REFERENCE ONLY

UNIVERSITY OF LONDON THESIS

Degree PhD Year 2005 Name of Author FERGUSON, B J

COPYRIGHT

This is a thesis accepted for a Higher Degree of the University of London. It is an unpublished typescript and the copyright is held by the author. All persons consulting the thesis must read and abide by the Copyright Declaration below.

COPYRIGHT DECLARATION

I recognise that the copyright of the above-described thesis rests with the author and that no quotation from it or information derived from it may be published without the prior written consent of the author.

LOANS

Theses may not be lent to individuals, but the Senate House Library may lend a copy to approved libraries within the United Kingdom, for consultation solely on the premises of those libraries. Application should be made to: Inter-Library Loans, Senate House Library, Senate House, Malet Street, London WC1E 7HU.

REPRODUCTION

University of London theses may not be reproduced without explicit written permission from the Senate House Library. Enquiries should be addressed to the Theses Section of the Library. Regulations concerning reproduction vary according to the date of acceptance of the thesis and are listed below as guidelines.

A. Before 1962. Permission granted only upon the prior written consent of the author. (The Senate House Library will provide addresses where possible).

B. 1962 - 1974. In many cases the author has agreed to permit copying upon completion of a Copyright Declaration.

C. 1975 - 1988. Most theses may be copied upon completion of a Copyright Declaration.

D. 1989 onwards. Most theses may be copied.

This thesis comes within category D.

☑ This copy has been deposited in the Library of UCL

☐ This copy has been deposited in the Senate House Library, Senate House, Malet Street, London WC1E 7HU.

Structural and biochemical analysis of the death domain complex formed at the Fas receptor

Brian James Ferguson

Department of Biochemistry and Molecular Biology

University College London

Submitted in fulfilment of the requirements for the degree of Doctor of Philosophy, February 2005

ProQuest LLC
789 East Eisenhower Parkway
P.O. Box 1346
Ann Arbor, MI 48106-1346

Abstract

Fas (CD95) is a member of the death receptor superfamily of proteins that are involved in the initiation of apoptosis as induced by the binding of extracellular ligands. At present, little is known about the precise mechanism by which the signal initiated by the interaction between Fas ligand (FasL) and Fas is transduced across the cell membrane to start the apoptotic signalling cascade. The first step in this pathway is the recruitment of the Fas-associated death domain protein (FADD) to the cytoplasmic death domain of Fas via a homotypic protein/protein interaction. This binding event occurs after receptor ligation apparently without any post translational modification such as phosphorylation. In order to better understand this event we have investigated the interaction between the death domains of the human Fas and FADD proteins both *in vitro* and in a cellular context.

The reported interaction between the Fas and FADD death domains (Fas-DD and FADD-DD) was recapitulated using the yeast 2-hybrid assay. Recombinant proteins were then produced for NMR spectroscopy experiments. FADD-DD is highly expressed, and easy to isolate soluble at physiological pH. This domain is readily expressed as a histidine tagged domain. Fas death domain expresses at low levels and produces soluble aggregates when concentrated at a pH above 4. However, it was found that using a Gb1 fusion protein to express Fas-DD overcomes these problems and allowed the production of Fas-DD for NMR experiments. NMR titration experiments showed that when these two proteins interact a large, soluble complex is formed. This may be significant in relation to the increasing evidence for the importance of Fas-receptor clustering in its signalling.

Mutational analysis of the Fas death domain was also carried out. Here, various previously described as well as several novel point mutations were made on the surface of the Fas death domain to investigate their effect on FADD-DD binding. These mutations were assayed using yeast 2-hybrid methods, NMR analysis and in a cell based assay. In the cell based assay wild type and mutant Fas receptors were overexpressed in a human cell line with no endogenous surface Fas expression. These cells were then

assayed for their ability to undergo FasL-induced apoptosis. It was found that residues from many surface regions of Fas-DD are crucial for the FADD-DD interaction. This observation has potentially important implications for the nature of the organisation of the death domains in the death inducing signalling complex (DISC) formed at the Fas receptor.

Acknowledgements

There are many people whom I must thank for their help and support during these studies. First and foremost I must acknowledge my supervisor Paul Driscoll for his unwavering support throughout my time at UCL and for all of the help and advice he has provided during this period.

Thanks must also go to the members of the Driscoll laboratory, Acely Garza, Mike Plevin, Beatriz Simas Magalhaes, Diego Esposito and Richard Harris who have provided invaluable teaching, help, support and general camaraderie during the last four years and special thanks to Mark Jeeves, Andrew Sankar, Stephan Millson and David Vines for their investments of time and effort in my practical training.

Outside of the laboratory, it has been a pleasure to work in the environment generated by members of the BSM groups. Thank you all for ensuring a constant supply of Friday evening entertainment and general social activity. A particular mention for the valiant work of James Bray and Stuart Rison in helping to rehabilitate my broken leg by dragging me to the gym on numerous occasions.

I must also thank my collaborators at the Hammersmith hospital for introducing me to the world of cell biology. Thanks to all of the members of the Weston lab, especially Nigel Kennea and Grisha Piranov for their help and advice and in particular, thanks to Huseyin Mehmet for his guidance and continuous injections of scientific enthusiasm.

Finally, special thanks to Joyce Wong for all of her love and support, particularly in the last few months. This thesis is dedicated to her.

Table of Contents

List of Figures

Chapter 1

Chapter 3

Chapter 4

Chapter 5

Chapter 6

List of Tables

Abbreviations

1^0	Primary
2^0	Secondary
2D	Two dimensional
3-AT	3-aminotriazole
3D	Three dimensional
Ab	Antibody
AD	GAL-4 RNA polymerase activation domain
AICD	Activation induced cell death
APAF-1	Apoptotic protease activating factor 1
APS	Ammonium persulphate
BD	GAL-4 DNA binding domain
BCA	Bicinchoninic acid
BH	Bcl-2 homology
CAD	Caspase-activated DNase
CARD	Caspase recruitment domain
CMV	Cytomegalovirus
CRD	Cysteine rich domain
CPS	Counts per second
DAPI	4-6-Diamidino-2-phenylindole
DD	Death domain
ddH_20	Distilled and deionised water
DED	Death effector domain
DISC	Death inducing signalling complex
DMEM	Dulbecco's modified Eagle's medium
DMF	Dimethylformamide
dNTP	Deoxynucleotide triphosphate
DNA	Deoxyribonucleic acid
Dox	Doxycyclin
DR	Death receptor
DTT	Dithiothreitol

EDTA	Ethylene diamine tetracetic acid
ELISA	Enzyme-linked immunosorbant assay
FADD	Fas associated death domain protein
FADD-DD	FADD death domain
Fas-DD	Fas death domain
FasL	Fas-ligand
FBS	Foetal bovine serum
GS	Glutathione-sepharose
HBSS	Hank's balanced salt solution
HI-FBS	Heat-inactivated foetal bovine serum
HRP	Horse-radish peroxidase
HSQC	Heteronuclear single quantum correlation spectroscopy
Hyg	Hygromycin
IAP	Inhibitor of apoptosis
IMAC	Immobilised metal ion chromatography
ICE	Interleukin-1β-converting enzyme
ICC	Immunocytochemistry
IPTG	Isopropyl-β-D-thiogalactopyranoside
LiAc	Lithium acetate
MHC	Major histocompatibility complex
mins	Minutes
MTT	Methylthiazoletetrazolium (3-(4,5-Dimethyl-2-thiazolyl)-2,5-diphenyl-2H-tetrazolium bromide)
NMR	Nuclear magnetic resonance
NEB	New England Biolabs
PCD	Programmed cell death
PCR	Polymerase chain reaction
PBS	Phosphate buffered saline
PLAD	Pre-ligand association domain
PVDF	Polyvinylidene Difluoride
rhsFasL	Recombinant, human, soluble Fas-ligand
RNA	Ribonucleic acid
rtTA	Tet-responsive transcriptional activator
PAGE	Polyacrylamide gel electrophoresis

S200	Superdex 200
SDH	Succinate dehydrogenase
SDS	Sodium dodecyl sulphate
SEC	Size-exclusion chromatography
SG	Structural genomics
ssp	Staurosporine
T7-pol	T7 RNA polymerase
TAE	Tris-acetate EDTA
TBS	Tris-buffered saline
TBS-T	Tris-buffered saline plus 0.1 % Tween20
TCR	T cell receptor
TdT	Terminal deoxynucleotide transferase
TEMED	N,N,N',N'-Tetramethylethylenediamine
TNF	Tumor necrosis factor
TNF-R	Tumor necrosis factor receptor
TRE	Tet-response element
TRAIL	TNF-related apoptosis-inducing ligand
TUNEL	TdT-mediated, dUTP nick-end labelling
UV	Ultra-violet

Chapter 1

Introduction

1.1 Apoptosis

THE balance between cell proliferation and death is essential for the development of multicellular organisms (Jacobson *et al.*, 1997) as well as in the maintenance of homeostasis in adult tissues (DeLong, 1998) and the fight against pathogens (Arends and Wyllie, 1991). It has been estimated that, in the human body, upwards of 100,000 cells are produced every minute and hence a similar number die in order to ensure the cellular populations remain constant (Vaux and Korsmeyer, 1999). Therefore, to assist in the control of cellular populations, multi-cellular organisms have evolved methods of removing damaged, unwanted or infected cells in a controlled manner that is non-detrimental to the surrounding tissues.

This concept, known as programmed cell death (PCD), has existed since 1842 when it was noticed that cells are removed during the normal development of amphibians (Vogt, 1842) The importance of PCD can be illustrated by its significant role in the development of multicellular organisms. For example, during the formation of the limbs, individual digits are sculpted by massive cell death of the interdigital mesenchymal tissue (Zuzarte-Luis and Hurle, 2002). Also, it is estimated that up to 50 percent of neurons that are initially created will be removed by PCD before the adult brain is fully formed (Meier *et al.*, 2000). However, as will be discussed in the following sections, PCD also plays significant roles in the maintenance of homeostasis and disease.

1.2 The morphological aspects of apoptosis

During the 1900's the idea of PCD was "rediscovered" on several occasions but it was not until the 1970s that these ideas were unified. The term apoptosis was coined in a paper by Kerr, Wyllie and Currie in 1972 to describe a quite characteristic variety of PCD involving a series of specific morphological changes (Kerr *et al.*, 1972). Cells being removed during embryonic development or through population regulation in normal human tissue as well as cells dying in pathological situations were all observed to undergo the exact same series of morphological changes. The sequence of gross rearrangements that have been identified – cellular shrinking, membrane blebbing, chromatic condensation, nuclear fragmentation and, finally, cellular fragmentation – have now become the hallmarks and, in many ways, the defining characteristics of apoptotic cell death (Hacker, 2000).

The concept of apoptosis is perhaps best illustrated by comparison with a separate variety of pathological cell death called caused by gross injury or uncontrolled infection. This second mode of cell death, known as necrosis, is characterised by swelling of the cell and its organelles, due to a loss of membrane potential control, which results in the dying cell bursting and releasing its contents into the local environment (Saraste and Pulkki, 2000). During necrosis there is no nuclear rearrangement or membrane blebbing, as seen in apoptosis, but perhaps the most crucial difference between these forms of cell death can be observed in the latter stages of apoptosis during which there is the formation of small membrane bound cellular fragments, known as "apoptotic bodies", which are subsequently phagocytosed by cells in the surrounding tissue. Since these apoptotic bodies serve to contain most, if not all, of the original contents of the now dead cell, there is no damage to the surrounding tissues and indeed the cellular contents can be reused following phagocytosis of the apoptotic bodies by other cells. This recycling process is in stark contrast to necrotic cell death whereby bursting of the plasma membrane and the release of cellular contents leads directly to a damaging, inflammatory response in the local tissue. A diagrammatic comparison of the morphological differences between apoptosis and necrosis, illustrating both the mechanism and consequences of these two distinct forms of cell death, is shown in Figure 1.1.

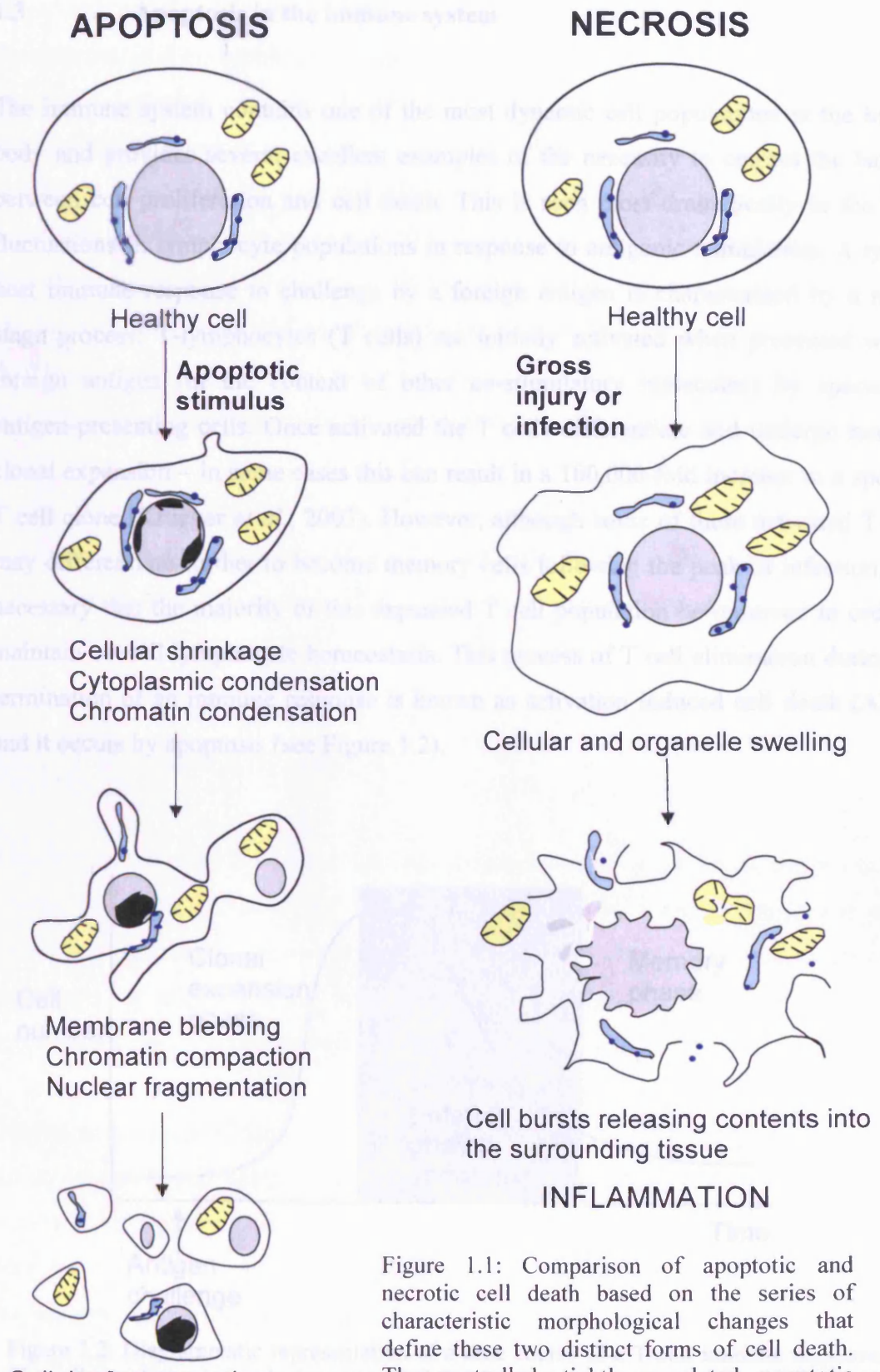

Figure 1.1: Comparison of apoptotic and necrotic cell death based on the series of characteristic morphological changes that define these two distinct forms of cell death. The controlled, tightly regulated apoptotic process that results in the formation of apoptotic bodies that are readily phagocytosed is contrasted with the uncontrolled nature of necrotic cell death that ends in the release of inflammatory molecules from the ruptured cell.

1.3 Apoptosis in the immune system

The immune system contains one of the most dynamic cell populations in the human body and provides several excellent examples of the necessity to control the balance between cell proliferation and cell death. This is seen most dramatically in the huge fluctuations in lymphocyte populations in response to antigenic stimulation. A typical host immune response to challenge by a foreign antigen is characterised by a multi-stage process: T-lymphocytes (T cells) are initially activated when presented with a foreign antigen (in the context of other co-stimulatory molecules) by specialised antigen-presenting cells. Once activated the T cells differentiate and undergo massive clonal expansion – in some cases this can result in a 100,000-fold increase in a specific T cell clone (Krueger *et al.*, 2003). However, although some of these activated T cells may differentiate further to become memory cells following the peak of infection, it is necessary that the majority of this expanded T cell population be removed in order to maintain overall lymphocyte homeostasis. This process of T cell elimination during the termination of an immune response is known as activation induced cell death (AICD) and it occurs by apoptosis (see Figure 1.2).

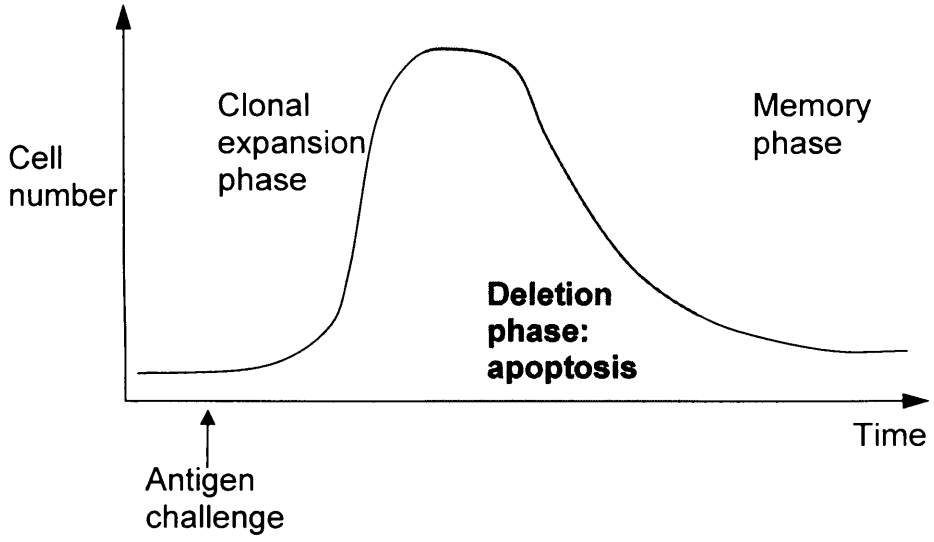

Figure 1.2: Diagrammatic representation of a time course of a T cell immune response. The cell population expands dramatically following antigen challenge. The removal of T cells following this clonal expansion is effected by apoptosis and is known as activation induced cell death. Adapted from (Krueger *et al.*, 2003).

A second, equally important, role for apoptosis in the immune system is in the development and maintenance of T cell self-tolerance. T cells recognise antigens via an interaction between their own T cell receptor (TCR) and a major histocompatibility complex (MHC)-peptide complex that is present on the surface of an antigen-presenting cell. Since the process that creates TCRs is an essentially random genetic recombination event it is inevitable that some T cells will be produced that recognise self-antigens. These self-reactive T cells are deleted by apoptosis both in the thymus by complex mechanisms of positive and negative selection, where the vast majority of tolerance is developed, and almost certainly also in the peripheral organs where a number of self-antigens are present which are not encountered in the thymus (Stuart and Hughes, 2002).

The tight control of the combination of proliferative and apoptotic events in the T cell population ensures that there is always a relatively constant number of functional but non-self reactive immune cells.

1.4 Apoptosis signalling

It is clear that in order for cells to undergo apoptosis in such a consistent manner in such a wide variety of physiological situations there must be a highly conserved set of underlying biochemical processes that control this mode of cell death. Reinforcing this hypothesis is the observed evolutionary conservation of apoptosis throughout multicellular invertebrate and vertebrate species (Jacobson *et al.*, 1997).

Despite intricate knowledge of the gross morphological changes that have now come to define apoptotic cell death, fifteen years ago the intracellular processes that control apoptosis were not well understood (Arends *et al.*, 1991). Since that time, however, there has been a vast effort to improve the understanding of the precise molecular mechanisms that underpin apoptosis and this is reflected in the exponential growth in the number of publications in the field since the early 1990's. A combination of cell biology, biochemical and genetic research has lead to the discovery that the way in which cells die by apoptosis is the consequence of highly organised and finely regulated

series of intracellular signalling pathways (see such reviews by Martin and Green, 1995; Chinnaiyan and Dixit, 1996; Strasser *et al.*, 2000; Hengartner, 2000).

The major impetus behind the deconstruction of these biochemical pathways was the genetic study of the nematode *Cœnorrahditis elegans* that uncovered several genes (denoted '*ced*' genes) which were found to be essential for the famously defined 131 PCD events that occur during the development of this organism. Of particular interest from this genetic research were several of the *ced* genes such as *ced-3, ced-4* and *ced-9* as these genes were subsequently found to have mammalian homologues (reviewed in (Metzstein *et al.*, 1998). The major route of initiation of apoptosis in *C. elegans* is the heterodimerisation of the *ced-3* and *ced-4* gene products. This complex can be negatively regulated by the *ced*-9 gene product, the activity of which can, in turn, be blocked by the *egl-1* gene product. The *ced-3* gene was discovered to encode a protein that is homologous to the human interleukin-1β-converting enzyme, ICE (Yuan *et al.*, 1993). ICE belongs to a family of proteases, of which 14 have been identified in mammals, which are now referred to as caspases as they are cysteine proteases that cleave their respective substrates on the C-terminal side of aspartic acid residues. The *ced-4* gene product is homologous to a mammalian protein known as apoptotic protease activating factor 1 (APAF-1) which is now known to be part of a caspase-activating signalling complex known as the apoptosome. The *ced-9* gene product, meanwhile, is homologous to Bcl-2, a mammalian inhibitor of apoptosis (Hengartner and Horvitz, 1994). The EGL-1 protein consists solely of a Bcl-2 homology 3 (BH3) domain and interacts with the CED-9 protein, directly inhibiting its function (Kaufmann and Hengartner, 2001).

Whilst evolution has led to an increase in the numbers of genes in the different "death gene" families recognised in *C. elegans* (exemplified by the inventory of 14 mammalian caspases and the large number of mammalian BH3-only proteins, such as Bid, Bad, Bik, Bim, Noxa and Puma), the conservation of these proteins is underlined by the presence of homologues not only in nematodes and mammals but also in *Drosophila* (Kaufmann *et al.*, 2001; Richardson and Kumar, 2002). The *Drosophila* PCD pathways are found to be of intermediate complexity relative to worms and mammals, as may be expected from the respective levels of complexity of these organisms.

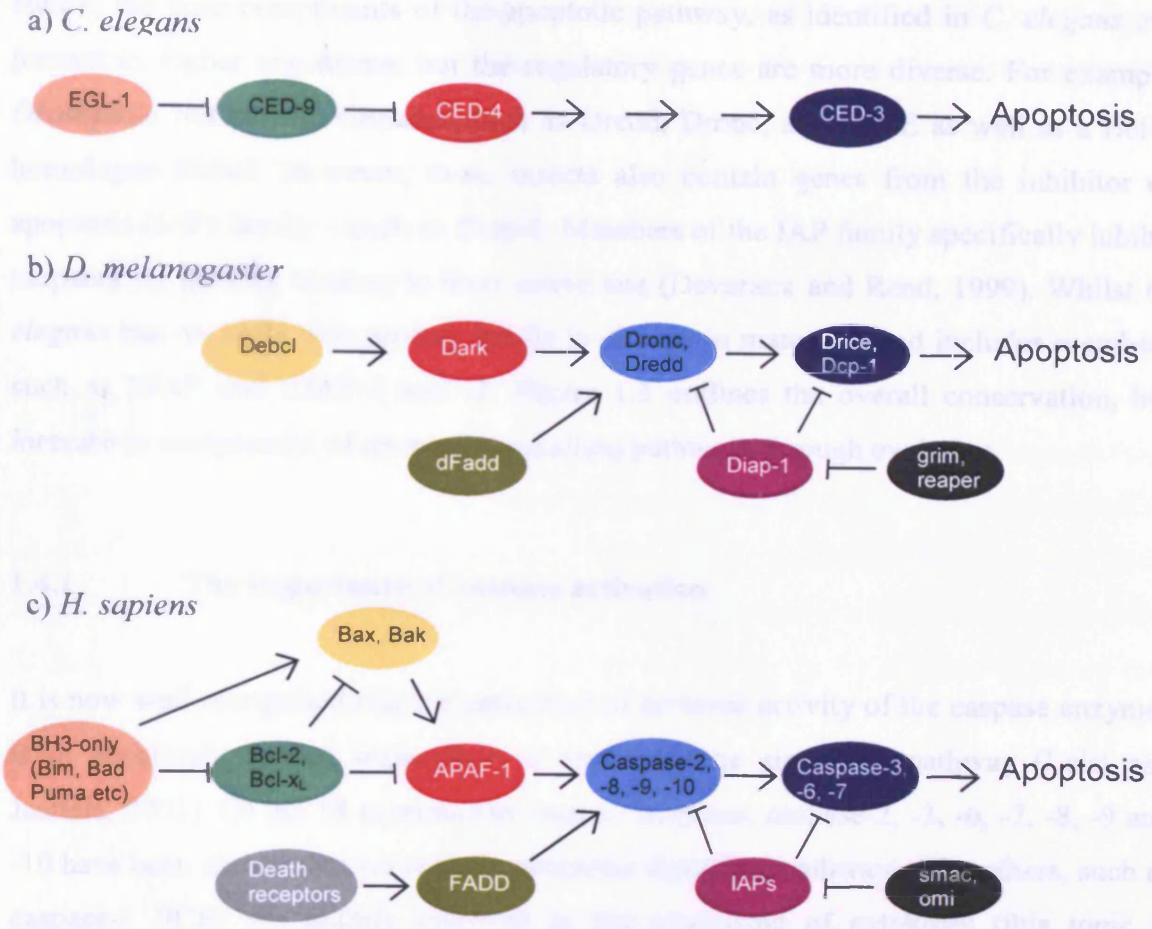

Figure 1.3: Apoptotic signaling pathways in (a) *C. elegans*, (b) *D. melanogaster* and (c) *H. sapiens*. The conservation of theses pathways is indicated in this diagram by the use of identical coloured boxes for homologous proteins across the different species. The *C. elegans* pathway is the least complex, involving direct interaction between CED-4 and CED-3 resulting in CED-3 (a caspase enzyme) activation. This action can be blocked by the Bcl-2 homologue CED-9 through direct binding to CED-4. The BH3-only protein EGL-1, can, in turn, interact directly with CED-9, blocking its activity (and is therefore indirectly pro-apoptotic). Mammals have evolved to have two sets of caspase enzymes, the initiators, such as caspase-8 and caspase-9 and the effectors, such as caspase-3 and caspase-6. These caspases are negatively regulated by the IAP family of proteins by direct interaction. IAP activity can, in turn, be blocked by smac and omi following the release of these pro-apoptotic proteins from the mitochondria. As in *C. elegans*, the activity of APAF-1 (the mammalian CED-4 homologue), can be blocked by Bcl-2 (as well as other anti-apoptotic members of this family, such as Bcl-x_L) and mammals have many BH3-only proteins that are capable of inhibiting these proteins in the same way as EGL-1. However, mammals have also evolved the use of the mitochondria in apoptotic signalling which is not observed in worms. Another set of pro-apoptotic Bcl-2 family members, Bax and Bak, control the release of cytochrome *c*, and other factors, from the mitochondria after receiving an apoptotic signal, often through the BH3-only proteins. Cytochrome *c* subsequently activates APAF-1 to form a complex known as the apoptosome that is responsible for procaspase-9 activation. Moreover, mammals have evolved a second pathway for the activation of caspases. The extrinsic pathway involves the activation of death receptors and proceeds via the adaptor protein FADD, which carries out a similar role to APAF-1 in activating initiator caspases (see Section 1.5). *Drosophila* show intermediate complexity in their apoptotic signalling. Although, like mammals, they have two sets of caspases, IAPs and smac homologues (such as grim and reaper), they have no extrinsic pathway (despite the presence of dFadd), no known BH3-only proteins and a poorly defined mitochondrional pathway.

Hence, the core components of the apoptotic pathway, as identified in *C. elegans* are present in higher organisms, but the regulatory genes are more diverse. For example *Drosophila* has several caspases, such as Dredd, Dronc, and drICE as well as a Bcl-2 homologue Debcl. However, these insects also contain genes from the inhibitor of apoptosis (IAP) family – such as Diap-1. Members of the IAP family specifically inhibit caspases by directly binding to their active site (Deveraux and Reed, 1999). Whilst *C. elegans* has no IAPs, this protein family is diverse in mammals and includes members such as XIAP and CIAP-1 and -2. Figure 1.3 outlines the overall conservation, but increase in complexity, of apoptotic signalling pathways through evolution.

1.4.1 The importance of caspase activation

It is now well recognised that the activation of protease activity of the caspase enzymes is of absolutely central importance to any apoptotic signalling pathway (Leist and Jaattela, 2001). Of the 14 mammalian caspase enzymes, caspase-2, -3, -6, -7, -8, -9 and -10 have been shown to have roles in apoptotic signalling pathways. The others, such as caspase-1 (ICE) are mainly involved in the processing of cytokines (this topic is reviewed extensively elsewhere, (for example see, Martin *et al.*, 1995; Li and Yuan, 1999; Budihardjo *et al.*, 1999).

All caspases are synthesised as essentially inactive zymogens, known as procaspases, which are activated by proteolytic cleavage and/or oligomerisation. Once activated each caspase recognises and cleaves target substrates at tetrapeptide motifs on the C-terminal side of an aspartate residue; for example caspase-8 attacks proteins that contain the amino-acid sequence Leu-Glu-Thr-Asp (Strasser *et al.*, 2000). It is both the mode of activation and the identity of its substrates that defines the role of the individual caspase in its particular apoptotic pathway. The apoptotic caspases can be divided into two main groups; those that initiate the individual apoptotic signalling pathways (caspase-2, -8, -9 and -10) and those that are themselves cleaved by the initiator caspases (caspase-3, -6 and -7) and go on to target the so-called "death substrates" for proteolysis (Nicholson and Thornberry, 1997).

All procaspases contain large and small subunits separated by a variable length linker peptide. As part of the activation process this linker is cleaved, thereby releasing the two subunits and allowing tetramerisation of two small and two large subunits to form the active caspase enzyme. As well as these two catalytic subunits, the initiator caspases are distinguished by their N-terminal prodomains. These prodomains contain protein/protein interaction motifs – a tandem pair of death effector domains (DEDs) in the case of caspase-8 and caspase-10 and a caspase recruitment domain (CARDs) in the case of caspase-2 and caspase-9. These protein/protein interaction domains are discussed in greater detail in Section 1.7.1. The role of the prodomains in the activation of the initiator caspases is to recruit the procaspases to death inducing signalling complexes (DISCs) where oligomerisation leads to their activation (Salvesen and Dixit, 1999). In contrast, the effector procaspases do not contain a functional prodomain. Rather, this set of procaspases is activated through cleavage by initiator caspases (see Figure 1.4).

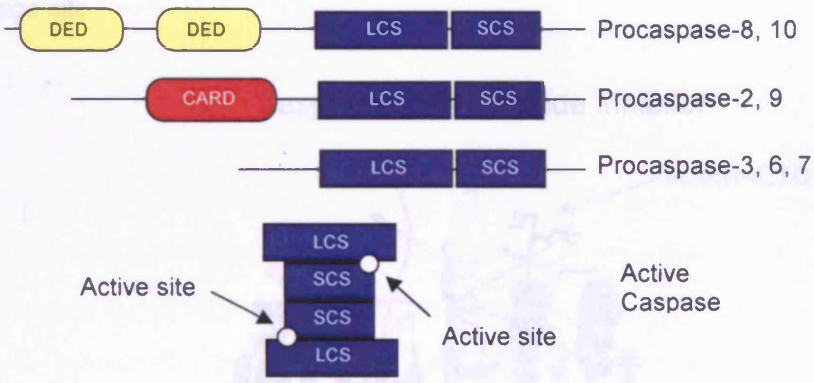

Figure 1.4: Schematic diagram of the domain architecture of mammalian apoptotic procaspases and the generalised form of an active caspase indicating the positions of the two active sites (white circles). LSC – large catalytic subunit, SCS – small catalytic subunit, DED – death effector domain, CARD – caspase recruitment domain.

The three dimensional structures of several human caspase enzymes have been solved, each of which exhibits a conserved topology consisting of a twisted β-sheet flanked by a series of α-helices (see Figure 1.5). The only available procaspase structure is that of procaspase-7 (see Figure 1.5a) (Chai *et al.*, 2001). Comparison of this zymogen structure with the 3D structure of active caspase-7 (Wei *et al.*, 2000), reveals that, following zymogen cleavage, it is the rearrangement of several flexible loops that connect the secondary structure elements that is responsible for the formation of the caspase active site (see Figure 1.5b). Also, the determination of 3D structures of

caspases with bound inhibitory peptides, such as the structure of caspase-8 bound to Ile-Glu-Thr-Asp (Watt *et al.*, 1999) (see Figure 1.5c) has improved the understanding of these enzymes' substrate specificities (Wei *et al.*, 2000).

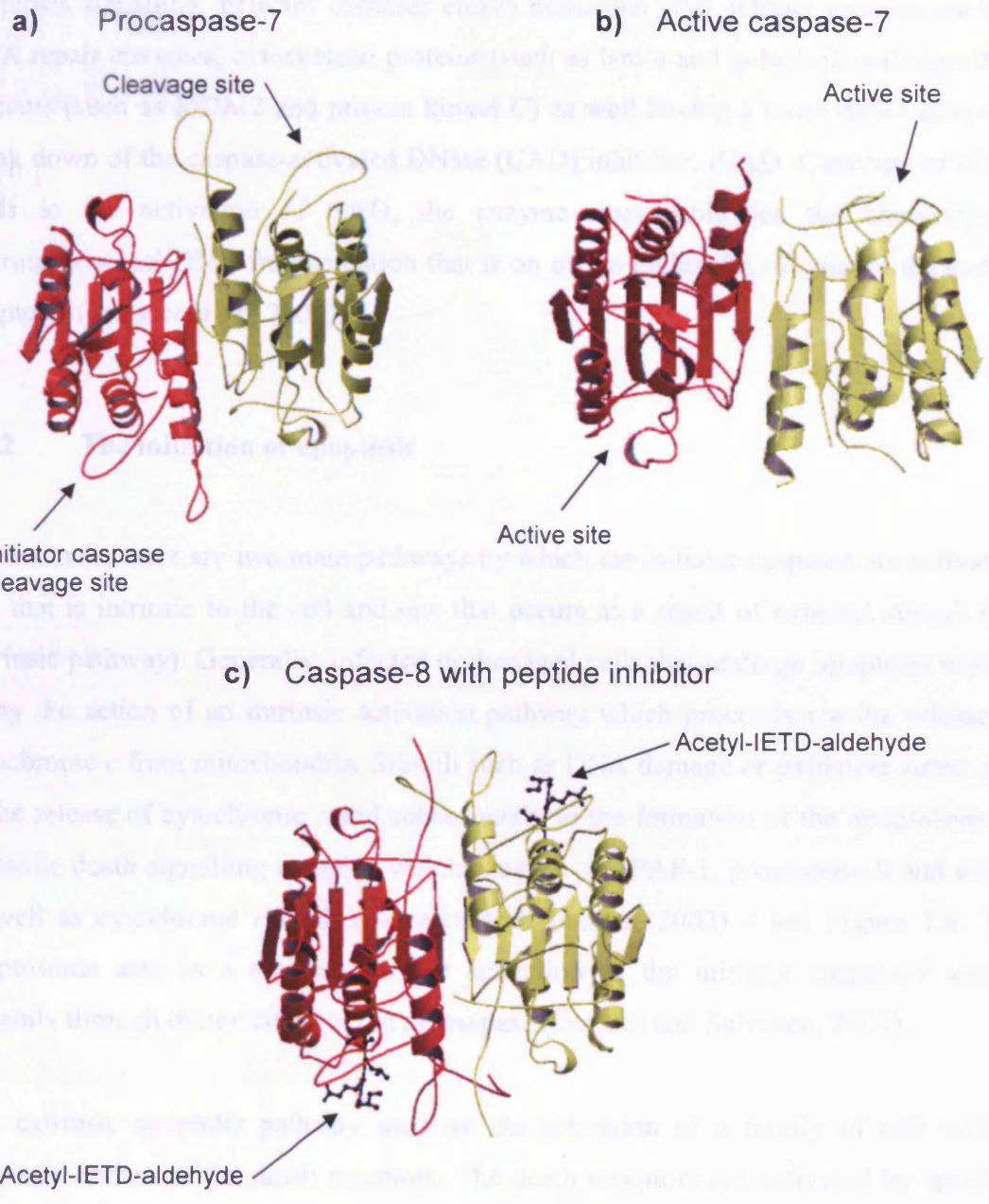

Figure 1.5: Three dimensional structures of caspase enzymes. Caspase-7 is shown in (a) the zymogen form (the only available 3D procaspase structure) and (b) the active, cleaved form. It can be seen how proteolytic cleavage of the flexible loop highlighted in (a) exposes the active site (highlighted in (b)) thereby activating the caspase enzyme. The 3D structure of active caspase-8 bound to a tetrapeptide (Ile-Glu-Thr-Asp) inhibitor is shown in (c). This inhibitor binds the active site of caspase-8. The homodimeric pairs shown in red and yellow in these figures each consist of one large and one small catalytic subunit which combine to form single globular entities as outlined in Figure 1.4. Figures generated with MolScript (Esnouf, 1997).

It is the specific proteolysis of death substrates by the effector caspases that is ultimately responsible for most of the morphological changes observed during apoptosis (Hacker, 2000) and for this reason the activation of caspases is one of the most critical events in apoptosis signalling. Effector caspases cleave numerous vital cellular proteins such as DNA repair enzymes, cytoskeletal proteins (such as lamin and gelsolin), cell signalling proteins (such as MDM2 and protein kinase C) as well having a more direct effect by break down of the caspase-activated DNase (CAD) inhibitor, iCAD. Cleavage of iCAD leads to the activation of CAD, the enzyme responsible for the characteristic internucleosomal DNA fragmentation that is on of the hallmarks of caspase dependent apoptosis (Strasser *et al.*, 2000).

1.4.2 The initiation of apoptosis

In mammals, there are two main pathways by which the initiator caspases are activated; one that is intrinsic to the cell and one that occurs as a result of external stimuli (the extrinsic pathway). Generally, infected or damaged cells that undergo apoptosis will do so by the action of an intrinsic activation pathway which proceeds via the release of cytochrome *c* from mitochondria. Stimuli such as DNA damage or oxidative stress lead to the release of cytochrome *c* and subsequently to the formation of the apoptosome, a cytosolic death signalling complex which consists of APAF-1, procaspase-9 and dATP as well as cytochrome *c* itself (Salvesen and Renatus, 2002) – see Figure 1.6. The apoptosome acts as a scaffold for the activation of the initiator caspase-9 almost certainly through dimerisation of the procaspase (Denault and Salvesen, 2002).

The extrinsic apoptotic pathway involves the activation of a family of cell surface receptors known as the death receptors. The death receptors are activated by specific, extracellular ligands and this pathway is vital for the regulation of cellular populations in the immune system where there is a need to send death signals between cells. This "death by communication" can be contrasted to the intrinsic pathway (which is essentially a means of autonomous cellular suicide).

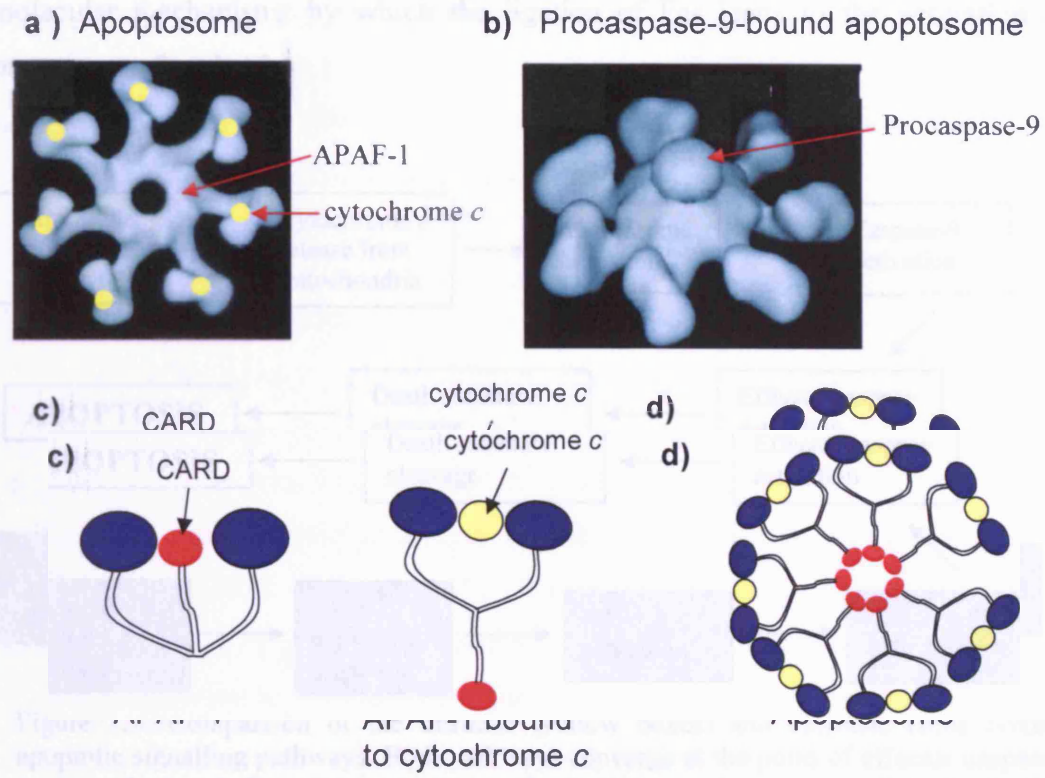

Figure 1.6: Three dimensional structure of the apoptosome. Upon release from the mitochondria, cytochrome *c* binds to APAF-1. This process (a model for which is shown diagrammatically in (c)) causes a conformational change in APAF-1, releasing its caspase recruitment domain (CARD) – shown in red – and allowing it to oligomerise with other APAF-1 molecules via homotypic CARD/CARD interactions. The cytochrome *c*/APAF-1 heterodimer heptamerises to form the apoptosome structure (shown in (a) and (d)). The position of cytochrome *c* is diagrammatically represented in these figures by yellow circles. The apoptosome subsequently recruits caspase-9 via the homotypic interaction between the CARD domains of caspase-9 and APAF-1. Diagram (b) shows the structure of the procaspase-9-bound form of the apoptosome. Following interaction with the apoptosome, procaspase-9 is activated by autoproteolysis. The 3D structures shown in (a) and (b) were solved by electron cryomicroscopy and are taken from (Acehan *et al.*, 2002).

Upon activation, the death receptors recruit several proteins to their cytoplasmic domains – to form DISCs – and these complexes include the initiator procaspase-8 and (in some cases) procaspase-10. Again, once activated by oligomerisation and autoproteolysis, the initiator caspases go target activation by proteolysis of effector procaspase-3, -6, and -7 in the caspase cascade that results in apoptosis (Thorburn, 2004). Figure 1.7 schematically outlines the two main apoptotic initiation pathways and their point of convergence at the stage of effector caspase initiation.

The aim of this project was to study one member of the death receptor family, namely the protein Fas, and its signalling pathway – of particular interest is the precise

molecular mechanisms by which the ligation of Fas leads to the activation of the procaspases-8 and -10.

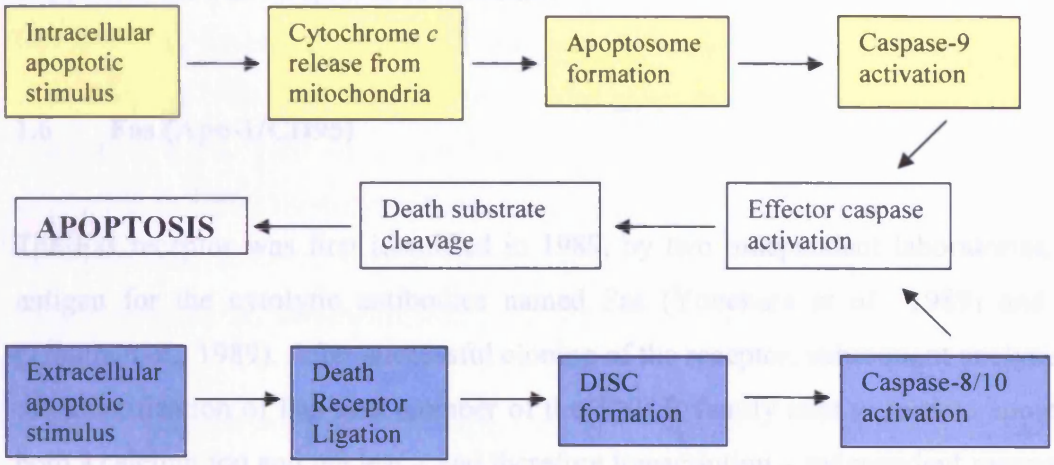

Figure 1.7: Comparison of the intrinsic (yellow boxes) and extrinsic (blue boxes) apoptotic signalling pathways. Both pathways converge at the point of effector caspases (caspase-3, -6,and -7) activation to initiate the final stages of apoptotic cell death. DISC= death inducing signalling complex.

1.5 The death receptor family

Death receptors (DRs) are type I transmembrane glycoproteins and are members of the tumour necrosis factor receptor (TNF-R) superfamily. The TNF-R family is characterised by the presence of two or more repeats of a specific cysteine rich domain (CRD) in the extracellular region of the receptor. The feature that sets the death receptors apart from the rest of the TNF-R family is the presence in the former of a conserved ~100 amino acid cytoplasmic domain. This domain governs the initiation of apoptotic signalling cascades and is known as the death domain (DD).

So far eight members of the death receptor family have been described – Fas (also known as CD95/Apo-1), TNF receptor-1 (TNF-R1/CD120a/p55R), TNF-related apoptosis-inducing ligand (TRAIL)-receptor 1 (DR4/Apo-2), TRAIL receptor 2 (DR5/KILLER/TRICKB), death receptor 3 (DR3/TRAMP/LARD/TR3/WSL1/ Apo3), death receptor 6 (DR6/TR7), nerve growth factor receptor (NGFR/ p75) and the ectodysplasin receptor (EDAR). Each death receptor plays specific roles in the immune

system and accordingly has unique downstream signalling pathways (as reviewed extensively elsewhere, e.g. (Gravestein and Borst, 1998; Wallach *et al.*, 1999; Schneider and Tschopp, 2000; Locksley *et al.*, 2001). It is in the interests of this thesis, however, to consider the Fas receptor in more detail.

1.6 Fas (Apo-1/CD95)

The Fas receptor was first identified in 1989, by two independent laboratories, as the antigen for the cytolytic antibodies named Fas (Yonehara *et al.*, 1989) and Apo-1 (Trauth *et al.*, 1989). After successful cloning of the receptor, subsequent analysis led to the identification of Fas as a member of the TNF-R family able to initiate apoptosis in both a calcium ion and nuclear – and therefore transcription – independent manner.

Following the discovery of a ligand for Fas, FasL (Suda and Nagata, 1994) and its ability to induce cell death, the Fas/FasL system has become the most intensively studied of the death receptor/ligand combinations and hence has become the major model for ligand-induced apoptotic signalling.

The discovery of mutations in the murine Fas (the *lpr* mutation) (Watanabe-Fukunaga *et al.*, 1992) and FasL (the *gld* mutation) (Roths *et al.*, 1984) genes was largely responsible for the unravelling of the physiological role of Fas induced apoptosis. The *lpr* mutation impairs the transcription of Fas due to the insertion of a transposable element into one of the gene's introns, whereas *gld* is a point mutation in the *FasL* gene resulting in the FasL protein being unable to interact with Fas. Interestingly both of these mutations result in mice with the same phenotype, namely the accumulation of lymphocytes in the lymph nodes and spleen. This data led to the conclusion that the major role of Fas-induced apoptosis is in the control of lymphocyte populations, and this has subsequently been shown to be the case. FasL-induced apoptosis is of particular importance in reducing the numbers of T- and B-cells in the periphery after antigen exposure-induced immune cell proliferation – as illustrated in Figure 1.2 (Ju *et al.*, 1995; Dhein *et al.*, 1995; Brunner *et al.*, 1995 and reviewed in Krammer, 2000).

As with all apoptotic pathways the Fas/FasL system must be tightly regulated so as to avoid adventitious depletion of immune surveillance and this is achieved on several levels. First, whilst the tissue distribution of Fas expression is almost ubiquitous, it appears that the transcription of FasL is only activated by signals specifically arising in the immune system compartment such as exposure to IL-2 and TCR activation (Lenardo, 1991) thereby keeping Fas-induced apoptosis specific to cells of the immune system. Also, as well as at the level of gene expression, both Fas and FasL are expressed into micro-vesicles before being translocated to the cell surface (Ivanov *et al.*, 2003) allowing scope for number of Fas and FasL molecules being expressed on the cell surface to be tightly controlled at in a post translational fashion.

These complex regulatory mechanisms are important for several reasons. Firstly, it is essential for the survival of an organism that the point at which a cell dies must be the correct one; having several points of regulation improves stringency for this process. Also, in the case of death receptors, these wide ranging methods of regulation allow for increased flexibility in response to activation (ligand binding). For example, as well as initiating apoptosis, the activation of Fas (and other death receptors) can induce the upregulation of transcription factors NF-κB and JNK which modulate the expression of many genes involved in inflammatory responses and cell survival (reviewed in Beyaert *et al.*, 2002). It is perhaps unusual for a single receptor to be able to initiate responses that are clearly in opposition to each other (in this case cell death and cell survival) and the balance of these effects may depend on the context in which activation occurs. However the precise mechanism by which one signalling pathway wins out over the other are not well understood.

1.6.1 Fas Receptor Signalling

1.6.1.1 Ligand binding

As Fas is a member of the TNF-R family it contains several extracellular, cysteine-rich domain (CRD) repeats characteristic of this family which govern ligand-binding. Fas contains three such CRD repeats, of which the second and third govern ligand binding (Starling *et al.*, 1997). Upon binding of FasL to Fas the intracellular part of the receptor, which is comprised mainly of the death domain, recruits intracellular signalling adaptor

proteins and, via a series of protein/protein interactions activates caspase-8 and caspase-10 (Algeciras-Schimnich *et al.*, 2002). Although both of these caspases-8 are known to be activated at the Fas receptor during Fas-dependent apoptosis it is only essential that caspase-8 is activated for apoptosis to take place (Sprick *et al.*, 2002) and hence the precise role of caspase-10 in this context activation remains unknown. Nevertheless, mutations in caspase-10 lead to a phenotype similar to that associated with Fas mutations (see Section 1.8), so it would appear that caspase-10 must play a significant, if not essential, role in Fas signalling.

The ligand binding event is key in any variety of receptor-mediated signalling process and the death receptors are no exception. The three dimensional crystal structures of two death receptor/ligand combinations are currently available, namely the ectodomain of TNF-R1 bound to TNF-β (Banner *et al.*, 1993) and the ectodomain of TRAIL-R2 bound to TRAIL (Cha *et al.*, 2000). These two 3D structures show homotrimeric ligands, TNF-β or TRAIL, bound to three separate receptor molecules, associated with the interface regions between the ligand protomers (see Figure 1.8). Since the three dimensional structures of other TNF family members, such as receptor activator of NF-κB ligand, RANKL, (Lam *et al.*, 2001), ectodysplasin (Hymowitz *et al.*, 2003), and CD40 (Karpusas *et al.*, 1995), have been shown to exhibit trimeric structures with essentially the same "jellyroll" topology and the receptors all appear to have a CRD repeat modular structure, despite an absence direct molecular evidence, the trimer structure has become the presumed consensus model for Fas/FasL interaction.

Once the ligand binding event has occurred the activation signal must be transduced across the cell membrane to initiate the signalling cascades. It is still unclear precisely how the binding event is promulgated inside the cell, particularly because the initial steps in the cytoplasmic signalling pathways of death receptors are governed purely by protein/protein interactions apparently without any requirement for post translational modifications such as phosphorylation. Present evidence suggests that the receptors may be constitutively oligomerised in the cell membrane through a region known as the pre-ligand association domain (PLAD) which exists at the N-terminal tip of the extracellular region (Siegel *et al.*, 2000).

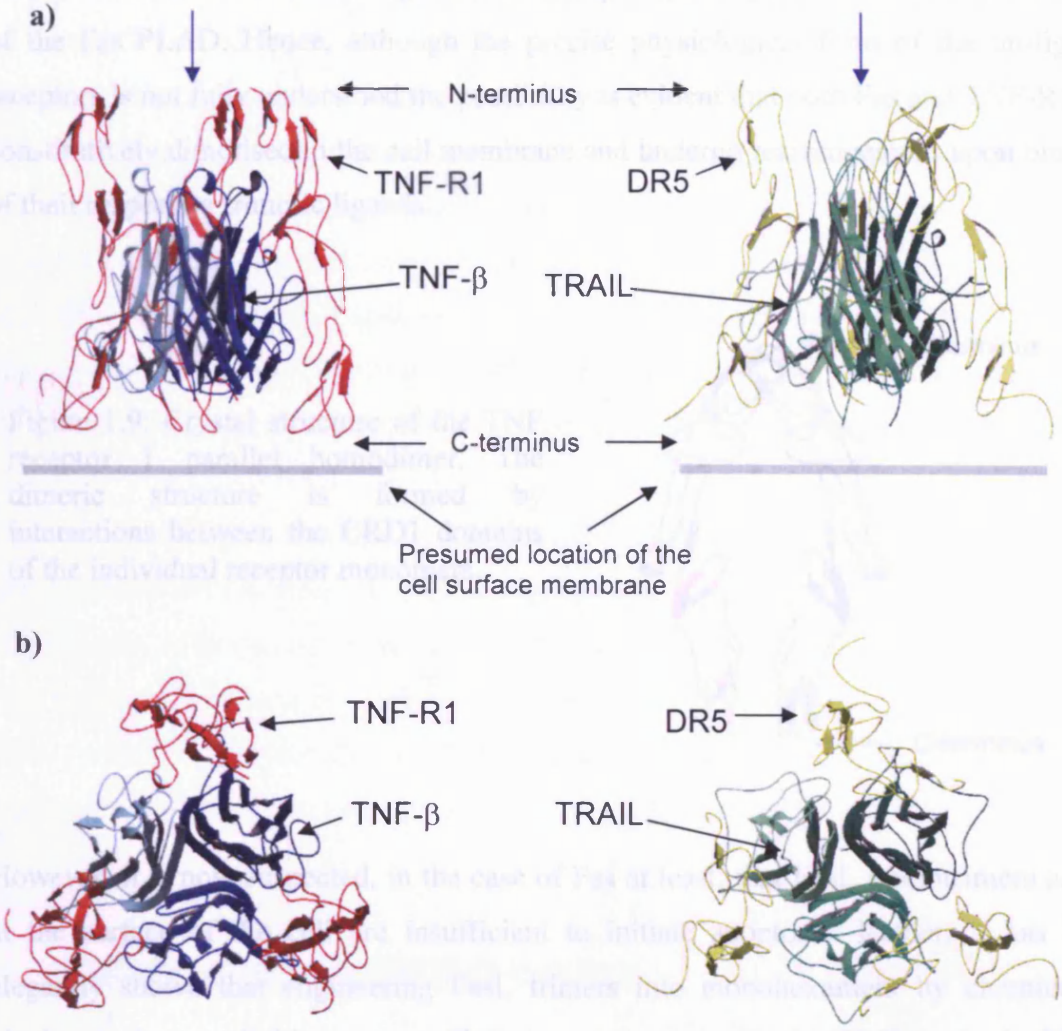

Figure 1.8. 3D structures of the TNF-β/TNF-R1 and TRAIL/DR5 complexes. The two complexes are shown in equivalent orientations from the side (a) and from above (b). The orientation of (b) is indicated by the blue arrow in (a). The structures show essentially identical conformations consisting of a trimeric ligand exhibiting the characteristic jellyroll topology (TNF-β - blue, or TRAIL – green) bound to three receptor molecules (TNF-R1 – red, or DR5 – yellow respectively).

The PLAD may exist to aid binding of the trimeric ligand, but its role may also be in holding the receptor cytoplasmic domains in an inactive configuration. If this is the case then when the ligand binds the receptor the intracellular domain may change conformation, reorganise or otherwise expose its binding sites to the adaptor molecules with which they interact. Evidence for the PLAD is given weight by the three dimensional structure of TNF-R1, solved without its ligand. The receptor was found to crystallise in two different forms – parallel and anti-parallel homodimers (Rodseth *et al.*, 1994; Naismith *et al.*, 1995). The interaction site of the two monomers in the

parallel dimer is in the CDR1 region of the receptor (see Figure 1.9) – the predicted site of the Fas PLAD. Hence, although the precise physiological form of the un-ligated receptors is not fully understood the possibility is evident that both Fas and TNF-R1 are constitutively dimerised in the cell membrane and undergo rearrangement upon binding of their respective trimeric ligands.

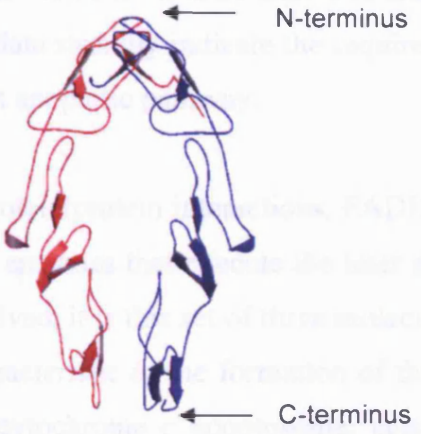

Figure 1.9: Crystal structure of the TNF receptor 1 parallel homodimer. The dimeric structure is formed by interactions between the CRD1 domains of the individual receptor monomers.

However, it is now suspected, in the case of Fas at least, that FasL homotrimers acting at the surface of the cell are insufficient to initiate apoptosis. Rather, it has been elegantly shown that engineering FasL trimers into monohexamers by chemical or biochemical cross linking was sufficient to induce apoptosis (Holler *et al.*, 2003). Combined with the knowledge that antibodies to Fas are sufficient to initiate apoptosis (presumably by cross linking the receptors) this leads to the hypothesis that it is aggregation of the receptors and therefore clustering of intra-cellular death receptor domains that is needed to trigger apoptosis. This argument is given weight by the evidence that both Fas, FasL and TNF-R1 are aggregated in ceramide-rich membrane "rafts" during signalling events (Grassme *et al.*, 2001a; Grassme *et al.*, 2001b; Scheel-Toellner *et al.*, 2002; Cottin *et al.*, 2002).

1.6.1.2 Formation of the Fas DISC

Upon activation of the Fas receptor by FasL, the adaptor molecule Fas associated death domain protein (FADD) is recruited to the receptor (Chinnaiyan *et al.*, 1995). FADD is a 208 amino acid residue protein comprising an N-terminal death effector domain

(DED) and a C-terminal death domain. FADD binds to the cytoplasmic Fas-DD through its own DD and subsequently recruits caspase-8 (Muzio *et al.*, 1996; Medema *et al.*, 1997) and/or caspase-10 (Wang *et al.*, 2001) via its DED. Embryonic fibroblast cells from FADD null mice are deficient in Fas-induced apoptosis (Yeh *et al.*, 1998) and both transformed and non-transformed cell lines overexpressing a construct consisting of the isolated FADD death domain are resistant to FasL (Chinnaiyan *et al.*, 1996; Newton *et al.*, 1998). Also a caspase-8 deficient T cell line has been shown to be unable to undergo FasL-induced apoptosis (Juo *et al.*, 1998). These data strongly indicate the requirement for both FADD and caspase-8 in the Fas dependent apoptotic pathway.

Figure 1.10 highlights how, through homotypic protein/protein interactions, FADD acts as a link between the receptor and the procaspase enzymes that execute the later stages of apoptosis. Although other proteins may be involved, it is this set of three molecules – Fas, FADD and caspase-8 – that has become characteristic of the formation of the Fas DISC, which, much like the APAF-1/caspase-9/cytochrome *c* apoptosome, acts as a scaffold for initiating caspase activation (Peter and Krammer, 2003).

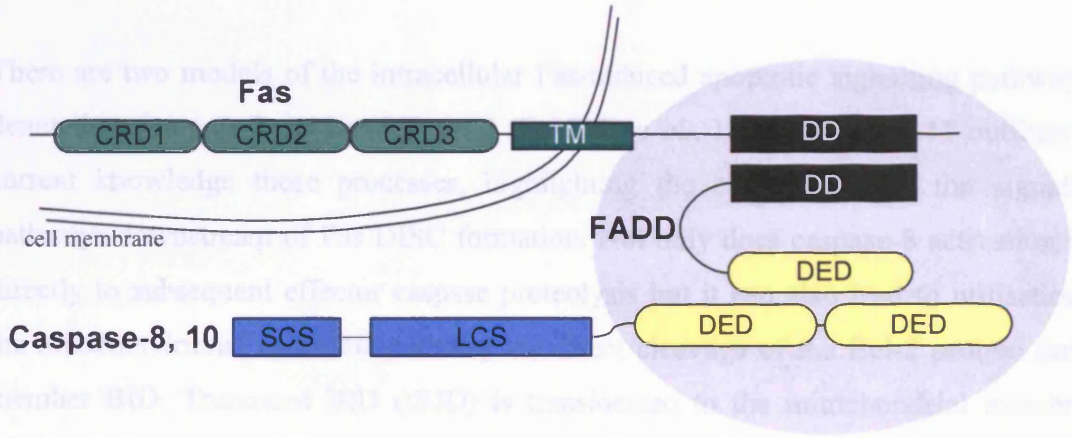

Figure 1.10: Schematic diagram of the proteins involved in apoptotic Fas DISC formation and their respective domain architectures. The Fas ligand binding domain is in CRD's 2 and 3 whilst the proposed PLAD lies in CRD1 (TM – transmembrane domain). The homotypic DD/DD and DED/DED protein-protein interactions between Fas, FADD and caspase-8 or 10 are highlighted in the grey circle.

The Fas apoptosis pathway is probably the best studied of all the death receptors but there is still much that is unknown, especially at the molecular level, about the interactions that govern the precise mechanism of the signalling processes. For example, it is known that if caspase-8 is artificially dimerised by fusion to a protein domain

responsive to non-covalent cross-linking reagents then apoptosis can be triggered efficiently (MacCorkle *et al.*, 1998). In contrast to the original view that caspases are activated by autoproteolysis induced by dimerisation there is now evidence to suggest that dimerisation by itself is sufficient for activation without the proteolysis step. In this model the processing step occurs after activation possibly to release the active caspase molecule from the membrane-bound DISC to carry out its cytoplasmic functions (Boatright *et al.*, 2003). How this simple requirement for caspase-8 dimerisation fits with the trimerised-receptor model in terms of the stoichiometry is unclear. Several models have been suggested relating to how the death signals are transmitted from the ligand to activate the caspases (Berglund *et al.*, 2000; Weber and Vincenz, 2001a). However, more work is needed to understand how these proteins join together spatially and temporally to activate the initial PCD signal. It is the aim of this thesis, therefore, to study the interaction between Fas and FADD, and specifically the contacts made between the death domains of these two proteins, in order to further the molecular understanding of the transduction of the apoptotic signal that proceeds through Fas, via FADD to activate caspase-8 and 10.

There are two models of the intracellular Fas-induced apoptotic signalling pathways – denoted as some as Type I and Type II (Scaffidi *et al.*, 1998). Figure 1.11 outlines the current knowledge these processes, highlighting the components of the signalling pathways downstream of Fas DISC formation. Not only does caspase-8 activation lead directly to subsequent effector caspase proteolysis but it can also lead to utilisation of the mitochondrional apoptotic pathway via direct cleavage of the Bcl-2 protein family member BID. Truncated BID (tBID) is translocated to the mitochondrial membrane where it promotes cytochrome *c* release and subsequent apoptosome formation. FasL-induced activation of the mitochondrial apoptotic pathway was first believed to be a positive feedback loop which accelerated the apoptotic response via the caspase-9 mediated cleavage of caspase-3 (Martin *et al.*, 1995). However, others have proposed that there is a cell type-specific dependence upon the two different pathways. Some cell-lines rely on DISC formation and direct caspase-3 cleavage by active caspase-8 (Type I cells), where as other cell line rely more heavily on utilisation of the mitochondrional pathway to induce apoptosis when stimulated with FasL (Type II cells) (Barnhart *et al.*, 2003).

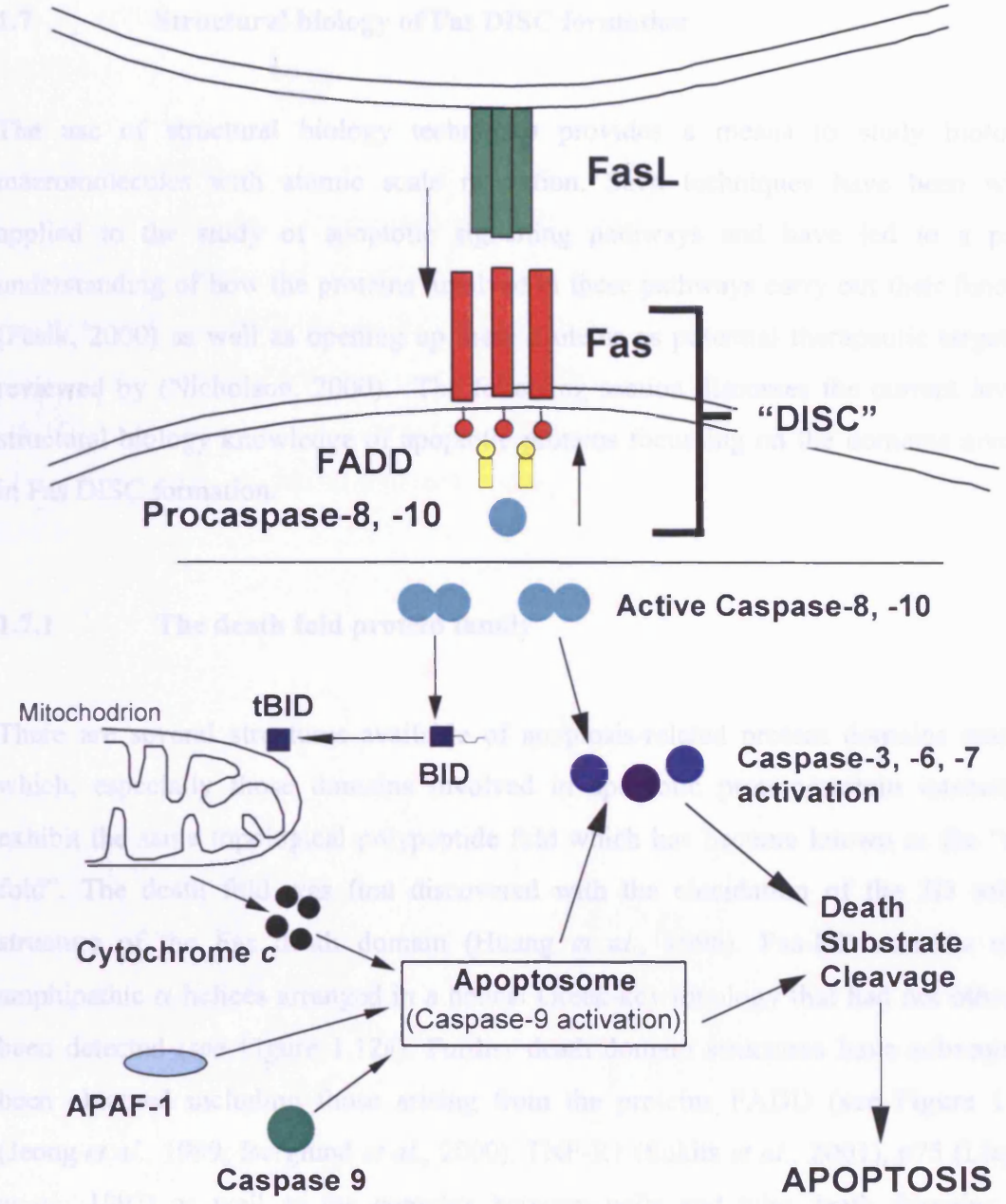

Figure 1.11: Canonical FasL-induced apoptotic signalling pathways. FasL binds to Fas leading to Fas DISC formation and subsequent caspase-8 and caspase-10 activation. Effector caspases are then activated either by direct caspase-8 or caspase-10-dependent cleavage or via the mitochondrional amplification loop following proteolytic truncation of BID. Effector caspases go on to cleave the "death substrates" leading to classical apoptotic cell death. It is postulated that, in Type I cells, direct caspase-3 cleavage is favoured over the mitochondrional amplification loop. Type II cells, however, produce low levels of activated caspase-8 and hence rely more heavily on caspase-9-mediated effector caspase cleavage.

1.7 Structural biology of Fas DISC formation

The use of structural biology techniques provides a means to study biological macromolecules with atomic scale resolution. Such techniques have been widely applied to the study of apoptotic signalling pathways and have led to a partial understanding of how the proteins involved in these pathways carry out their functions (Fesik, 2000) as well as opening up these proteins as potential therapeutic targets (as reviewed by (Nicholson, 2000). The following section discusses the current level of structural biology knowledge of apoptotic proteins focussing on the domains involved in Fas DISC formation.

1.7.1 The death fold protein family

There are several structures available of apoptosis-related protein domains many of which, especially those domains involved in apoptotic protein/protein interactions, exhibit the same topological polypeptide fold which has become known as the "death fold". The death fold was first discovered with the elucidation of the 3D solution structure of the Fas death domain (Huang *et al.*, 1996). Fas-DD consists of six amphipathic α-helices arranged in a helical Greek-key topology that had not otherwise been detected (see Figure 1.12a). Further death domain structures have subsequently been obtained including those arising from the proteins FADD (see Figure 1.12b) (Jeong *et al.*, 1999; Berglund *et al.*, 2000), TNF-R1 (Sukits *et al.*, 2001), p75 (Liepinsh *et al.*, 1997) as well as the complex between pelle and tube death domains from *Drosophila melongaster* (Xiao *et al.*, 1999). Despite a high level of amino acid sequence diversity, all of these death domains are structurally very similar exhibiting the same fold and several conserved hydrophobic residues that stabilise the core of the fold structures.

The death fold is also exhibited by members of three other protein families and 3D structures are available for representative examples of each; the death effector domains, for example FADD (Eberstadt *et al.*, 1998) and PEA-15 (Hill *et al.*, 2002)), caspase recruitment domains, CARDs, for example caspase-9 (Qin *et al.*, 1999) and APAF-1 (Vaughn *et al.*, 1999) and pyrin domains, for example NALP1 (Hiller *et al.*, 2003) and

ASC (Liepinsh *et al.*, 2003). The structures of several of these domains are shown in Figure 1.13.

Despite exhibiting a conserved secondary structure fold and pattern of buried hydrophobic residues, a high degree of variation is found in the solvent exposed residues – and hence the electrostatic charge distribution – at the protein surface of members of this death fold superfamily (as illustrated in Figure 1.13). In the absence of any evidence that the conformation of the death fold domains is altered at any point in the apoptotic pathway, this variation is highlighted in the low levels of homology amongst the primary amino-acid sequences of these domains (Weber and Vincenz, 2001b).

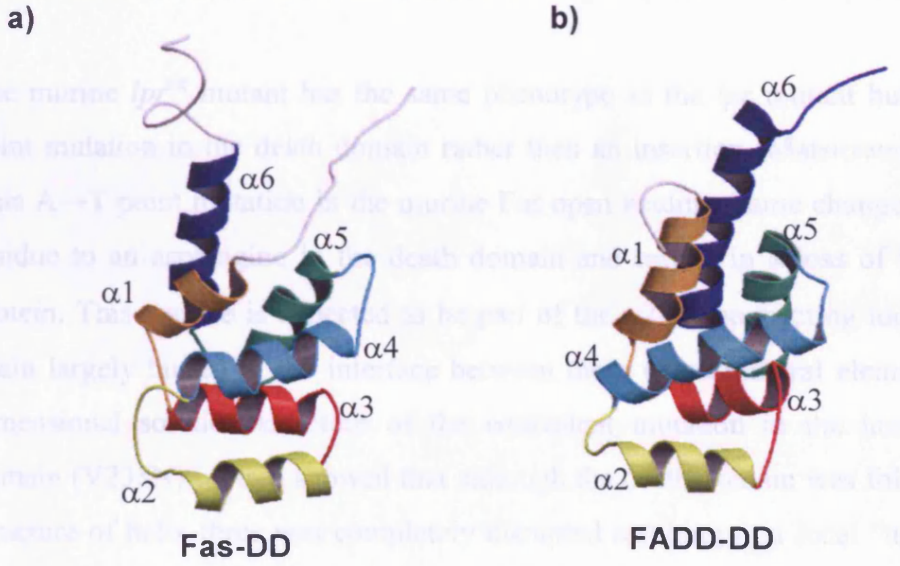

Figure 1.12: Three dimensional solution structures of a) Fas-DD and b) FADD-DD showing the conserved secondary structure elements typical of the death fold domain protein family. Each death domain exhibits the same "helical greek-key" motif consisting of 6 α-helices (α1-α6 in the above diagrams). Both domains are shown in the same orientation and each helix is given a separate colour to highlight the conservation of these structural elements. Figures generated with MolScript.

It is highly likely that the surface characteristics of these domains govern the nature of their interactions with other proteins. At present two 3D structures are known of complexes between death fold family members. The structure of the complex between the caspase 9 and APAF-1 CARD domains shows the interface to lie between the surface of helices 2 and 3 of caspase-9 and the surface of helices 1 and 4 of APAF-1 (Qin *et al.*, 1999) (see Figure 1.14a). The interface between these two domains is dominated by charged residues (basic residues on the caspase-9 CARD domain and acidic residues on the APAF-1 CARD domain) indicating the interaction is probably governed by electrostatic forces. Initial mutagenic evidence suggested that this type of interaction is reproduced in other death fold interactions such as the pairwise Fas-DD/FADD-DD and TNFR-1-DD/TRADD-DD death domain interactions, and in the self-association of the pyrin domain of ASC (Liepinsh *et al.*, 2003). The importance of helices 2 and 3 in the Fas death domain is highlighted by the three dimensional structure of a mutant form of the death domain known as lpr^{cg} (Eberstadt *et al.*, 1997).

The murine lpr^{cg} mutant has the same phenotype as the *lpr* mutant but arises from a point mutation in the death domain rather than an insertion (Matsuzawa *et al.*, 1990). This A→T point mutation in the murine Fas open reading frame changes an isoleucine residue to an asparagine in the death domain and results in a loss of function of the protein. This residue is expected to be part of the α2-α3 connecting loop with its side chain largely buried in the interface between these two structural elements. The three dimensional solution structure of the equivalent mutation in the human Fas death domain (V238N) protein showed that although the death domain was folded the regular structure of helix three was completely disrupted resulting in a local "unfolding" of in the region of the substitution (Eberstadt *et al.*, 1997).

One other complex structure is available in this superfamily and this is of the death domains of pelle and tube from *D. melongaster* (Xiao *et al.*, 1999). The pelle-DD/ tube-DD complex exhibits a different binding conformation from the APAF-1/caspase-9 CARD/CARD complex, instead involving the insertion of helix 4 of pelle-DD into a groove in the surface of tube-DD and the C-terminus of tube-DD into a groove in the surface of pelle-DD (see Figure 1.14)

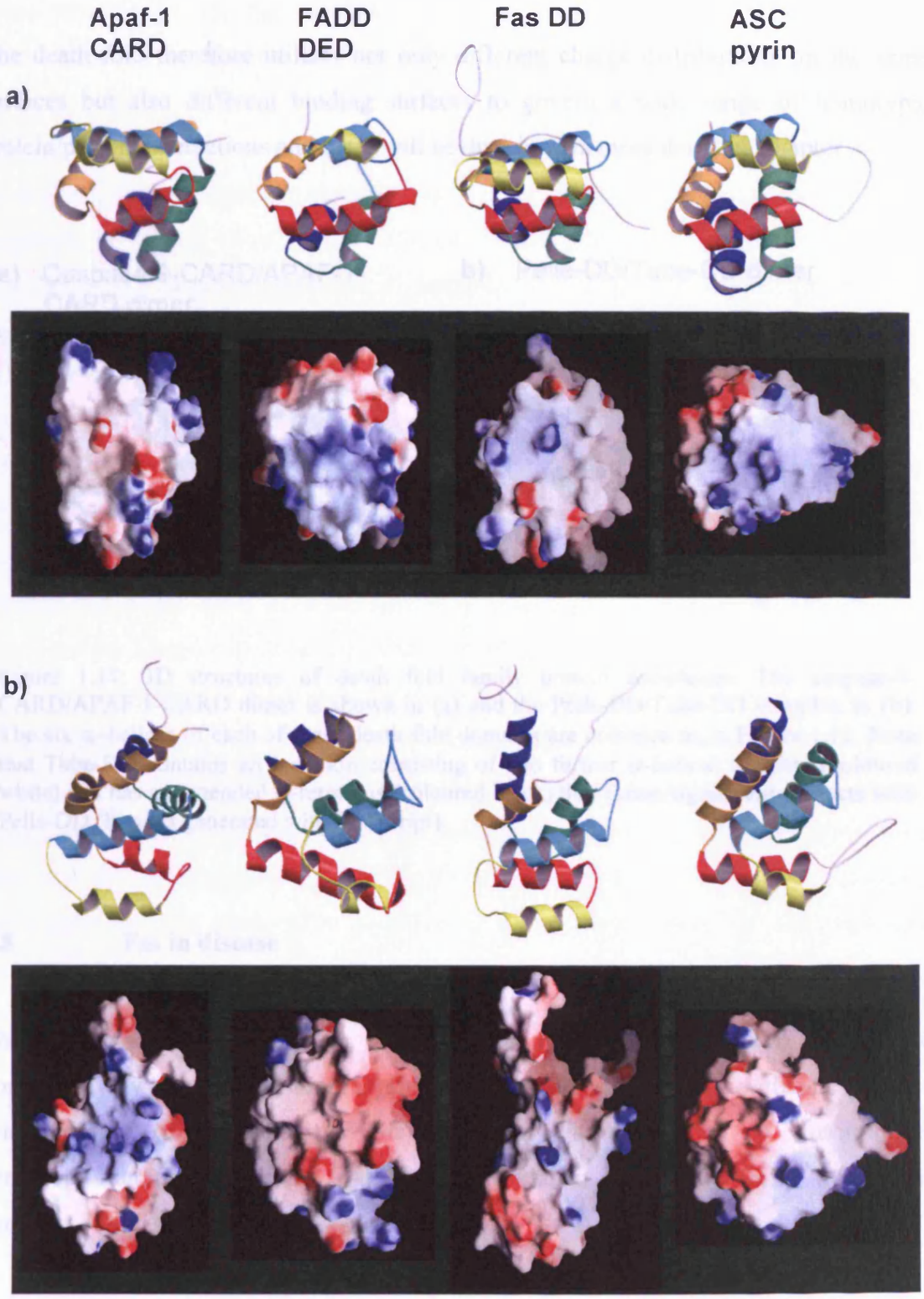

Figure 1.13: The death fold family of protein domains. Secondary structure (generated with MolScript) and solvent accessible surface (generated with GRASP (Nicholls *et al.*, 1991)) representations of the CARD domain of APAF-1, the death effector domain of FADD, the death domain of Fas and the pyrin domain of ASC-1 are shown in two separate orientations (a and b respectively). Helices 1-6 of each domain are plotted in separate colours as per Figure 1.12. Solvent accessible surfaces are coloured according to the electrostatic in a gradient from red (high density of negative potential) through white (no electrostatic potential) to blue (high density of positive potential). Each domain has the conserved death fold but exhibits dramatic differences in electrostatic surface charge distribution.

The death fold therefore utilises not only different charge distributions on the same surfaces but also different binding surfaces to govern a wide range of homotypic protein/protein interactions and these will be discussed in more detail in Chapter 4.

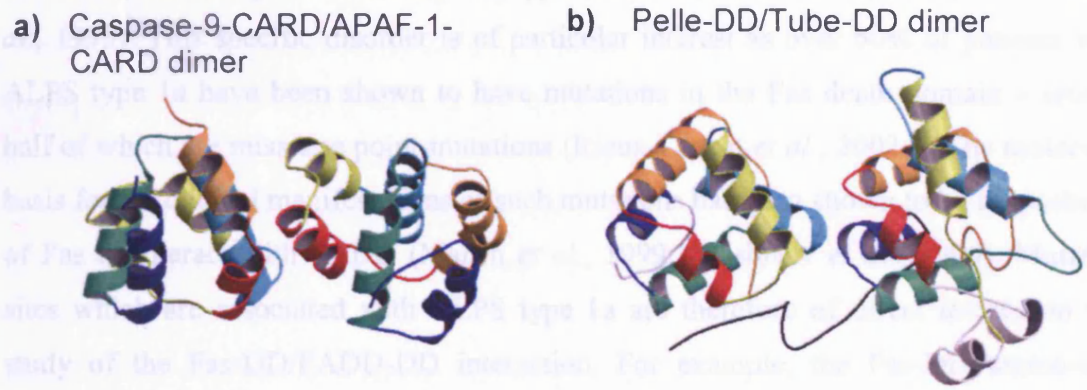

Figure 1.14: 3D structures of death fold family protein complexes. The caspase-9-CARD/APAF-1-CARD dimer is shown in (a) and the Pelle-DD/Tube-DD complex in (b). The six α–helices of each of these death fold domains are coloured as in Figure 1.12. Note that Tube-DD contains an insertion consisting of two further α-helical segmets (coloured white) and has an extended C-terminus (coloured black) that forms significant contacts with Pelle-DD (Figures generated with MolScript).

1.8 Fas in disease

The importance of apoptosis in the regulation of cell populations is highlighted consistently by its role in disease. Dysfunction of apoptosis plays a significant part in a wide variety of diseases and the effect of Fas mutations in autoimmune lymphoproliferation syndrome (ALPS - also known as Canale-Smith syndrome) provides a fine example.

Patients with mutations in Fas (the cause of ALPS type 0 and type 1a), FasL (ALPS type 1b) or caspase-10 (ALPS type 2) are found to have phenotypes that are very similar to the respective murine *gld* and *lpr* models, displaying at least three of the following disease manifestations: tumoral syndrome (splenomegaly or lymphadenopathy), autoimmunity, hypergammaglobulinemia, and detection of double negative ($CD4^-$, $CD8^-$) T cells in the blood (Rieux-Laucat *et al.*, 2003b). All of these symptoms stem

from the inability of the Fas/FasL system to induce T cell apoptosis for these individuals (Rieux-Laucat *et al.*, 2003a).

Of particular interest to this study is the molecular basis of ALPS type 1a. ALPS type 1a is defined by heterozygous mutations in the Fas receptor. Such mutations show a dominant interfering effect on the wild-type receptor (Martin *et al.*, 1999; Vaishnaw *et al.*, 1999). This specific disorder is of particular interest as over 60% of patients with ALPS type 1a have been shown to have mutations in the Fas death domain – around half of which are missense point-mutations (Rieux-Laucat *et al.*, 2003a). The molecular basis for the clinical manifestations of such mutations has been shown to be the inability of Fas to interact with FADD (Martin *et al.*, 1999; Vaishnaw *et al.*, 1999). Mutation sites which are associated with ALPS type 1a are therefore of direct interest to this study of the Fas-DD/FADD-DD interaction. For example, the Fas-DD amino-acid residue Asp 244is found to be mutated more often than any other single site in ALPS type 1a (see Chapter 4).Structural studies have suggested that the mutation does not influence the folding or stability of the Fas receptor, implying that the mutation must act at the level of interaction of Fas with downstream effectors, for example FADD (Huang *et al.*, 1996). Mutation D244 therefore provided a useful negative control for the interaction studies developed throughout this study. Also of interest to this study is the fact that the heterozygous ALPS type 1a mutations exhibit a dominant interfering phenotype as this observation must be a direct consequence of the molecular mechanisms of Fas-induced apoptosis. This dominant interfering phenotype is manifested by the absolute abrogation of FasL-induced T cell apoptosis in cell lines from patients with heterozygous ALPS type 1a mutations (Martin *et al.*, 1999). The simplest explanation for this observation is that oligomerisation of the Fas receptor (and therefore the death domain) following FasL binding is crucial for signal transduction to caspase-8.

1.9 Outline of this thesis

In general, despite much research activity in the field of death receptor signalling, we still do not fully understand how the death fold protein interactions are regulated, particularly with respect to DISC formation and the subsequent activation of caspases and other downstream signalling pathways. Therefore, more work is required to understand the exact molecular details of these protein/protein interactions before we can uncover the full details of death receptor activation and signalling regulation. It is the aim of this study to utilise a multidisciplinary approach to probe the interaction between the death domains of Fas and FADD in an attempt to further the understanding of this binding event in the context of Fas-dependent apoptosis.

This thesis is divided into a further four chapters as follows.

Chapter 2 outlines technical details of the materials and methods utilised throughout this study. Chapter 3 introduces the use of structural biology to probe the interaction between the Fas and FADD death domains. First, a productive interaction between the DDs was established using the yeast two-hybrid assay. Recombinant production of the individual DDs in bacteria was then used to provide these two proteins in a tractable form for nuclear magnetic resonance (NMR) spectroscopy experiments to probe the interaction between these two domains in solution. A significant proportion of this chapter focuses on the specific problem of producing the Fas death domain (Fas-DD) in sufficient quantities for structural studies at physiological pH.

In Chapter 4, both of the yeast two-hybrid and NMR-based interaction assays were used to carry out a mutagenesis study of the Fas death domain. Here, mutants of Fas-DD with substitutions of amino acid residues on solvent-exposed surface regions of the domain were analysed for their ability to interact with FADD-DD. This study allowed the identification of those regions of the Fas-DD surface that are important for this interaction. Having uncovered several significant novel Fas-DD mutants the remainder of this chapter focuses on the analysis of these mutations in the context of other death fold family protein/protein interactions.

Chapter 5 outlines the development of a functional, cell-based apoptosis assay for Fas mutants. Here the Fas receptor, and three Fas death domain mutants, are individually expressed in a human cell line that expresses no endogenous Fas. A controllable expression system is used to ensure that the cell lines express equal amounts of the receptor and the cell lines are then tested for their ability to undergo Fas-induced apoptosis.

This thesis concludes with a Discussion (Chapter 6) of the results obtained in the course of this work, and speculates on what these results mean for the mechanism of Fas signalling and DISC formation in the physiological situation, as well as looking forward to how else this intriguing system maybe probed by further investigation.

Chapter 2

Materials and Methods

2.1 Molecular biology protocols

Chapter two outlines the experimental protocols used to carry out the investigations in this study. Reagents were obtained from Sigma or VWR unless otherwise stated. Cell culture plastics were obtained from Orange scientific.

2.1.1 *Escherichia coli* growth

Liquid cultures of *E. Coli* were grown at 37^0C in a shaking incubator in autoclaved LB media (1% w/v tryptone, 0.5% w/v yeast extract and 0.5% w/v NaCl) (unless otherwise stated) containing the relevant antibiotics for plasmid selection. For antibiotic selection of transformed cells, *E. coli* were grown overnight at 37^0C on 10mm plates containing LB media supplemented with 1% agar. Antibiotic concentrations, where used, were as follows: 100 mg/ml carbenicillin (an analogue of ampicillin with increased stability) or 100 mg/ml kanamycin.

2.1.2 Plasmid DNA propagation

Supercoiled plasmid DNA was transformed into the DH5α strain of *E. coli* as outlined in Section 2.1.3. DH5α is a nuclease deficient (*recA*$^-$ *endA*$^-$) strain of *E. coli* suitable for DNA propagation. Single colonies from the resultant plates were grown overnight in 10ml (or 100ml) of liquid culture. Pure plasmid DNA was extracted from these cells using the Qiagen Miniprep (or Midiprep) kits. The final elution step in these purifications – and in all other Qiagen kit purifications – was carried out using sterile filtered dd$H_2$0.

2.1.3 Preparation of competent *E. coli*

For the transformation of supercoiled plasmid DNA *E. coli* cells were made chemically competent using the following protocol:

1) 10 ml of liquid culture containing the relevant strain of *E. coli* were grown overnight in LB medium containing no antibiotics.
2) Cells were harvested in a centrifuge by spinning for 10 minutes (mins) at 1250 g.
3) The resultant cell pellet was resuspended gently in 25 ml of an ice cold solution of 10 mM $CaCl_2$ and left on ice for 20mins.
4) Cells were harvested by spinning at 500 g for 10 mins and the supernatant discarded.
5) Steps 3 and 4 were repeated twice and the competent cells finally resuspended in a volume of 1.5 ml $CaCl_2$. These chemically competent cells were either used immediately for transformations or stored at -80^{0}C after the addition of sterile filtered glycerol to a final concentration of 15%.

2.1.4 Transformation of *E. coli*

Plasmid DNA (50-100 ng in ddH_2O) was added to 50μl of competent cells and incubated on ice for 30 mins. Cells were heat shocked at 42^{0}C for exactly 45 seconds before being returned to the ice for a further 2 mins. Following the heat shock, 300 μl of SOC media (2% w/v tryptone, 0.5% w/v yeast extract, 0.05% w/v NaCl, 2.5 mM KCl,

10 mM MgCl, 20 mM glucose, pH 7) pre-warmed to 37^0C was added to the cells. After incubation at 37^0C 1 hour, 150 µl of the transformed cells were spread onto an agar plate containing the antibiotic suitable for selection of the transformed plasmid.

2.1.5 Agarose gel electrophoresis

Agarose gels were prepared using the RunOne system (EmbiTech). Agarose was dissolved in TAE buffer (40 mM Tris-Acetate pH8.4, 1mM EDTA) to a final concentration of 1% or 2% w/v. Gels were cast and set in the apparatus provided. DNA samples were prepared by addition of DNA gel loading buffer (30% v/v glycerol, 0.1% w/v bromophenol blue in water). Electrophoresis was carried out in TAE buffer at a constant voltage of 100 V. On all gels molecular weight markers were included as a reference. In 1% gels 1 kilobase markers were used and in 2% gels 100 base markers were used (New England Biolabs)

Following electrophoresis, gels were stained in a 0.01% solution of ethidium bromide for 30 mins, destained in water for 10 mins and photographed under long-wave ultra-violet (UV) light.

2.1.6 Polymerase chain reaction (PCR)

PCR mixtures were prepared on ice to the following recipe in thin-walled 200 µl PCR tubes:

Plasmid DNA template	50-100 ng
dNTP* mix	2 mM
5' primer	1 mM
3' primer	1 mM
Pfu** DNA polymerase	3 units
10x Pfu buffer**	10 µl
ddH_20	To a final volume of 100 µl

*An equimolar mixture of dATP, dCTP, dTTP and dGTP (Promega)

**Promega

PCR was carried out using a Primus thermocycler (MWG-Biotech). The heating block of the thermocycler was pre-heated to 95^0C and the PCR samples added to the block

straight from ice (a technique known as "hot start" PCR) to improve the efficiency of the initial primer annealing event.

Samples were subjected to 30 rounds of thermal cycling (95^0C for 30 seconds, 55^0C for 30 seconds and 72^0C for 90 seconds) to amplify the required stretch of DNA.

Following the thermal cycling, PCR products were purified using the Qiagen PCR clean-up kit and analysed on 2% agarose gels.

2.1.7 Restriction enzyme digestion of DNA

For subcloning purposes, plasmid DNA and PCR products were digested with the relevant restriction enzymes. Restriction enzymes were purchased from New England Biolabs (NEB) and were supplied with individual buffers. Digests were carried out in these buffers as recommended by the manufacturer with 3 µl of enzyme (and 1 mM BSA where advised) in a total volume of 60 µl. Where necessary, digests with two enzymes were carried out by including 3 µl of the second enzyme in the same reaction mixture. In this case the reaction was carried out in a buffer compatible with both enzymes as advised by the manufacturer. All digests were performed at 37^0C for 2 hours.

Digested DNA was electrophoresed on agarose gels (1% agarose for digested plasmid DNA and 2% agarose for digested PCR products). Gels were stained with ethidium bromide and the required bands, as identified by size comparison with the molecular weight markers, were excised from the gel under UV light. DNA was purified from the excised pieces of agarose using the Qiagen gel extraction kit.

2.1.8 DNA ligation

Purified inserts were ligated into digested plasmid vectors using the following protocol:

The ligation mix consisted of 10-50 ng of digested plasmid, between 0.1-1 µg of digested PCR product , 0.5 µl of T4 DNA ligase (NEB) and buffer as supplied by the

manufacturer in a total volume of 20 µl. This mixture was incubated at 15^0C overnight. Subsequently, the ligation reaction was heat inactivated at 55^0C for 10 mins before being transformed into subcloning efficiency supercompetent *E. coli* DH5α cells (Invitrogen). The heat shock when transforming these particular cells was carried out at 37^0C for 30 seconds as recommended by the manufacturer. Transformed cells were plated onto antibiotic selective agar plates.

2.1.9 Selection of positive clones

Typically 10 colonies from each ligation were suspended in 20 µl of sterile ddH_20, 10 µl of which was grown up in 10 ml of media containing the relevant antibiotics, the remaining 10 µl was heated at 95^0C for 10 mins. 1 µl of the heated sample was used as the template in a PCR reaction with primers specific for the ligated insert. 10 µl of this PCR reaction was run on a 2% agarose gel to check for the presence of a PCR product of the correct size. Plasmid DNA was extracted from those cultures found to contain the insert and sent for DNA sequencing.

2.1.10 DNA concentration and purity estimation

Where only small volumes (<100 µl) of DNA were available, DNA concentrations were estimated by comparison to a DNA mass ladder (Invitrogen) on an agarose gel. When large volumes were available (>100 µl) concentrations were estimated by optical absorbance at 260 nm (A_{260}) using a Biomate-3 UV/visible spectrometer (Thermo). In this case the purity of the DNA was also estimated by measuring the A_{260}:A_{280} ratio. This purity measurement takes into consideration the absorbance at 280 nm from any contaminating proteins present in the sample.

2.1.11 Site directed mutagenesis

Point mutations were made in genes of interest by using the QuickChange site directed mutagenesis kit (Stratagene) following the manufacturer's protocol. All selected clones

were subjected to DNA sequencing to ensure only the required mutations had been introduced.

2.2 Yeast protocols

2.2.1 *Saccharomyces cerevisiae* growth

S. cerevisiae was grown, when no selection was required, in liquid culture either in YPD (1% w/v yeast extract, 2% w/v peptone, 2% glucose, pH 5.8) or on 10mM plates containing YPD with 1.5% w/v agar. In both cases yeast was grown at 30^0C in an incubator.

When auxotrophic selection of yeast cells was required, media was prepared with minimal SD base (Clontech) and DO -trp, -leu, -his supplements (Clontech). As required, this media was supplemented with 20 mg/L tryptophan, 60 mg/L leucine or 20 mg/L histidine to create single or double deficient media. For growth on 10 mM plates these media were supplemented with 1.5% w/v agar.

2.2.2 Cloning into pOAD and $pOBD_2$ vectors by homologous recombination

Recombination cloning techniques were used to insert the required genes into the pOAD and $pOBD_2$ plasmids. A two-step PCR protocol was used to generate DNA which had sufficient homology at its terminal ends to allow homologous recombination with linearised vector inside the yeast cell.

The first PCR reaction utilised primers designed to specifically amplify the coding region of interest. Additionally, both primers contained "tails" of 20 nucleotides that were homologous to sequences in the pOAD and $pOBD_2$ plasmids. The second PCR reaction used "re-PCR" primers that were specific for the tails from the first reaction and extended the homologous region by a further 50 bases.

Generalised yeast two-hybrid PCR primer sequences:

First round PCR:
Forward primer: 5' AA TTC CAG CTG ACC AAC ATG xxx xxx xxx xxx xxx xxx 3'
The xxx's represent the base sequence of the start of the coding region of interest
Reverse primer: 5' xxx xxx xxx xxx xxx xxx *** GTA CCG TTA AGG CGG CCT AG 3'
Where the xxx's represent the base sequence of end of the coding region of interest and *** represents a stop codon.

Re-PCR:
Forward primer: 5' C TAT CTA TTC GAT GAA GAT ACC CCA CCA AAC CCA AAA AAA GAG ATC GAA TTC CAG CTG ACC ACC ATG 3'
Reverse primer: 5' GTA CCG TTA AGG GCC CCT AGG CAG CTG GAC GTC TCT AGA TAC TTA GCA TCT ATG ACT TTT TGG GGC GTT C 3'

In order to ensure accurate recombination pOAD and $pOBD_2$ were linearised by digesting with the restriction enzymes *PvuII* and *NcoI*.

By transforming the re-PCR products into the yeast cells along with the linearised plasmids, homologous recombination would take place inside the yeast cells to result in the gene of interest being incorporated into the plasmids.

2.2.3 Transformation of yeast cells

Yeast cells were made competent and transformed with plasmid DNA using the following protocol:

1) 10 ml cultures of yeast cells were grown overnight in YPD medium. 1 ml of this culture was used to inoculate 100 ml of YPD medium the next day. This 100 ml culture was grown for 4 hours before the cells were harvested in a centrifuge by spinning at 3000*g* for 5 mins.
2) The harvested cells were washed once with sterile ddH_2O before being resuspended in 1 ml of 100 mM lithium acetate (LiAc) and incubated at 30^0C for 30 mins

3) Cells were pelleted in a microfuge and resuspended in 400 µl of 100 mM LiAc. 50 µl aliquots of these competent cells were used immediately for transformations.

4) The following components were added, in the order listed, to the competent yeast cells for transformation.

- 240 µl of 50% w/v PEG-3500
- 36 µl of 1M LiAc
- 25 µl of 2 mg/ml single stranded carrier DNA*
- 0.2 µg linearised plasmid DNA (in a volume of 50 µl in ddH_2O)
- 0.5 µg re-PCR product DNA

5) The transformation mixture was vortexed and incubated at 30^0C for 30 mins.
6) The cells were heat shocked for 20 mins at 42^0C before being pelleted in a microfuge at 6000 rpm and the supernatant discarded.
7) Pelleted cells were resuspended gently in 0.5 ml ddH_2O and 200 µl spread onto selective plates.

* ssDNA was prepared from double stranded salmon sperm DNA (Sigma) by heating at 95^0C for 10 mins.

2.2.4 Selection of positive yeast transformants

4 colonies from each successfully transformed plate were individually re-streaked onto fresh selective plates. Single colonies from these plates were picked and resuspended in 20 µl of spheroblasting solution (1.2M sorbitol, 100mM $NaPO_4$, 2.5 mg/ml zymolase, pH 7.4). These cells were heated in a water bath at 37^0C for 30 mins and 1 µl of the sample used as template in a PCR reaction using the re-PCR primers. 10 µl of this PCR reaction was run on an agarose gel to check for the presence of a PCR product of the correct size.

2.2.5 3-aminotriazole (3-AT) self-activation assay

Individually transformed colonies were grown on selective plates (his^-/leu^- or his^-/trp^-) containing different concentrations of 3-AT (0, 0.5, 1, 2, 4 and 8 mM) for seven days. If, after this time, any growth was seen on the plates with 2 mM 3-AT or above then use of that particular construct was discontinued.

2.2.6 Mating of two-hybrid yeast strains

Selected colonies of PJ694A (transformed with pOAD) and PJ694α (transformed with $pOBD_2$) were grown overnight in 1 ml of leu^- or trp^- media respectively. These cells were harvested and resuspended in 1 ml YPD. 25 µl of the PJ694A strain was mixed with 25 µl of the PJ694α strain and the resultant mixture was left overnight to mate and grow in 1 ml YPD.

Cells were plated the next day on leu^-/trp^- plates to select for mated yeast containing both pOAD and $pOBD_2$ plasmids. After 3 days these plates were replicated (using velvet cloth) onto $leu^-/trp^-/his^-$ plates with 4 mM 3-AT and incubated for 10-14 days.

2.3 Protein expression and purification

2.3.1 Small scale protein expression tests

Plasmid vectors were transformed into the *E. coli* BL21 Star (Invitrogen) protein expression strain. Single colonies were picked from the transformation plates into 10 ml LB with the relevant antibiotics. These cultures were grown until the optical density (as measured at 600 nm) (OD_{600}) was 0.8 when protein expression was induced by the addition of 0.75 mM isopropyl-β-D-thiogalactopyranoside (IPTG). Cultures were left to express protein for 3-6 hrs.

Both before and after the induction of protein expression a 1 ml sample was taken. The post-induction sample was sonicated for three 15 second bursts (with 10 second gaps) in

order to lyse the cells. Sonicated samples were spun in a microfuge for 10 mins at 13000 rpm, the supernatant retained and the pellet resuspended in 1 ml of water. 15 μl of the pre-induction and post-induction soluble and insoluble fractions were run on a polyacrylamide gel (see Section 2.3.7) to test for protein expression.

2.3.2 Large scale protein expression

Plasmid vectors were transformed into *E. coli* BL21 Star cells (Invitrogen). Four single colonies were picked from the transformation plates and grown overnight in 20 ml of LB with the relevant antibiotics. The next day these cultures were used to inoculate four separate 500 ml LB cultures in 2 L flasks. When the OD_{600} of the 500ml cultures reached 0.8 protein expression was induced with 0.75 mM IPTG. Induced cultures were left to express protein for 4-6 hours. Cells were then harvested in a Sorvall RN30 centrifuge by spinning for 15 mins at 5000 g.

2.3.2.1 Large scale expression of isotope labelled proteins

^{15}N-labelled proteins were expressed in the following manner: Plasmid vectors were transformed into the BL21 Star cells. Four single colonies were picked from the transformation plates and grown overnight in 20 ml of LB with the relevant antibiotics. The next day the cells were harvested by centrifugation and the cells resuspended into 100 ml of ^{15}N-labelled minimal media with antibiotics. This culture was grown until $A_{600}\approx0.6$ when the cells were harvested again. Finally these harvested cells were resuspended into 500 ml ^{15}N-labelled minimal media with antibiotics, grown to $A_{600}=0.8$ and protein expression induced by the addition of 0.75 mM IPTG. Following 4-6 hours protein expression, cells were harvested by centrifugation at 5000 g for 15 mins in a Sorvall RC-B5 centrifuge.

The composition of minimal media was as follows:

Per litre:

6 g Na_2HPO_4
3 g KH_2PO_4
0.5 g NaCl
1 g ^{15}N-labelled $(NH4)_2SO_4$ (Cambridge Isotopes Ltd.)

The pH of this solution was adjusted to 7.4 and autoclaved.
The following components were then filtered sterilised and added:

2 ml 1M MgCl
10 µl 1M $CaCl_2$
1 ml 0.01 M $FeSO_4$
2 g glucose
1 ml 1000x Vitamins solution*
1 ml 1000x micronutrient solution**

*1000X Vitamins solution

Per litre:

0.4 g Choline chloride
0.5 g Folic acid
0.5 g Pantothenic acid
0.5 g Nicotinamide
1.0 g Myo-inositol
0.5 g Pyridoxal HCl
0.5 g Thiamine HCl
0.05 g Riboflavin
1.0 g Biotin

** 1000x micronutrient solution

3 µM Ammonium Molybdate
400 µM H_3BO_3
30 µM $CoCl_2$
10 µM $CuSO_4$
80 µM $MnCl_2$
10 µM $ZnSO_4$

2.3.3 Protein purification

2.3.3.1 Purification of polyhistidine-tagged proteins

Cells harvested from 2 L of culture were resuspended in 25 ml of lysis buffer (100 mM Tris-HCl, pH 8, 300 mM NaCl) and lysed by passing three times through a French Press (American Instrument Company) at 1000 Psi. Lysed cells were then spun in a Sorvall RC-B5 centrifuge at 12000 g in an SS34 rotor for 1 hour to remove any insoluble particles and general cell debris.

Uncharged His-bind resin (Novagen) was prepared as follows: Resin was washed three times with 10ml ddH_2O then incubated with 10 ml of 100 mM $NiSO_4$ for 30 mins to

charge the matrix with nickel (II) ions. The charged resin was then washed three times with 10 ml ddH_2O before being equilibrated in 10 ml of lysis buffer for 30 mins and finally washed twice with 10 ml of lysis buffer. Between each washing step the resin was centrifuged for 3 mins at 1250 g and the supernatant discarded.

The lysed cell supernatant was incubated with equilibrated resin for 1 hour at 4^0C to allow the six histidine residue (His)-tagged protein to bind to the nickel ions. The resin was washed three times with 15 ml of wash buffer (lysis buffer with 10 mM imidazole) to remove contaminating proteins. Purified protein was eluted in three steps with 5 ml of elution buffer (lysis buffer plus imidazole) containing increasing concentrations of imidazole (200 mM, 400mM and 600mM).

At each stage of the purification process a 15 µl sample was removed for later analysis by SDS polyacrylamide gel electrophoresis (SDS-PAGE).

Both unlabelled and ^{15}N-labelled proteins were purified in exactly the same manner.

2.3.3.2 Purification of GST-tagged proteins

Glutathione-S-transferase (GST) tagged proteins were purified using glutathione-sepharose (GS) resin (Amersham). Cells were resuspended in phosphate buffered saline (PBS) and lysed as described in Section 2.3.4.

GS resin was prepared by washing three times with ddH_2O and equilibrated with PBS for 30 mins. The lysed cell supernatant was incubated with 5 ml of equilibrated resin for 1 hour at 4^0C or to allow the GST-tagged protein to bind to the glutathione. The resin was then washed three times with 15 ml of PBS. Purified protein was eluted in three washes of 5 ml of elution buffer (PBS plus 25 mM reduced glutathione).

As with His-tagged protein purifications, at each stage of the process a 15 µl sample was removed for later analysis by SDS-PAGE.

2.3.3.3 Preparative size exclusion chromatography

Size exclusion chromatography was carried out on a Biocad Sprint (Perceptive Biosystems) or an ÄKTA purifier (Amersham) chromatography system. Samples of no more than 2 ml were applied to 120 ml Superdex 75 or Superdex 200 (Amersham) columns and eluted with NMR buffer (50 mM phosphate, pH 6.2, 100 mM NaCl, 1 mM EDTA, 4 mM DTT) at a flow rate of 0.5 ml/min. 5 ml fractions were collected and analysed by SDS-PAGE. Fractions containing pure protein were pooled for future use and stored at 4^0C.

2.3.4 Polyacrylamide gel electrophoresis (PAGE)

Protein samples were electrophoresed on one of two types of SDS-PAGE gels. Gels were either prepared and run using the Biorad Protean system (as described below), or pre-cast Novex (Invitrogen) gels were electrophoresed using the XCell-SureLock system.

2.3.4.1 Protean gels

12% or 16% polyacrylamide separating gels were prepared to the following recipe:

- 3 ml (for 12% gels) or 4 ml (for 16% gels) 40% acrylamide solution
- 2.5 ml separating gel buffer (1.5 M Tris, pH 8.8, 4% w/v SDS)
- ddH_2O to a final volume of 10 ml
- 50 µl of 20% ammonium persulphate (APS)
- 25 µl N,N,N',N'-Tetramethylethylenediamine (TEMED)

Approximately 4 ml of this gel mixture was poured between two glass plates in the ProteanII apparatus. A small volume of ddH_2O was then layered on top of this liquid to avoid dehydration of the gel as it set.

A 6 % stacking gel was prepared to the following recipe:

- 0.5 ml of 40% acrylamide solution
- 1.25 ml stacking gel buffer (1.0 M Tris, pH 6.8, 4% w/v SDS)
- ddH_2O to a final volume of 5 ml
- 25 µl of 20% APS
- 25 µl TEMED

Once the separating gel had set excess water was poured away and the stacking gel mix poured on top to fill the glass plates. A 15-well comb was placed in the top of the staking gel to create the sample wells.

Protein samples were prepared by boiling for 5 mins in loading buffer (50 mM Tris, pH 6.8, 100 mM DTT, 2% w/v SDS, 0.1% bromophenol blue, 10% w/v glycerol) before being loaded onto the gel. Gels were run at a constant voltage of 180 V for 45 mins in the ProteanII gel tank in SDS-PAGE running buffer (25 mM Tris, pH 8.3, 250 mM glycine, 0.1% w/v SDS).

2.3.4.2 Novex Gels

12-16% Bis-Tris Novex gradient gels were electrophoresed as recommended by the manufacturer using the XCell-SureLock gel tank using the loading and running buffers provided. These gels were run at constant voltage of 200 V for 30 mins.

All SDS-PAGE gels were stained with coomassie blue stain (45% methanol, 10% acetic acid, 0.25% coomassie blue R-250) for 20 mins and destained with destaining solution (20% methanol, 7% acetic acid) until clear protein bands became visible.

2.3.5 Concentration of purified proteins

Pure proteins were concentrated using Vivaspin centrifugal concentrators with a 5000 kDa molecular weight cut-off. Concentrators were washed with 25 ml ddH_2O before sample addition and were spun at 3000 g.

2.3.6 Protein concentration determination

A Biomate-4 spectrometer was used to measure the UV light absorbance of concentrated proteins at 280 nm in a 1 ml quartz cuvette. Each protein concentration was measured twice using two different dilutions, both relative to the flowthrough from the Vivaspin concentrator used to concentrate that protein. Protein dilutions were chosen to give an A_{280} measurement between 0.01 and 0.5 to reflect the accurate dynamic range of such a measurement. Protein concentrations were calculated using the Beer-Lambert law, stating that A_{280} = e.c.l (where l is the path length, c the protein concentration, and e the extinction co-efficient). Theoretical extinction co-efficients for individual proteins were calculated from their primary sequences using the Expasy ProtParam tool (Gill and von Hippel, 1989).

2.4 Nuclear magnetic resonance (NMR) spectroscopy

[^{1}H-^{15}N]-HSQC experiments were carried out on UCL/Ludwig Institute Varian UNITYplus spectrometers (operating at nominal ^{1}H frequencies of 500 MHz and 600 MHz) equipped with a triple resonance (^{1}H, ^{13}C, ^{15}N) probe including z-axis pulse field gradients.

[^{1}H-^{15}N]-HSQC spectra of protein samples in NMR buffer (50 mM phosphate, pH 6.2, 100 mM NaCl, 1 mM EDTA, 4 mM DTT) were recorded at 25^{O}C using gradient coherence selection, sensitivity enhancement and a water flip-back pulse (Zhang *et al.*, 1994). All spectra were recorded with 1024 complex points in the direct dimension and 256 complex points in the indirect dimension. For experiments recorded at 500 MHz ^{1}H frequency sweep widths of 4000 Hz in the direct, ^{1}H dimension and 1650 Hz in the indirect, ^{15}N dimension were used. For experiments recorded at 600 MHz ^{1}H frequency sweep widths of 4200 Hz (^{1}H) and 2000 Hz (^{15}N) were used. The number of scans varied depending on the protein concentration. However, during titration experiments the number of scans was kept constant for each point in the titration.

NMR data was processed using the NMRPipe (Delaglio *et al.*, 1995) and AZARA (Boucher 2002) software packages and images of spectra were produced using the program PLOT2 from the AZARA package.

2.5 Cell culture

The three adherent human carcinoma cell lines, Huh7, A549 and Hep-3b, were grown and maintained in Dulbecco's modified Eagle's medium (DMEM) supplemented with 10% heat-inactivated foetal bovine serum (HI-FBS) and penicillin/streptomycin (100 units/ml penicillin and 0.1 mg/ml streptomycin) in 10 mm tissue-culture dishes. Cells were passaged (see Section 5.2.2) when confluent and replated at a density of $2.5x10^5$ cells/dish. FBS was heat-inactivated by incubation at 55^0C for 30 mins.

The murine B-cell line, A20, was cultured in suspension in 75 cm^2 flasks in RPMI 1640 medium supplemented with 10% HI-FBS, 2 mM L-Glutamine, penicillin/streptomycin solution and 0.05 mM β-mercaptoethanol. When cells reached a density of $2x10^6$ cells/ml they were harvested by centrifugation at 1100 rpm for 4 mins and resuspended in fresh medium at a concentration of $2x10^4$ cells/ml.

For experiments, cells were plated in 96 well plates at a density of 15000 cells/well (or 50000 cells/well in the case of A20 cells) in 100 µl of standard medium containing 0.1% HI-FBS.

All cells were grown in humidified incubators at 37^0C with 10% carbon dioxide for adherent cells lines and 5% carbon dioxide for the A20 cells.

2.5.1 Passage of cultured adherent cells

Cells were washed twice with 5 ml Hank's balanced salt solution (HBSS) and detached with 0.5 ml 0.5 mg/ml bovine trypsin solution (in HBSS supplemented with 0.2 mM EDTA). Trypsinisation was allowed to proceed for 2-3 mins at 37^0C before being stopped by the addition of 5 ml 10% HI-FBS in DMEM. A 20 µl aliquot of cells was

removed for counting and the remaining cells were harvested by centrifugation at 500g for 4 mins.

2.5.2 Cell counts

Cells were counted by addition of an equal volume of 0.4% w/v trypan blue dye to a 20 µl aliquot of cell suspension. Trypan blue is impermeable to the plasma membranes of living cells but penetrates and stains dead cells. A haemocytometer was used to count the number of viable (unstained) cells in the sample.

2.5.3 MTT assay

25 µl of 0.5 mg/ml methylthiazoletetrazolium (MTT) in PBS was added per well to cell cultures in 96-well plates. Plates were incubated at 37^0C for 2 hours before the addition of 100 µl lysis buffer (10% SDS in 50% Dimethylformamide (DMF)) to each well. After incubation overnight at 37^0C the absorbance of each well was measured at 540 nm in an Optimax plate reader (Molecular Devices) relative to a blank well containing no cells.

2.5.4 Fas-ligand treatment

In order to test the sensitivity of cell lines to apoptosis through the Fas receptor, cells were treated with various concentrations of recombinant, human, soluble Fas-ligand (rhsFasL – Alexis) plus enhancer (at ten times the concentration of the ligand – as recommended by the manufacturer). Cells were incubated overnight at 37^0C before being analysed.

2.5.5 Western Blotting

Western blots were carried out on whole cell lysates to test for the presence of Fas and other proteins.

2.5.5.1 Cell lysate preparation

Adherent cells were washed twice with PBS and scraped from the dish surface using a sterile cell-scraper. Cells were lysed by the addition of 250 µl of 1 % SDS, pre-heated to 95^0C, to the dish and the resultant lysate was collected into a 1.5 ml centrifuge tube.

A20 cells were harvested by centrifugation at 500g for 5 mins, washed with 5 ml PBS and lysed by addition of 250 µl of 1 % SDS pre-heated to 95^0C.

DNA in the lysates was sheared by passing twice through a 0.6 mm gauge sterile needle and they were subsequently centrifuged at 13000 g for 15 mins to remove insoluble debris. Clear supernatant was collected and stored at -20^0C.

2.5.5.2 Protein concentration determination of cell lysates

The bicinchoninic acid (BCA) assay (Pierce) was used to analyse the total protein content in cell lysates. 2 µl of cell lysate was added to two wells of a 96-well plate followed by addition of 100 µl BCA assay reagent (prepared as recommended by the manufacturer). The reaction was left to proceed in the dark for 15 mins before absorbance was measured at 562 nm in an Optimax spectrophotometer (Molecular Devices). The absorbance was compared to that of a set of bovine serum albumin (BSA) standards – 0, 2, 4, 8, 10 and 20 µg/ml – as assessed in duplicate on the same plate – to allow accurate determination of protein concentration in the lysates.

2.5.5.3 Blotting and detection procedures

The appropriate volume of cell lysates calculated to contain 50 µg of total protein was electrophoresed on 10 % SDS-PAGE gels (prepared using the Protean system as described in Section 2.3.4) at 200 V for 45 mins. Rainbow Markers (Amersham) were used for molecular weight comparison. Gels, along with sections of blotting paper (Biorad) and a section of Immobilon-P Polyvinylidene Difluoride (PVDF) membrane (Millipore) cut to the size of the gel, were equilibrated in western transfer buffer (50

mM Tris, 200 mM glycine, 0.03 % w/v SDS, 20% v/v methanol) for 15 mins. Following equilibration proteins were transferred from the gel to the PVDF membrane using a semi-dry transfer electrophoresis system (ESA) run for 1 hour at 20 V. Membranes were then washed once with 20 ml Tris-buffered saline supplemented with 0.1 % Tween20 (TBS-T) before being incubated in 20 ml blocking buffer (TBS-T, 10% w/v skimmed milk powder) for 1 hour at 20^0C to block the remaining protein binding sites on the membrane.

An indirect detection method was utilised for visualising specific proteins on the membrane. Indirect detection uses an unmodified primary antibody (1^o ab) to bind to the protein of interest followed by a modified secondary antibody (2^o ab) which binds to the 1^oab. This type of secondary antibody is readily commercially available for many different species and with several types of modification for different uses. In this study horseradish peroxidase (HRP)-conjugated 2^o antibodies were used for detection allowing sensitive detection since light being emitted from the enzyme can be detected using x-ray film (following addition of a specific substrate).

Membranes were then washed three times with 20 ml TBS-T before incubation with the primary antibody overnight at 4^0C. Primary antibodies were prepared diluted in 5 ml TBS, 5% w/v skimmed milk powder. Specific monoclonal antibodies used in this study are outlined in Table 2.1.

Target	Species	Clone	Company	Working Dilution
Fas (IC)	mouse	3D5	Alexis	1/500
Fas (EC)	mouse	610197	BD Biosciences	1/1000
FADD	mouse	610399	BD Biosciences	1/250
Caspase-8	rabbit	H-134	Santa Cruz	1/250
Fas Ligand	rabbit	N-20	Santa Cruz	1/1000

Table 2.1: Primary antibodies used in Western blotting and ICC experiments. All antibodies are specific for the human protein but show cross-reactivity with murine isoforms. Optimal working concentrations (given as dilutions from the supplied stock solutions) for Western blotting analysis are shown in this table. Note that for ICC experiments all antibodies were used at a 1/50 dilution (see Section 2.5.6)

Following primary antibody incubation membranes were washed three times with 20 ml TBS-T before being incubated with a horse-radish peroxidase (HRP) conjugated secondary antibody for 1 hour at 20^0C (diluted in 15 ml TBS, 5% w/v skimmed milk powder). For murine primary antibodies a polyclonal, HRP-conjugated, goat-anti-mouse secondary antibody (Amersham) was used at a 1/1000 dilution and for the lapine primary antibodies a polyclonal, HRP-conjugated, goat-anti-rabbit secondary antibody (DAKO) was used at a 1/2000 dilution (these concentrations are as recommended by the manufacturers).

Membranes were then washed three times with 20 ml TBS-T before being incubated with 2 ml Lumiglow peroxidase substrate (KPL) for 2 mins at 20^0C. Excess liquid was drained from the membranes which were analysed by autoradiography by exposure to Hyperfilm x-ray film (Amersham) in an autoradiography cassette (Amersham) and development in an Optimax x-ray film processor (IGP). Exposure times were varied depending on the strength of the signal.

During experiments to equalise the expression levels of Fas mutants, in order to ensure that the total amount of protein in each cell lysate was consistent, blots were probed with an anti-β tubulin antibody (Santa Cruz) following the detection of Fas. The β tubulin protein is expressed at a constant level in any particular cell line (and is unaffected by doxycyclin) and hence serves as a good loading control for western blotting experiments.

2.5.6 Immunocytochemistry

For immunocytochemistry (ICC) experiments cells were seeded onto eight-well chamber slides (Nalge Nunc) at a density of 15,000 cells per chamber in the relevant medium containing 0.1% FBS and left overnight to recover.

Cells were fixed in 500 μl of 4% paraformaldehyde for 10 mins at 20^0C, washed twice with 500 μl PBS and, where required, permeablised by incubation with 250 μl, 0.1% Triton (in PBS) for 10 mins 20^0C. The cells were then washed twice with 500 μl PBS and excess protein-binding sites were blocked with 4% normal goat serum and 1% BSA for 1 hour at 20^0C. Following blocking were then washed again twice with 500 μl PBS

and incubated overnight at 4^0C in a humidified chamber with 50 µl of primary antibody diluted in PBS. Following primary antibody incubation, cells were washed three times with PBS in a Coplin jar, incubated for 1 hour at 20^0C with 50 µl of biotin conjugated secondary antibody diluted in PBS and washed again three times with PBS. Finally the cells were incubated for 30 mins at 20^0C in the dark with fluorecsein (FITC)-streptavidin, washed with PBS and mounted under coverslips using Vectashield (Vector) with 4-6-Diamidino-2-phenylindole (DAPI) counterstain. DAPI fluoresces when specifically bound to double stranded DNA and this counterstaining procedure helps to visualise intact, healthy cell nuclei when labelling cell cultures.

For all ICC experiments the 1^0 ab was used at a dilution of 1/50 and the 2^0 ab used was a polyclonal biotin-conjugated goat-anti-mouse ab (DAKO), also used at a 1/50 dilution.

Fluorescent labelling was visualised and photographed using a Nikon Eclipse E600 fluorescence microscope using the Lucia G software package (Nikon). FITC was detected using with 465-495 nm excitation and 515-555 nm emission wavelengths. DAPI staining was detected using wavelengths 340-380 nm (excitation) and 435-485 nm (emission).

2.5.7 Transfection of adherent cells

The reagent selected for the transfection of the three cell lines was Fugene6 (Roche). Such lipid-based reagents rely on the formation of lipid-DNA complexes formed simply by incubation with plasmid DNA. The lipid-DNA complex can then be added to a cell culture for transfection to take place by fusion of the lipids with the cell-membrane and subsequent uptake of the DNA by endocytosis. However, the efficiency of different transfection methods can vary greatly according to cell-type, so Fugene6 was specifically chosen in this study because it is previously reported to have been successfully used to transfect the three cells lines; Huh7, Hep3b and A459 (transfection database at http://www.roche-applied-science.com/).

Mammalian cell transfection protocols rely on the use of pure DNA in multi-microgram quantities. Plasmids used in this study were produced by propagation in *E. coli* cells and

by extraction with the Qiagen Midiprep kit from 100 ml cultures of bacteria. DNA purity was estimated as described in Section 2.1.10 using an A_{260}:A_{280} absorbance ratio. It is generally accepted that an absorbance ratio above 1.7 indicates the DNA is pure enough to use for transfection. By eluting DNA from the Midiprep kits in sterile-filtered, distilled, deionised water, DNA was generally found to have an absorbance ratio of 1.7-1.9 and was hence pure enough for transfection. The concentration of plasmid samples from this purification method was also in the correct region (between 0.2-0.5 μg/μl) to carry out the chosen transfection protocol.

For the transfection of each cell line with the pTET-on plasmid all six wells of a six well tissue-culture plate were seeded with $2x10^5$ cells and left overnight to recover. For each of the three cell-lines the six wells (labelled A-F below) were treated as follows:

A) Cell control – no Fugene6, no DNA
B) Reagent control – 6 μl Fugene6, no DNA
C) DNA control – no Fugene6, 2 μg DNA
D) 3:1 ratio – 3 μl Fugene6, 1 μg DNA
E) 3:2 ratio – 3 μl Fugene6, 2 μg DNA
F) 6:1 ratio – 6 μl Fugene6, 1 μg DNA

This system allows the toxicity of both the reagent and the plasmid DNA to be tested as well as three reagent:DNA ratios. The reagent:DNA ratio is an important variable in lipid-based transfection protocols and one that can only be optimised empirically since it depends both on cell-type and the quality of the DNA used in the experiment.

At 48 hours post-transfection the cells from each well were split into two 100 mm dishes containing standard medium supplemented with 750 μg/ml G418. G418 is a soluble analogue of neomycin used here to select for cells that had been successfully transfected with the pTet-on plasmid. There were no adverse effects noted from the reagent and DNA control wells suggesting that Fugene6 is non-toxic to these three cell lines and that the plasmid DNA preparation was pure enough not to damage the cells. Antibiotic selection was allowed to proceed for fourteen days, with medium changes every three days.

The second stable transfection procedure (using pTRE2 plasmids) was carried out in the same manner as the pTet-on transfection with the following exceptions: Firstly, for each of the five pTRE2 plasmids only one Fugene6:DNA ratio was used (the 6:1 ratio) for transfection as this was found to be the most successful from the previous experiments. Secondly, antibiotic selection of the pTRE2 plasmid was carried out using 75 μg/ml hygromycin B as this plasmid contains a hygromycin resistance gene. Finally, the double stable transfected cell lines were cultured in standard medium supplemented with 200 μg/ml G418 and 50 μg/ml hygromycin B (double selective medium)

2.5.8 Luminescence Assay

Cells that were transiently transfected with the pTRE2-luciferase plasmid were analysed using the Luclite luminescence assay (Perkin Elmer) according to the manufacturer's protocol. Luminescence was measured in white 96-well plates (Corning) using a Victor2 multilabel plate reader (Perkin Elmer). The Luclite assay works by lysing the cells and providing a substrate for firefly luciferase – the light emitted from this assay can be measured in a luminometer and is proportional to the amount of luciferase expression in the cells.

2.5.9 DNA fragmentation assays

The fluorescent-detection TUNEL assay used in this study utilises a terminal deoxynucleotide transferase (TdT) enzyme to add FITC-labelled nucleotides to the 3' termini of fragmented DNA strands. These nucleotides can be directly observed under a fluorescent microscope. For this purpose cells from the four Fas-expressing cell lines were seeded on chamber slides, induced with doxycyclin, treated with 200 ng/ml rhsFasL and then subjected to the TUNEL assay using the Apoptag Fluorescein Direct *In Situ* Apoptosis Detection Kit (Chemicon) following the manufacturer's protocol. Control experiments for each cell line were carried out where cells were treated with 500 nM staurosporine (as a positive control for the assay) or left untreated (to test the background level of apoptosis). Also, as a negative control for the TUNEL assay, one chamber of the wild-type Fas expressing cell line was treated with rhsFasL but addition

of the TdT enzyme was omitted during the assay protocol. Cells were counterstained with Hoechst stain by incubation with a 2 mg/ml solution for 10 mins at room temperature in the dark, washed twice with PBS and mounted under glass coverslips using Vectorshield (Vector). Fluorescence microscopy of these slides was carried out as described in Section 2.5.6.

Chapter 3

Investigation of the interaction between the death domains of Fas and FADD

3.1 *In vitro* studies of Fas-DD and FADD-DD

THIS chapter will cover the initial approaches taken to study the interaction between the death domains of Fas and FADD *in vitro*. Particular attention is given to the resolution of the problem of expression and purification of Fas-DD. This is followed by an account of a series of NMR-based protein/protein interaction experiments.

The aim of this study is to further the understanding of the interaction between Fas-DD and FADD-DD *in vitro* in order to improve the understanding of how these proteins interact to carry out their physiological roles *in vivo*. Structural biology techniques, such as nuclear magnetic resonance (NMR) spectroscopy and X-ray crystallography, provide us with the most powerful tools for such *in vitro* studies of proteins as, in principle, they allow atomic scale resolution of these biological molecules.

However, the use of NMR techniques, in particular, for studying proteins in solution is often limited by the requirement for multi-milligram quantities of protein that is soluble in aqueous buffers at millimolar concentrations. Arguably, it is either technically impossible or economically unfeasible to produce the majority of proteins and polypeptides in such quantities. Even if a protein can be expressed in a recombinant fashion, at high enough levels, it is often the case that the resultant molecule is not sufficiently stable (with respect to aggregation and precipitation) at the concentrations required for structural studies.

As outlined in Chapter 1, the NMR solution structures of Fas-DD (Huang *et al.*, 1996) and FADD-DD (Jeong *et al.*, 1999; Berglund *et al.*, 2000) are already available and this may lead to the conclusion that the production of these two domains for NMR-based interaction studies should be straightforward. Unfortunately this is not the case as these two structures were determined with a large difference in one key variable – the pH of the buffer used for the NMR experiments. It was reported by Huang *et al.* that Fas-DD is prone to aggregation at physiological pH and that this problem could be overcome using a pH 4 buffer to carry out the NMR experiments. It may be presumed that the protonation of acidic side chains of Fas-DD helps to stop the intrinsic self-aggregation properties of this protein in solution. In contrast, the FADD-DD structure was solved in the Driscoll group laboratory at pH 6.2 (Berglund *et al.*, 2000) and in this case FADD-DD presented no reported problems with self-aggregation.

It is clear that in order to carry out a biologically relevant study of the interaction between these two domains the buffer conditions must be kept as close to physiological pH (and salt concentration) as possible. It was therefore necessary to discover a method to recombinantly express and purify both of these domains in such a way that they would both be soluble enough for NMR experiments at a pH as close to 7.4 as possible. In practical terms, this relied on the discovery of a method to produce Fas-DD in a recombinant manner such that it would not aggregate at the required concentrations.

However, before attempting the large scale expression and purification of Fas-DD and FADD-DD it was first necessary to find an interaction assay to confirm that the domains used for structural studies would productively interact. In this case, the yeast two-hybrid assay was chosen.

3.2 Use of the yeast two-hybrid assay system

The yeast-two hybrid assay was chosen as the primary method for studying the interaction between Fas-DD and FADD-DD for two main reasons. Firstly this experiment would replicate the original study documenting the existence of a direct interaction between these two domains (Chinnaiyan *et al.*, 1995). Secondly, this assay provides a convenient method of screening many potential alternative protein interactions in parallel.

The potential of the yeast two-hybrid assay to screen many interactions is important when considering the difficulties in production of recombinant proteins for NMR studies. There are several ways to overcome such problems, many of which involve altering the genetic construct used for recombinant expression of the protein of interest. For example, when working with domains that represent only a fragment of the intact protein, as is the situation with the death domains of Fas and FADD, it is often the case that only slight alterations in the amino-acid sequence selected to define the limits of that domain (i.e. the predicted domain "boundaries") can lead to dramatic changes in the expression levels or solubility of the resultant protein product. Another common strategy that is adopted to improve the solubility of a particular protein domain is to make point mutations in amino-acid residues known (or predicted) to be on the surface of that domain. Alteration of the distribution of electrostatic charges or the hydrophobic character of the protein surface with point mutations can greatly enhance the intrinsic solubility of the protein target (for example (Eberstadt *et al.*, 1998; Waldo *et al.*, 1999) etc.) Therefore, according to the strategy we were obliged to adopt, if it proved necessary to alter the Fas-DD or FADD-DD constructs in either of these ways then the yeast two-hybrid assay would provide a facile means to screen many of these alterations in parallel in order to check whether the altered domains are still able to interact.

3.2.1 Mechanism of the yeast two-hybrid assay

The yeast two-hybrid assay was developed as a powerful method for studying protein/protein interactions in a cellular environment (Fields and Song, 1989). The main application of this non-ubiquitous methodology has become the medium- to high-throughput screening of large numbers of potential interactions involving the use of whole libraries of candidate interacting genes or partial cDNAs, but it remains just as

applicable on a smaller scale. The mechanism underlying the yeast two-hybrid assay is outlined in Figure 3.1 where it is illustrated how this technique takes advantage of the modular nature of the yeast GAL-4 transcriptional activator. GAL-4 has two independently functioning domains that can be separated onto different polypeptide chains and only need to be brought into close proximity to restore full functionality (Keegan *et al.*, 1986). These two domains are named BD for the DNA binding domain (residues 1-147 of GAL-4) and AD for the transcriptional activation domain (residues 768-881 of GAL-4). The experimenter arranges that one protein of interest (the "bait") is genetically fused to BD whilst a potential binding partner (the "prey") is fused to AD. These two proteins, the bait-BD fusion and the prey-AD fusion, are then expressed in the same yeast cell. If the prey protein interacts with the bait protein then BD is brought close enough to AD to initiate the transcription of a reporter gene via recruitment of the endogenous RNA polymerase complex. In the illustrated example the reporter gene produces a histidine biosynthesis enzyme – the *HIS3* gene product – the expression of which allows the specifically chosen yeast strain to grow on medium lacking histidine. In the absence of the bait-prey interaction, expression of HIS3 is extremely low and the yeast will not grow in the absence of histidine.

There are now many commercial systems available for application of the yeast two-hybrid assay but the non-commercial system used here – kindly provided by colleagues in the laboratory of Professor Peter Piper at University College London – was very similar to that described by the laboratory that originally introduced the assay (Cagney *et al.*, 2000). This system uses two plasmid vectors to express the GAL-4 AD and GAL-4 BD fusion proteins; these vectors are known as pOAD and $pOBD_2$ respectively (see Appendix 4). The DNA constructs encoding the target bait and prey proteins are subcloned into these vectors (to create pOAD-prey and $pOBD_2$-bait plasmids) such that when transformed into *Saccharomyces cerevisiae* yeast these plasmids express the BD-bait and AD-prey fusion proteins under the control of the constitutive yeast alcohol dehydrogenase, ADH, promoter.

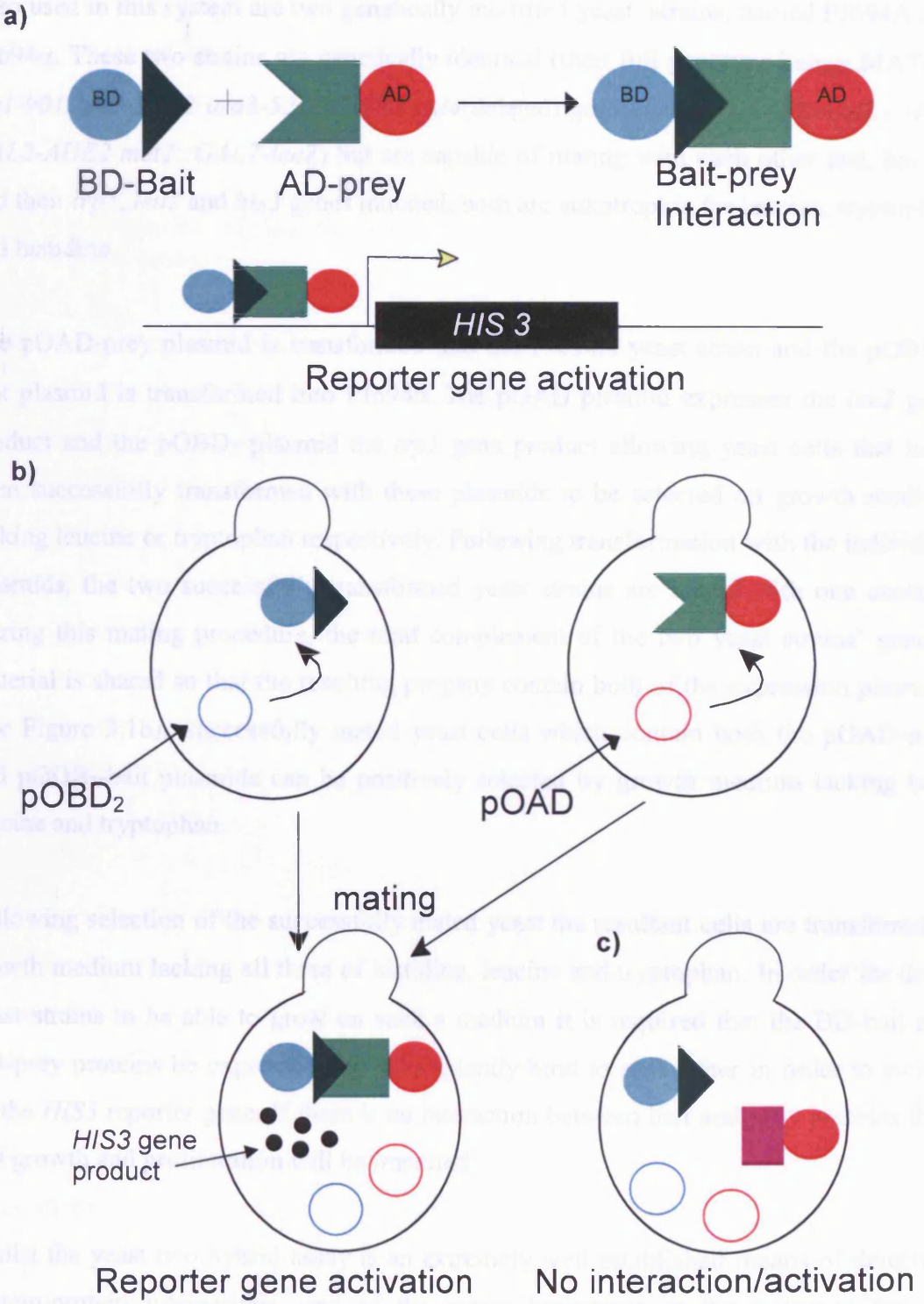

Figure 3.1: Mechanism of the yeast two-hybrid assay. a) This panel shows the GAL4-BD/bait fusion protein interacting with the GAL4-AD/prey fusion protein. The resultant complex is capable of activating transcription of the *HIS3* reporter gene. b) This mechanism is carried out in yeast cells by initial transformation of the pOAD and $pOBD_2$ plasmids into separate yeast strains. Mating of these two strains allows the two fusion proteins to be expressed in the same cell. Subsequently, mated cells are grown on medium lacking histidine to probe the bait-prey protein/protein interaction. If the two proteins interact the *HIS3* gene product is synthesised allowing the yeast to grow on his^- medium. In contrast, as shown in c), a lack of bait/prey interaction results in no HIS3 production and these yeast are unable to grow on medium lacking histidine

Also used in this system are two genetically modified yeast strains, named PJ694A and PJ694α. These two strains are genetically identical (their full genotype being: MATa/α *trp1-901 leu2-3,112 ura3-52 his3-200 gal4*(deleted) *gal80*(deleted) *LYS2::GAL1-HIS3 GAL2-ADE2 met2::GAL7-lacZ*) but are capable of mating with each other and, having had their *trp1*, *leu2* and *his3* genes mutated, both are auxotrophic for leucine, tryptophan and histidine.

The pOAD-prey plasmid is transformed into the PJ694A yeast strain and the $pOBD_2$-bait plasmid is transformed into PJ694α. The pOAD plasmid expresses the *leu2* gene product and the $pOBD_2$ plasmid the *trp1* gene product allowing yeast cells that have been successfully transformed with these plasmids to be selected on growth medium lacking leucine or tryptophan respectively. Following transformation with the individual plasmids, the two successfully transformed yeast strains are mated with one another. During this mating procedure, the total complement of the two yeast strains' genetic material is shared so that the resulting progeny contain both of the expression plasmids (see Figure 3.1b). Successfully mated yeast cells which contain both the pOAD-prey and $pODB_2$-bait plasmids can be positively selected by growth medium lacking both leucine and tryptophan.

Following selection of the successfully mated yeast the resultant cells are transferred to growth medium lacking all three of histidine, leucine and tryptophan. In order for these yeast strains to be able to grow on such a medium it is required that the BD-bait and AD-prey proteins be expressed and subsequently bind to each other in order to switch on the *HIS3* reporter gene. If there is no interaction between bait and prey proteins then cell growth and proliferation will be impaired.

Whilst the yeast two-hybrid assay is an extremely well established means of detecting protein-protein interactions, one of the major limitations is the potential for the reporting of false positive indications. This is suspected to occur when either of the fusion proteins on its own is able individually activate transcription of the reporter gene. In order to overcome this problem a self-activation assay was used to filter out any bait or prey constructs that may give false positive results. This self-activation assay (described in Section 2.2.5) involves the use of 3-aminotriazole (3-AT), a competitive inhibitor of the *HIS3* gene product. It is widely accepted for this system that if

transformation of a particular construct allows the yeast to grow on selective media (lacking histidine) in the presence of greater than 2 mM 3-AT then that construct is "self-activating" and must not be used for further experiments.

3.2.2 Investigation of the Fas-DD/FADD-DD interaction with the yeast two-hybrid assay

Plasmids encoding the death domains of Fas and FADD were available in the laboratory – a kind gift from Professor Neil McDonald of Birkbeck College School of Crystallography – and were used as templates for the first round of PCR (using PCR primers 1 and 2 or 3 and 4 respectively – see Appendix 3 for a list of all PCR primers used in this study) for sub-cloning into the yeast two-hybrid expression plasmids (see Section 2.2.2). Initially the amino-acid sequence boundaries of these two domains were chosen to mimic those found in the respective three dimensional structure papers, as these constructs would provide suitable starting points for subsequent large scale protein expression tests. Therefore human Fas-DD was defined as encompassing amino-acid residues 202-307 (Huang *et al.*, 1996), and human FADD-DD as residues 93-192 (Berglund *et al.*, 2000).

DNA encoding Fas-DD was sub-cloned into pOAD and transformed into yeast strain PJ694A with successful transformants being selected for by growth on agar plates with medium lacking leucine – leu^- plates (see Section 2.2.3). As a negative control the DNA encoding the Fas-DD point mutant D244A was sub-cloned and transformed into PJ694A in the same way – see Chapter 4 for a more detailed description of this point mutation. DNA encoding FADD-DD was sub-cloned into $pOBD_2$ and transformed into yeast strain PJ694α with successful transformants being selected for by growth on trp^- plates.

Selected clones were tested for self-activation by growth on 3-AT plates (see Section 2.2.5) and found to be non-self-activating (see Figure 3.2c). Wild-type and mutant Fas-DD clones were separately mated with the FADD-DD clone and in each case, following mating, the resultant positively selected (on trp^-/leu^- plates) yeast were transferred onto $leu^-/trp^-/his^-$ plates with 4 mM 3-AT.

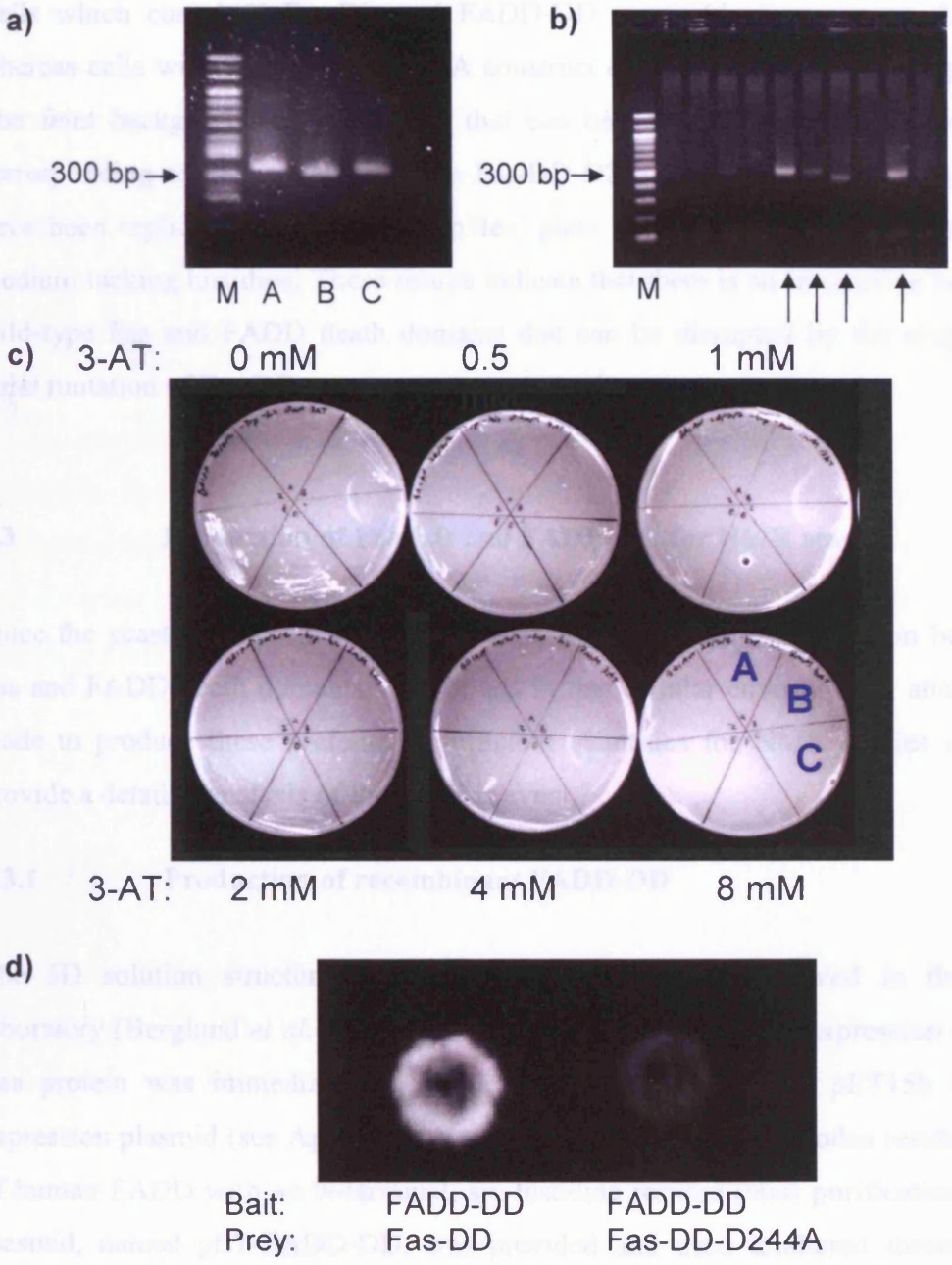

Figure 3.2 Interaction between Fas-DD and FADD-DD shown by the yeast 2-hybrid assay. a) re-PCR of DNA constructs encoding: A:FADD-DD, B:Fas-DD, C:Fas-DD-D244A (M: DNA size ladder). b) Colony screen of various Fas-DD and FADD-DD transformants showing bands of the correct size to confirm accurate transformation of these constructs into yeast cells (lanes from positive colonies are indicated by arrows). c) Self-activation assay of A:FADD-DD, B:Fas-DD and C:Fas-DD-D244A. Cells are plated in sections onto increasing concentrations of 3-AT. No growth is seen above 1 mM indicating no self-activation (the unlabelled segments correspond to an unrelated experiment). d) Mated cells are grown on $trp^-/leu^-/his^-$ plates with 4 mM 3-AT. Proliferation is seen when FADD-DD cells are mated with Fas-DD cells but not when FADD-DD cells are mated with Fas-DD-D244A cells.

Cells which contained Fas-DD and FADD-DD were able to grow on these plates whereas cells with the Fas-DD-D244A construct did not proliferate (see Figure 3.2d). The feint background of yeast cells that can be seen in Figure 3.2d in the region corresponding to cells containing the Fas-DD-D244A mutant results from cells that have been replica-plated from the trp^-/leu^- plate but are unable to proliferate on the medium lacking histidine. These results indicate that there is an interaction between the wild-type Fas and FADD death domains that can be disrupted by the single D244A point mutation of Fas-DD.

3.3 Production of Fas-DD and FADD-DD for NMR studies

Since the yeast two-hybrid assay confirmed that a productive interaction between the Fas and FADD death domains was formed in this cellular environment, attempts were made to produce these proteins in sufficient quantities for NMR studies in order to provide a detailed analysis of this binding event.

3.3.1 Production of recombinant FADD-DD

The 3D solution structure of FADD-DD was previously solved in the Driscoll laboratory (Berglund *et al.*, 2000) and hence a robust, high-level expression system for this protein was immediately available. This system uses the pET15b (Novagen) expression plasmid (see Appendix 4) containing an insert that encodes residues 93-192 of human FADD with an N-terminal, six histidine residue (His) purification tag. This plasmid, named pET-FADD-DD, was provided and used unaltered throughout this project. pET-FADD-DD was freshly transformed into *E. coli* BL21 Star cells (Invitrogen) on each occasion that a batch of FADD-DD protein was required.

The BL21 Star strain of *E. coli* is engineered by integration of genes from the modified "DE3" bacteriophage into the host chromosome. This modification allows these cells to express T7 RNA polymerase (T7pol) under control of the *lac* operon (outlined in Figure 3.3). Under normal conditions of bacterial cell growth, expression of the T7-pol gene is suppressed by binding of the *lac* repressor protein to the *lac* operator sequence in the promoter of the T7-pol gene. Addition of allolactose (or a stable analogue thereof) to the bacterial cell culture results in this sugar binding to the *lac* repressor. This binding

event causes the dissociation of the *lac* repressor from the *lac* operator and hence allows the T7-pol gene to be transcribed by the endogenous RNA polymerase. The majority of commercially available *E. coli* protein expression vectors (including those employed in this study) place the target gene downstream of a T7 promoter sequence. This promoter sequence is not present elsewhere in the *E. coli* genome so the induction of T7-pol expression leads solely to the expression of the target gene(s) within the expression plasmid. The vectors used in this study also contain the *lac* repressor gene and the *lac* operator sequence (as part of the T7 promoter) thus allowing double repression of target protein expression in the absence of allolactose. Isopropyl-β-D-thiogalactopyranoside (IPTG) is the most commonly used allolactose analogue for induction of protein expression in this system. Since IPTG cannot be broken down by *E. coli* the addition of this chemical to the bacterial cell culture allows a constant, high level of heterologous protein expression.

The BL21 Star strain is also specially engineered to be deficient in RNAse E and the protease OmpT which results in increased stability of both the transcribed RNA the translated protein in the *E. coli* cell.

A reproducibly high level of expression of FADD-DD from the pET-FADD-DD vector was possible using BL21 Star cells. The His-tag present on FADD-DD, when expressed in this manner, allowed the protein to be easily purified away from unwanted *E. coli* proteins by immobilised metal ion affinity chromatography (IMAC) on nickel (II)-charged resin. Nickel (II) binds strongly to the His-tag at pH 8 and retained protein can be easily eluted using an increasing concentration of imidazole which competes with histidine for the nickel-ion binding sites (see Section 2.3.4).

After IMAC purification, proteins were further purified using preparative scale size-exclusion chromatography (SEC) (see section 2.3.6). SEC primarily separates molecules by their hydrodynamic size so can be used to purify small proteins away from other contaminating biological macromolecules. SEC is normally carried out under non-denaturing conditions in aqueous buffers and so this method is ideal for the purification of proteins for structural biology. In this project, all proteins purified in this two-stage manner were found to be sufficiently pure for NMR spectroscopy and other solution-based experiments (>95% pure as analysed by SDS-PAGE).

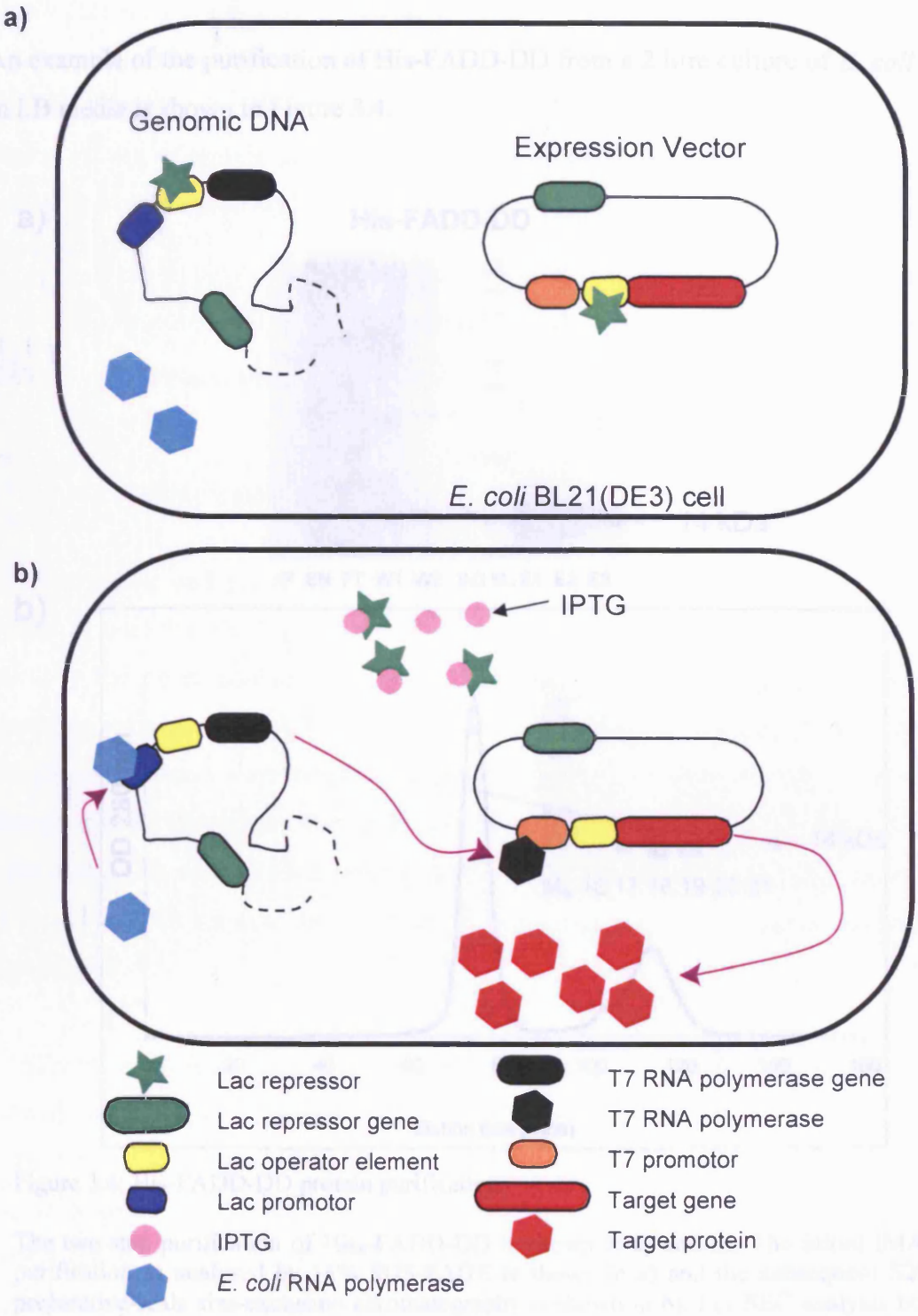

Figure 3.3 : Expression of recombinant protein in *E. coli* BL21 cells.

a) Before induction, the lac repressor is bound to the lac operator elements thereby suppressing expression of the T7 RNA polymerase gene and the target gene. b) IPTG added to the cell culture binds to the lac repressor, changing its conformation and effecting its dissociation from the lac operator sequences both in the chromosomal DNA and on the expression plasmid. This leads to the initiation of expression of theT7 RNA polymerase by endogenous *E. coli* polymerases. The T7 polymerase then binds to the T7 promoter in the expression vector leading to a high level of expression of the target protein.

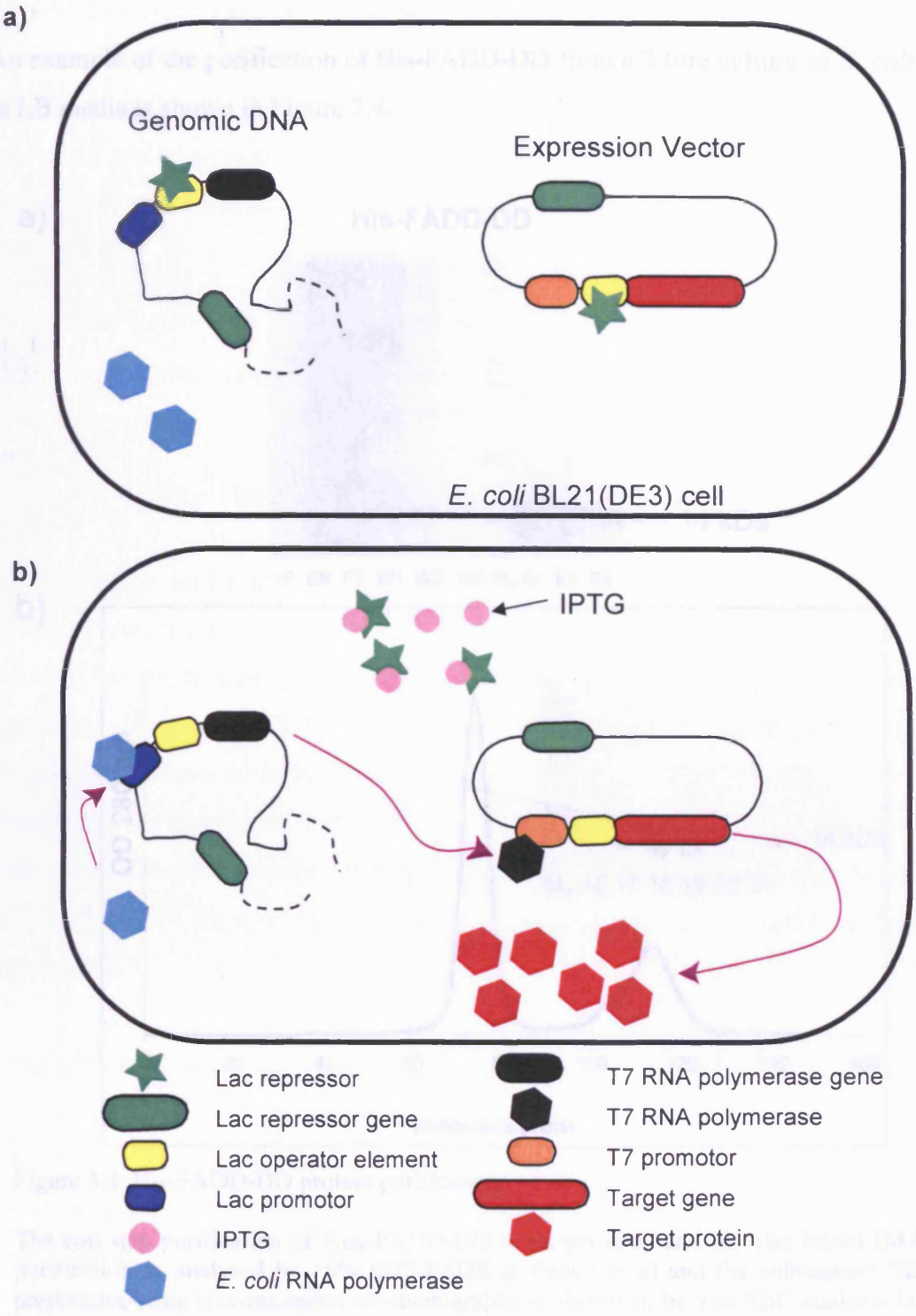

Figure 3.3 : Expression of recombinant protein in *E. coli* BL21 cells.

a) Before induction, the lac repressor is bound to the lac operator elements thereby suppressing expression of the T7 RNA polymerase gene and the target gene. b) IPTG added to the cell culture binds to the lac repressor, changing its conformation and effecting its dissociation from the lac operator sequences both in the chromosomal DNA and on the expression plasmid. This leads to the initiation of expression of theT7 RNA polymerase by endogenous *E. coli* polymerases. The T7 polymerase then binds to the T7 promoter in the expression vector leading to a high level of expression of the target protein.

An example of the purification of His-FADD-DD from a 2 litre culture of *E. coli* grown in LB media is shown in Figure 3.4.

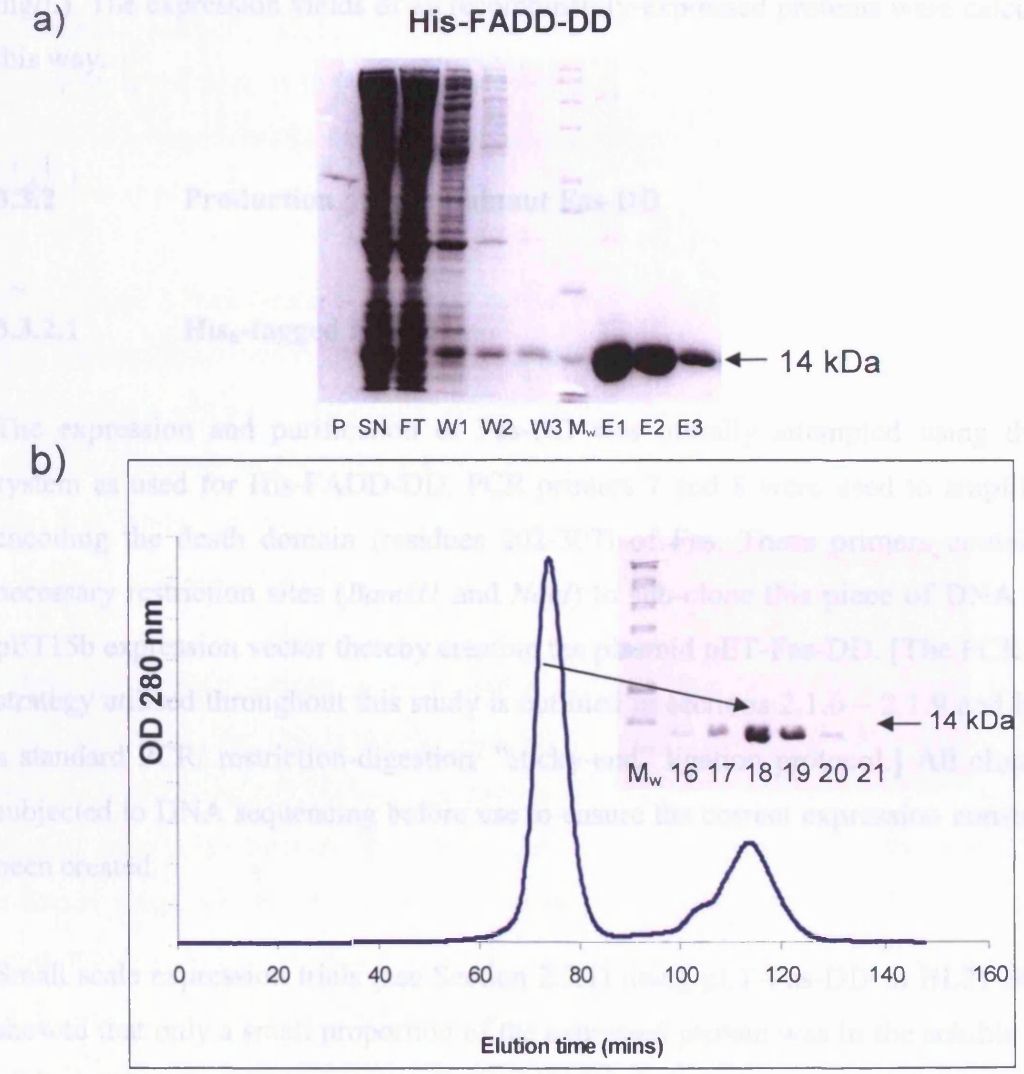

Figure 3.4: His-FADD-DD protein purification.

The two step purification of His_6-FADD-DD is shown in a) and b). The initial IMAC purification as analysed by 16% SDS-PAGE is shown in a) and the subsequent S200 preparative-scale size-exclusion chromatography is shown in b). For SEC analysis both the elution profile, as monitored by UV absorbance, and SDS-PAGE analysis of the chromatographic fractions are shown (the numbers correspond to eluted fractions).

Key: M_w – molecular weight markers. P – pellet, SN – supernatant, FT – flow through, W – wash, E – elution.

The figures illustrate that His-FADD-DD was produced in high yields and was readily purified by a combination of IMAC and SEC. Then, in order to produce a sample suitable for NMR experiments, the eluted fractions from SEC that contained pure

FADD-DD protein were concentrated to a volume of ~1 ml (see Section 2.3.8). The protein concentration of this sample was determined (see Section 2.3.9) and found to be 2.2 mM. Since His-FADD-DD has a molecular mass of 14.5 kDa, this corresponds to a total of 40 mg of protein and hence an expression yield of 20 mg per litre of cells (20 mg/L). The expression yields of all recombinantly-expressed proteins were calculated in this way.

3.3.2 Production of recombinant Fas-DD

3.3.2.1 His_6-tagged Fas-DD

The expression and purification of Fas-DD was initially attempted using the same system as used for His-FADD-DD. PCR primers 7 and 8 were used to amplify DNA encoding the death domain (residues 202-307) of Fas. These primers contained the necessary restriction sites (*BamH1* and *NdeI*) to sub-clone this piece of DNA into the pET15b expression vector thereby creating the plasmid pET-Fas-DD. [The PCR cloning strategy utilised throughout this study is outlined in sections 2.1.6 – 2.1.9 and involved a standard PCR/ restriction-digestion/ "sticky-end" ligation protocol.] All clones were subjected to DNA sequencing before use to ensure the correct expression construct had been created.

Small scale expression trials (see Section 2.3.1) using pET-Fas-DD in BL21 Star cells showed that only a small proportion of the expressed protein was in the soluble fraction of the cell lysate. Attempts to purify the soluble fraction of this protein in a buffer at pH 6.2 on a larger scale resulted in only a relatively small amount of pure protein – approximately 2 mg/L. Crucially, attempts to concentrate pure His-Fas-DD resulted in the formation of a viscous, gel-like fluid caused by self-aggregation of this protein. This observation is perhaps unsurprising as the solution structure of this domain was solved at pH 4 precisely to overcome these aggregation problems (Huang *et al.*, 1996). The combination of low expression level and self-aggregation meant that this expression strategy was not suitable for producing Fas-DD for NMR-based interaction studies with FADD-DD and hence alternative strategies were needed to improve the expression of this domain.

3.3.2.2 GST-tagged Fas-DD

One strategy that has been developed to increase the expression levels and solubility of previously insoluble target proteins is the use of fusion protein systems. Expression of a target protein fused, at the C-terminus, to a highly expressed, soluble protein has been shown to be a successful way of increasing its expression yield and solubility reviewed in (Davis *et al.*, 1999).

Glutathione-S-transferase (GST) one of the most commonly used fusion partners as it has the combined advantage of an intrinsically generally high expression level coupled with a facile affinity purification system (Smith and Johnson, 1988). GST has a very specific and high affinity for glutathione and hence the fusion protein can be easily purified using an affinity chromatography system employing a resin chemically modified with glutathione.

There are many a commercially available plasmid vectors for the expression of GST-fusion proteins. For this study the plasmid pGEX-2T (see Appendix 4) was chosen to express Fas-DD as a GST-fusion protein (GST-Fas-DD). As with all commercial GST-fusion expression vectors, the target gene of interest must be sub-cloned into this plasmid using a cloning site that lies immediately downstream of the DNA sequence that encodes the GST protein. DNA encoding Fas-DD was therefore sub-cloned into the pGEX-2T vector (Amersham) – PCR primers 9 and 10 were used to amplify the relevant sequence of DNA and these primers contained the *BamHI* and *EcoRI* restriction enzyme sites required for sticky-end ligation of the amplified fragment into the multiple cloning site of this vector. The resultant plasmid – pGEX-Fas-DD – was used to express the GST-Fas-DD fusion protein.

Recombinant protein expression from pGEX-Fas-DD in Bl21 Star cells resulted in only a small amount of soluble protein (approximately 2.5 mg/L). The purification of this protein (GST-Fas-DD1) is shown in Figure 3.5 a, c and d. As with His-Fas-DD, attempts to concentrate the pure GST-Fas-DD protein resulted in aggregation and also precipitation. It was therefore decided to try altering the Fas-DD domain itself in an attempt to improve its expression characteristics.

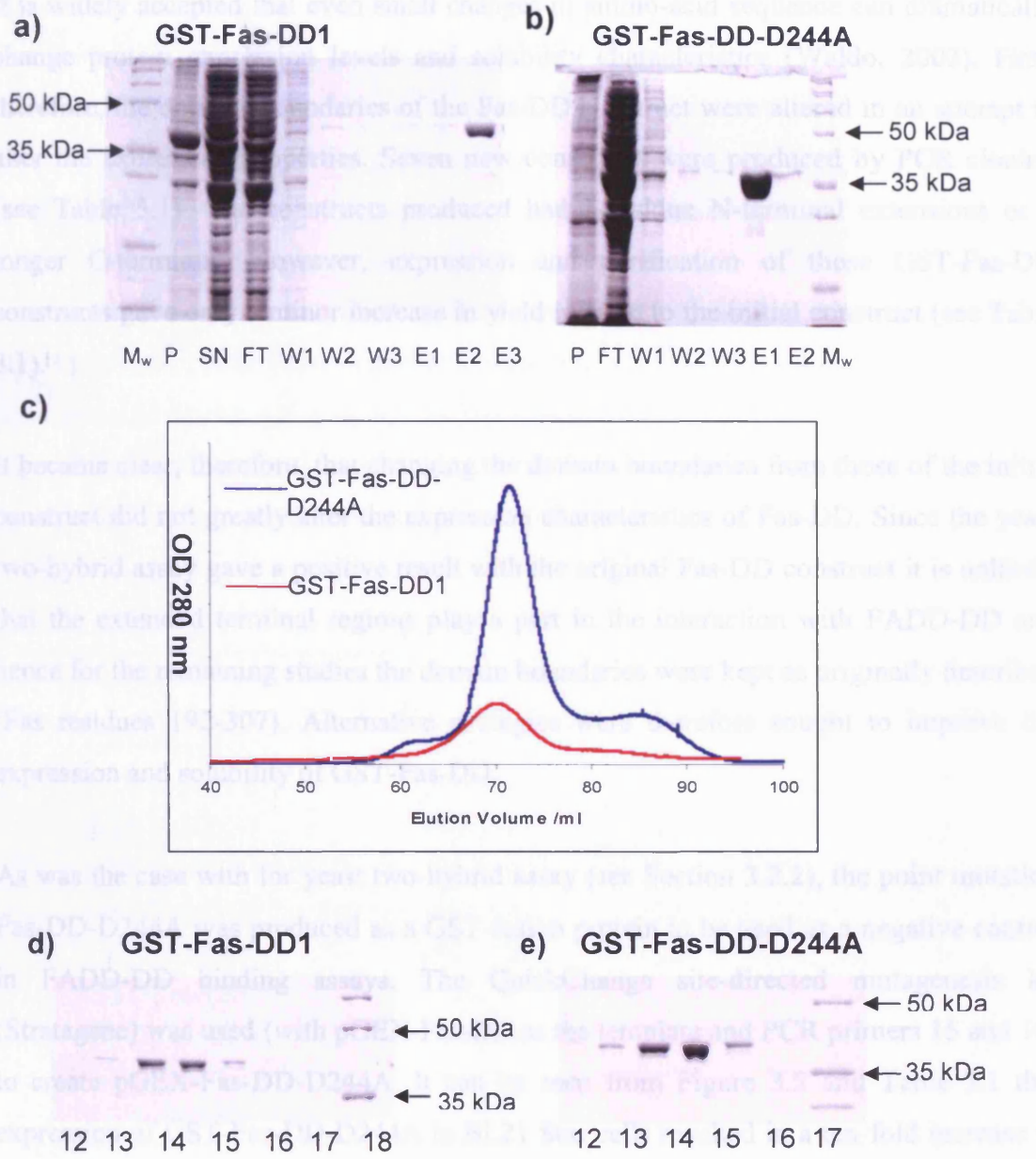

Figure 3.5: GST-Fas-DD purification

Analysis of the two-step purification of GST-Fas-DD1 (wild type) and GST-Fas-DD-D244A. a) and b) show SDS-PAGE analysis of the GST affinity purification step. c), d) and e) show the respective S200 size-exclusion chromatograms and subsequent fractional analysis by SDS-PAGE from these two protein purifications. There is a clear difference in protein yield between wild-type GST-Fas-DD and the D244A mutant.

Key: Mw – molecular weight markers. P – pellet, SN – supernatant, FT – flow through, W – wash, E – elution.

It is widely accepted that even small changes in amino-acid sequence can dramatically change protein expression levels and solubility characteristics (Waldo, 2003). First, therefore, the domain boundaries of the Fas-DD construct were altered in an attempt to alter the expression properties. Seven new constructs were produced by PCR cloning (see Table 3.1). The constructs produced had 3-residue N-terminal extensions or a longer C-terminus. However, expression and purification of these GST-Fas-DD constructs gave only a minor increase in yield relative to the initial construct (see Table 3.1).

It became clear, therefore, that changing the domain boundaries from those of the initial construct did not greatly alter the expression characteristics of Fas-DD. Since the yeast two-hybrid assay gave a positive result with the original Fas-DD construct it is unlikely that the extended terminal regions play a part in the interaction with FADD-DD and hence for the remaining studies the domain boundaries were kept as originally described (Fas residues 192-307). Alternative strategies were therefore sought to improve the expression and solubility of GST-Fas-DD.

As was the case with for yeast two-hybrid assay (see Section 3.2.2), the point mutation Fas-DD-D244A was produced as a GST-fusion protein to be used as a negative control in FADD-DD binding assays. The QuickChange site-directed mutagenesis kit (Stratagene) was used (with pGEX-Fas-DD as the template and PCR primers 15 and 16) to create pGEX-Fas-DD-D244A. It can be seen from Figure 3.5 and Table 3.1 that expression of GST-Fas-DD-D244A in BL21 Star cells resulted in a ten-fold increase in the yield of soluble, purified protein when compared to expression of the wild type protein. This type of remarkable result from a single point mutation has been noted before in the expression of death fold protein domains. For example the F25Y mutation has a very similar effect on the expression of the death effector domain of FADD (Eberstadt *et al.*, 1998), allowing the solution structure of this domain to be solved. It is likely that both of the D244A and F25Y mutations are disrupting the self-aggregation properties of these proteins by altering the charge distribution or enhancing the polarity on the surface of their respective domains. Adding weight to this argument is the difference in behaviour of wild-type Fas-DD – which seems to have an aggregated, gel-like composition when concentrated – and the GST-Fas-DD-D244A protein which remains free in solution at higher concentrations.

The success of the D244A mutation suggested that it may be possible to find a point mutation that substantially reduced the self-aggregation properties of Fas-DD but did not disrupt its FADD-DD binding activity – the D244A mutation only provided a solution to the first of these requirements as it completely abrogates FADD-DD binding in the yeast two-hybrid experiment. A reasonably extensive mutational analysis had been previously presented in the Fas-DD structure determination publication (Huang *et al.*, 1996). Here, both Fas-DD self-aggregation and a FADD-DD binding assays were described and applied to several Fas-DD mutants. One point mutation, K247A, was described as having significantly reduced Fas-DD self-aggregation properties relative to the wild type protein, whilst maintaining FADD-DD binding activity.

Construct Name	Fas-DD residue Boundaries	5' PCR primer	3' PCR primer	Expression yield mg/L
GST-Fas-DD1	192-307	9	10	2
GST-Fas-DD2	192-319	9	14	2
GST-Fas-DD3	196-307	11	10	3
GST-Fas-DD4	196-319	11	14	3
GST-Fas-DD5	199-307	12	10	3
GST-Fas-DD6	199-319	12	14	3
GST-Fas-DD7	202-307	13	10	3
GST-Fas-DD8	202-319	13	14	3
GST-Fas-DD-D244A	192-307	13	14	25
GST-Fas-DD-K247A	192-307	15	16	25

Table 3.1: GST-Fas-DD constructs, their corresponding PCR cloning primers and expression yields of pure protein per litre of bacterial culture grown in LB medium (as described in Section 3.3.1).

GST-Fas-DD-K247A was therefore produced by site-directed mutagenesis using the pGEX-Fas-DD plasmid as the template and the mutagenic PCR primers 17 and 18. The expression yield of GST-Fas-DD-K247A in BL21 Star cells was very similar to GST-Fas-DD-D244A (~25 mg/L, see Table 3.1) and, as such, both of these proteins could be expressed, purified and concentrated as necessary for NMR spectroscopy at pH 6.2.

Although the GST-Fas-DD-K247A construct was well expressed and highly soluble at the desired pH, this construct was not ideal for NMR studies of Fas-DD for several reasons. Firstly, its size makes it difficult to study by NMR. GST is an obligate homodimer (Lim *et al.*, 1994) and hence, in solution, GST-Fas-DD-K247A has a molecular mass of 76 kDa. Despite a series of recent technological improvements proteins larger than ~50 kDa are refractory to the application of many of the standard triple resonance NMR pulse schemes (Kay, 2001). Also, and probably more importantly, the fact that this protein has a point mutation means there was a chance that it would not interact with FADD-DD in the same manner as wild-type Fas-DD. These issues meant that whilst the K247A mutant was being fully analysed by methods including NMR, attempts to produce the wild-type Fas-DD domain in a soluble form were continued.

3.3.2.3 Gb1-tagged Fas-DD

The problems presented by the use of GST as the fusion partner for Fas-DD were eventually overcome by the utilisation of a different fusion protein construct. There are many fusion partners that are available for protein expression in *E. coli* (Davis *et al.*, 1999) but it has turned out that the most appropriate choice in the case of wild-type Fas-DD was the B1 domain of protein G (Gb1). Gb1 is an excellent fusion partner for the production of fusion proteins for NMR studies because, as well as potentially enhancing expression levels and solubility of the target protein, it is monomeric in solution and has a molecular mass of only 6 kDa (Zhou *et al.*, 2001). It is worthy of note that this fusion partner has been used successfully with another member of the death fold protein family – the solution structure of the NALP1 PYRIN domain was solved using NMR spectroscopy as an intact Gb1 fusion protein (Hiller *et al.*, 2003).

A modified form of the pET30a vector that expresses the Gb1 domain as an N-terminal tag was a provided by Professor Gerhard Wagner of the Harvard Medical School (see Appendix 4). DNA encoding Fas-DD was sub-cloned into the single *BamHI* site in this vector to create the plasmid pETGb1-Fas-DD. This plasmid was used as the template in two separate site-directed mutagenesis reactions to create two further plasmids encoding point mutant forms of Fas-DD, pETGb1-Fas-DD-D244A and pETGb1-Fas-DD-K247A.

These three plasmids were subsequently used to express wild-type and mutant Gb1-Fas-DD fusion proteins in BL21 Star cells.

As well as the addition of an N-terminal Gb1 tag, expression of protein from the pETGb1-Fas-DD vectors results in the addition of a C-terminal polyhistidine tag to allow the target proteins to be purified using Ni (II) IMAC. All three Gb1-Fas-DD proteins, importantly including the wild type Fas death domain fusion, were solubly expressed at high levels – the yield of all three of these proteins was approximately 40 mg/L – and successfully purified using IMAC and SEC. It was found that the pure wild-type Gb1-Fas-DD protein was soluble up to 0.7 mM and the two Fas-DD mutants were soluble to at least 1.5 mM in a pH 6.2 phosphate buffer. An example of the two-stage purification of wild type Gb1-Fas-DD is shown in Figure 3.6.

The rationalisation of the success of this Gb1-fusion expression strategy remains unclear. Presumably the Gb1 fusion partner suppresses the self-aggregation properties of Fas-DD allowing a high level of soluble protein expression. Quite why this is the case remains a mystery.

3.3.3 Protein expression summary

The reproducible expression of His-FADD-DD was well established giving a high level of soluble protein as expressed in *E. coli* BL21 Star cells. This protein is soluble up to at least 2.5 mM in the pH 6.2 phosphate buffer in which the solution NMR structure was solved (Berglund *et al.*, 2000).

Previously it had not been possible to express Fas-DD in a soluble form such that it was suitable for NMR spectroscopy at physiological pH. In the process of trying to solve this problem two separate solutions were discovered. First, it was established that expression of wild-type Fas-DD as a Gb1-Fas-DD fusion protein enhances its expression level and promotes its solubility in the optimal FADD-DD NMR buffer. Second, it was found that the self-aggregation properties of Fas-DD could be overcome by mutation of certain charged residues on the protein's surface.

Both the K247A and D244A mutations, when made as either GST or Gb1 fusion proteins, are well expressed and highly soluble. Interestingly, these mutations have similar effects on the expression and solubility characteristics of Fas-DD even though they remove oppositely charged residues from surface of the protein – the K247A substitution removes a positively charged amino group and the D244A substitution a negatively charged carboxylate group. It is therefore possible that both residues are implicated in the self-aggregation of this death domain.

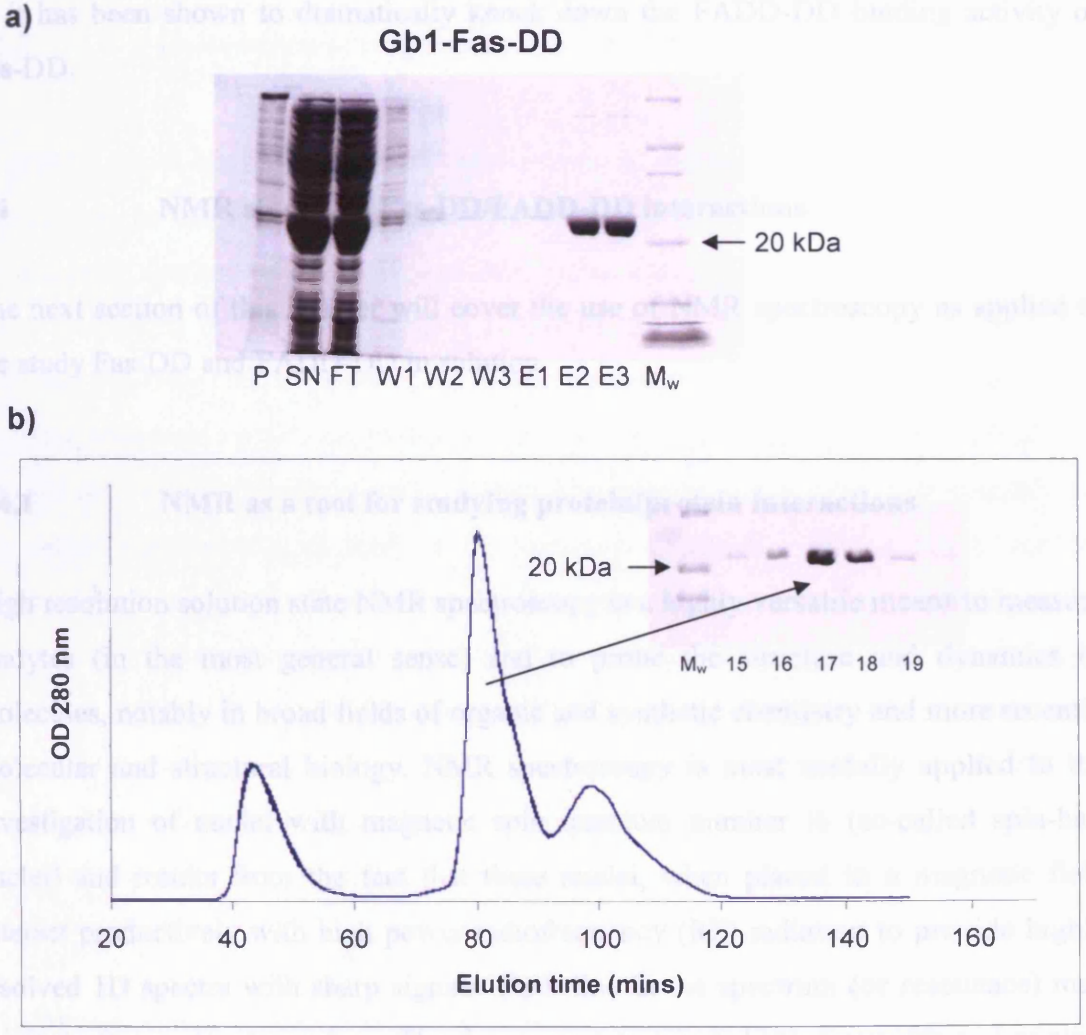

Figure 3.6: Gb1-Fas-DD purification

Both the IMAC purification (a) – utilising this protein's C-terminal polyhistidine tag – and the SEC purification (b) stages are shown as analysed by SDS page.

Key: Mw – molecular weight markers. P – pellet, SN – supernatant, FT – flow through, W – wash, E – elution.

The combination of these highly soluble protein constructs allowed the detailed study of the Fas-DD/FADD-DD interaction using NMR spectroscopy – the subject of the next section. Fas-DD has been engineered in such a way that for first time it can be expressed as a wild-type domain that is stable as a monomer at physiological pH. The GST-Fas-DD-K247A construct allows us to observe whether there is any impact of the effective dimerisation of Fas-DD on the interaction with FADD-DD. Finally, the Fas-DD-D244A mutant is an excellent negative control for FADD-DD binding experiments as it has been shown to dramatically knock down the FADD-DD binding activity of Fas-DD.

3.4 NMR studies of Fas-DD/FADD-DD interactions

The next section of this chapter will cover the use of NMR spectroscopy as applied to the study Fas-DD and FADD-DD in solution.

3.4.1 NMR as a tool for studying protein/protein interactions

High resolution solution state NMR spectroscopy is a highly versatile means to measure analytes (in the most general sense) and to probe the structure and dynamics of molecules, notably in broad fields of organic and synthetic chemistry and more recently molecular and structural biology. NMR spectroscopy is most usefully applied to the investigation of nuclei with magnetic spin quantum number ½ (so-called spin-half nuclei) and results from the fact that these nuclei, when placed in a magnetic field interact productively with high power radiofrequency (RF) radiation to provide highly resolved 1D spectra with sharp signals. Each line in the spectrum (or resonance) may originate from a single nucleus. The frequency (chemical shift), linewidth and nuclear relaxation rates of each resonance may reveal some aspect of the physical state of the target molecule. In proteins, the only spin-half nuclei of reasonable natural abundance is the ^{1}H proton (~100%); ^{13}C carbon is present at about 1.1% but this is presently not so useful. 1D ^{1}H spectra of proteins can have sharp lines (particularly for small proteins), but are more often than not highly overlapped, making analysis less than straightforward. Partly inspired by this difficulty, as well as by the extraordinarily rich

physics of interacting spin-half nuclei, NMR spectroscopists have invested a great deal of effort in the development of multi-dimensional NMR spectroscopy that provides information concerning the connectivities embedded within networks of spin-half nuclei, or 'spin systems'. This field of research is necessarily large and intrinsically complex and, as such a full theoretical description of this technique is beyond the scope of this thesis. However, the following provides a cursory description of the particular NMR method used routinely in this work, namely 2D [^{15}N-^{1}H]-HSQC spectroscopy.

3.4.2 Heteronuclear single quantum coherence (HSQC) spectroscopy

In general, multi-dimensional NMR spectroscopy of macromolecules provides spectral information in the form of chemical shift correlations, or cross-peaks, that connect resonances either because the corresponding nuclei are coupled 'through bonds' (i.e. via scalar couplings) or 'through space' (i.e. through dipole-dipole interactions). Here the discussion is only concerned with the former type of nuclear coupling. For unlabelled proteins, observable scalar couplings between protons are typically of the order of <18 Hz, and the correlated spectroscopy – COSY-type spectra that exploit these connections are rather insensitive and tend to be highly overlapped. Whilst much can be accomplished using two-dimensional homonuclear ^{1}H spectroscopy, particularly for very small proteins, the majority of multi-dimensional NMR experiments in common use today exploit ^{15}N and/or ^{13}C-isotope labelling because of the relatively large one-bond scalar couplings (typically > 40Hz). The larger scalar couplings that can then be exploited in heteronuclear experiments provide for relative high sensitivity, and the fact the spectra produced have non-identical frequency axes, which dramatically reduces spectral complexity.

One heteronuclear NMR experiment in particular has come to be particularly useful for the characterisation and monitoring of the chemical state of protein molecules: the ^{15}N, ^{1}H-COSY experiment, which is most often referred to as [^{15}N-^{1}H]-heteronuclear single quantum coherence (HSQC) spectroscopy. In the pulse sequence which delivers the HSQC spectrum (illustrated in highly schematic form in Figure 3.7), ^{1}H nuclear polarisation is first transferred from the NH proton onto the NH nitrogen-15 atom (providing for an increase in sensitivity for the low gyromagnetic ratio nucleus). At the end of this so-called INEPT transfer, the magnetisation components on the ^{15}N atom are

in antiphase with respect to the attached proton. A period of free precession (t_1) allows this "coherence" to be labelled with the resonance frequency (chemical shift) of the ^{15}N-atom and then combined 90 degree RF pulses applied to both N and NH atoms convert this magnetisation into antiphase magnetisation of the NH proton. Following a period for refocusing of this ^{1}H magnetisation into an in-phase transverse magnetisation, the signal is detected (as a function of time t_2) whilst the ^{15}N atoms are decoupled using a train of low power ^{15}N pulse. The signal recorded for each NH group is a collapsed doublet (singlet) with the ^{15}N-^{1}H coupling removed.

A full description of the theory and practice of pulse sequence design is rather beyond the scope of this thesis. However, it is important to note that the 2D Fourier transformation of the dataset provided by the HQSC pulse sequence provides a 2D spectrum that correlates each ^{15}N nucleus to its attached proton(s). Therefore the [^{15}N-^{1}H]-HSQC spectrum of a typical protein contains only slightly more signals than the number of amino acid residues – one signal for each backbone amide NH group, and several more corresponding to side chain $N^{\varepsilon}H$ (Arg, Trp) and NH_2 (Asn, Gln, Arg) groups. Experience shows that the dispersion of chemical shifts in this type of spectrum is characteristic for the folding status of the protein. Moreover the spectrum provides an extremely convenient way to monitor the effects of external perturbations to the protein, e.g. the addition of binding partners, or a change in the buffer or temperature conditions. Because the chemical shift of both the NH group ^{15}N and ^{1}H atoms is sensitive to the local chemical environment, changes to these parameters are interpreted to indicate that the NH is close to the site of interaction with the ligand, or point to a local change in the protein conformation in each of these circumstances. To that end the [^{15}N-^{1}H]-HSQC spectrum is referred to as providing a snapshot 'fingerprint' for the protein. This is now the NMR experiment of choice for monitoring the binding and conformational state of the target protein in a number of experimental situations. Here ^{15}N isotope labelling and [^{15}N-^{1}H]-HSQC spectroscopy has been used to monitor the interaction of the Fas and FADD death domains, as well as the folding of various mutant forms of the Fas-DD protein.

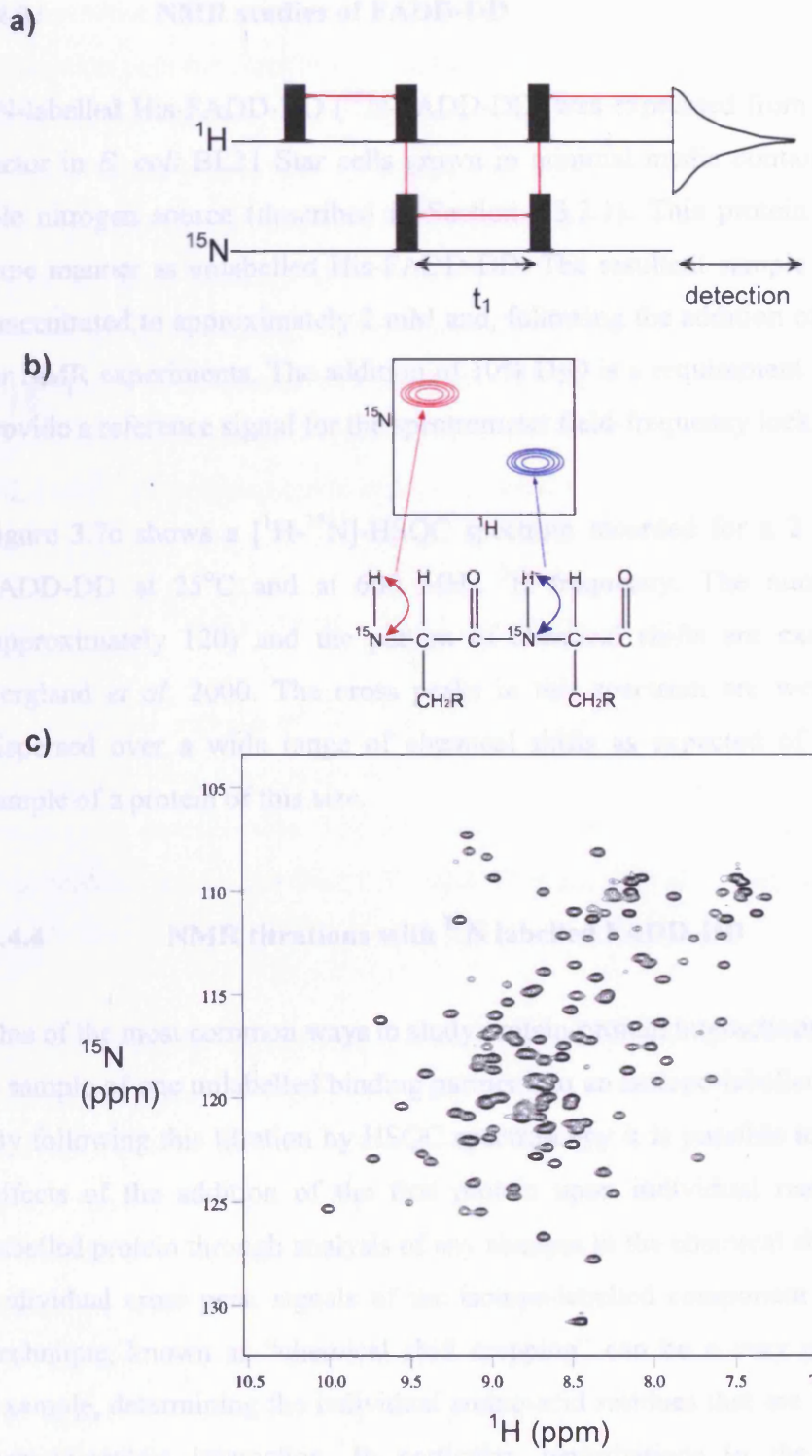

Figure 3.7: The [^{1}H-^{15}N]-HSQC experiment. a) Shows a highly simplistic representation of the coherence transfers utilised in this experiment where the red line corresponds to the "path" of coherence as it is transferred from ^{1}H nuclei to ^{15}N nuclei and back before being detected. t_1 is the time delay that is varied to produce a two dimensional data set. b) Shows the theoretical effect of this experiment on a fully ^{15}N-labelled polypeptide chain. A signal is produced from each amide group in the chain and where these groups lie in different chemical environments (as is the case for a fully folded protein domain) each generated signal will have a different chemical shift value. An example of a [^{1}H-^{15}N]-HSQC spectrum of a fully ^{15}N-labelled sample of His-FADD-DD is shown in (c).

3.4.3 NMR studies of FADD-DD

^{15}N-labelled His-FADD-DD (^{15}N-FADD-DD) was expressed from the pET-FADD-DD vector in *E. coli* BL21 Star cells grown in minimal media containing $^{15}NH_4Cl$ as the sole nitrogen source (described in Section 2.3.2.1). This protein was purified in the same manner as unlabelled His-FADD-DD. The resultant sample of pure protein was concentrated to approximately 2 mM and, following the addition of 10% v/v D_2O, used for NMR experiments. The addition of 10% D_2O is a requirement for NMR samples to provide a reference signal for the spectrometer field-frequency lock system.

Figure 3.7c shows a [^{1}H-^{15}N]-HSQC spectrum recorded for a 2 mM sample of ^{15}N-FADD-DD at 25°C and at 600 MHz ^{1}H frequency. The number of cross peaks (approximately 120) and the pattern of chemical shifts are exactly as reported by Bergland *et al.* 2000. The cross peaks in this spectrum are well resolved and well dispersed over a wide range of chemical shifts as expected of a pure, fully folded sample of a protein of this size.

3.4.4 NMR titrations with ^{15}N labelled FADD-DD

One of the most common ways to study protein-protein interactions by NMR is to titrate a sample of one unlabelled binding partner into an isotope-labelled sample of the other. By following this titration by HSQC spectroscopy it is possible to selectively track the effects of the addition of the first protein upon individual residues of the second, labelled protein through analysis of any changes in the chemical shifts and intensities of individual cross peak signals of the isotope-labelled component of the mixture. This technique, known as "chemical shift mapping" can be a very powerful tool for, for example, determining the individual amino-acid residues that are involved in a specific protein-protein interaction. In particular, perturbations in the chemical shifts are presumed to occur when the chemical environment of the nucleus in question is altered, reflecting a change in the immediate nature and arrangement of the atoms in the vicinity. Where these effects are of sufficient magnitude, they are often interpreted as defining the scope of the binding surface (van Nuland *et al.*, 1993; Zuiderweg, 2002).

One limitation of this approach is that, in order to extract the greatest amount of information possible from such experiments, knowledge is required of which cross peak in the HSQC spectrum corresponds to which individual amino-acid residue in the protein's primary structure. Generally, the assignment of these cross peaks to their corresponding residues can only be reliably accomplished by the recording and analysis of a set of three-dimensional heteronuclear NMR experiments. However, since the full three-dimensional structure of FADD-DD had been solved in the same laboratory a full set of resonance assignments of the FADD-DD spectrum were already available for this project. Hence, titrations of Gb1-Fas-DD or GST-Fas-DD-K247A into a sample of ^{15}N-FADD-DD were carried out in order to probe the Fas-DD/FADD-DD interaction.

3.4.4.1 ^{15}N-FADD-DD/ Gb1-Fas-DD titrations

An unlabelled sample of Gb1-Fas-DD was prepared and concentrated to 0.7 mM. Although the ideal concentration for an NMR protein sample is above 1 mM, in practice this is often unachievable. The Gb1-Fas-DD sample, for example, began to precipitate at concentrations higher than 0.75 mM. This unlabelled protein sample was used in a titration with a sample of ^{15}N-FADD-DD.

When carrying out any titration it is essential to avoid any dilution effects that can occur from the addition the two samples. This dilution effect can often be overcome, especially when titrating small molecules, by using a stock solution of one component of the titration at a much higher concentration than is required in the final mixture. When added to the larger volume of the first component, the small incremental volume associated with the addition of the highly concentrated sample can be considered insignificant. This approach, however, breaks down when the two samples to be titrated are limited by their maximum concentration – as is often the case when studying proteins by NMR. For example, the addition a 0.7 mM sample of Gb1-Fas-DD to a 1 mM sample of ^{15}N-FADD-DD would lead to a two-and-a-half-fold volume change by the time stoichiometric equivalence (a 1:1 molar ratio) is reached.
In order to avoid this problem, an alternative titration strategy was used. Here, two 600 µl NMR samples were initially produced, one containing 0.5 mM ^{15}N-FADD-DD (sample A) and one containing 0.5 mM ^{15}N-FADD-DD mixed with 0.5 mM Gb1-Fas-DD (sample B). These two samples effectively correspond to the start (A) and end (B)

points of the required titration. HSQC spectra were recorded for both samples, A and B, using exactly the same NMR parameters. Then, by simultaneously swapping a small volume aliquot out of sample A and adding it to sample B, and vice versa, and recording spectra for these new mixtures, two more points in the titration could be recorded. By repeating this series of swapping volume aliquots between the A and B samples and recording HSQC spectra a whole titration series can be filled in.

Figure 3.8 shows the titration of Gb1-Fas-DD into ^{15}N-FADD-DD. Here, the initial ^{15}N-FADD-DD HSQC is the same as the spectrum shown in Figure 3.7c and corresponds to the pure FADD-DD protein. However, as increasing amounts of Gb1-Fas-DD were added to the ^{15}N-FADD-DD sample it was observed that the majority of the ^{15}N-FADD-DD cross peaks exhibited a fall in intensity. As one molar equivalence is reached the majority of the ^{15}N-FADD-DD cross peaks are no longer visible. The positions of few remaining cross peaks in the spectrum were compared to the available FADD-DD resonance assignments (Berglund *et al.*, 2000). All such remaining cross peaks were found to correspond to residues from the flexible N- and C- termini of FADD-DD.

In order to quantitatively analyse the results from the Fas-DD/FADD-DD titration the ANSIG software package (Helgstrand *et al.*, 2000) was used to extract peak intensity values from each of the HSQC spectra recorded at different titration points. All cross peaks from the initial ^{15}N-FADD-DD spectrum were selected and their intensities determined as a function of the relative concentration of Gb1-Fas-DD. Figure 3.8b shows the mean peak intensity values from these spectra, relative to the initial spectrum of pure ^{15}N-FADD-DD, plotted against the molar ratio of Gb1-Fas-DD to ^{15}N-FADD-DD. It can be seen from this graph that there is a monotonic loss of signal from the ^{15}N-FADD-DD protein upon titration of Gb1-Fas-DD. It would appear from the graph in Figure 3.8b that the ^{15}N-FADD-DD signals decay essentially to zero at a concentration of Gb1-Fas-DD that is less than the FADD-DD concentration.

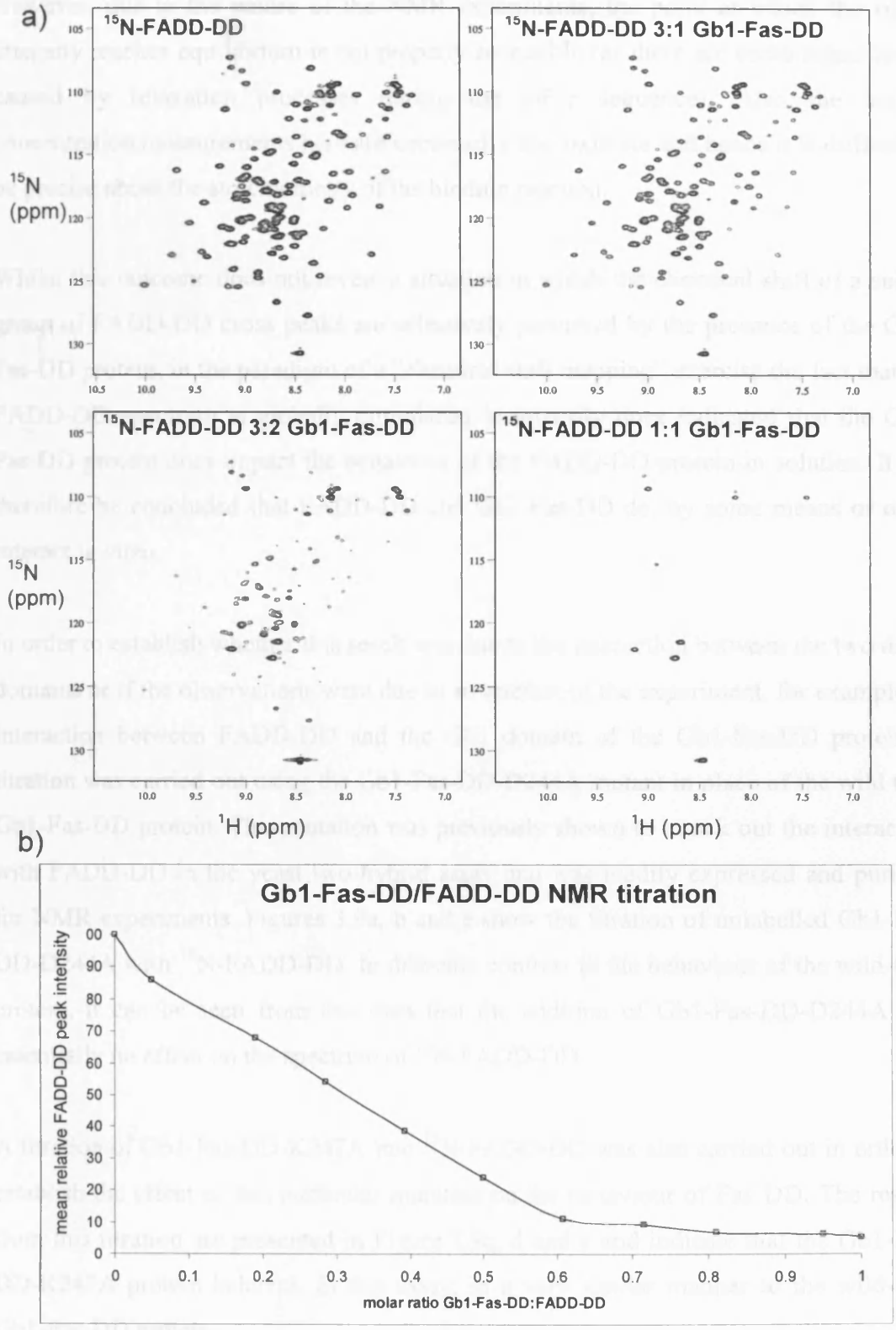

Figure 3.8: NMR titration of Gb1-Fas-DD into ^{15}N-FADD-DD. a) HSQC spectra of ^{15}N-FADD-DD following the addition of increasing concentrations of unlabelled Gb1-Fas-DD. b) A graph of mean cross peak intensities from HSQC spectra recorded during the titration. Values are calculated relative to the mean intensity of the peaks from the initial ^{15}N-FADD-DD spectrum.

However, due to the nature of the NMR experiments, the point at which the signal intensity reaches equilibrium is not properly accessible (as there are some signal losses caused by relaxation processes during the pulse sequence). Also the protein concentration measurements here are necessarily approximate and hence it is difficult to be precise about the stoichiometry of the binding reaction.

Whilst this outcome does not reveal a situation in which the chemical shift of a subset group of FADD-DD cross peaks are selectively perturbed by the presence of the Gb1-Fas-DD protein, in the paradigm of a "chemical shift mapping" exercise the fact that the FADD-DD spectrum is globally diminished in intensity does indicated that the Gb1-Fas-DD protein does impact the behaviour of the FADD-DD protein in solution. It can therefore be concluded that FADD-DD and Gb1-Fas-DD do, by some means or other interact *in vitro*.

In order to establish whether this result was due to the interaction between the two death domains or if the observations were due to an artefact of the experiment, for example an interaction between FADD-DD and the Gb1 domain of the Gb1-Fas-DD protein, a titration was carried out using the Gb1-Fas-DD-D244A mutant in place of the wild type Gb1-Fas-DD protein. This mutation was previously shown to knock out the interaction with FADD-DD in the yeast two-hybrid assay and was readily expressed and purified for NMR experiments. Figures 3.9a, b and e show the titration of unlabelled Gb1-Fas-DD-D244A with ^{15}N-FADD-DD. In dramatic contrast to the behaviour of the wild-type protein, it can be seen from this data that the addition of Gb1-Fas-DD-D244A had essentially no effect on the spectrum of ^{15}N-FADD-DD.

A titration of Gb1-Fas-DD-K247A into ^{15}N-FADD-DD was also carried out in order to establish the effect of this particular mutation on the behaviour of Fas-DD. The results from this titration are presented in Figure 3.9c, d and e and indicate that the Gb1-Fas-DD-K247A protein behaves, in this assay, in a very similar manner to the wild-type Gb1-Fas-DD protein.

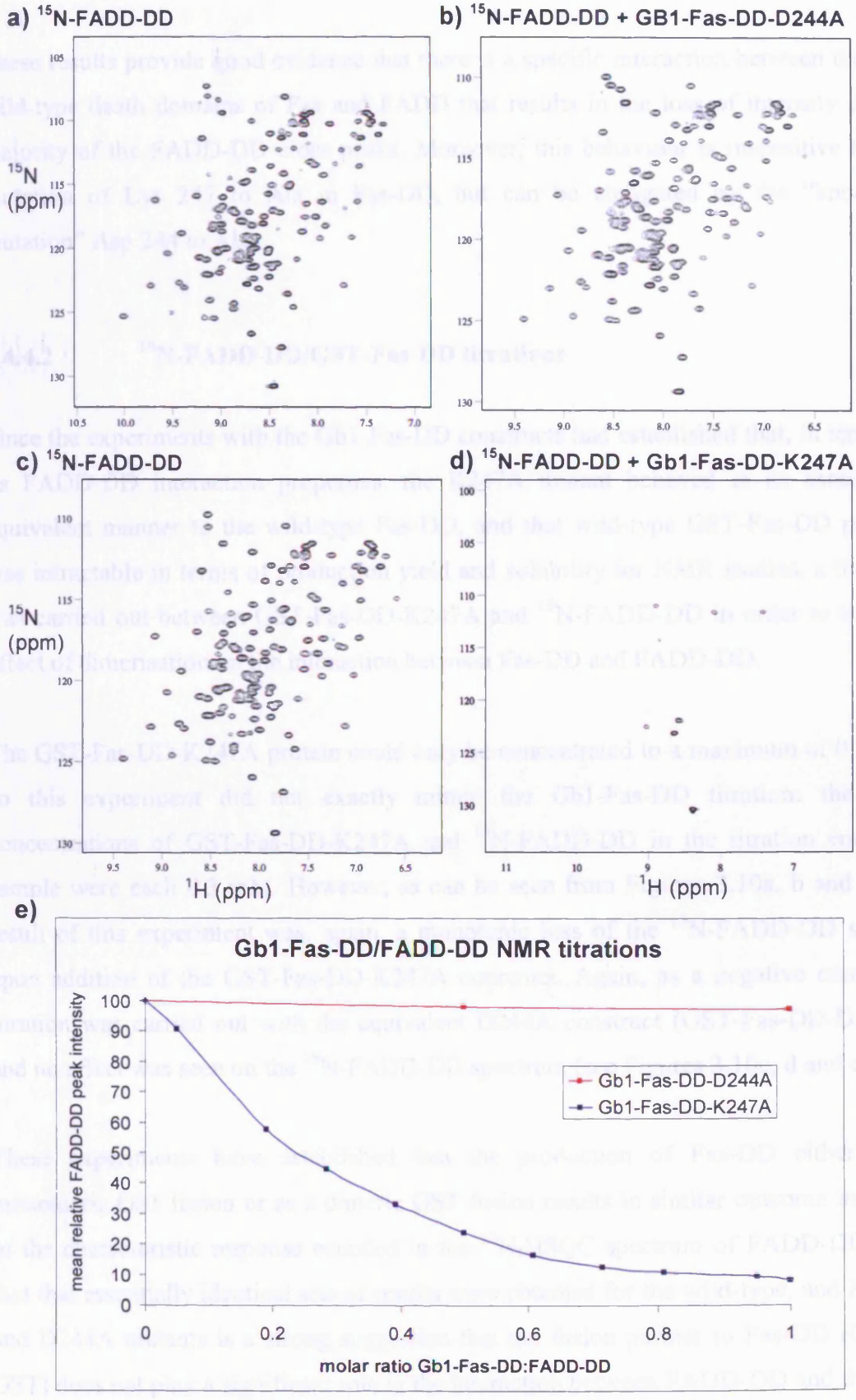

Figure 3.9: NMR titrations of Gb1-Fas-DD constructs into ^{15}N-FADD-DD. HSQC spectra of a) and c) FADD-DD alone and with a 1:1 molar ratio of unlabelled b) Gb1-Fas-DD-K247A and d) Gb1-Fas-DD-D244A. The full titration data are summarised in graph e).

These results provide good evidence that there is a specific interaction between the two wild-type death domains of Fas and FADD that results in the loss of intensity of the majority of the FADD-DD cross peaks. Moreover, this behaviour is insensitive to the mutation of Lys 247 to Ala in Fas-DD, but can be abrogated by the "knockout mutation" Asp 244 to Ala.

3.4.4.2 ^{15}N-FADD-DD/GST-Fas-DD titrations

Since the experiments with the Gb1-Fas-DD constructs had established that, in terms of its FADD-DD interaction properties, the K247A mutant behaved in an essentially equivalent manner to the wild-type Fas-DD, and that wild-type GST-Fas-DD protein was intractable in terms of production yield and solubility for NMR studies, a titration was carried out between GST-Fas-DD-K247A and ^{15}N-FADD-DD in order to test the effect of dimerisation on the interaction between Fas-DD and FADD-DD.

The GST-Fas-DD-K247A protein could only be concentrated to a maximum of 0.5 mM so this experiment did not exactly mimic the Gb1-Fas-DD titration: the final concentrations of GST-Fas-DD-K247A and ^{15}N-FADD-DD in the titration endpoint sample were each 0.3 mM. However, as can be seen from Figures 3.10a, b and e, the result of this experiment was, again, a monotonic loss of the ^{15}N-FADD-DD signals upon addition of the GST-Fas-DD-K247A construct. Again, as a negative control, a titration was carried out with the equivalent D244A construct (GST-Fas-DD-D244A) and no effect was seen on the ^{15}N-FADD-DD spectrum (see Figures 3.10c, d and e).

These experiments have established that the production of Fas-DD either as a monomeric Gb1 fusion or as a dimeric GST fusion results in similar outcome in terms of the characteristic response encoded in the ^{15}N-HSQC spectrum of FADD-DD. The fact that essentially identical sets of results were obtained for the wild-type, and K247A and D244A mutants is a strong suggestion that the fusion partner to Fas-DD (Gb1 or GST) does not play a significant role in the interaction between FADD-DD and the Fas-DD proteins.

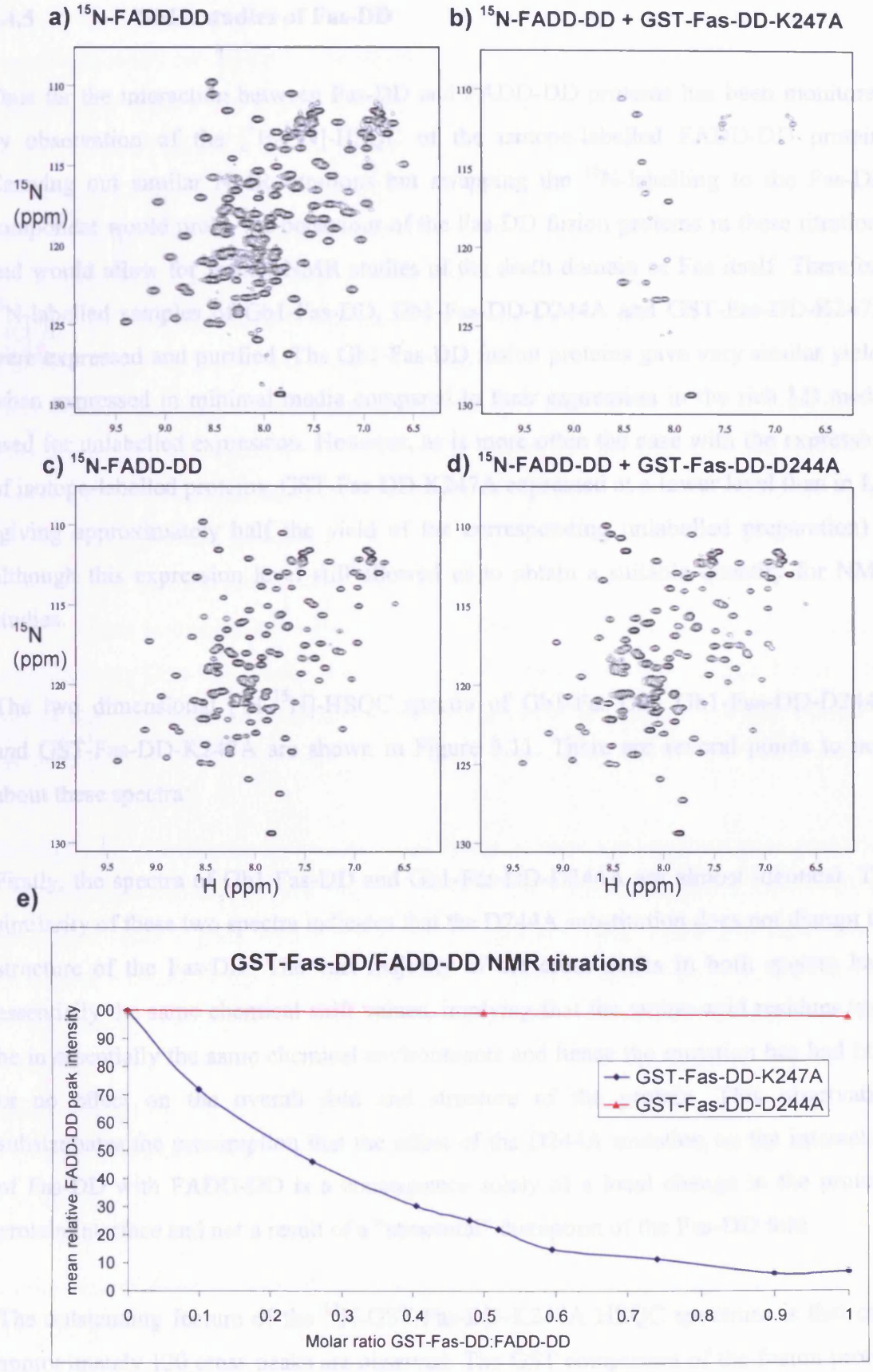

Figure 3.10: NMR Titrations of GST-Fas-DD constructs into ^{15}N-FADD-DD. HSQC spectra of a) and c) FADD-DD alone and with a 1:1 molar ratio of unlabelled b) GST-Fas-DD-K247A and d) GST-Fas-DD-D244A. The full titration data are summarised in graph e).

3.4.5 NMR studies of Fas-DD

Thus far the interaction between Fas-DD and FADD-DD proteins has been monitored by observation of the [^{1}H-^{15}N]-HSQC of the isotope-labelled FADD-DD protein. Carrying out similar NMR titrations but swapping the ^{15}N-labelling to the Fas-DD component would probe the behaviour of the Fas-DD fusion proteins in these titrations and would allow for further NMR studies of the death domain of Fas itself. Therefore ^{15}N-labelled samples of Gb1-Fas-DD, Gb1-Fas-DD-D244A and GST-Fas-DD-K247A were expressed and purified. The Gb1-Fas-DD fusion proteins gave very similar yields when expressed in minimal media compared to their expression in the rich LB media used for unlabelled expression. However, as is more often the case with the expression of isotope-labelled proteins, GST-Fas-DD-K247A expressed at a lower level than in LB (giving approximately half the yield of the corresponding unlabelled preparation) – although this expression level still allowed us to obtain a suitable quantity for NMR studies.

The two dimensional [^{1}H-^{15}N]-HSQC spectra of Gb1-Fas-DD, Gb1-Fas-DD-D244A and GST-Fas-DD-K247A are shown in Figure 3.11. There are several points to note about these spectra:

Firstly, the spectra of Gb1-Fas-DD and Gb1-Fas-DD-D244A are almost identical. The similarity of these two spectra indicates that the D244A substitution does not disrupt the structure of the Fas-DD. The vast majority of the cross peaks in both spectra have essentially the same chemical shift values, implying that the amino-acid residues must be in essentially the same chemical environments and hence the mutation has had little or no effect on the overall fold and structure of the protein. This observation substantiates the presumption that the effect of the D244A mutation on the interaction of Fas-DD with FADD-DD is a consequence solely of a local change in the protein-protein interface and not a result of a "structural" disruption of the Fas-DD fold.

The outstanding feature of the ^{15}N-GST-Fas-DD-K247A HSQC spectrum is that only approximately 120 cross peaks are observed. The GST component of the fusion protein has 218 residues and Fas-DD 105 residues so, naively, the expected number of cross peaks in this spectrum is of the order of 320. It was initially assumed that the cross

peaks in this spectrum corresponded only to signals from Fas-DD residues and this idea was subsequently confirmed by the superposition of ^{15}N-GST-Fas-DD-K247A and ^{15}N-Gb1-Fas-DD spectra (see Figure 3.11d). The vast majority of the cross peaks from the ^{15}N-GST-Fas-DD-K247A spectra precisely align with cross peaks in the ^{15}N-Gb1-Fas-DD spectrum. This overlap would only occur if both of these sets of cross peaks were from the same folded protein domain in the fusion – in this case Fas-DD. The fact that few signals from the GST protein are observed is an interesting phenomenon which can be explained by the modular composition and hydrodynamic properties of the GST-Fas-DD fusion protein. When expressing a protein from the pGEX-2T vector a flexible, protease cleavable, eight-residue linker between GST and the target protein is encoded. This linker does not appear to affect the ability of GST to enhance the solubility of the fusion partner. However, apparently it does allow the two individual domains of the whole fusion protein to behave independently in a hydrodynamic sense. There is presumably a low activation barrier to conformational averaging of the backbone Φ, Ψ torsion angles in this linker region, permitting the Fas-DD domain to rotate essentially independently from the heavier GST. In terms of NMR experiments, this free rotation means that the two domains will have the potential to display nuclear relaxation parameters.

Relaxation is the process by which nuclei return to their resting state after excitation. The relaxation rate of a specific nucleus is key to the determination of the linewidth the associated NMR signal. In a compact protein domain most nuclei will have similar transverse relaxation rates that are determined by the overall rotational correlation time of that domain. Generally, smaller proteins (or protein domains) tumble in solution with faster correlation times and hence their transverse nuclear relaxation rates are slower than those of larger proteins. Slower relaxation rates lead to more NMR resonances with narrower linewidths and greater intensities in multidimensional heteronuclear NMR spectra.

In the case of the GST-Fas-DD-K247A molecule, therefore, it seems that the dimeric, 54 kDa GST moiety tumbles sufficiently slowly such that the HSQC experiment is not sensitive enough to detect it under the conditions of the experiments recorded in this study (i.e. at 25°C and 600 MHz ^{1}H frequency). The Fas-DD domain, however, is

behaving like an essentially independent, fast rotating, monomeric 12 kDa moiety that gives rise to typically narrow lines and relatively intense HSQC cross peaks.

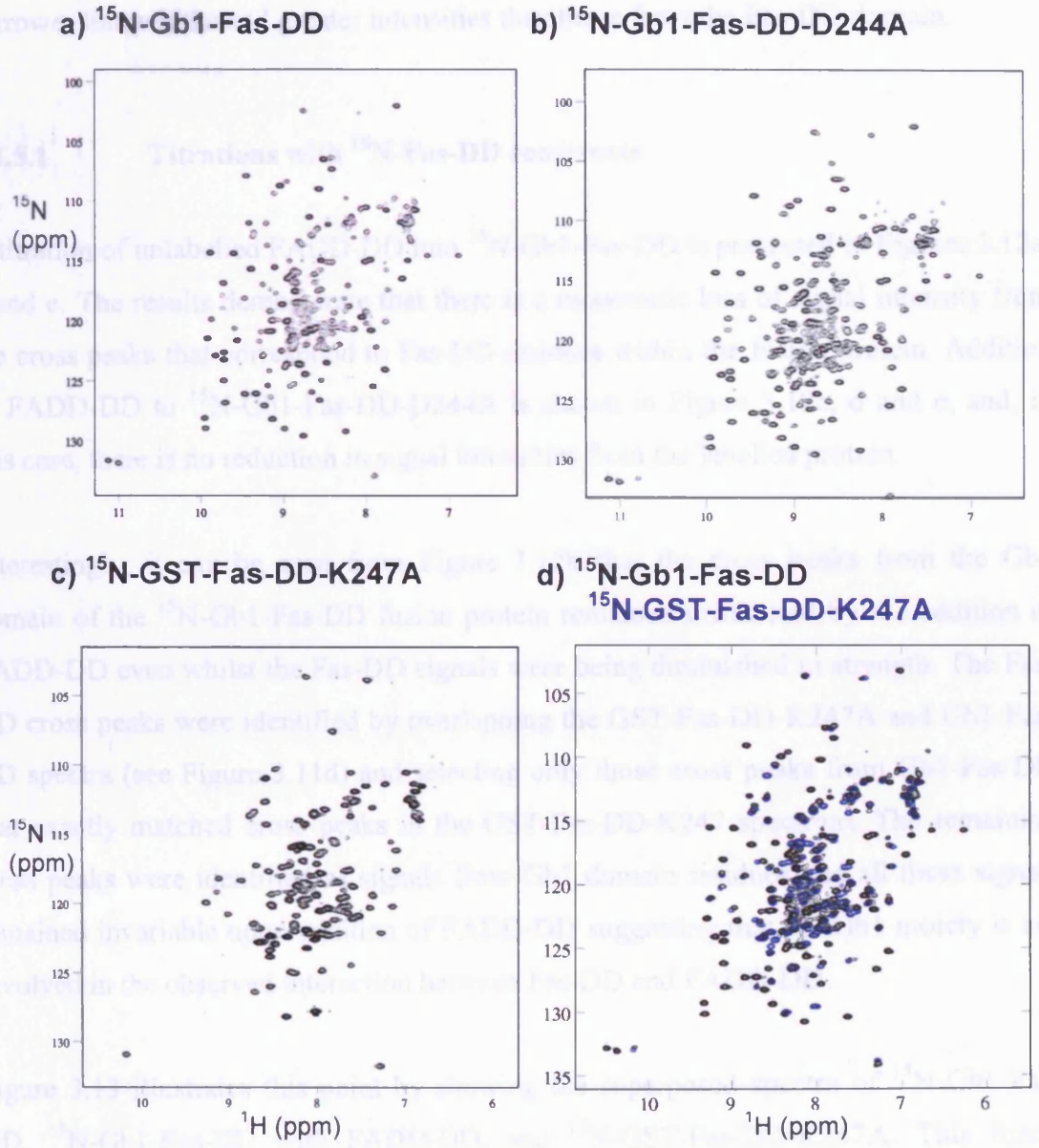

Figure 3.11: 2D HSQC spectra of ^{15}N-labelled Fas-DD constructs. Spectra of ^{15}N-Gb1-Fas-DD, ^{15}N-Gb1-Fas-DD-D244A and ^{15}N-GST-Fas-DD-K247A are shown in (a), (b) and (c) respectively. d) shows a superposition of spectrum (c) in blue on spectrum (a) in black.

This transverse relaxation "contrast" phenomenon is also observed with the Gb1-Fas-DD fusion proteins. Here, the Gb1 moiety is again linked to Fas-DD through a flexible peptide linker allowing the two domains to rotate in solution effectively independently. In this case, however, because the Gb1 domain is smaller than the Fas-DD moiety (6 kDa compared to 12 kDa), signals from the Gb1 residues are detected and indeed have narrower line-widths and greater intensities than those from the Fas-DD domain.

3.4.5.1 Titrations with ^{15}N-Fas-DD constructs

A titration of unlabelled FADD-DD into ^{15}N-Gb1-Fas-DD is presented in Figures 3.12a, b and e. The results demonstrate that there is a monotonic loss of signal intensity from the cross peaks that correspond to Fas-DD residues within the fusion protein. Addition of FADD-DD to ^{15}N-Gb1-Fas-DD-D244A is shown in Figure 3.12c, d and e, and, in this case, there is no reduction in signal intensities from the labelled protein.

Interestingly, it can be seen from Figure 3.12b that the cross peaks from the Gb1 domain of the ^{15}N-Gb1-Fas-DD fusion protein remained unaffected by the addition of FADD-DD even whilst the Fas-DD signals were being diminished in strength. The Fas-DD cross peaks were identified by overlapping the GST-Fas-DD-K247A and Gb1-Fas-DD spectra (see Figure 3.11d) and selecting only those cross peaks from Gb1-Fas-DD that exactly matched cross peaks in the GST-Fas-DD-K247 spectrum. The remaining cross peaks were identified as signals from Gb1 domain residues and all these signals remained invariable upon addition of FADD-DD suggesting that the Gb1 moiety is not involved in the observed interaction between Fas-DD and FADD-DD.

Figure 3.13 illustrates this point by showing the superposed spectra of ^{15}N-Gb1-Fas-DD, ^{15}N-Gb1-Fas-DD with FADD-DD, and ^{15}N-GST-Fas-DD-K247A. This figure emphasises the presence of two distinct sets of cross peaks in the ^{15}N-Gb1-Fas-DD spectrum, one set corresponding to Gb1 residues (that remain visible upon addition of FADD-DD), and a second set corresponding to Fas-DD residues (that overlap with the signals from ^{15}N-GST-Fas-DD-K247A and are lost upon addition of FADD-DD).

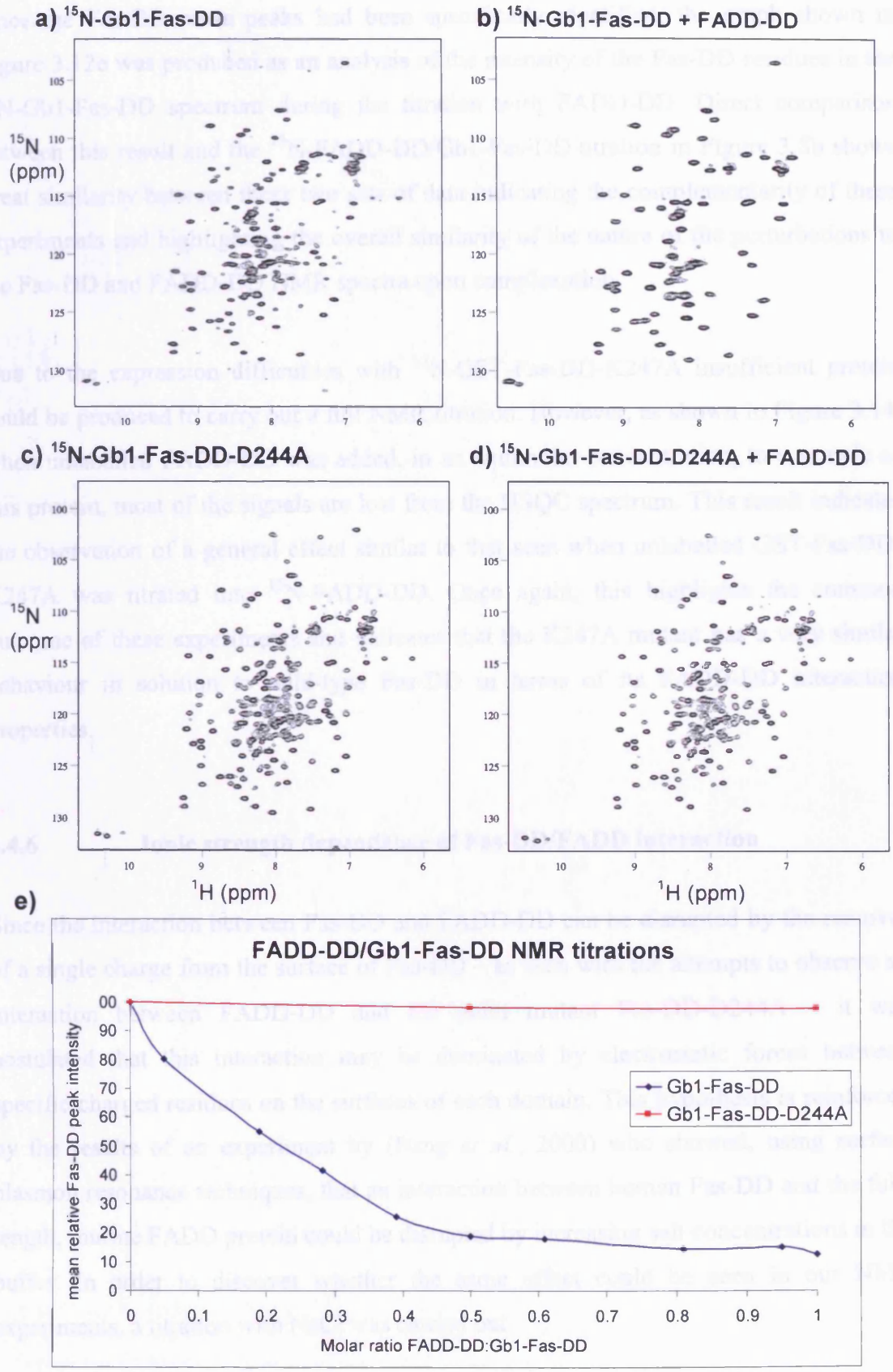

Figure 3.12: NMR titrations of FADD-DD into different forms of ^{15}N-Gb1-Fas-DD. HSQC spectra of a) Gb1-Fas-DD alone and b) with a 1:1 molar ratio of unlabelled FADD-DD. Spectra of (c) Gb1-Fas-DD-D244A alone and d) with a 1:1 molar ratio of unlabelled FADD-DD. The full titration data are summarised in graph (e).

Once the Fas-DD cross peaks had been specifically identified, the graph shown in Figure 3.12e was produced as an analysis of the intensity of the Fas-DD residues in the ^{15}N-Gb1-Fas-DD spectrum during the titration with FADD-DD. Direct comparison between this result and the ^{15}N-FADD-DD/Gb1-Fas-DD titration in Figure 3.8b shows great similarity between these two sets of data indicating the complementarity of these experiments and highlighting the overall similarity of the nature of the perturbations to the Fas-DD and FADD-DD NMR spectra upon complexation.

Due to the expression difficulties with ^{15}N-GST-Fas-DD-K247A insufficient protein could be produced to carry out a full NMR titration. However, as shown in Figure 3.14, when unlabelled FADD-DD was added, in an equimolar concentration, to a sample of this protein, most of the signals are lost from the HSQC spectrum. This result indicates the observation of a general effect similar to that seen when unlabelled GST-Fas-DD-K247A was titrated into ^{15}N-FADD-DD. Once again, this highlights the common outcome of these experiments and indicates that the K247A mutant has a very similar behaviour in solution to wild-type Fas-DD in terms of its FADD-DD interaction properties.

3.4.6 Ionic strength dependence of Fas-DD/FADD interaction

Since the interaction between Fas-DD and FADD-DD can be disrupted by the removal of a single charge from the surface of Fas-DD – as seen with the attempts to observe an interaction between FADD-DD and the point mutant Fas-DD-D244A – it was postulated that this interaction may be dominated by electrostatic forces between specific charged residues on the surfaces of each domain. This hypothesis is reinforced by the results of an experiment by (Bang *et al.*, 2000) who showed, using surface plasmon resonance techniques, that an interaction between human Fas-DD and the full-length, murine FADD protein could be disrupted by increasing salt concentrations in the buffer. In order to discover whether the same effect could be seen in our NMR experiments, a titration with NaCl was carried out

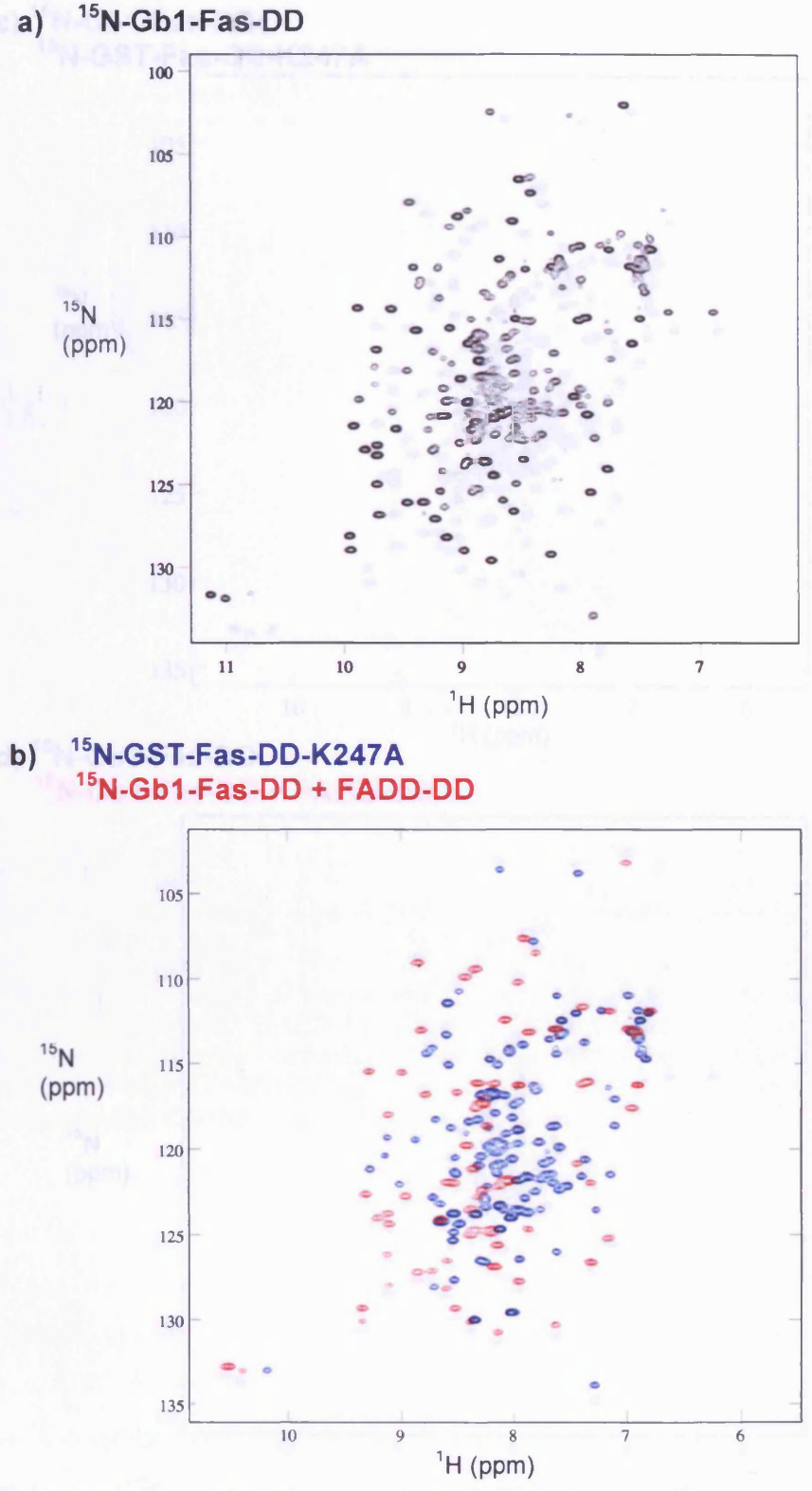

Figure 3.13: Superposition of 2D [^{1}H-^{15}N]-HSQC spectra of ^{15}N-Gb1-Fas-DD, ^{15}N-GST-Fas-DD-K247A and ^{15}N-GB1-Fas-DD+FADD-DD. a) HSQC spectrum of ^{15}N-Gb1-Fas-DD alone. b) superimposed HSQC spectra of ^{15}N-GST-Fas-DD-K247A and ^{15}N-GB1-Fas-DD+FADD-DD. If visualised in black and white the figure (b) is seen to be highly similar to spectrum in (a), allowing the identification of two sets of cross-peaks in the [^{1}H-^{15}N]-HSQC spectrum, one set corresponding to signals from Gb1 residues and the other to signals from Fas-DD residues. Note that coloured names correspond to the colour of the respective HSQC spectra.

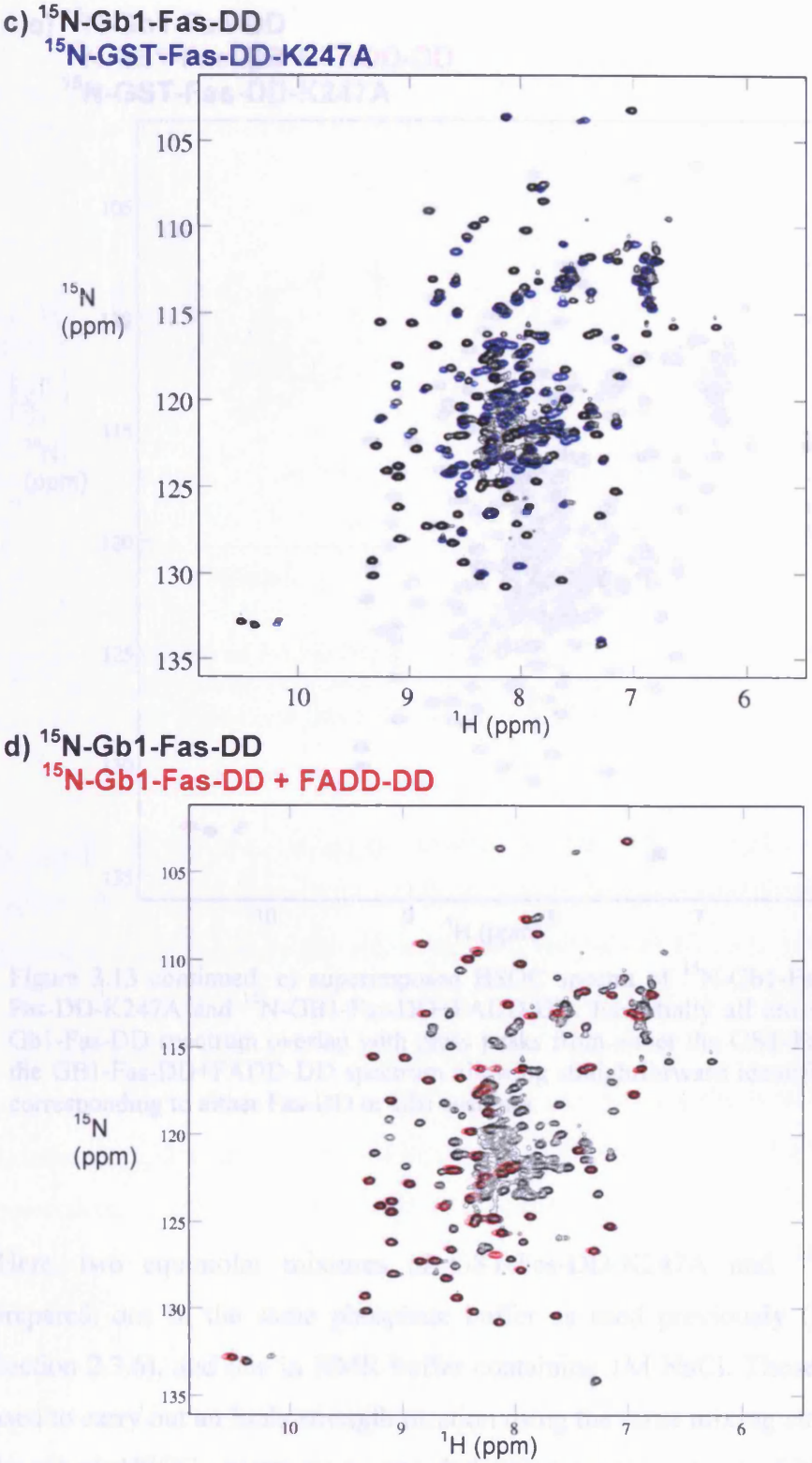

Figure 3.13 continued: c) Superposition of HSQC spectra of ^{15}N-Gb1-Fas-DD and ^{15}N-GST-Fas-DD-K247A. All of the cross peaks from the GST-Fas-DD-K247A spectrum essentially overlap with cross peaks from the Gb1-Fas-DD spectrum highlighting the lack of signals from the GST moiety in the GST-Fas-DD spectrum as well allowing the identification of Fas-DD cross peaks in the Gb1-Fas-DD spectrum. Moreover this figure indicates that the K247A mutant does not disrupt the Fas-DD structure. A superposition of HSQC spectra of ^{15}N-Gb1-Fas-DD and ^{15}N-GB1-Fas-DD+FADD-DD is shown in (d). This figure highlights the loss of Fas-DD signals upon addition of FADD-DD to Gb1-Fas-DD and that the chemical shifts of the Gb1 signals are unperturbed, indicating that the Gb1 moiety is not involved in the DD/DD interaction.

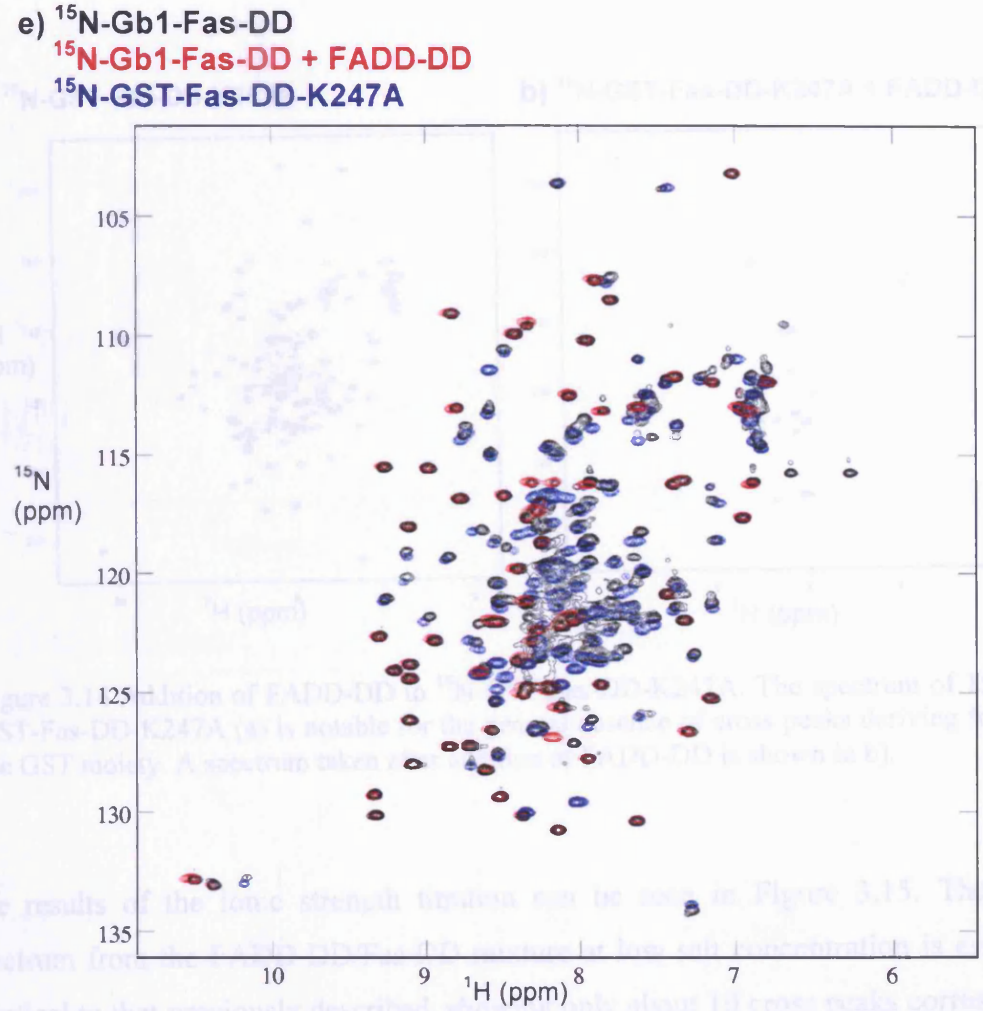

Figure 3.13 continued: e) superimposed HSQC spectra of ^{15}N-Gb1-Fas-DD, ^{15}N-GST-Fas-DD-K247A and ^{15}N-GB1-Fas-DD+FADD-DD. Essentially all cross peaks from the Gb1-Fas-DD spectrum overlap with cross peaks from either the GST-Fas-DD-K247A or the GB1-Fas-DD+FADD-DD spectrum allowing straightforward identification of signals corresponding to either Fas-DD or Gb1 residues.

Here, two equimolar mixtures of GST-Fas-DD-K247A and ^{15}N-FADD-DD was prepared, one in the same phosphate buffer as used previously (NMR buffer – see Section 2.3.6), and one in NMR buffer containing 1M NaCl. These two samples were used to carry out an ionic strength titration using the same mixing strategy as previously described. HSQC spectra were recorded, using a common set of NMR parameters, at each point in the titration in order to follow the effect of the addition of NaCl to the Fas-DD/FADD-DD complex.

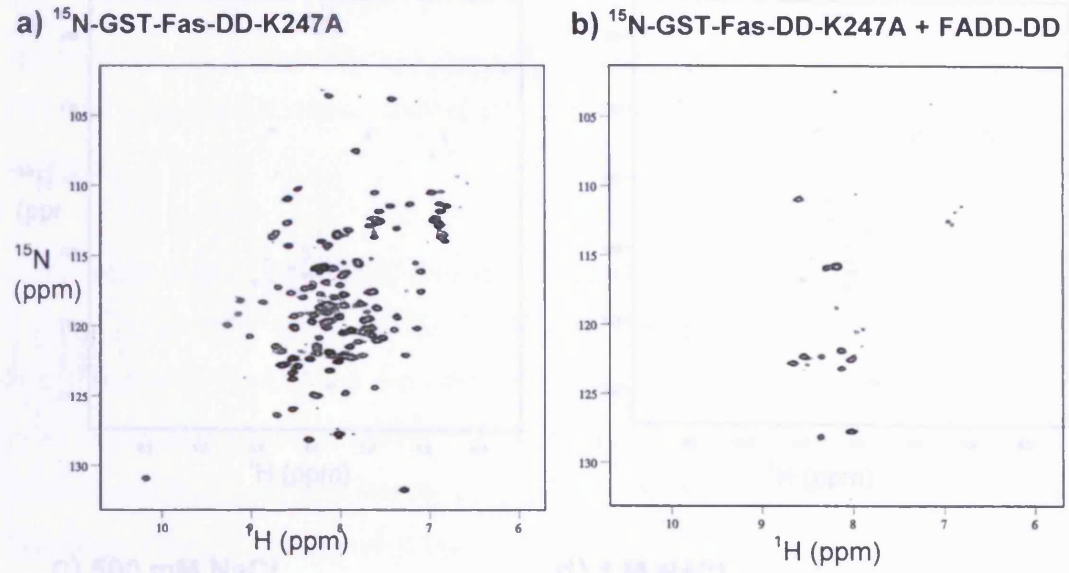

Figure 3.14 Addition of FADD-DD to ^{15}N-GST-Fas-DD-K247A. The spectrum of 15N-GST-Fas-DD-K247A (a) is notable for the general absence of cross peaks deriving from the GST moiety. A spectrum taken after addition of FADD-DD is shown in b).

The results of the ionic strength titration can be seen in Figure 3.15. The HSQC spectrum from the FADD-DD/Fas-DD mixture at low salt concentration is essentially identical to that previously described, showing only about 10 cross peaks corresponding to the flexible, terminal residues of FADD-DD. However, upon addition of NaCl, the remaining FADD-DD cross peaks were fully recovered. This result shows that the observed interaction between the two domains can be fully disrupted by an increase in the ionic strength of the buffer and hence would appear to be dominated by electrostatic interactions, presumably between the many charged residues on the surfaces of these two death domains.

It is worth noting that the chemical shift values of the FADD-DD residue cross peaks changed slightly during the salt titration. This is because the addition of salt to the sample changes the chemical environment of the amide groups in FADD-DD sufficiently to give a small but significant alteration in amide group chemical shifts. However these shift changes are unrelated to the interaction between the two domains.

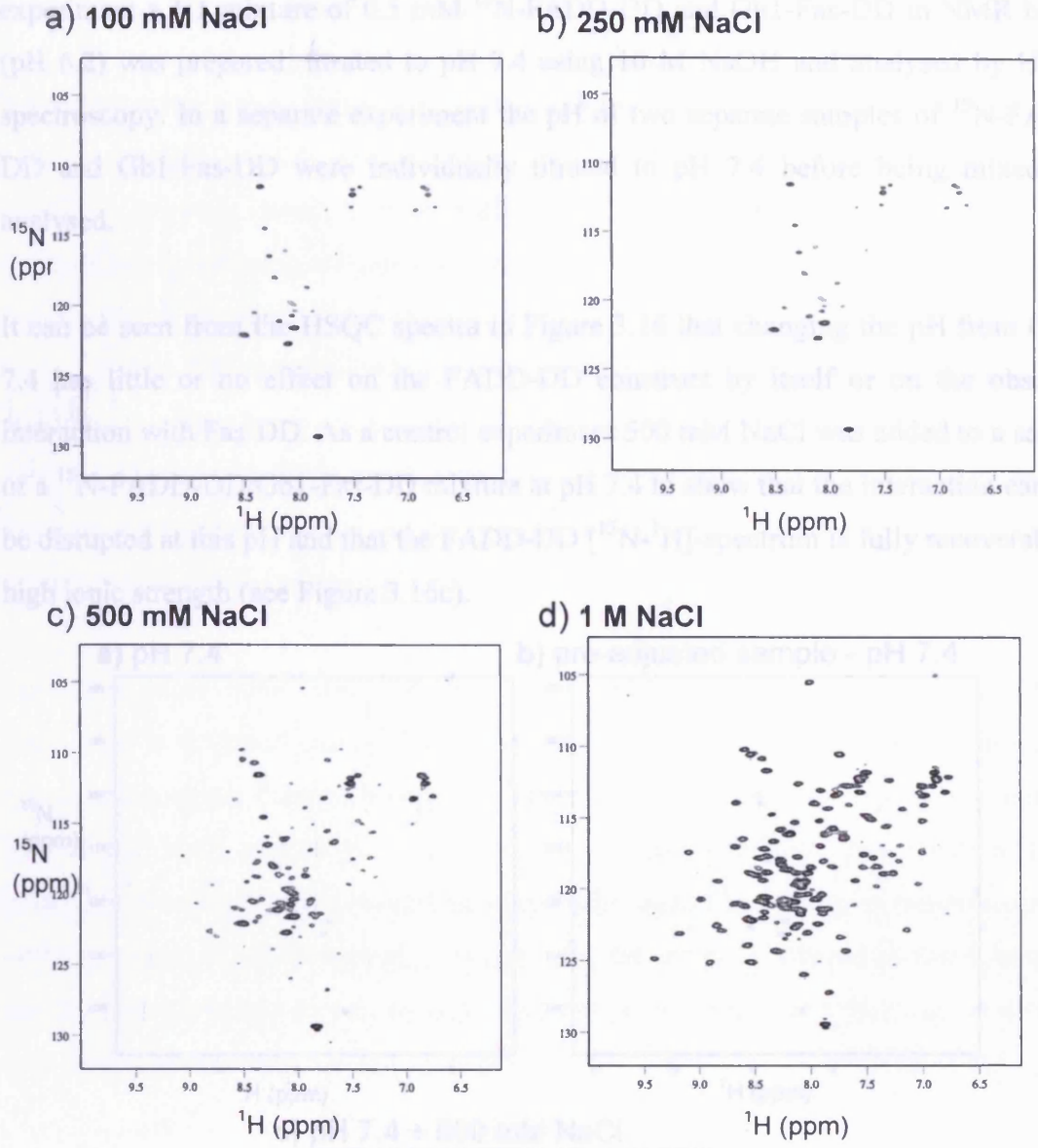

Figure 3.15 Ionic strength titration of the Fas-DD/FADD-DD complex. A 1:1 molar ratio mixture of ^{15}N-FADD-DD and GST-Fas-DD-K247A was titrated with NaCl from 100 mM to 1 M. a) – d) show spectra of several points from this titration indicating that as the salt concentration is increased signals from ^{15}N-FADD-DD are recovered, suggesting disruption of the complex formed between these two proteins.

3.4.7 Analysis of the effect of pH on the Fas-DD/FADD-DD interaction

All the experiments described previously in this study were carried out at pH 6.2 using a buffer identical to that in the three dimensional structure determination of FADD-DD (Berglund *et al.*, 2000). However, in order to test the physiological relevance of the previous titration results, it was felt that the observations should be tested at physiological pH (=7.4). Two experiments were therefore carried out. In the first

experiment a 1:1 mixture of 0.5 mM ^{15}N-FADD-DD and Gb1-Fas-DD in NMR buffer (pH 6.2) was prepared, titrated to pH 7.4 using 10 M NaOH and analysed by HSQC spectroscopy. In a separate experiment the pH of two separate samples of ^{15}N-FADD-DD and Gb1-Fas-DD were individually titrated to pH 7.4 before being mixed and analysed.

It can be seen from the HSQC spectra in Figure 3.16 that changing the pH from 6.2 to 7.4 has little or no effect on the FADD-DD construct by itself or on the observed interaction with Fas-DD. As a control experiment 500 mM NaCl was added to a sample of a ^{15}N-FADD-DD/Gb1-Fas-DD mixture at pH 7.4 to show that the interaction can still be disrupted at this pH and that the FADD-DD [^{15}N-^{1}H]-spectrum is fully recoverable at high ionic strength (see Figure 3.16c).

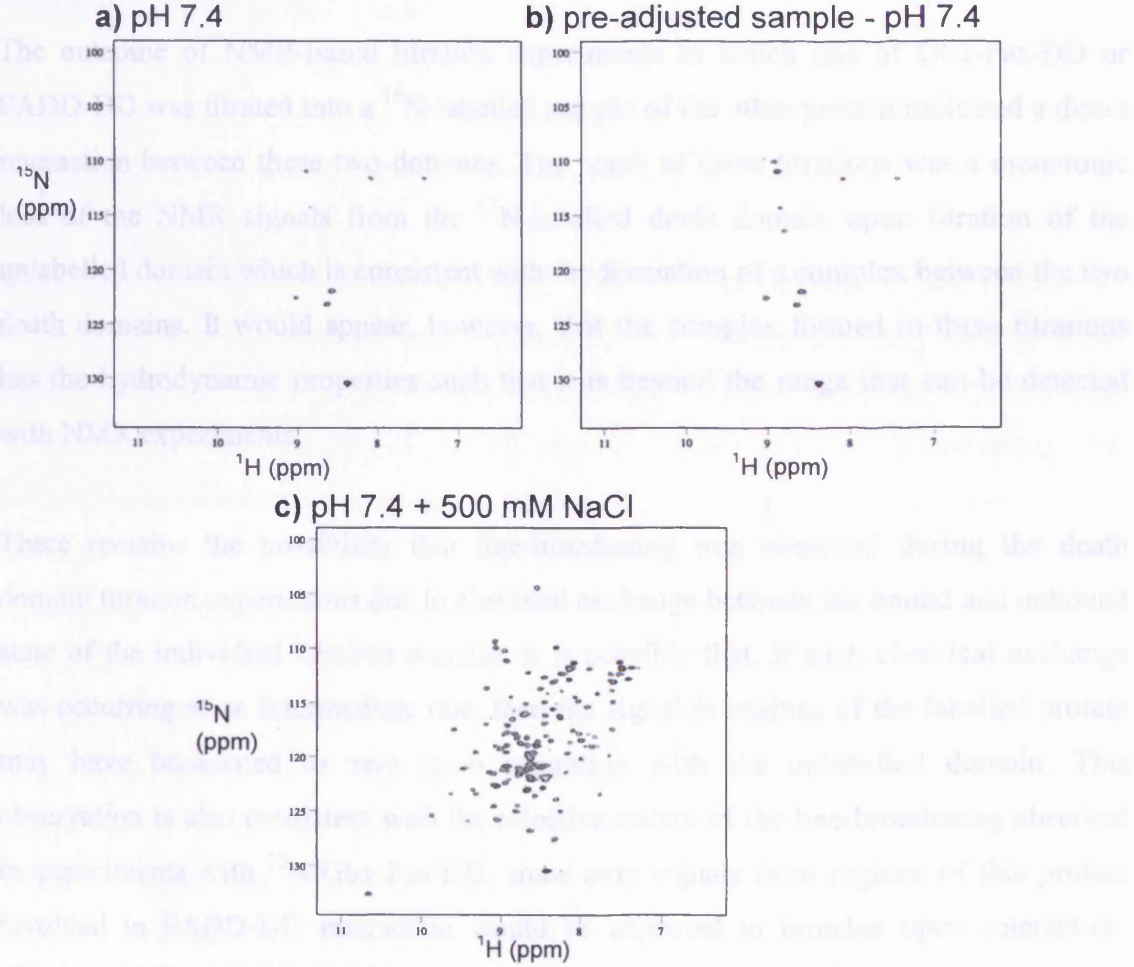

Figure 3.16 Studies of the FADD-DD/Gb1-Fas-DD complex at pH 7.4. HSQC spectra of: a) a sample of 15N-FADD-DD + Gb1-Fas-DD mixed in a 1:1 ratio and adjusted to pH7.4. b) Samples of 15N-FADD-DD and Gb1-Fas-DD separately adjusted to pH 7.4 before being mixed together. Spectrum (c) shows an HSQC spectrum of sample (a) after addition of 500 mM NaCl.

3.5 Conclusions from NMR titrations

To our knowledge this chapter has described the first time that NMR spectroscopy has been successfully used to study the interaction between the death domains of Fas and FADD. It has been shown how several different strategies were used to overcome the difficulties of producing suitable quantities of recombinant proteins that are sufficiently soluble for NMR studies. In particular, the production of Fas-DD was initially limited by its intrinsic self-aggregation properties. However it was found that by producing this domain as a Gb1 fusion protein or by mutating amino acid residues on its surface (specifically residues D244 and K247), the poor expression yields and, to some extent, the poor solubility of Fas-DD could be overcome allowing NMR studies to be carried out at physiologically relevant pH values.

The outcome of NMR-based titration experiments in which one of Gb1-Fas-DD or FADD-DD was titrated into a ^{15}N-labelled sample of the other protein indicated a direct interaction between these two domains. The result of these titrations was a monotonic loss of the NMR signals from the ^{15}N-labelled death domain upon titration of the unlabelled domain which is consistent with the formation of a complex between the two death domains. It would appear, however, that the complex formed in these titrations has the hydrodynamic properties such that it is beyond the range that can be detected with NMR experiments.

There remains the possibility that line-broadening was observed during the death domain titration experiments due to chemical exchange between the bound and unbound state of the individual labelled domain. It is possible that, if such chemical exchange was occurring at an intermediate rate, then the signal intensities of the labelled protein may have broadened to zero upon saturation with the unlabelled domain. This observation is also consistent with the selective nature of the line-broadening observed in experiments with ^{15}N-Gb1-Fas-DD, since only signals from regions of this protein involved in FADD-DD interaction would be expected to broaden upon interaction. However, if intermediate exchange was occurring then, associated with this process, would be chemical shift changes of those broadening signals. Since no chemical shift changes were observed in the titration experiments in ths study it is unlikely that exchange processes were responsible for the effects detected by these titrations.

Curiously, mobile elements within the complex are still observed in the spectrum indicating that the interacting proteins remain in solution and that these elements retain a substantial degree of rotational independence from the interacting death domains. Indeed, the solubility of this complex was also shown indirectly by its disruption with increased ionic strength buffers which led to the recovery of signals from the labelled death domain component. Importantly, the observed interaction between Fas-DD and FADD-DD could be entirely disrupted by mutation of the Fas-DD aspartate 244 residue to alanine. These *in vitro* data obtained by NMR are consistent with both the results of the yeast two-hybrid assay presented at the start of this chapter and the prior knowledge of this residue as a mutational hotspot in the disease ALPS which is known to be caused by a disruption of Fas-DD/FADD interactions. Also, the titration of FADD-DD into a ^{15}N-labelled sample of Gb1-Fas-DD indicated that the interaction did not affect residues from the Gb1 domain since the loss of NMR signals was only observed from Fas-DD residue cross peaks. The nature of this observed interaction, therefore, despite lacking in any real molecular detail at this stage, does appear to be highly specific.

Speculation as to the exact size of the complex formed between Fas-DD and FADD-DD in this study is, at this stage, at best, tentative. The observation that the intensity of the majority of cross peaks for the isotope-labelled death domain monotonically diminish upon titration with the unlabelled death domain implies that, in all probability, the hydrodynamic radius of the complex is in the order of, or greater than, other proteins that do not give rise to significant cross peak intensity under the conditions of the NMR experiments used here. A lower limit for this size might be provided by the molecular weight of the GST homodimer (58 kDa) which is essentially not visible in the spectra of the ^{15}N-GST-Fas-DD fusion proteins recorded in this study (for example see Figure 3.9d). Also, since the predicted size of a simple 1:1 FADD-DD/Gb1-Fas-DD heterodimer is lower than 35 kDa, it is reasonable to suggest that it would have been possible to record tractable NMR spectra of such a complex had it been formed. This prediction, combined with extensive experience of biomolecular NMR within the local protein NMR community suggests that the complex is larger than 35 kDa indicating that a heterodimeric, low molecular weight complex is not formed.

In an attempt to charaterise the exact size of such a complex, several preliminary biophysical and biochemical measurements were made by a variety of techniques. Dynamic light scattering carried out on a complex between GST-Fas-DD-K247A and FADD-DD indicated that this species may be very much larger than 30 kDa and possibly in the megadalton range. Attempts to analyse this complex by analytical size exclusion chromatography proved to be unproductive since the protein mixture would not enter a size exclusion (S200) column – although this data is, in itself, indicative of a large complex further investigation must be carried for confirmation. Finally, chemical crosslinking with either gluteraldehyde (a non-specific protein crosslinking reagent) or 1-Ethyl-3-[3-dimethylaminopropyl]carbodiimide hydrochloride (a homobifunctional amide-amide crosslinking reagent) was attempted using samples of FADD-DD and Gb1-Fas-DD. Using these reagents, however, it was not possible to specifically crosslink the two death domains to each other. Therefore, although some of the data obtained in attempts to characterise the exact size of the Fas-DD/FADD-DD complex formed in solution is suggestive of a large, mulitmeric complex (and, as such, is in disagreement with the suggestion that chemical exchange processes may be involved in the observations from the NMR titrations), such data is too preliminary to present in this thesis and hence more work is required to establish the veracity of such indications.

The next chapter describes the extension of the use of the Fas-DD/FADD-DD interaction assays developed in this section, to investigate the effects of a range of Fas-DD mutations on FADD-DD binding.

Chapter 4

Mutational analysis of the Fas death domain

4.1 Mutations in Fas-DD

THE focus of Chapter four is on the mutational analysis of the Fas death domain and the implications of these mutations for Fas-DD/FADD-DD signalling. The aim of the analysis presented in this chapter is to identify amino-acid residues in Fas-DD that may be crucial in mediating Fas-DD/FADD-DD interactions. The identification of these residues will help to further the understanding of the mechanism of this interaction by providing insight into how the complex between these two domains is formed.

The methods used in this chapter echo those described in Chapter 3. Since the yeast two-hybrid assay is capable of screening a large number of protein/protein interactions in parallel and in a cellular context, it was used here to test many mutant forms of Fas-DD simultaneously for their ability to bind FADD-DD. NMR spectroscopy then provides an attractive means to further analyse these mutants and the death domain interactions *in vitro*.

4.1.1 Previous reports of mutational analysis of Fas-DD

There have been several previous studies of mutations of FasL, Fas and FADD; this is unsurprising since mutations in the Fas signalling pathway lead to the onset of the autoimmune disease ALPS, as discussed in Chapter 1. The symptoms of ALPS type 1a are attributed to failure of the FasL-induced apoptotic signalling pathways specifically resulting from mutations in Fas. Interestingly, it has been observed that the death domain of Fas is particularly disposed to mutation since more patients presenting with the symptoms of ALPS have mutations in the death domain than in any other region of Fas (Martin *et al.*, 1999). Such Fas-DD mutations apparently lead to a disruption of the Fas/FADD interaction and abrogate Fas-induced apoptosis leading to the ALPS phenotype (Vaishnaw *et al.*, 1999).

The strong link between Fas and disease allows the acquisition of data on Fas-DD mutations from both clinical (Fisher *et al.*, 1995; Bettinardi *et al.*, 1997; Sneller *et al.*, 1997; Jackson *et al.*, 1999; Martin *et al.*, 1999; Rieux-Laucat *et al.*, 1999; Vaishnaw *et al.*, 1999; Peters *et al.*, 1999; Siegel *et al.*, 2000; Straus *et al.*, 2001; van den Berg *et al.*, 2002; Rieux-Laucat *et al.*, 2003b) as well as biochemical studies (Huang *et al.*, 1996; Eberstadt *et al.*, 1997)). Table 4.1 outlines the known naturally occurring and artificially engineered Fas-DD mutations and their effects. Since this study is solely interested in finding individual amino-acid residues that affect FADD binding, only missense mutations are listed (i.e. nonsense, deletion and insertion mutants are not directly relevant to this study and are not included in Table 4.1).

Missense mutations in Fas-DD have also been found in examples of other conditions such as non-Hodgkin's lymphoma (Gronbaek *et al.*, 1998), gastric cancer (Park *et al.*, 2001), non-small cell lung cancer (Lee *et al.*, 1999) and squamous cell carcinoma (Lee *et al.*, 2000). However the role of Fas mutations in these diseases remains unclear and hence, unlike many of the ALPS-related mutations, they cannot be presumed to affect FADD binding.

The mutation data from Table 4.1 is summarised in Figure 4.1 in the form of a linear map of the structure of Fas-DD indicating the positions of individual mutation sites. It can be seen from this figure that there is no obvious clustering of these mutation sites in

any specific region of the death domain and hence there is no clear indication of how this data fits with FADD binding. One problem with the analysis of the mutations presented in Table 4.1 is that the majority of these mutants have not been analysed at the molecular level. Without such molecular analysis it remains unknown as to whether these mutations affect the overall structure of Fas-DD. This aspect is the subject of the next section.

4.1.2 Structural mutations

Before drawing any conclusions about the residues outlined in Table/Figure 4.1 in terms of their relevance for FADD interaction, it is imperative to understand the effects of these mutations on the three-dimensional structure of Fas-DD. Since the biological function of a protein is intrinsically linked to its 3D structure, any disruption to its structure resulting from amino acid substitutions of critical residues will almost certainly cause the loss of that function.

It is quite possible for a single amino-acid change to disrupt the whole, or key parts of, a protein's structure. Therefore, one must distinguish between mutations that disrupt Fas/FADD interactions by altering the surface characteristics of Fas-DD without a major impact on the polypeptide fold (and are therefore of interest to this study) and those mutations that knock out the function of Fas-DD through global or partial disruption of its 3D structure. An example of one such "structural mutation" is the *lpr*^{cg} mutation. Originally *lpr*^{cg} was discovered as a point mutation in murine Fas-DD that causes an ALPS-like syndrome including lymphoproliferation and splenomegaly (Matsuzawa *et al.*, 1990). This mutation was later mapped to residue I246 in murine Fas-DD (which is mutated to asparagine in the *lpr*^{cg} mouse). The solution structure of human Fas-DD with the equivalent mutation – Fas-DD-V238N – was later investigated by NMR spectroscopy (Eberstadt *et al.*, 1997) and this structure reveals a unfolded and disordered region of the polypeptide chain corresponding to the α3 helix. This result suggests that the buried V238 side chain, part of the loop that connects α2 and α3, is important in maintaining the regular structure of the a3 helix and suggests that the side chains projecting from α3 may play a significant role in the interaction with FADD.

Mutation	Effects	Reference
Y216C	ALPS type 1a, reduced FasL-induced apoptosis	A
T225P	ALPS type 1a, no FADD binding, reduced FasL-induced apoptosis, death domain unfolded	B, C
T225K	ALPS type 1a	D
G231A	ALPS type 1a, no FADD binding, reduced FasL-induced apoptosis, death domain unfolded	B
V233F	ALPS type 1a	K
V233L	ALPS type 1a	K
R234A	Reduced FADD binding	E
R234Q	ALPS type 1a, no FADD binding, reduced FasL-induced apoptosis	B, F
R234P	ALPS type 1a, no FADD binding, reduced FasL-induced apoptosis, death domain unfolded	G
G237D	ALPS type 1a	K
G237S	ALPS type 1a	K
V238N	Human equivalent of the murine *lpr*^{cg} mutation. Murine Fas-I246N mutation has ALPS-like phenotype, death domain partially unfolded, knocks out FADD binding,	H
E240A	Reduces FADD binding	E
A241D	ALPS type 1a, abrogated FasL-induced apoptosis,	B
A241V	ALPS type 1a, no FADD binding, abrogated FasL-induced apoptosis	G
I243R	ALPS	K
I243T	ALPS	K
D244A	No FADD binding	E
D244V	ALPS type 1a, no FADD binding, abrogated FasL-induced apoptosis	B
D244Y	ALPS type 1a, no FADD binding, reduced FasL-induced apoptosis, death domain unfolded	G
D244G	ALPS type 1a, no FADD binding, abrogated FasL-induced apoptosis	G
E245A	Reduced FADD binding	E
K247A	No Fas-DD self-aggregation	E
T254I	ALPS type 1a	G, C
T254K	ALPS type 1a	K
E256G	ALPS type 1a	C, I
W265C	ALPS type 1a	K
L268P	ALPS type 1a	K
D276A	No reported effect	E
K283A	Reduced FADD binding	E
I294S	ALPS type 1a, no FADD binding, reduced FasL-induced apoptosis, death domain unfolded	B, J
L299A	No reported effect	E

Table 4.1: Human Fas-DD missense mutations reported in the literature and their effects in relation to FADD binding and disease.

Reference key: A: (Bettinardi *et al.*, 1997); B: (Martin *et al.*, 1999); C: (Straus *et al.*, 2001); D: (Jackson *et al.*, 1999); E: (Huang *et al.*, 1996); F: (van den Berg A. *et al.*, 2002); G: (Vaishnaw *et al.*, 1999); H: (Eberstadt *et al.*, 1997); I: (Peters *et al.*, 1999); J: (Sneller *et al.*, 1997); K: (Rieux-Laucat *et al.*, 2003b)

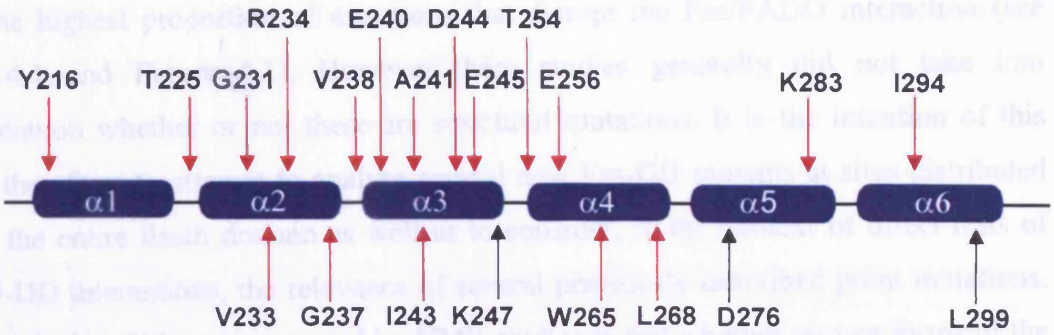

Figure 4.1: Sites of previously reported missense point mutations in Fas-DD mapped onto a linear representation of the domain. Residues reported to be disrupt FADD binding when mutated are shown by red arrows. Those residues that, when mutated, have no effect on FADD binding are indicated by black arrows. α1-α6 denote the six α-helices of Fas-DD.

However, because the helix is completely disrupted in this mutant, it is not possible to precisely identify which of the α3 side chains are important in the interaction of the wild-type protein with FADD.

A convenient method to establish whether a particular mutant alters the overall structure of a protein is to use NMR spectroscopy. Comparison of the [^{1}H-^{15}N]-HSQC spectrum of the wild-type protein to that of a mutant variants of the same protein is an excellent way to identify and characterise the nature and extent of a structural mutation. Any change in the overall structure of a protein will lead to gross changes in its HSQC spectrum – such as loss of chemical shift dispersion and/or cross-peak intensity. This technique was employed by (Martin *et al.*, 1999) in an excellent study on the molecular basis of ALPS. Here six Fas-DD missense mutations derived from patients with ALPS were analysed not only for their ability to induce apoptosis, but also for the structural integrity of the death domain by 2D [^{15}N-^{1}H]-HSQC spectroscopy. In this paper three out of the six point mutations analysed (T225P, G231A and I294S) were shown to disrupt the structure of Fas-DD. However, three other single residue mutations also derived from ALPS patients (R234Q, A241D and D244V) were shown to give HSQC spectra very similar to the wild-type domain and so these three side-chains can be presumed to be important in FADD-binding.

Previous studies on Fas-DD mutations have concluded that the region around α-helices 2 and 3 is the most important region for FADD binding because this region seems to

have the highest proportion of mutations that disrupt the Fas/FADD interaction (see Table 4.1 and Figure 4.1). However these studies generally did not take into consideration whether or not these are structural mutations. It is the intention of this study, therefore, to attempt to analyse several new Fas-DD mutants at sites distributed across the entire death domain as well as to consider, in the context of direct tests of FADD-DD interactions, the relevance of several previously described point mutations. Such analysis will be accompanied by NMR studies to test whether mutant forms of the domain are still correctly folded.

4.2 Fas-DD mutations chosen for analysis

Several criteria were used in the selection of sites in Fas-DD to mutate for this study. First, in an attempt to preserve the overall 3D structure of the protein, and because we it can be presumed that only solvent-exposed residues can interact with FADD, only residues from the surface of the protein were chosen for mutation. The program "NACCESS" (Hubbard *et al.*, 1991) was used to determine the solvent accessibility of all of the Fas-DD side-chains based on the NMR solution structure of this domain (Huang *et al.*, 1996), PDB entry 1ddf. The NACCESS algorithm simulates the rolling of a probe over the van der Waals surface of a protein structure and subsequently calculates the percentage surface exposure of each residue relative to a fully exposed side chain (relative surface exposure – RSE). The NACCESS output data for Fas-DD is shown in Table 4.2. The utility of this approach is reflected in the data for the mostly exposed R234, A241 and D244 side chains and for the highly buried V238 side chain (the lpr^{cg} mutation site) – the RSE value for this residue is 0.2%. It is straightforward to understand from this information how mutation of the hydrophobic valine side chain to the more polar asparagine could lead to a local unfolding of the Fas-DD structure. Observation of the Fas-DD 3D structure – using Swiss-PDB Viewer – was also used to confirm that the side-chains of the residues selected for mutation are on the surface of the protein. Secondly, due to the evidence that the Fas-DD/FADD-DD interaction is almost certainly dominated by electrostatic forces (Bang *et al.*, 2000), it was decided to focus on the charged residues. It was also decided to select residues from several different surface regions of the protein in order to test whether areas other than the α2-α3 region are important in the FADD-DD interaction. Finally, several previously

reported substitutions were also selected to help validate the assays used in this study, as well as, in some cases, to check whether these alterations correspond to structural mutations.

Residue	No.	RSE	Residue	No.	RSE	Residue	No.	RSE
GLU	202	72.2	GLY	237	71.5	LYS	272	84.8
THR	203	77.8	VAL	238	0.20	GLU	273	63.1
VAL	204	89.0	ASN	239	60.7	ALA	274	4.30
ALA	205	61.7	GLU	240	59.7	TYR	275	13.2
ILE	206	57.7	ALA	241	75.7	ASP	276	43.2
ASN	207	95.8	LYS	242	51.6	THR	277	22.4
LEU	208	29.5	ILE	243	0.50	LEU	278	0.00
SER	209	80.5	ASP	244	60.3	ILE	279	16.4
ASP	210	86.2	GLU	245	78.2	LYS	280	67.1
VAL	211	9.60	ILE	246	12.4	ASP	281	16.2
ASP	212	71.1	LYS	247	40.5	LEU	282	0.00
LEU	213	6.60	ASN	248	84.1	LYS	283	57.4
SER	214	53.5	ASP	249	66.6	LYS	284	82.4
LYS	215	86.0	ASN	250	19.5	ALA	285	4.70
TYR	216	12.4	VAL	251	64.9	ASN	286	100
ILE	217	0.20	GLN	252	98.0	LEU	287	16.7
THR	218	53.9	ASP	253	35.2	CYS	288	57.7
THR	219	52.0	THR	254	49.6	THR	289	47.3
ILE	220	0.00	ALA	255	71.2	LEU	290	1.30
ALA	221	0.00	GLU	256	62.9	ALA	291	3.70
GLY	222	61.8	GLN	257	4.20	GLU	292	66.1
VAL	223	46.9	LYS	258	15.0	LYS	293	37.8
MET	224	1.90	VAL	259	18.3	ILE	294	0.00
THR	225	48.3	GLN	260	48.3	GLN	295	51.2
LEU	226	9.70	LEU	261	0.10	THR	296	55.6
SER	227	71.6	LEU	262	0.00	ILE	297	17.8
GLN	228	38.0	ARG	263	59.3	ILE	298	3.10
VAL	229	0.00	ASN	264	25.6	LEU	299	61.0
LYS	230	18.3	TRP	265	0.30	LYS	300	42.4
GLY	231	33.5	HIS	266	19.6	ASP	301	54.0
PHE	232	0.00	GLN	267	81.5	ILE	302	58.5
VAL	233	0.00	LEU	268	37.6	THR	303	55.7
ARG	234	29.8	HIS	269	54.5	SER	304	12.9
LYS	235	58.8	GLY	270	42.0	ASP	305	45.4
ASN	236	17.0	LYS	271	89.8	SER	306	92.4
						GLU	307	71.3

Table 4.2: NACCESS data from Fas-DD (PDB file 1ddf). RSE – relative solvent exposure – is the calculated percentage exposure of individual residues in the structure relative to a fully exposed side-chain. Residues with an RSE value of less than 30 % have been shaded in grey and were not considered as candidates for mutation in this study. The *lpr*^{cg} mutation site V238 is highlighted in yellow.

Tables 4.3 and 4.4 present a list of the Fas-DD mutations as chosen for analysis together with a rationale for each selection. Table 4.3 describes previously reported mutants that are further characterised in this study and Table 4.4 describes the novel mutants designed and characterised in this work. PCR primers (see Appendix 3) were designed and used to introduce the mutations into the Gb1-Fas-DD-His construct using the QuickChange site directed mutagenesis kit (Stratagene). All mutant constructs were confirmed by DNA sequencing.

Table 4.3: Previously reported Fas-DD mutations also analysed in this study

Substitution	Rationale	Reference
D244A	Already characterised, this ALPS mutation is an excellent negative control for the assays used in this study.	(Huang *et al.*, 1996)
K247A	This mutation was used in previously reported NMR studies but has not yet been tested by yeast two-hybrid analysis.	(Huang *et al.*, 1996)
A241D	Corresponds to a naturally occurring ALPS mutation and a surface exposed residue. Requires confirmation as a non-structural mutation.	(Martin *et al.*, 1999)
R234A	R234 is a common ALPS mutation site that has also been characterised *in vitro* but is not confirmed as a non-structural mutation.	(Huang *et al.*, 1996)
E240A	Characterised *in vitro* as a non-FADD-DD binding mutant, but not characterised at the structural level.	(Huang *et al.*, 1996)
D267N	Mutation of this residue is reported to have no effect on FADD binding. This mutation therefore provides another control for this study.	(Huang *et al.*, 1996)

4.3 Yeast two-hybrid analysis of Fas-DD mutations

The wild-type and the twenty different mutant Fas-DD constructs listed in Tables 4.3 and 4.4 were tested for FADD-DD interaction using the yeast two-hybrid assay in exactly the same way as described in Section 3.2.2. Each mutant pOAD-Fas-DD construct was individually tested for self-activation by growth on medium lacking leucine and histidine with a range of 3-AT concentrations. None of the mutant Fas-DD constructs showed any growth on plates with medium containing more than 2 mM 3-AT indicating that they were all suitable for interaction analysis with $pOBD_2$-FADD-DD. The yeast strains containing each Fas-DD construct was individually mated with the strain transformed with the $pOBD_2$-FADD-DD construct and the resulting cells were

tested for their ability to grow on leu$^-$/trp$^-$/his$^-$ plates. Mating experiments were repeated twice using two separate colonies of each Fas-DD mutant to ensure reproducibility. Cells expressing wild–type or mutant forms of Fas-DD that were able to interact with FADD-DD showed signs of proliferation within seven days. Cells containing Fas-DD mutants that were unable to productively interact with FADD-DD showed no sign of proliferation after two weeks incubation at 30°C.

Table 4.4: Novel mutations in Fas-DD designed and analysed in this study

Substitution	Rationale
S227A	S227 is a solvent-exposed polar residue on helix 2. This mutation should give an idea of how sensitive the Fas-DD/FADD-DD interaction is to small alterations in polarity at the protein surface.
N239Q	This mutation, in the putatively important helix 3 will test the sensitivity of the interaction to slight increases in steric bulk through the introduction of an extra methylene group.
E240Q	This mutant is very similar to, but more conservative than the E240A mutation as only the charged group is blocked – it is less likely to be a structural mutation.
K242A	K242 is a charged, solvent exposed residue on helix 3. Mutation of this residue to alanine will test the importance of this side chain in a region of Fas-DD thought to be associated with FADD-DD binding.
N248D	This mutant will test the effect of the introduction of a charged group in the putatively important helix 3 region of Fas-DD.
V251Q	Mutation of this hydrophobic surface residue to glutamine will test the effect of subtle changes in the exposed hydrophobic surface of the Fas-DD domain.
Q252A	This mutation will test the importance of residue 252, sited in helix 4, by removing the large, solvent-exposed glutamine side-chain.
E256Q	E256 is a charged, surface exposed residue that, when mutated to glycine, causes ALPS. This mutation simply removes the negative charge and should keep the domain structurally intact.
R263A	R263 is a charged, surface exposed residue sited in helix 4, a region of Fas-DD not previously thought to be important in FADD binding
Q267E	Residue 267 is sited very close to R263 (on the same surface of helix 4) and is also highly solvent exposed. This mutation will test the introduction of an extra negative charge to this region of the protein surface.
K272A	K272 is a charged, solvent exposed residue sited in the loop between helices 4 and 5 of Fas-DD, a region not previously thought to be important in FADD binding.
K280A	Mutation of residue K280 will test the effect of removing a positive charge from the surface of helix 5, a region of Fas-DD not previously thought to be important in FADD binding.
K284Q	K284 is on the surface of helix 5, a region not previously thought to be important in FADD binding. Glutamine was chosen as the replacement residue in order to remove the charge from the side chain whilst conserving the structural integrity of the domain.

The results from one of these mating experiments are shown in Figure 4.2 and the overall results from this yeast two-hybrid experiment are summarised in Table 4.5. The second experiment gave essentially the same results as the experiment shown in Figure 4.2 except in the case of the R234A mutation which exhibited positive FADD-DD interaction properties in one experiment but not in the other and hence had to be further analysed *in vitro* by NMR (see Section 4.4).

To facilitate discussion of the results of the yeast two-hybrid experiment, the set of Fas-DD constructs employed is divided into three sets of mutations in Table 4.5. Those mutations that resulted in no yeast growth in the two-hybrid assay are defined as "knock-out" mutations. Those mutations that resulted in some growth, but lower growth than wild-type Fas-DD, are defined as "reduced interaction". It is probable – but it requires confirmation by other methods – that the reduced interaction behaviour corresponds to a death domain that can still interact with FADD-DD but with a weaker affinity than the wild-type protein. Finally there are six Fas-DD mutants that show no change in the amount of yeast growth relative to wild-type Fas-DD. This last group is listed in Table 4.4 as "no effect" mutations.

"Knock-out" mutations	**Reduced interaction**	**No effect**
N239Q	V251Q	S227A
E240A	K280A	K247A
E240Q	N286K	R263A
A241D		Q267E
K242A		D276N
D244A		
N248D		
Q252A		
E256Q		
K272A		
K284Q		
R234A*		

Table 4.5: Summary of the effects of Fas-DD mutations on FADD-DD binding based on yeast two-hybrid assay data. *R234A appears in the knock-out mutation column only after further NMR analysis (see Section 4.4).

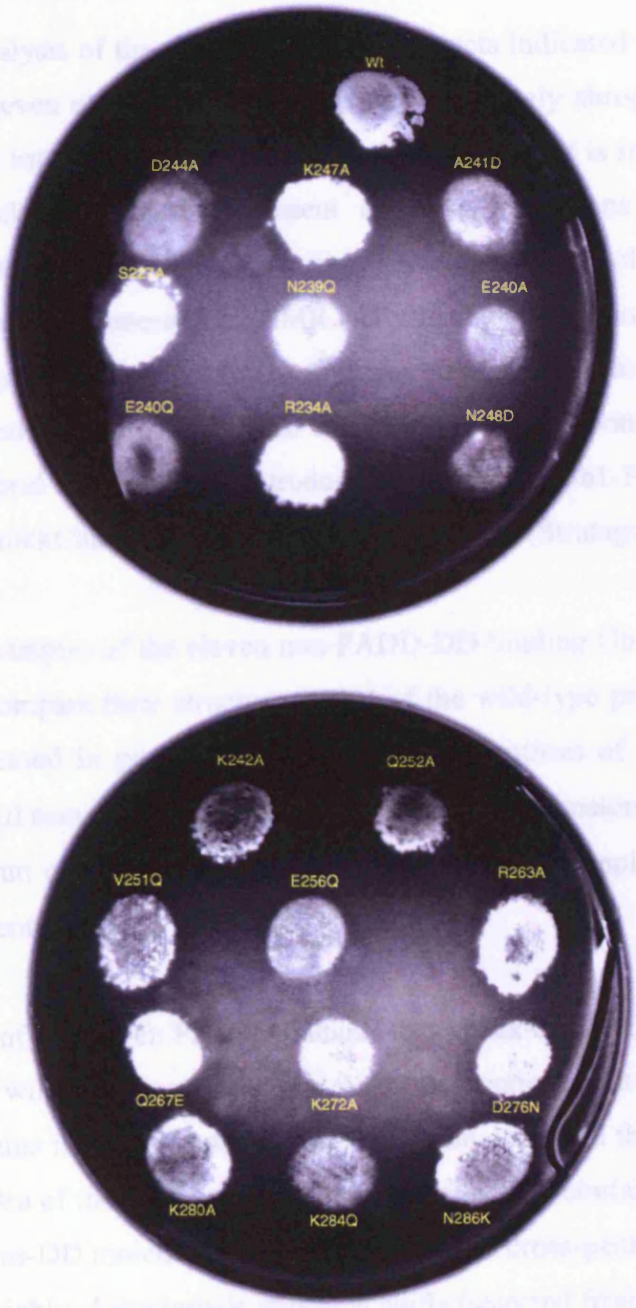

Figure 4.2 Analysis of Fas-DD mutations using yeast two-hybrid assay. The assay was carried out using FADD-DD as the bait protein and wild-type or mutant Fas-DD as the prey. The plates photographed here contain $trp^-/leu^-/his^-$ medium and hence growth on these plates indicates a positive bait/prey interaction. For this experiment plates were photographed after ten days incubation at 30^0C.

The plates shown here are representative of two independent experiments – with the exception of the R234A mutant (see text for details).

4.4 NMR studies of Fas-DD mutants

Yeast two-hybrid analysis of the mutant Fas-DD constructs indicated that eleven of the mutants (including seven of the novel mutation set) completely abrogate the ability of this death domain to interact with the death domain of FADD. It is important to assess whether these knock-out mutants represent structural mutations or whether the individually substituted side chains are significant in terms of the FADD-DD interaction. This issue was assessed by NMR analysis of Fas-DD mutants expressed in the form of His-tagged Gb1-Fas-DD fusion proteins, similar to the analysis of the wild-type protein described in Chapter 3. To that end, mutations corresponding to those used in the yeast two-hybrid analysis were introduced into the pETGb1-Fas-DD expression plasmid using the QuickChange site directed mutagenesis kit (Stratagene).

^{15}N-labelled NMR samples of the eleven non-FADD-DD-binding Gb1-Fas-DD mutants were produced to compare their structure to that of the wild-type protein. All of these proteins were expressed in good yield and sufficient quantities of each protein were produced for a 500 µl sample of greater than 0.4 mM. Two dimensional [^{1}H-^{15}N]-HSQC experiments were run on each of the twelve mutant Fas-DD samples and the spectra from these experiments are shown in Figure 4.3.

The HSQC spectra of the eleven Fas-DD mutants that knock-out FADD-DD binding are very similar to the wild-type protein and so it can be assumed that the overall fold of these mutated proteins is the same as the wild-type domain. Since the HSQC spectra in Figure 4.3 are spectra of the Gb1-Fas-DD fusion proteins they contain cross peaks from both the Gb1 and Fas-DD moieties. For clarity, then, three cross-peaks arising from Fas-DD residues with highly characteristic chemical shifts (selected from the analysis of the wild-type Gb1-Fas-DD spectrum presented in Chapter 3) have been highlighted in each spectrum in Figure 4.3. The presence of these cross peaks in the mutant spectra, where they have essentially the same chemical shifts as in the wild-type spectrum, helps to indicate that Fas-DD has the same fold in these mutant constructs as in the wild-type domain. An important conclusion from these observations is that each of these mutations must disrupt the Fas-DD/FADD-DD interaction in the yeast two-hybrid assay by altering the surface of the Fas-DD domain in such a way that FADD-DD can no-longer bind.

The remaining Fas-DD mutants that retain FADD-DD binding in the yeast two-hybrid assay were then compared to the wild-type protein in an NMR-based binding assay. These experiments were carried out for two reasons, first to assess the validity of the yeast two-hybrid assay and second to test the theory that the subset of mutant forms of Fas-DD that appeared to show a reduced affinity in the yeast two-hybrid assay might show a correspondingly weaker interaction with FADD-DD in the *in vitro* NMR experiments.

Unlabelled protein samples of the six Fas-DD mutants that showed binding activity close to wild-type levels in the yeast two-hybrid assay and the three reduced interaction mutants were produced as Gb1-Fas-DD constructs. All but one of these proteins were well expressed and could be concentrated to at least 0.4 mM without showing signs of precipitation. The Gb1-Fas-DD-Q267E construct gave a lower yield of soluble expressed protein (~10 mg/L of culture compared to >20 mg/L for the other mutants) and showed signs of precipitation at concentrations above 0.25 mM. A ^{15}N-labelled sample of this protein was produced to examine whether the protein was becoming aggregated as the concentration was increased.

Figure 4.3n shows an HSQC spectrum of a ~0.2mM sample of Gb1-Fas-DD-Q267E which shows many overlapping peaks and poor resolution compared to the spectrum of the wild-type protein. The most prominent peaks appear to derive from the Gb1 part of the fusion protein. These spectral features are indicative of an aggregated protein and so, although giving a positive yeast two-hybrid result, this mutant was not further analysed *in vitro*. It is not clear whether the aggregation also operates at the concentrations of protein relevant inside the nucleus of a yeast cell, so this result may represent artifactual behaviour that is a result of the high concentration required for NMR spectroscopy.

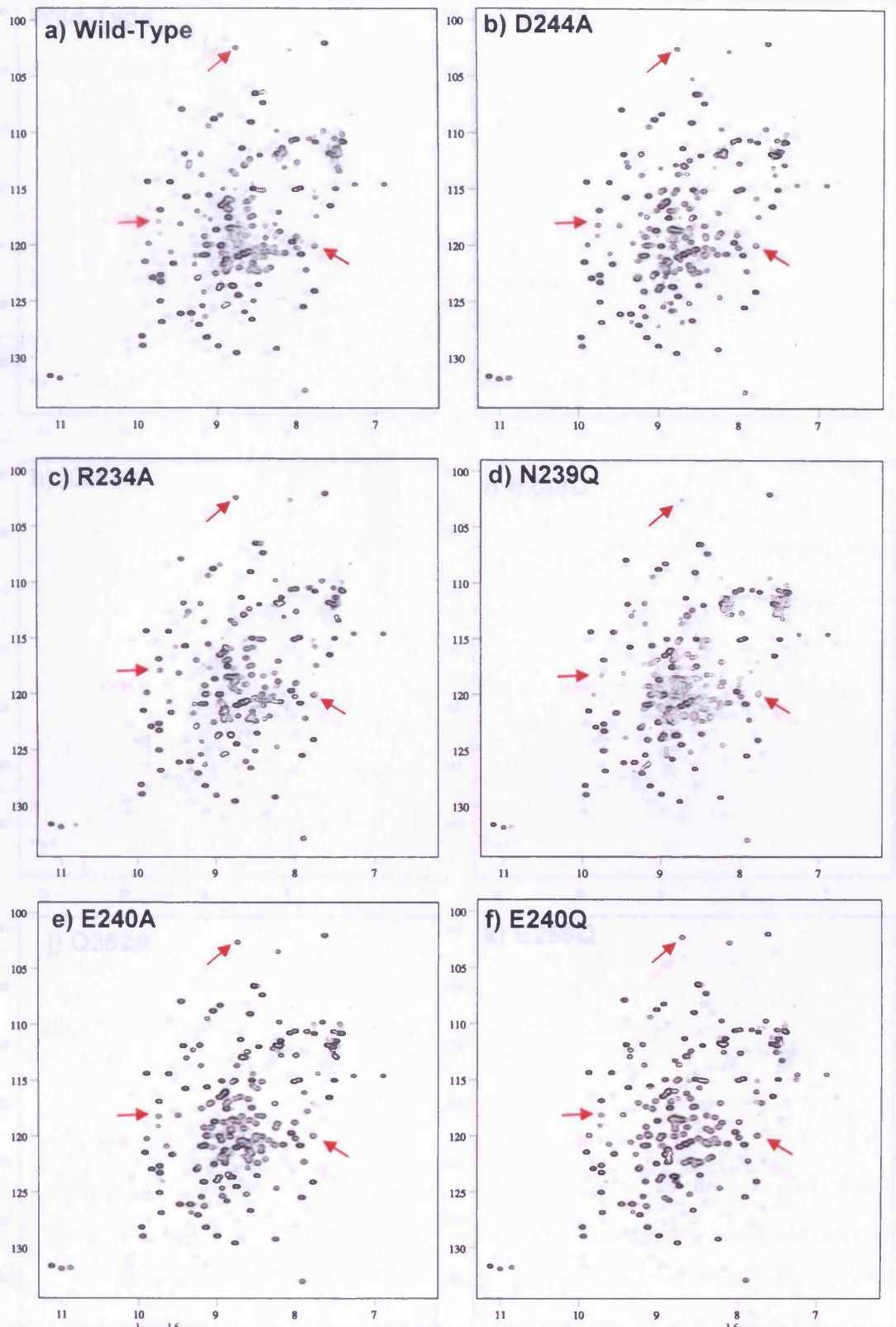

Figure 4.3: [^{1}H-^{15}N]-HSQC spectra of wild-type (a) and mutant (b-k) ^{15}N-Gb1-Fas-DD proteins. In all spectra the horizontal axis represents ^{1}H frequency (in ppm) and the vertical axis the ^{15}N frequency (in ppm). All mutated Fas-DD proteins that have no FADD-DD binding capacity (b-j) show essentially the same chemical shift dispersion as the wild-type domain. Red arrows indicate three examples of cross peaks from Fas-DD residues.

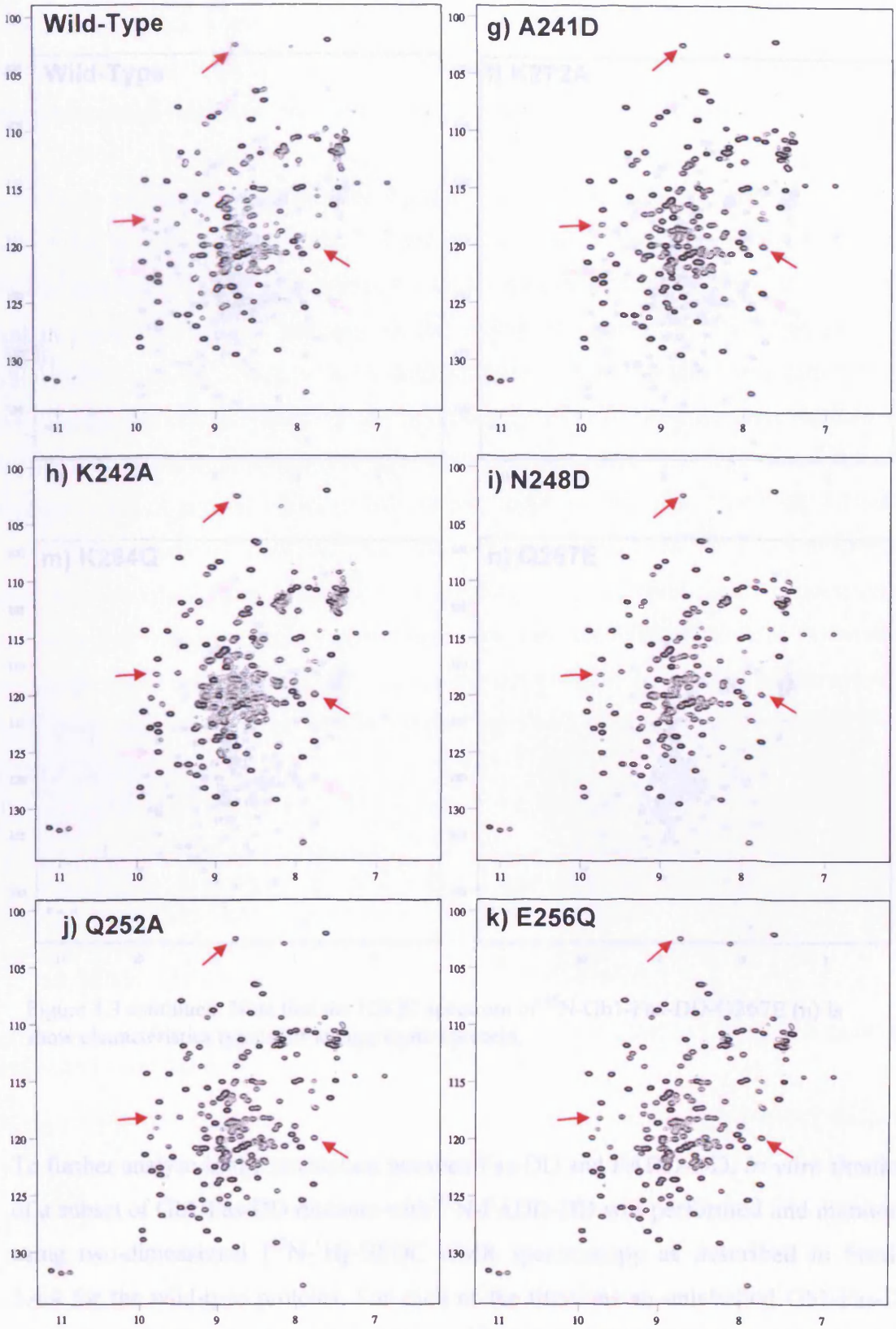

Figure 4.3 continued.

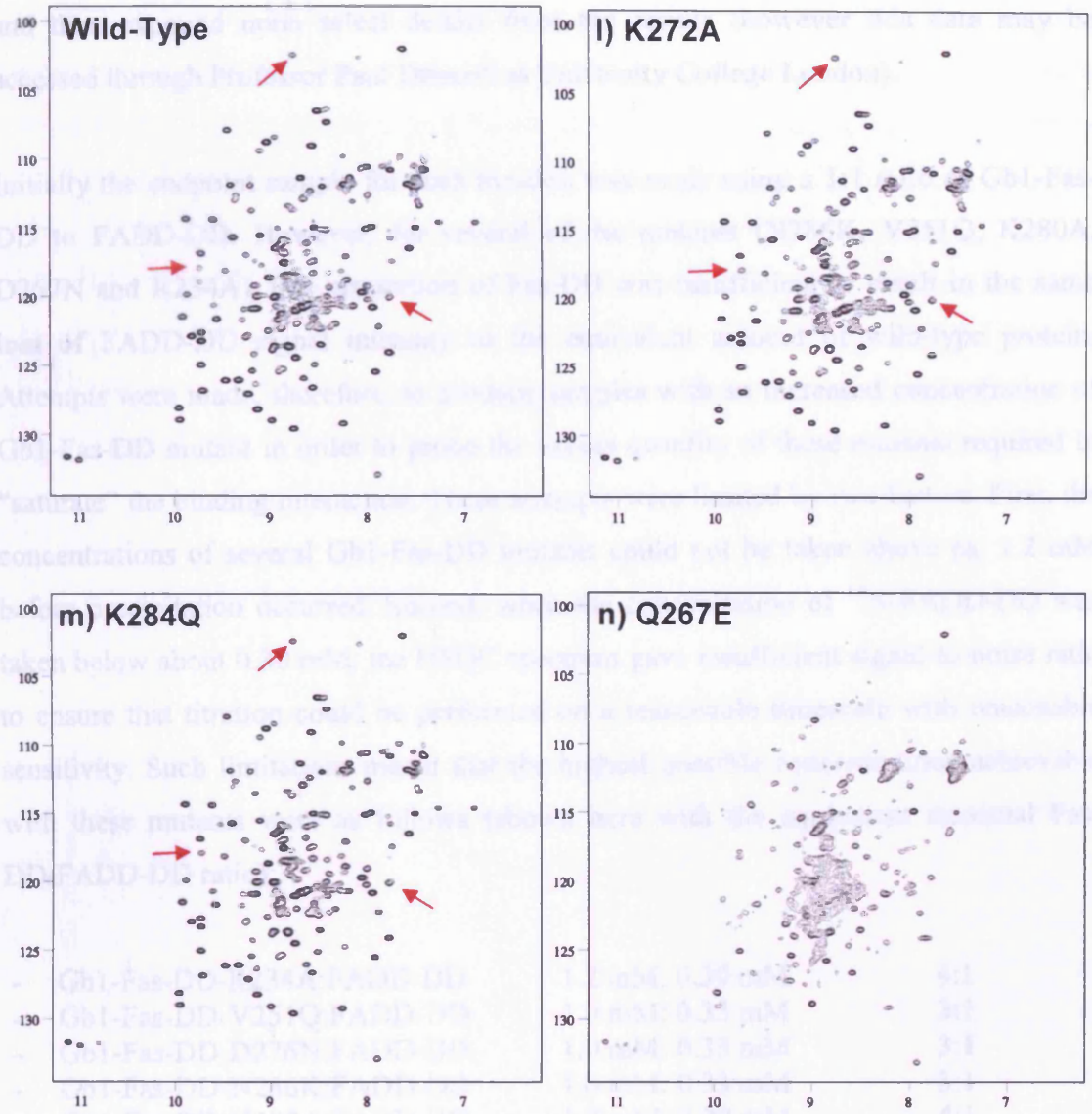

Figure 4.3 continued. Note that the HSQC spectrum of ^{15}N-Gb1-Fas-DD-Q267E (n) is show characteristics typical of an aggregated protein.

To further analyse in the interaction between Fas-DD and FADD-DD, *in vitro* titrations of a subset of Gb1-Fas-DD mutants with ^{15}N-FADD-DD was performed and monitored using two-dimensional [^{15}N-^{1}H]-HSQC NMR spectroscopy as described in Section 3.4.4 for the wild-type proteins. For each of the titrations an unlabelled Gb1-Fas-DD mutant protein sample was titrated into a ^{15}N-labelled FADD-DD sample using the same mixing strategy that keeps the concentration of FADD-DD constant throughout the titration (see Section 3.4.4.1). The amount of data recorded in these titration experiments is large and it is not sensible to reproduce the NMR spectra here. Rather,

for simplicity, I state here the general conclusions deriving from these NMR titrations and then expound upon select details from the results (however this data may be accessed through Professor Paul Driscoll at University College London).

Initially the endpoint sample for each titration was made using a 1:1 ratio of Gb1-Fas-DD to FADD-DD. However, for several of the mutants (N286K, V251Q, K280A, D267N and R234A), this proportion of Fas-DD was insufficient to result in the same loss of FADD-DD signal intensity as the equivalent amount of wild-type protein. Attempts were made, therefore, to produce samples with an increased concentration of Gb1-Fas-DD mutant in order to probe the excess quantity of these mutants required to "saturate" the binding interaction. These attempts were limited by two factors. First, the concentrations of several Gb1-Fas-DD mutants could not be taken above ca. 1.2 mM before precipitation occurred. Second, when the concentration of ^{15}N-FADD-DD was taken below about 0.30 mM, the HSQC spectrum gave insufficient signal-to-noise ratio to ensure that titration could be performed on a reasonable timescale with reasonable sensitivity. Such limitations meant that the highest possible concentrations achievable with these mutants were as follows (shown here with the equivalent maximal Fas-DD/FADD-DD ratio):

- Gb1-Fas-DD-R234A:FADD-DD	1.2 mM: 0.30 mM	4:1
- Gb1-Fas-DD-V251Q:FADD-DD	1.0 mM: 0.33 mM	3:1
- Gb1-Fas-DD-D276N:FADD-DD	1.0 mM: 0.33 mM	3:1
- Gb1-Fas-DD-N286K:FADD-DD	1.0 mM: 0.33 mM	3:1
- Gb1-Fas-DD-K280A:FADD-DD	1.2 mM: 0.30 mM	4:1

(Higher ratios were possible for the R234A and K280A mutants as these two proteins could be concentrated to a maximum of roughly 1.4 mM)

Figure 4.4 shows combined results of the titrations of the seven Gb1-Fas-DD mutants that were shown by yeast two-hybrid analysis to still interact with FADD-DD and that were tractable for NMR studies (the wild-type Gb1-Fas-DD and the Gb1-Fas-DD-D244A mutant titrations are also presented for comparison). None of the mutants exhibited an alternate behaviour in which increasing concentrations of Fas-DD gave rise to selective chemical shift changes of the FADD-DD cross peaks without the loss of signal intensity. It can be seen that the K247A and R263A Gb1-Fas-DD mutants behave in essentially the same way as the wild-type Gb1-Fas-DD protein providing further evidence that the corresponding substitutions have no bearing on the interaction of Fas-

DD with FADD-DD. The D267N mutation, although observed to have a similar level of interaction to wild-type Fas-DD in the yeast two-hybrid assay was shown to slightly attenuate the FADD-DD interaction in the NMR assay. However, such an attenuation was seen to a much greater extent by the three Fas-DD mutants, V251Q, N286K and K280A all of which required approximately five-times as much protein as the wild-type Gb1-Fas-DD to produce an equivalent diminution of the FADD-DD signal intensity. This behaviour in the NMR titrations may be associated with a lower FADD-DD binding activity and this data correlates well with the yeast two-hybrid results for the same three mutants which were described as having a "reduced activity" relative to wild-type Fas-DD.

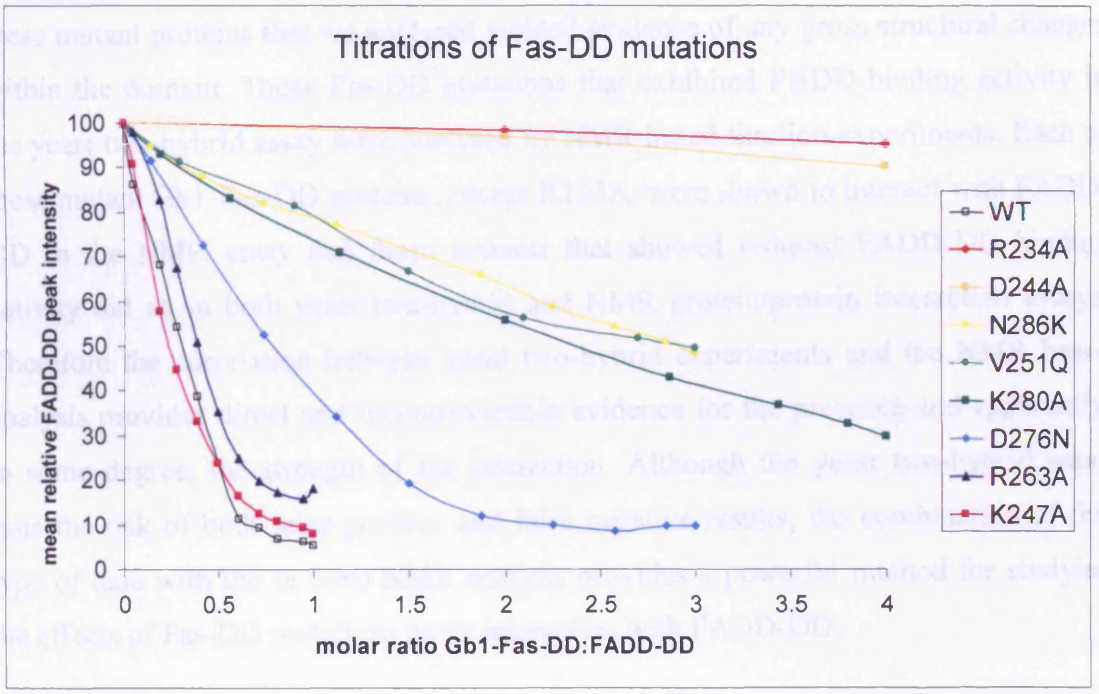

Figure 4.4 NMR titrations of Fas-DD mutants. Titrations of various Gb1-Fas-DD constructs into ^{15}N-FADD-DD followed by the measurement of the relative aggregate FADD-DD cross peak intensities from HSQC experiments.

Overall, therefore, there is a very high degree of correlation between the results from the yeast two-hybrid assay and those from the assessment of protein-protein interaction by NMR spectroscopy. All but one of the Fas-DD mutants show agreement between the two assays. The R234A mutant gave inconsistent results in the yeast-two hybrid assay, although, as it is a previously described naturally occurring ALPS mutation it represents a form of Fas-DD that is not expected to bind FADD-DD, and indeed, when analysed

by NMR, no binding activity could be seen. It remains unclear how this particular mutation gave rise to a false positive result in one instance of the yeast two-hybrid trials.

4.5 Conclusions from mutational analysis of the Fas death domain

Several conclusions can be drawn from this mutational study of Fas-DD. Firstly yeast two-hybrid analysis of a bank of 20 Fas-DD mutants gave reproducible results and showed that most of the mutations either significantly reduced or effectively eliminated the interaction with FADD-DD. Those side chain substitutions that knocked out the FADD-DD interaction were tested for their effect on 3D structure of Fas-DD by [^{1}H-^{15}N]-HSQC spectroscopy. Comparison with the wild-type spectrum showed that none of these mutant proteins that we analysed yielded evidence of any gross structural changes within the domain. Those Fas-DD mutations that exhibited FADD-binding activity in the yeast two-hybrid assay were analysed by NMR-based titration experiments. Each of these mutant Gb1-Fas-DD proteins, except R234A, were shown to interact with FADD-DD in the NMR assay and those mutants that showed reduced FADD-DD binding activity did so in both yeast two-hybrid and NMR protein/protein interaction assays. Therefore the correlation between yeast two-hybrid experiments and the NMR based analysis provides direct and incontrovertible evidence for the presence and apparently, to some degree, the strength of the interaction. Although the yeast two-hybrid assay runs the risk of both false positive and false negative results, the combination of this type of data with the *in vitro* NMR analysis provides a powerful method for studying the effects of Fas-DD mutations on its interaction with FADD-DD.

The results from NMR-based titrations showed that each mutant Gb1-Fas-DD protein (apart from Gb1-Fas-DD-D244A) titrated into ^{15}N-FADD-DD exhibited the same type of behaviour as the wild-type domain in producing an overall loss of signal intensity from the FADD-DD [^{1}H-^{15}N]-HSQC spectrum. As the simplest interpretation of this behaviour, we equate this progressive loss of signal with the formation of a hydrodynamically large complex between the two domains. Importantly, in each titration, several sharp FADD-DD signals – corresponding to side chains and residues from the flexible tails of the domain – were still observed, indicating that FADD-DD, and therefore the complex between the two death domains, remained in solution

throughout the titrations. Some differences are seen, however, between the relative concentrations of the mutant proteins that are required to reduce the FADD-DD signal intensity by an equivalent amount. The D276N, V251Q, K280A and N286K Fas-DD mutants required relatively higher protein concentrations to effect complete diminution of the FADD-DD signals. Presumably this behaviour can be attributed to these mutants possessing a reduced FADD-DD interaction affinity and, in the case of 3 out of 4 of these mutations (V251Q, K280A and N286K), is correlated with the decreased, but not abolished, interaction strength suggested by the results of the corresponding yeast two-hybrid assay trials.

From this mutational analysis several Fas-DD residues have been identified, that, when substituted, appear to knock out the FADD-DD interaction. This set of residues includes four previously described in the literature – D244A, R234A, A241D and E240A – which have all been shown to disrupt the interaction either *in vivo* or *in vitro* (see Table 4.1), but which have been analysed to varying levels. Of these four, only A241D has been previously fully described as a non-structural, ALPS-causing mutation (Martin *et al.*, 1999). Two others, R234A and D244A, had been described as FADD-DD knockout mutants in a biochemical (ELISA-based) study (Huang *et al.*, 1996) but had not been confirmed as non-structural mutations (although two very similar ALPS-causing mutations, R234Q and D244V had been shown to maintain the fold of Fas-DD (Martin *et al.*, 1999)). The present study has now confirmed that the R234A and D244A mutants have a native death domain fold. This result is especially important in the case of D244A mutation as this mutant was used previously as a negative control for FADD-DD binding (see Chapter 3). Finally the E240A mutant of Fas-DD had been shown in a biochemical study to knock out FADD interaction (Huang *et al.*, 1996) but in this work the protein has been proven to be a non-structural mutant. This study has therefore confirmed information about the D244A, R234A, A241D and E240A mutants and extended the knowledge of D244A, R234A and E240A as these proteins had not previously been structurally analysed.

Of the set of mutant Fas-DD proteins examined in this study, there are eight remaining, previously uncharacterised, Fas-DD mutations that have been shown by this work to knock out FADD-DD interaction in the yeast two-hybrid assay and yet to maintain the Fas-DD death domain structure as determined by NMR spectroscopy. These eight

mutants are as follows: N239Q, E240Q, K242A, N248D, Q252A, E256Q, K272A and K284Q. The E240Q mutation, perhaps unsurprisingly, has the same affect as the E240A mutation and it was chosen for analysis as a more conservative mutation in case the E240A mutation gave rise to structural perturbations. E256Q is a novel Fas-DD mutant but was chosen to test the importance of this residue that, when mutated to glycine, is reported to cause ALPS.

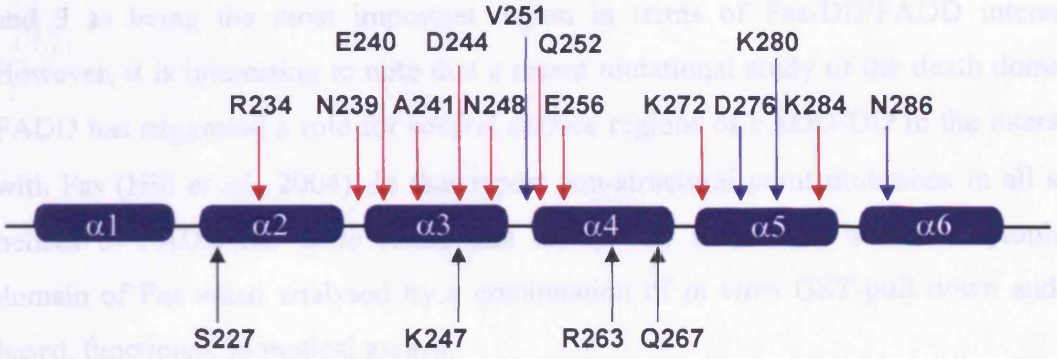

Figure 4.5: Sites of those point mutations in Fas-DD used in this study mapped onto a linear representation of the death domain. Residues that disrupt FADD-DD binding when mutated are indicated by red arrows. Blue arrows denote mutation sites that partially disrupt FADD binding. Those residues that, when mutated, have no effect on FADD binding are indicated by black arrows.

Taken as a whole this set of data represents the novel identification of six residues on the surface of Fas-DD that are apparently important for FADD-DD binding: N239, K242, N248, Q252, K272 and K284. Moreover, the importance of several other Fas-DD surface residues that have been previously described through their role in ALPS have been confirmed as being vital for FADD-DD binding: R234, E240, A241, D244, and E256. Four other Fas-DD residues – V251, D276, K280 and N286 – are shown to contribute to FADD-DD interaction as, when any of these residues is mutated, Fas-DD exhibits significantly reduced FADD-DD binding activity. Another interesting point is that two uncharged residues have been discovered, N239 and Q252, that, when mutated to other uncharged amino acids (glutamine and alanine respectively), abrogate the FADD-DD binding. This observation shows that, despite the observation that the Fas-DD/FADD-DD interaction appears to rely heavily on electrostatic interactions, there is almost certainly a hydrophobic and/or shape recognition component as well. This is an important observation since previous studies of the interactions between these domains have focussed purely on the charged residues. Finally, of the 20 residues analysed, only

four show no apparent effect on FADD-DD binding upon mutation: mutations of Fas-DD-S227, -K247, -R263 and -Q267 gave rise to behaviour indistinguishable from the wild-type protein in our binding assays.

The mutation data is summarised in Figure 4.5. Here we can see that there are residues from Fas-DD α-helices 2, 3, 4, 5 and 6 that appear to be important for FADD-DD interaction. This is perhaps unexpected as previous studies have focussed on helices 2 and 3 as being the most important region in terms of Fas-DD/FADD interaction. However, it is interesting to note that a recent mutational study of the death domain of FADD has suggested a role for several surface regions of FADD-DD in the interaction with Fas (Hill *et al.*, 2004). In that report non-structural point mutations in all six α-helices of FADD-DD were found that disrupt the interaction with the cytoplasmic domain of Fas when analysed by a combination of *in vitro* GST-pull down and cell-based, functional, biological assays.

Figure 4.6 summarises the Fas-DD and FADD-DD mutagenesis data from the present study together with that of Hill *et al.* 2004. This figure indicates that there are expansive surfaces on both of these death domains that are implicated by the various mutagenesis and assay data in the interaction between the two proteins. It is important to note that we can only draw conclusions for those residues that have been mutated but there are many other residues on the surface of these proteins that remain to be thoroughly examined and that may also play a role in this interaction. However, we can see that the two sets of data presented in Figure 4.6 are sufficient to allow for further analysis of this interaction in the context of other death-fold interactions.

4.6 A model for Fas-DD/FADD-DD interaction?

We have seen from the mutagenesis data that both the Fas and FADD death domains appear to utilise multiple surface regions in their mutual interaction. This observation is consistent with the data from Chapter 3 that illustrated the formation of an apparently hydrodynamically large, stable but reversible complex between the two death domains in solution.

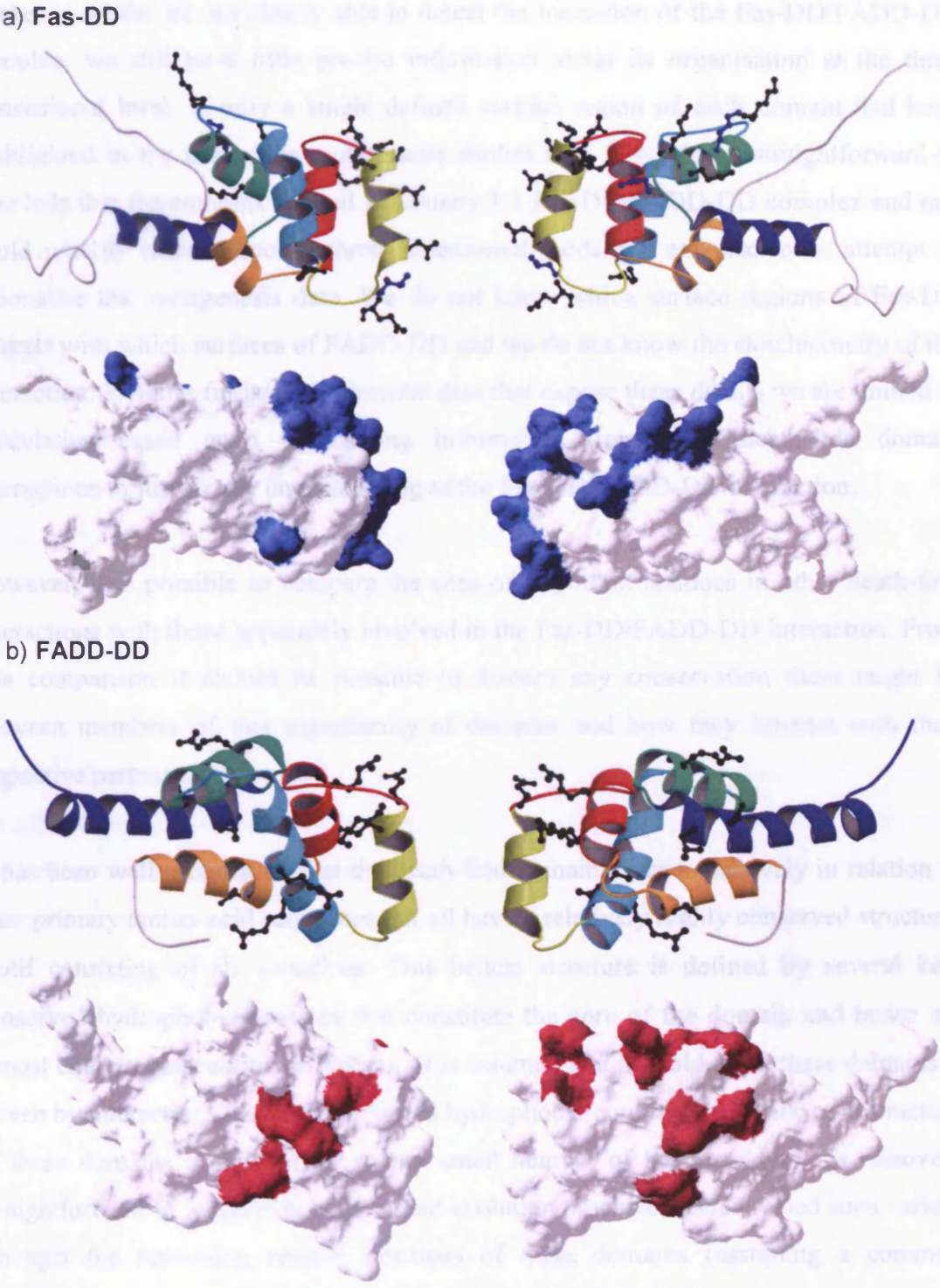

Figure 4.6 Backbone and surface representations of the Fas and FADD death domains in the same orientations indicating sites of non-structural point mutations that disrupt their mutual interaction. Backbone images (created with MolScript) are coloured by helices – α1: orange, α2: red, α3 yellow, α4: cyan, α5: green, α6 blue – and mutations sites are indicated with ball-and-stick representations. Surface images (generated with Swiss PDBViewer) are oriented exactly as the backbone image above and have mutation sites coloured blue (Fas-DD) and crimson (FADD-DD). Images on the right are rotated 180° about the y-axis relative to those on the left.

The surface representations show the expansive regions involved in the interaction between these two domains.

However, whilst we are clearly able to detect the formation of the Fas-DD/FADD-DD complex, we still have little precise information about its organisation at the three dimensional level. If only a single defined surface region of each domain had been highlighted in the respective mutagenesis studies then it would be straightforward to conclude that the complex formed is a binary 1:1 Fas-DD/FADD-DD complex and one could reliably embark upon a three dimensional modelling exercise in an attempt to rationalise the mutagenesis data. We do not know which surface regions of Fas-DD interact with which surfaces of FADD-DD and we do not know the stoichiometry of the interaction. Without further experimental data that expose these details we are limited to speculation based upon pre-existing information from other death-fold domain interactions to further our understanding of the Fas-DD/FADD-DD interaction.

However, it is possible to compare the sites of important residues in other death-fold interactions with those apparently involved in the Fas-DD/FADD-DD interaction. From this comparison it should be possible to discern any conservation there might be between members of this superfamily of domains and how they interact with their respective partners.

It has been well established that the death-fold domains vary extensively in relation to their primary amino-acid sequences but all have a relatively highly conserved structural motif consisting of six α-helices. This helical structure is defined by several key, conserved hydrophobic residues that constitute the core of the domain and hence are almost entirely inaccessible to solvent. It is assumed that the folding of these domains is driven by interactions between the buried hydrophobic core residues. Since the structure of these domains is defined by such a small number of key residues it is relatively straightforward to imagine how divergent evolution processes have created such variety amongst the remaining residue positions of these domains (assuming a common ancestor for all members of the death fold superfamily). The evolution process has created a family of protein domains each with unique surface characteristics, the specific nature of which governs how they interact specifically with their respective partners (or sets of partners).

Unfortunately this diversity makes accurate primary sequence alignment of these domains extremely difficult, especially when comparing members from different

subfamilies. However, in order to test whether there is any conservation of residues in the interactions between these domains it is first necessary to create such an alignment. Fortunately, computer-based tools are now available that generate the alignment of protein sequences based on their three-dimensional structures. Such a tool is ideal for this particular situation. The program DALI (http://www.ebi.ac.uk/dali/) was therefore used to generate structural alignments between FADD-DD and eight other members of the death-fold superfamily – including at least one member of each subfamily – for which structures were available: Fas-DD (Huang *et al.*, 1996), TNFR1-DD (Sukits *et al.*, 2001), Tube-DD and Pelle-DD (Xiao *et al.*, 1999), FADD-DED (Eberstadt *et al.*, 1998), APAF-1 CARD and Caspase-9 CARD (Qin *et al.*, 1999) and ASC pyrin (Liepinsh *et al.*, 2003). The structural alignment was repeated using Fas-DD as the template in place of FADD-DD to generate a total of 15 structural alignments. This alternation of the template structure was carried out to remove any bias generated by using a single structure as the alignment platform. Once the alignments had been generated they were collated using the program BioEdit (Hall, 1999) to produce an overall structure-based sequence alignment between the nine family members – see Figure 4.7. In order to test the accuracy of this essentially automatically derived structure-based alignment, and to observe if the core residues are conserved between subfamilies, primary sequence alignments from the PFAM database (Bateman *et al.*, 2004) were used to extract the conserved core residues for each of the four death-fold sub-families – DD, DED, CARD and pyrin. The positions of these conserved hydrophobic core residues for each sub-family were mapped back onto the full structural alignment and are shaded in grey in Figure 4.7.

The sequence alignment in Figure 4.7 reveals several points. First, it is interesting to note that there is excellent conservation of the positions of the hydrophobic core residues throughout the death-fold family (across all four sub-families). Although some residues have altered through evolution as the family has diverged into four separate subfamilies, the structural distribution and hydrophobicity of these residues remains consistent. From preliminary observation of the primary sequences this level of conservation was not immediately apparent.

Figure 4.7: Structural alignment of members of the death fold family of proteins. The conserved hydrophobic residues (shaded in grey) were extracted from the PFAM database sequence alignments for each death fold sub-family and are mapped back onto this structural alignment. The α-helices are boxed and the residues shown to be important for domain/domain interactions are highlighted in red. There is a 26 residue insert in the Tube death domain which has been omitted for clarity – indicated by ***.

However, analysis of the structural alignment indicates that these core residues are positionally conserved throughout all six helices of the death fold and across all four sequence sub-families. The presence of the death domains from *Drosophila melongaster* proteins Pelle and Tube in this alignment alongside the other seven human proteins also indicates a cross-species conservation of the death-fold structure.

It is clear then, that the structure of these domains is generally conserved and is maintained by the preservation of a set of hydrophobic core residues. However, observation of the amino-acid sequences that lie outside the core regions shows that there is very little conservation in any other elements of these domains. This is true when comparing members both across and within sub-families. Naively, it would be predicted therefore, that there is not likely to be any similarities between the surface properties of these individual domains. Indeed, as we have seen from Figure 1.9 the charge distributions on the surfaces of those death fold domains with known structures do appear to be remarkably diverse. Such diversity suggests that there is no particular reason why there should be a common interaction surface shared by members of this family of domains.

The availability of the three dimensional structures the complexes between the death domains of Pelle and Tube (Xiao *et al.*, 1999) and the CARD domains of caspase-9 and APAF-1 (Qin *et al.*, 1999) allows for the further analysis of death-fold protein interactions. The residues involved in the interaction surfaces of these two complexes were identified from their PDB files (1d2z and 3ygs respectively) using the program CNS (Brunger *et al.*, 1998). A residues was defined as an "interface residue" if the side chain β-carbon atom was within 8 Å of the β-carbon atom of any residue from the other chain in the complex. This information was mapped onto the sequence alignment in Figure 4.7. Residues at the interfaces of these two complexes are highlighted in red for comparison with the positions of characterised mutations in Fas-DD, FADD-DD and TNFR1-DD (Telliez *et al.*, 2000). The data for TNFR-1 is from a study to identify mutants of this domain that are important for the interaction with the death domain of the adapter protein TNF-receptor associated death domain protein (TRADD). It is important to note that the information from the TNFR1-DD mutations does not demonstrate whether these are structural mutants, however all the residues chosen in the study were highly solvent exposed on the domain. Hence it is reasonable to presume

that the substitutions do not disrupt the TNFR1-DD structure and that at least a proportion of these residues are directly involved in intermolecular contacts with TRADD-DD.

Comparison of the positions of the red-shaded residues in Figure 4.7 shows no obvious conservation of regions that may be important in the respective death-fold domain interactions. However, more information about the Fas-DD/FADD-DD interaction could potentially be gained by modelling these two domains onto the structures of the two known binary death-fold complexes – Pelle-DD/Tube-DD and caspase-9-CARD/APAF-1-CARD. Comparison of the mutagenesis data from the Fas and FADD death domains with the residues at the protein-protein interfaces of these modelled complexes should permit the detection of any potential relationship between the Fas-DD/FADD-DD interaction and the other, known death fold interactions.

Four structural models were built in order to test this hypothesis. The NMR solution structures of Fas-DD and FADD-DD were modelled onto the DDs of Pelle and Tube and onto the CARD domains of caspase-9 and APAF-1. For clarity, these four models have been numbered as show below:

Model 1: Fas-DD → Tube-DD / FADD-DD → Pelle-DD

Model 2: Fas-DD → Pelle-DD / FADD-DD→ Tube-DD

Model 3: Fas-DD → Caspase-9 CARD / FADD-DD → APAF-1 CARD

Model 4: Fas-DD → APAF-1 CARD / FADD-DD → Caspase-9 CARD

Each model was produced by adopting the same procedure outlined below using Model 1 as an example. In order to create Model 1 the Fas-DD and FADD-DD structures (PDB files 1ddf and 1e3y respectively) were first structurally aligned to Tube-DD and Pelle-DD (extracted from the PDB file 1d2z) respectively using the program SSAP (Orengo and Taylor, 1990). The program PROFIT (Martin, A.C.R., http://www.bioinf.org.uk/software/profit/) was then used to fit the Fas-DD and FADD-DD structures onto the Pelle-DD/Tube-DD heterodimer (chains A and B from the PDB

file 1d2z*) using the previously created structural alignments as templates. The PROFIT program outputs a new PDB format file containing the atomic coordinates of the new three dimensional model.

Figure 4.8 shows Models 1-4, represented by their polypeptide ribbon structures, both individually and superimposed onto their respective templates. It can be seen that the models are all reasonably well aligned to the templates in respect of their regular secondary structure elements. Once these models had been created it was then possible to generate information about the inter-domain interfacial surfaces that are formed by these hypothetical complexes. The residues at the interfaces of these four models were detected using an objective pairwise distance search coded in CNS exactly as described above for the analysis of crystal structure interfaces. The output of this analysis data is shown in Table 4.6.

From Table 4.6 it is possible to see that whilst three of the models include a subset of residues in the knockout mutation list no single model can wholly account for all of them. Model 1 is the least interesting of the four as it shares no common interface residues with the mutagenesis data. Model 2 suggests that there may exist a shared binding interface between FADD-DD and Tube-DD However, it is clear that this surface does not account for the full interaction between FADD-DD and Fas-DD as several other surface regions are also involved, particularly in the case of Fas-DD.

Similar observations apply to Models 3 and 4, where, in each case, there is a significant degree of overlap between the interface residues from one partner in the model and their knockout mutations but where each model fails to accommodate all of the mutagenesis observations. Interestingly, in both Models 3 and 4, the surface region corresponding to

---

* A note about the crystal structure of the Pelle-DD/Tube-DD complex: Four molecules are shown in the asymmetric unit of the structure in a linear Pelle-Tube-Pelle-Tube arrangement and hence this arrangement provides three distinct Tube-DD/Pelle-DD interfaces. Whilst two of these interaction sites are almost identical, the second (middle) interface is dissimilar and is almost certainly an artefact of crystal packing (N. Gay, personal communication) – an observation that is backed up by the presence of a HEPES molecule from the buffer buried at this interface. For the present study, therefore, only the conserved interface was chosen for comparison with the Fas-DD/FADD-DD data. For this purpose a new atomic coordinate file was created consisting of only one pair of Tube-DD/Pelle-DD molecules (chains A and B from the original 1d2z file) as a template for the modelling exercise.

the caspase-9 CARD interaction site is the one that yields the highest concordance with knockout mutation sites. However, in these cases the partner domain appears to be in a largely inconsistent orientation as it shares only one contact residue with the mutation list.

"Knockout mutations"		Interface residues				Interface residues			
		Model 1		Model 2		Model 3		Model 4	
Fas-DD	FADD-DD	Fas-DD → Tube	FADD-DD → Pelle	Fas-DD → Pelle	FADD-DD → Tube	Fas-DD → APAF-1	FADD-DD → Casp-9	Fas-DD → Casp-9	FADD-DD → APAF-1
R234	D106	T219	I147	V238	Q169	T217	R113	R234	R132
N239	R113	V223	N150	N239	M170	T218	R114	K235	Y133
E240	R117	K293	T151	A241	N171	A255	A116	N239	N136
A241	D123	T296	K153	K242	L172	Q256	R117	E240	T138
D244	K125	I297	E154	R263	V173	V259	Q118	A241	E139
N248	R142	K300	N155	N264	A174	Q260	K120	I243	R140
V251	R146	T303	T157	W265	N175	L262	S122	D244	R142
Q252	R166	T304	R189	H266	L176	R263	D123		E143
E256	L172	S306	S190	Q267	Q178	N264	T124		
K272	D175	E307		L268	Q179		K125		
D276				H269	Q181		C168		
K280				K271	Q182		Q169		
K284				K272					
N286				A274					

Table 4.6: List of interface resides from the four generated models of the Fas-DD/FADD-DD complex models. The "knockout mutations" are defined from this study and the study of (Hill *et al.*, 2004) as the sites of residues which, when mutated, lead to an apparent total loss of respective Fas-DD/FADD-DD binding without perturbing the overall three dimensional fold of the respective death domain. Yellow highlights indicate model interface residues that also appear in the list of knockout mutation sites.

Overall we can see from these models that the Fas-DD/FADD-DD interaction cannot be readily explained by the current observations of death-fold domain interactions. This failure stems from the fact that the surface regions involved in the interaction appear to be extended over a greater surface area than those interactions of the known death-fold family interactions. It may be possible to conclude that the Tube-DD and caspase-9 CARD interactions use similar interacting surface regions (in complexes with Pelle and APAF-1) to the Fas and FADD death domains. However, the fact that we see such highly dispersed interaction surfaces for these two domains, in an interaction that our NMR data suggest is almost certainly not as simple as 1:1 heterodimer formation, suggests that there is no genuine similarity between the Fas-DD/FADD-DD and other death fold interactions.

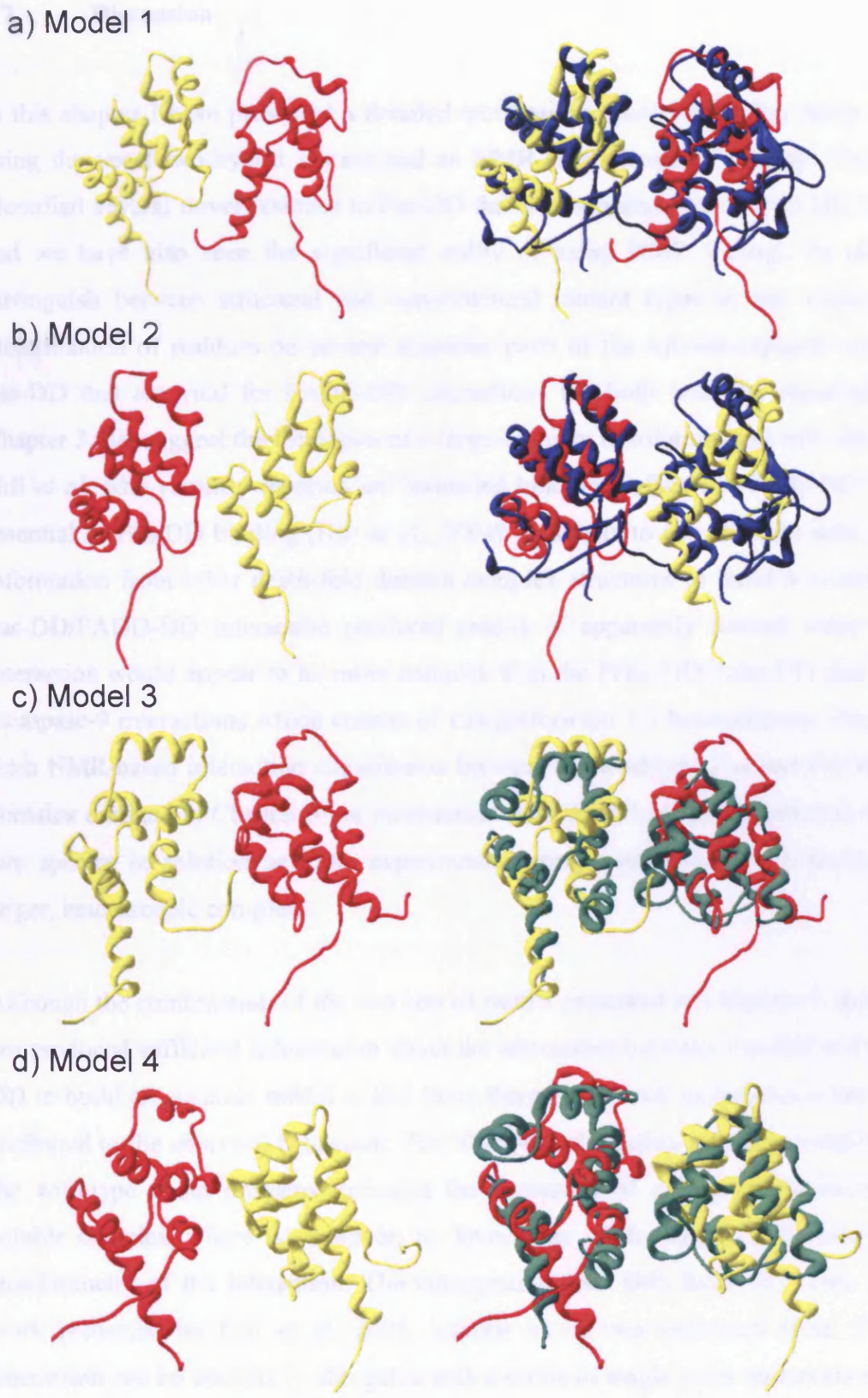

Figure 4.8: Models of Fas-DD/FADD-DD interactions based on the Pelle-DD/Tube-DD complex and the caspase-9 CARD/APAF-1 CARD complex. On the left are the four individual heterodimer models and on the right as shown superimposed with their template structures. Fas-DD is coloured red, FADD-DD yellow, the Pelle/Tube complex blue and the caspase-9/APAF-1 complex green.

4.7 Discussion

In this chapter I have presented a detailed mutagenesis study of the Fas death domain using the yeast two-hybrid system and an NMR-based interaction assay. This study identified several novel residues in Fas-DD that are important for FADD-DD binding, and we have also seen the significant utility of using NMR through its ability to distinguish between structural and non-structural mutant types in this context. The identification of residues on several disparate parts of the solvent-exposed surface of Fas-DD that are vital for FADD-DD interactions fits both with the observations of Chapter 3 that suggest the formation of a large complex in solution, and with the data of Hill *et al.* who recently reported an "extended binding surface of FADD-DD" that is essential of Fas-DD binding (Hill *et al.*, 2004). Attempts to use all these data and the information from other death-fold domain complex structures to build a model of the Fas-DD/FADD-DD interaction produced results of apparently limited value as this interaction would appear to be more complex than the Pelle-DD/Tube-DD and APAF-1/caspase-9 interactions which consist of straightforward 1:1 heterodimers. The results from NMR-based interaction experiments between the wild-type Fas and FADD death domains outlined in Chapter 3 are inconsistent with the 1:1 heterodimerisation of these two species in solution as these experiments strongly suggested the formation of a larger, macroscopic complex.

Although the combination of the two sets of results presented in Chapters 3 and 4 have not produced sufficient information about the interaction between Fas-DD and FADD-DD to build an accurate model at this time, there are several explanations that can be attributed to the observed behaviour. The NMR-based titration studies carried out with the wild-type death domains indicated the formation of a hydrodynamically large, soluble complex. There is, however, no knowledge of the size of this complex and stoichiometry of the interaction. The mutagenesis data, both from this work and the work presented by Hill *et al.* 2004, informs us of two important facts. First the interaction can be essentially abrogated with a series of single point mutations either in Fas-DD or FADD-DD, and second that such "knockout" mutations result from side-chain substitutions on multiple surface regions of each domain.

The combination of these observations leads to a number of conclusions. Firstly this interaction is not a simple 1:1 heterodimerisation but instead probably involves the co-aggregation of these domains into higher-order hetero-oligomers. Whether this co-aggregation event results in a homogenous, monodisperse complex, in the experiments carried out here, is unknown. However, the fact that this large complex, involving multiple surface regions of each domain can be disrupted by single point mutations on those surface regions indicates that the formation of this complex probably involves a co-operative binding event. Such a co-operative binding event must be initiated by the interaction between Fas-DD and FADD-DD but the subsequent formation of the higher-order complex may be driven by pairwise interactions of Fas-DD:Fas-DD, FADD-DD:FADD-DD or Fas-DD/FADD-DD:Fas-DD/FADD-DD death domain interactions. Taking into consideration the limited utility of the complex-modelling exercise based on known death fold domain interactions and without further work to analyse the hydrodynamic properties of this complex in solution it is impractical to conclude anything more about the molecular details of the Fas-DD/FADD-DD interaction at this stage.

Future work to characterise the Fas-DD/FADD-DD complex formed in solution should involve the biophysical characterisation of its homogeneity and hydrodynamic size. If found to be homogenous, attempts could be made to use electron microscopy to visualise the gross morphology of the complex or to co-crystallise the two proteins for structural analysis. There is also scope for further mutagenesis work of both death domains. Although FADD-DD mutants have been studied by other groups in different Fas/FADD interaction assays, it would be useful to investigate the effects of several FADD-DD mutations, particularly those utilised by Hill *et al.*, in the NMR-based assay developed in this study. Also, in order to further analyse the effects of altering the Fas-DD charge distribution it may be useful to create second-site mutants in the Fas-DD-K247A background. This type of experiment would directly address the issue whether one could detect discrete Fas-DD/FADD-DD complexes lacking the characteristic of apparent higher-order association witnessed in the study presented here.

In the final chapter of this thesis I describe the development of a cell-based, functional assay that was provides essential corroboration of the mutagenesis data presented in this chapter.

Chapter 5

A functional assay for the Fas-DD/FADD-DD interaction

5.1 The importance of a biological assay

IN the preceding chapters the interaction between the death domains of the Fas receptor and the adaptor protein FADD has been studied both *in vitro* (in an NMR-based assay) and in a heterologous cellular environment (in the yeast two-hybrid assay). However, neither of these methods allows this interaction to be studied in the context of the normal physiological roles of these two proteins. This problem is particularly relevant to the extensively studied Fas-DD mutants. In order to draw conclusions about Fas signalling from the mutational studies of its death domain is was important to correlate the behaviour of these mutants in the NMR assay and their behaviour in a cellular environment.

To address this issue an assay was developed to investigate the biological effects of several of these mutants.

5.2 FasL-induced apoptosis as an assay for Fas/FADD interaction

The study of apoptotic pathways has the advantage of providing an obvious biological readout – cell death. The death receptor-induced apoptotic pathways have the added advantage of being highly specific and inducible by the application of external ligands to the cells being studied. It has been extensively shown that the induction of apoptosis through the Fas receptor in cell culture is possible simply by the addition of FasL to the medium (Suda *et al.*, 1994) and that this apoptosis is absolutely dependent on the ability of Fas to bind FADD (Newton *et al.*, 1998; Yeh *et al.*, 1998). These facts allow the development of a Fas-DD/FADD-DD interaction assay based on the ability of FasL to induce apoptosis in a cell line that is artificially induced to expressing the Fas receptor so long as those cells also express the remaining components of the Fas-dependent apoptosis signalling pathway. Once developed, this assay could then be used to test the effects of mutations in Fas-DD on FADD-DD binding in a biological context.

5.3 Development of a functional cell-based assay

The basic concept of the biological assay of Fas function was as follows: wild-type and mutant forms of the Fas receptor were to be expressed in individual human cell lines and these cell lines then would be tested for their ability to undergo apoptosis upon addition of FasL. Such an assay would provide a direct biological readout of the effect of the Fas mutants on their ability to induce apoptosis and this data could then be directly compared with the NMR and yeast two-hybrid results for the same mutants.

There were several important factors to be considered in the development of the assay. A cell line had to be selected that fulfilled a number of defined criteria. First, since human Fas and FADD proteins have been used throughout this study, the cell line chosen was of human origin. Second, the cell line must not endogenously express the Fas receptor. Recombinant Fas, and importantly, mutants of Fas, could therefore be expressed by transfection of an appropriate plasmid, in these cells without any background interference from endogenous, wild-type Fas already present in the cells. Quantitative measurements on the effects of the Fas-DD mutations would then be possible. Finally, it was important that the chosen cell line functionally expressed the

remaining components of the apoptotic machinery such that when the Fas receptor was expressed the cells could undergo apoptosis through the canonical death receptor pathway.

Also of importance in the development of this assay was the system used to recombinantly express Fas in the chosen cell line. The most important factor in this case was to ensure that the level of expression of the receptor was essentially equal for the wild-type and each mutant chosen for analysis. Without consistent expression levels it would be difficult to quantitatively compare the effects of any Fas mutations. Traditional methods of recombinant expression in mammalian cells rely on the use of constitutively active promoters, such as the cytomegalovius (CMV) promoter, to drive the expression of a protein of interest from a plasmid that is transfected into the cells. However, this method cannot guarantee that equal amounts of protein will be expressed from one experiment to the next. For this reason it was decided to use a more controllable method of protein expression that takes advantage of an inducible promoter system to express the protein of interest. In this case the "Tet-on" system (BD Biosciences) was selected to create cell lines that express Fas (or Fas mutants) under the control of a titratable promoter system. The Tet-on system allows the amount of protein expression to be directly controlled by the addition of tetracycline (or its analogue, doxycyclin) to the cell culture medium. Subsequent experiments with these cell lines would then give more accurate, quantitative data for the effects of the expression of wild-type and mutant forms of Fas.

The molecular basis of the tetracycline-regulated expression system is outlined in Figure 5.1. Here it can be seen how the use of doxycyclin (an analogue of tetracycline) is used to initiate the transcription of a target gene – in this case encoding for the Fas receptor. The system relies on the use of the tetracycline responsive transcriptional activator (rtRA) protein that binds specifically to the tet-response element (TRE), a promoter region of DNA, encoded so as to initiate the expression of the target gene. The level of expression of the target gene is directly proportional to the concentration of doxycyclin present in the culture medium allowing the expression of wild-type and mutant forms of Fas in individual stable cell lines to be titrated to similar levels. The two plasmids required for these experiments – pTet-on and pTRE2-hyg (Clontech) (see Appendix 4) – contain ampicillin resistance genes to allow their propagation in *E. coli.*

Each plasmid also contains a second antibiotic resistance gene (neomycin in the case of pTet-on and hygromycin (hyg) in the case of pTRE2-hyg) to allow separate and combined selection of successfully transfected mammalian cells.

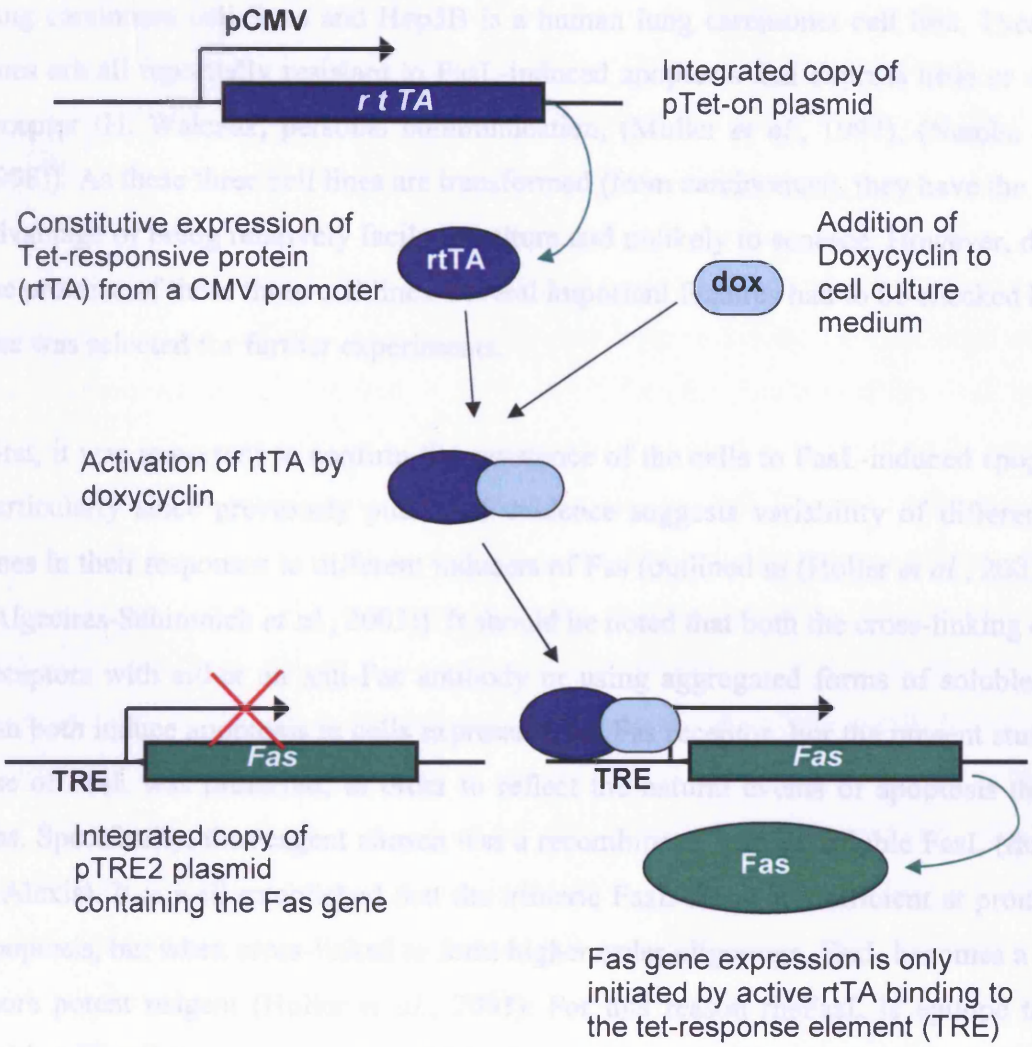

Figure 5.1: The Tet-on mammalian expression system as used to express the Fas receptor. Here the Fas gene has been cloned into the pTRE2 plasmid and both the pTet-on and pTRE2-Fas plasmids have been stably transfected into a mammalian cell line. The constitutively expressed tet-responsive transcriptional activator protein (rtTA) is activated by doxycyclin. Once active, the rtTA protein binds to the tet-response element (TRE) to initiate expression of the target gene (in this case, Fas).

5.4 Choice of cell line

Initially three human cell lines were found that potentially fulfilled the criteria outlined in Section 5.3. These cell lines were A549, Hep3B and Huh7 (kind gifts from Henning Walczak of the University of Heidelberg, Germany). A549 and Huh7 represent human lung carcinoma cell lines and Hep3B is a human lung carcinoma cell line. These cell lines are all reportedly resistant to FasL-induced apoptosis and express little or no Fas receptor (H. Walczak, personal communication, (Muller *et al.*, 1997), (Nambu *et al.*, 1998)). As these three cell lines are transformed (from carcinomas), they have the added advantage of being relatively facile to culture and unlikely to senesce. However, despite the promise of these three cell lines, several important features had to be checked before one was selected for further experiments.

First, it was important to confirm the resistance of the cells to FasL-induced apoptosis, particularly since previously published evidence suggests variability of different cell lines in their responses to different inducers of Fas (outlined in (Holler *et al.*, 2003) and (Algeciras-Schimnich *et al.*, 2003)). It should be noted that both the cross-linking of Fas receptors with either an anti-Fas antibody or using aggregated forms of soluble FasL can both induce apoptosis in cells expressing the Fas receptor. For the present study the use of FasL was preferred, in order to reflect the natural events of apoptosis through Fas. Specifically, the reagent chosen was a recombinant, human, soluble FasL (rhsFasL – Alexis). It is well established that the trimeric FasL alone is inefficient at promoting apoptosis, but when cross-linked to form higher order oligomers, FasL becomes a much more potent reagent (Holler *et al.*, 2003). For this reason rhsFasL is epitope tagged (with a FLAG-tag – a sequence of 26 amino-acids at the N-terminus) and is supplied with a cross-linking anti-FLAG antibody (the "enhancer"). Combining rhsFasL with the enhancer results in potent and highly specific induction of apoptosis through the Fas receptor.

5.4.1 The MTT assay

An assay using the compound methylthiazoletetrazolium (MTT) in order to test the effect of rhsFasL on cell survival was adopted. In live cells, MTT is metabolised to a

purple formazan compound by the metabolic enzyme succinate dehydrogenase (SDH), while in dead cells the SDH substrate remains yellow (Hansen *et al.*, 1989). Following incubation with MTT, cells were lysed with a solution containing SDS detergent (along with DMF to solublise the dye) and the absorbance of the resulting solution was measured at 540 nm (see Section 2.5.3). Because the amount of dye turned over is proportional to the number of MTT-metabolising cells, this assay provided an accurate measure of the number of living cells in a culture. The combination of rhsFasL treatment followed by the MTT assay therefore provided a simple method to quantitatively assess Fas-dependent cell death in our cultures.

The three cell lines were tested for their response to FasL by incubation with increasing concentrations of rhsFasL (up to 50 ng/ml, see Section 2.5.4). Two different controls were carried out in parallel: first, in order to confirm the function of the FasL reagent, the cell line A20 was tested alongside the other cell lines. A20 is a murine B-lymphoma cell line that is especially susceptible to apoptosis through Fas and hence provides a useful positive control for this part of the assay. The use of a murine cell line for this purpose is possible since human FasL is known to activate murine Fas. Second all four cell lines were treated with a high dose of staurosporine – a general protein kinase inhibitor that is known to initiate caspase-dependent apoptosis independent of Fas (Kabir *et al.*, 2002). The application of staurosporine here serves as a useful control for the MTT assay as well as confirming the integrity of the apoptotic machinery downstream of caspase activation. As illustrated in Figure 5.2, all four cell lines showed significant death in response to treatment with 0.5 μM staurosporine, whereas only the A20 cell line showed a response to rhsFasL. As little as 2 ng/ml rhsFasL resulted in a 40 % reduction in A20 viability but doses up to 50 ng/ml had essentially no effect on the A549, Huh7 and Hep3B cell lines.

Having established that all three human cell lines were resistant to Fas ligand it was necessary to check for their expression of Fas, FADD, caspase-8 and FasL. The expression of the Fas machinery was investigated by Western blotting and the expression of FADD by immunocytochemistry as outlined below.

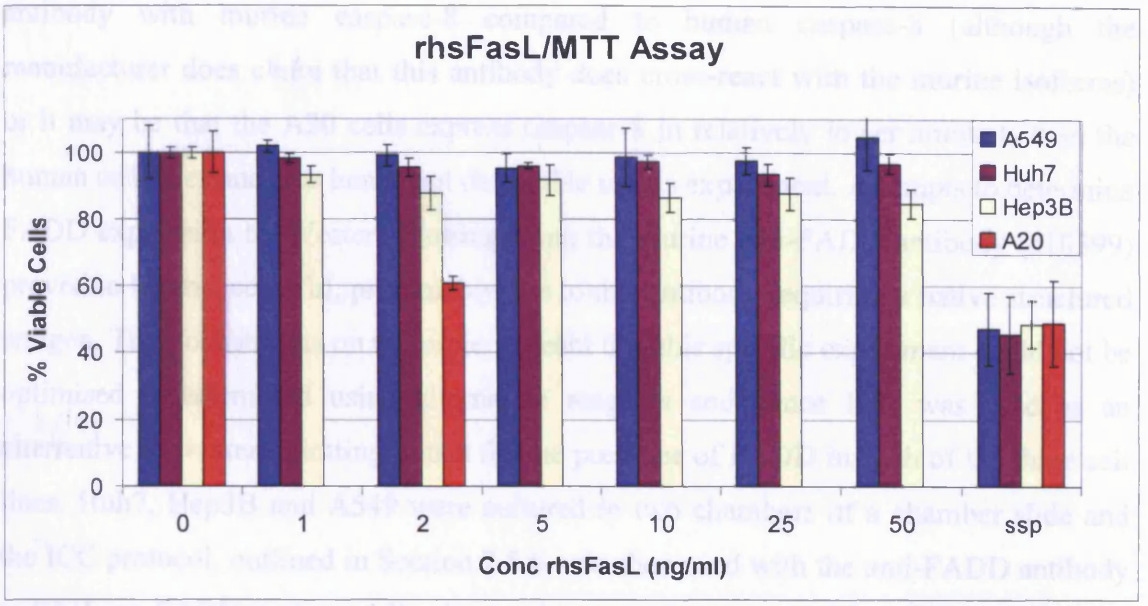

Figure 5.2: A549, Huh7 and Hep3B cell lines are not responsive to Fas-ligand. Treatment of these three cell lines followed by the MTT assay to count the numbers of remaining, viable cells showed no significant reduction in cell number. The A20 cell did respond to FasL at a concentration of 2 ng/ml and all four lines showed a significant decrease in cell number in response to treatment with 0.5 μM staurosporine. Note that the A20 cell line was only treated with a single concentration of FasL (2 ng/ml). Data is displayed as the mean of three independent experiments with error bars showing ± one standard deviation from the mean.

5.4.2 Western blotting and immunocytochemistry

Western blotting and "ICC" are two complementary techniques that are used to probe cells or cell-lysates for the presence of particular macromolecules. Each technique requires the application of specific antibodies raised against the protein(s) of interest. In each case a secondary antibody system is used to amplify the signal and provide a quantitative readout (see Section 2.5.5).

Cell lysates were prepared from the three cell lines, Huh7, Hep3B and A549, as well as from the A20 cells as a control, and Western blotting analysis was carried out as described in Section 2.5.5. Initial results of these analyses are shown in Figure 5.3. These images are produced by digitally scanning the x-ray films used to detect antibody binding. Fas was only detectable in the A20 cell line, but importantly not in the three human cell lines. In contrast, caspase-8 was detected in all three human cell lines, while FasL was present in all but the Hep3B cell line. It is unclear why no caspase-8 was detected in the A20 cell-line. This may be due to a lower binding affinity of this

antibody with murine caspase-8 compared to human caspase-8 (although the manufacturer does claim that this antibody does cross-react with the murine isoforms) or it may be that the A20 cells express caspase-8 in relatively lower amounts than the human cell lines and was hence not detectable in this experiment. Attempts to determine FADD expression by Western blotting using the murine anti-FADD antibody (610399) proved to be unsuccessful, presumably due to this antibody requiring a native structured antigen. Time constraints on the project meant that this specific experiment could not be optimised or attempted using alternative reagents and hence ICC was used as an alternative to western blotting to test for the presence of FADD in each of the three cell lines. Huh7, Hep3B and A549 were cultured in two chambers of a chamber slide and the ICC protocol, outlined in Section 2.5.6, was then used with the anti-FADD antibody to label any FADD in these cell cultures. As a negative control, for each cell line one of the chambers in these experiments was incubated without primary antibody. This was to ensure that any background staining from the secondary antibody could be detected and accounted for.

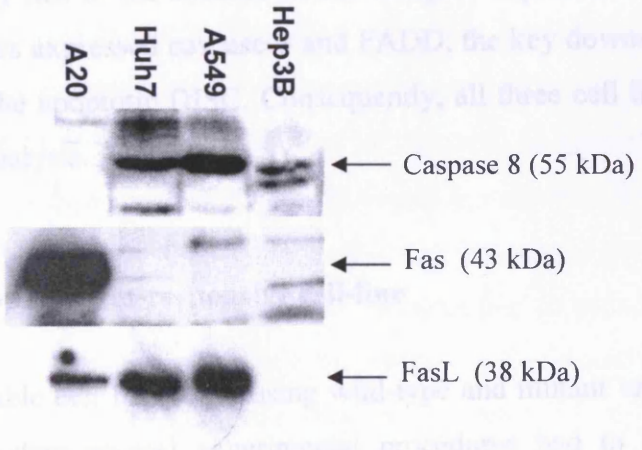

Figure 5.3: Western blotting analysis of cell lysates probed for the presence of Fas, FasL and caspase-8. Results shown here originate from three separate blots.

Figure 5.4 shows images of labelled cells from the three cell lines taken at 60x magnification. To create such two-colour images the same microscope field was digitally captured twice, once with a FITC-filter and once with a DAPI-filter, and the two resulting images overlaid to show healthy DAPI-stained nuclei surrounded by the green FITC fluorescent-labelled cytoplasm, indicating the presence of FADD protein. FADD staining was confirmed for all three cell lines and fluorescence was absent from all negative-control wells.

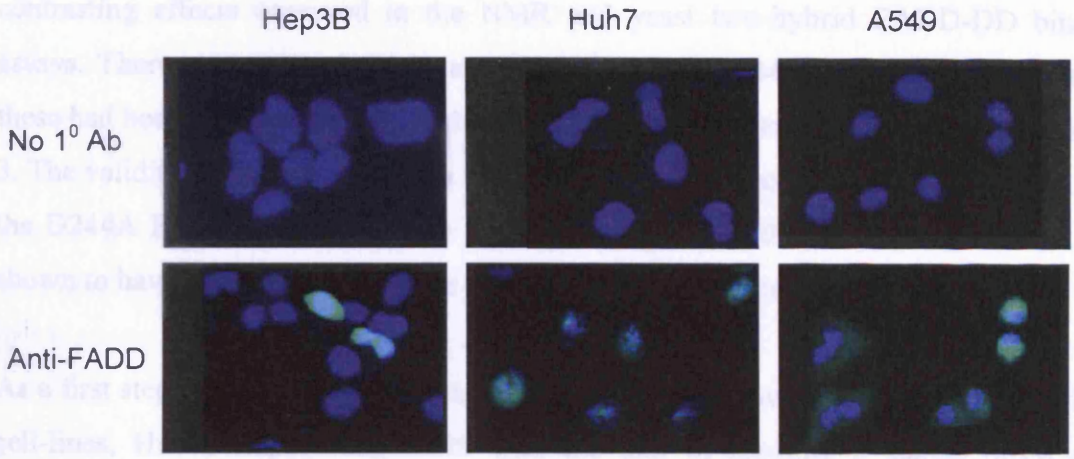

Figure 5.4. Immunocytochemistry analysis of FADD in the three cell lines Hep3B, Huh7 and A549. FADD is detected with FITC and appears as green fluorescence in these cells. Nuclei are stained blue with DAPI. Images were taken at 60x magnification.

These initial experiments confirm that all three human cell lines were resistant to FasL and this was probably due to the absence of Fas receptor expression. It was also clear that the three cell lines expressed caspase-8 and FADD, the key downstream molecules in the formation of the apoptotic DISC. Consequently, all three cell lines were carried forward for further analysis.

5.5 Creation of a Tet-responsive cell-line

In order to create stable cell lines expressing wild-type and mutant variants of Fas and using the Tet-on system several experimental procedures had to be performed as outlined below.

1) Stable transfection of the pTet-on plasmid into the cell line of interest.
2) Selection of the transfected clone that gives the best response to doxycyclin.
3) Cloning of the target genes of interest into the pTRE2-hyg vector.
4) Stable transfection of the pTRE2 plasmids into the selected Tet-on cell line.
5) Selection of clones that show expression of the target gene.

The three mutant forms of Fas, D244A, K280A and K247A were selected for their contrasting effects observed in the NMR and yeast two-hybrid FADD-DD binding assays. There was particular relevance in testing the D244A and K247A mutants as these had been used extensively in the initial NMR experiments, as described in Chapter 3. The validity of the structural data would be greatly enhanced if it could be shown that the D244A Fas mutant was unable to induce apoptosis and if the K247A mutant was shown to have similar activity to the wild-type Fas receptor in a biological system.

As a first step to achieving this goal, the pTet-on plasmid was transfected into the three cell-lines, Huh7, Hep3B and A549 with the aim of creating a stable, doxycyclin responsive cell line.

5.5.1 Stable mammalian cell transfection

The transfection of mammalian cells with plasmid, or other types of DNA constructs, is now a well established technology that has become routine in many cell biology experiments. However, unlike transformation of DNA into bacterial cells, stable expression of recombinant proteins in a mammalian cell relies on the integration of target genes into a suitable position in genome of that cell. In general, this process of integration cannot be precisely controlled and hence transfection can be inefficient. Furthermore, as is the case with the Tet-on system, it is not only to the target genes, but also the antibiotic resistance gene(s) that must be integrated in order to allow for the selection of successful transformants in medium containing those antibiotics. Therefore, following transfection (and after antibiotic selection has occurred) several clones must be tested for expression of the protein(s) of interest.

For the present experiment, transfection with the pTet-on plasmid was carried out in the 6 well plates as directed by the manufacturer's protocol outlined in Section 2.5.7. For all three candidate cell-lines a greater percentage of cell survival was observed on the plates originating from well F, suggesting that the 6:1 transfection reagent:DNA ratio was optimal in these experiments.

The surviving cells were cultured for a further ten days in medium with a reduced concentration of G418 (200 μg/ml). After ten days individual colonies of cells began to grow. Fifteen such colonies from each cell-line these were picked from the 100 mm culture plates using a sterile pipette tip and transferred to an individual well of a half-area 96-well tissue culture plate. In this way, individual clones were selected and separated from the rest of the cells for further culturing. This process of clonal selection enables the detection of successfully transfected clones that have integrated the plasmid genes successfully into their genome.

5.6.1 Tet-on clone selection

After transfection with the pTet-on plasmid the clone that gave the best response to induction of target gene expression with doxycyclin was selected. This was achieved by transiently transfecting the individual clones with the pTRE2-Luc plasmid (Clontech). The pTRE2-Luc plasmid is a modified form of the pTRE2-hyg plasmid that is engineered to produce the firefly luciferase enzyme under control of the Tet response element.

Each of the 13 Tet-on clones was seeded into three wells of a 96-well plate. Two of the three wells of each cell line were transfected with 40 ng of pTRE2-Luc plasmid DNA using 0.25 μl of the transfection reagent Fugene6. Doxycyclin was added to one of the two transfected wells to a final concentration of 2.5 μg/ml. After 48 hours the cells were subjected to the Luclite luminescence assay to measure the activity of any expressed luciferase. By comparing the amount of luciferase expression in the pTRE2-Luc transfected cells with and without the addition of doxycyclin the most responsive Tet-on clone could be selected.

Figure 5.5 shows the data from the luminescence assay as carried out on the 13 available clones. This data is presented as figures corrected by subtraction of the background luciferase activity (measured for the untransfected cells) from the raw luminescence values. It is worth noting, however, that the background luminescence was always below the essentially insignificant level of 100 counts per second (CPS). It can be seen from these results that the Huh7 cell line provided the most strongly

inducible clones (namely Huh7-3 and Huh7-4). These two clones represented the only derived cell lines that showed an increase in luciferase expression in response to the addition of doxycyclin and were selected for further use. The remaining clones (and the two cell lines A549 and Hep3B) were excluded from further experiments.

During attempts to culture the two Tet-responsive clones Huh7-3 and Huh7-4, it became clear that Huh7-3 grew more slowly than Huh7-4. For this reason the Huh7-3 clone was also excluded from the remaining experiments.

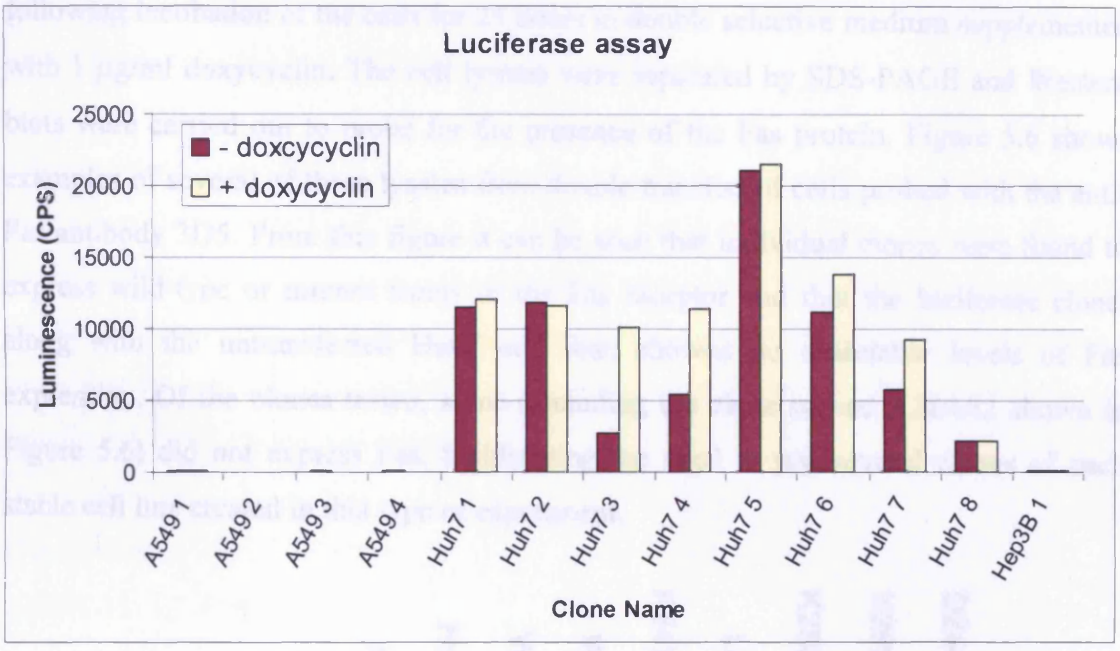

Figure 5.5 Selection of a single Tet-responsive clone using the luciferase assay. Light emitted from the luciferase enzyme expressed in Tet-responsive clones transiently transfected with the pTRE2-Luc plasmid was detected as luminescence and recorded as counts per second (CPS).

5.7 Creation of Tet-responsive Fas-expressing cell lines

Once the Tet-responsive cell line had been created, a second round of transfections was necessary in order to create cells that would express Fas (and the chosen mutants of Fas) in a controllable fashion. Therefore, DNA encoding the full length human Fas receptor (a kind gift from Jürg Tschopp, University of Lausanne, Switzerland) was subcloned between the *Mlu1* and *Not1* restriction sites in the pTRE2-hyg plasmid, using PCR primers 57 and 58, to create the plasmid pTRE2-Fas. The pTRE2-Fas plasmid was used

as a template to create the three chosen single residue mutants, D244A, K247A and K280A with the QuickChange site directed mutagenesis kit (Stratagene) and the resulting four plasmids were used for stable transfection into the Huh7-4 cell line. A fifth plasmid, the pTRE2-Luc plasmid, was also transfected into this cell line as a negative control for the apoptosis experiments.

Two stable clones were produced for each of the five transfected pTRE2 plasmids (containing DNA encoding wild-type Fas, the three Fas mutants and firefly luciferase). In order to check for expression of Fas in these clones, cell lysates were prepared following incubation of the cells for 24 hours in double selective medium supplemented with 1 μg/ml doxycyclin. The cell lysates were separated by SDS-PAGE and Western blots were carried out to probe for the presence of the Fas protein. Figure 5.6 shows examples of several of these lysates from double transfected cells probed with the anti-Fas antibody 3D5. From this figure it can be seen that individual clones were found to express wild-type or mutant forms of the Fas receptor and that the luciferase clone, along with the untransfected Huh7 cell line, showed no detectable levels of Fas expression. Of the clones tested, some (including the clone named K280A2 shown in Figure 5.6) did not express Fas, highlighting the need to test several clones of each stable cell line created in this type of experiment.

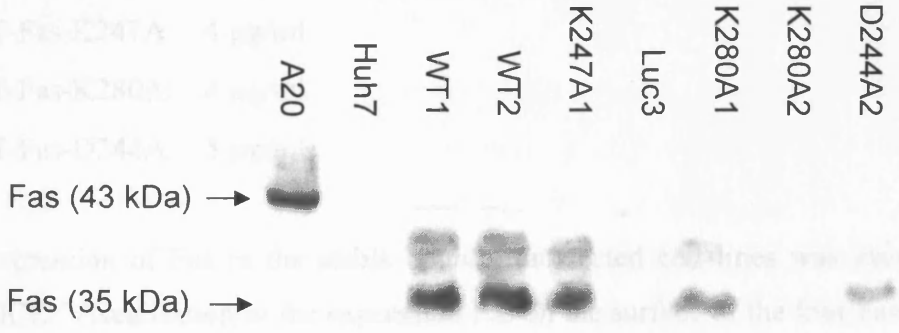

Figure 5.6: Selection of Tet-inducible Fas-expressing cell-lines. Lysates prepared from individual double-stable clones, A20 and untransfected Huh7 cells were probed with anti-Fas antibody (3D5).

From the full set of stable, doubly transfected clones, five were chosen that separately expressed the different genes of interest: Wild-type Fas (named Huh7T-Fas), Fas-D244A (Huh7T-FasD244A), Fas-K247A (Huh7T-Fas-K247A), Fas-K280A (Huh7T-

FasK280A) and Luciferase (Huh7T-Luc). The remaining experiments were carried out with these five cell lines.

5.8 Equalisation of Fas expression

Next, it was next necessary to normalise the levels of expression in the four Fas-expressing cell lines before carrying out further experiments by finding conditions where equivalent levels of the target gene was expressed. This normalisation was achieved by incubating each cell line with a range of concentrations of doxycyclin (between 1 and 5 μg/ml) for a period of 24 hours, before carrying out Western blotting experiments to quantify the level of Fas protein expression.

The precise concentration of doxycyclin used to induce comparable levels of Fas (or Fas mutant) protein expression varied for each of the four cell lines. In each case, the appropriate level of doxycyclin was established empirically using Western blotting with the anti-Fas monoclonal antibody to quantify the expression level. Using this laborious procedure we settled upon the following doxycyclin concentrations for the set of doubly transfected Huh7 clones (see Figure 5.7):

Huh7T-Fas: 1 μg/ml
Huh7T-Fas-K247A: 4 μg/ml
Huh7T-Fas-K280A: 4 μg/ml
Huh7T-Fas-D244A: 5 μg/ml

The expression of Fas in the stable doubly transfected cell lines was also confirmed using ICC. Visualisation of the expression Fas on the surface of the four Fas-expressing cell lines was possible by carrying out ICC experiments without permeablising the cells before probing with anti-Fas antibody. This experiment required the use of a second anti-Fas antibody as the antibody used in previous experiments (monoclonal antibody 3D5) was raised against the cytoplasmic domain of Fas. In this case it was necessary to use an antibody raised against the extracellular domain of Fas, hence a monoclonal, mouse anti-human Fas antibody from BD Biosciences (#610197) was selected.

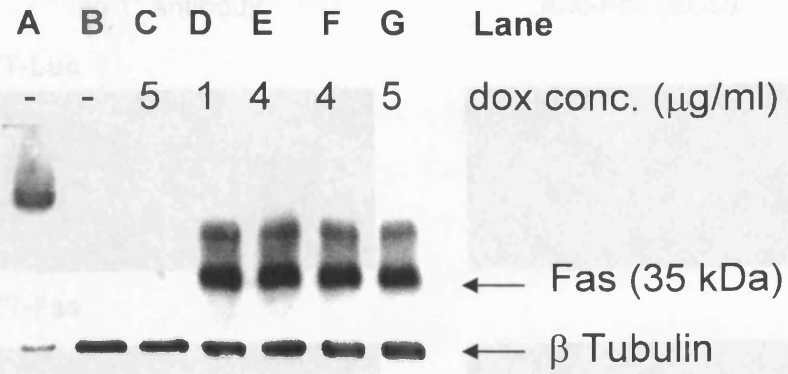

Figure 5.7 Equalisation of Fas expression levels in double-stable Tet-responsive cell lines. Cells were incubated for 24 hours with the indicated doxycyclin (dox) concentrations. Cell lysates were then probed for Fas expression and for β-tubulin as a loading control. A: A20, B:Huh7, C: Huh7-Luc, D:Huh7T-Fas, E: Huh7T-Fas-K280A, F:Huh7T-Fas-K247A, G:Huh7T-Fas-D244A. By using these specific dox concentrations the level of Fas expression was the same in the four Tet-inducible Fas-expressing cell lines. In contrast, no Fas expression was seen in the luciferase-expressing cell line, after incubation with the highest used dox concentration, or in the untransfected Huh7 cells.

ICC experiments on the five double-stable cell lines were carried out in the same manner as outlined in Section 2.5.6 but omitting the detergent permeablistion step. Sample images obtained from two replicate experiments are shown in Figure 5.8. These results indicate that there is surface expression of the Fas receptor in all four Fas-expressing cell lines but not in the cell line expressing firefly luciferase.

Following these procedures, I was in the position where stable cell lines had been created that express either wild-type Fas or one of three Fas mutants (D244A, K247A or K280) under control of the Tet-on expression system, which permits Fas expression to be titrated to the same level in all four cell lines. A fifth cell stable cell line, expressing firefly luciferase under control of the same Tet-inducible promoter, had also been created to be used as a negative control in the remaining experiments. In the final set of experiments these cell lines were tested for their ability to undergo Fas-induced apoptosis.

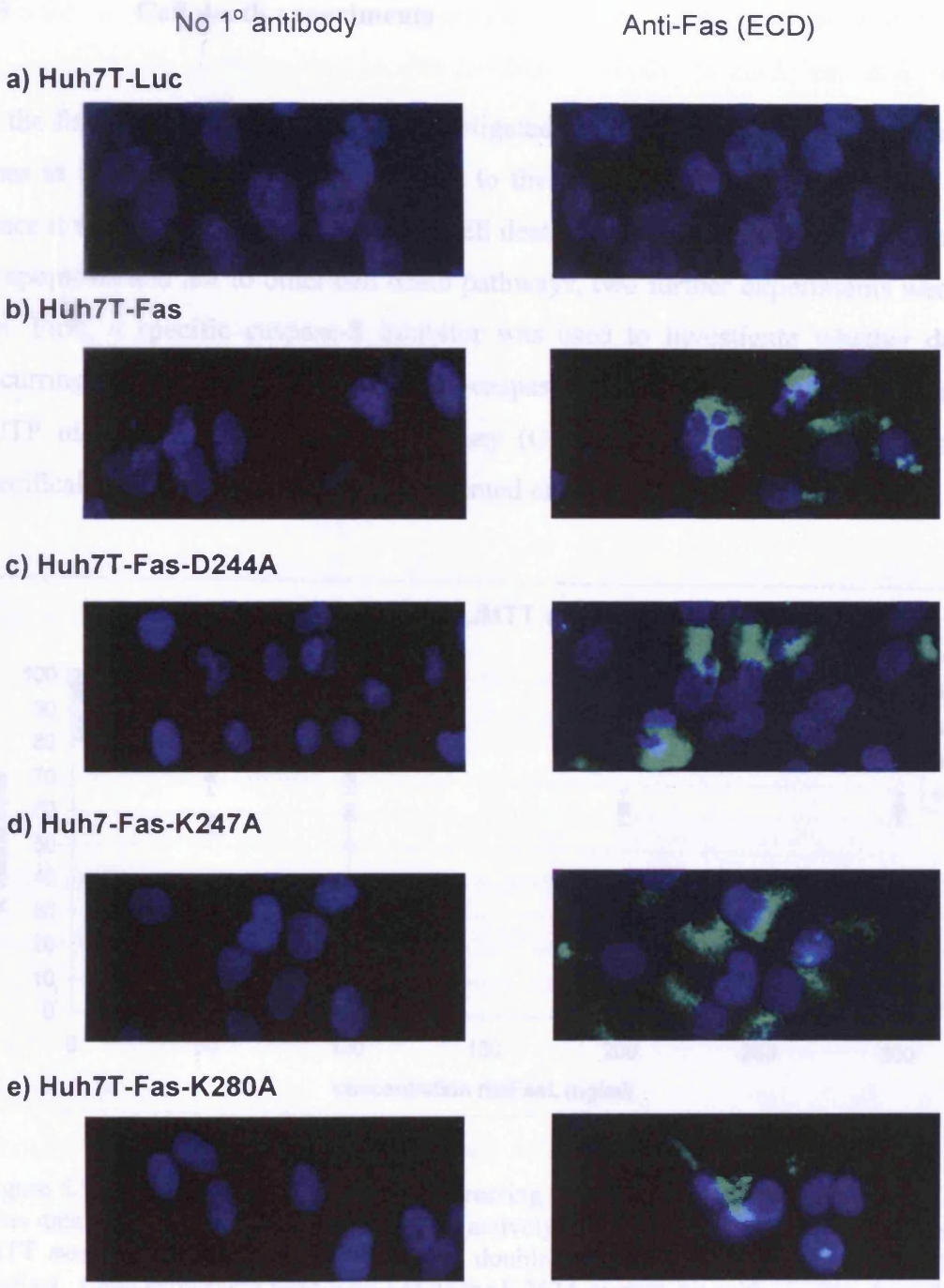

Figure 5.8 ICC experiments carried out on unpermeablised double-stable cell lines. Cells were probed with an antibody raised against the extracellular domain (ECD) of Fas and a FITC-labelled secondary antibody. Cells were counterstained with DAPI (blue). FITC staining (green) was only observed in cells shown to expressing Fas by Western blotting and only in the presence of the anti-Fas antibody. This data indicates the surface expression of recombinant wild-type or mutant Fas receptors in the Tet-responsive cell lines. Images were taken at 60x magnification

5.9 Cell death experiments

In the final series of experiments I investigated the ability of the five double-stable cell lines to undergo cell death in response to the administration of FasL to the medium. Since it was important to confirm that cell death recorded in these experiments was due to apoptosis and not to other cell death pathways, two further experiments were carried out. First, a specific caspase-8 inhibitor was used to investigate whether death was occurring via the expected Fas-FADD-caspase-8 pathway. Second, a TdT-mediated, dUTP nick-end labelling (TUNEL) assay (Gavrieli *et al.*, 1992) was performed to specifically label cells containing fragmented chromosomal DNA.

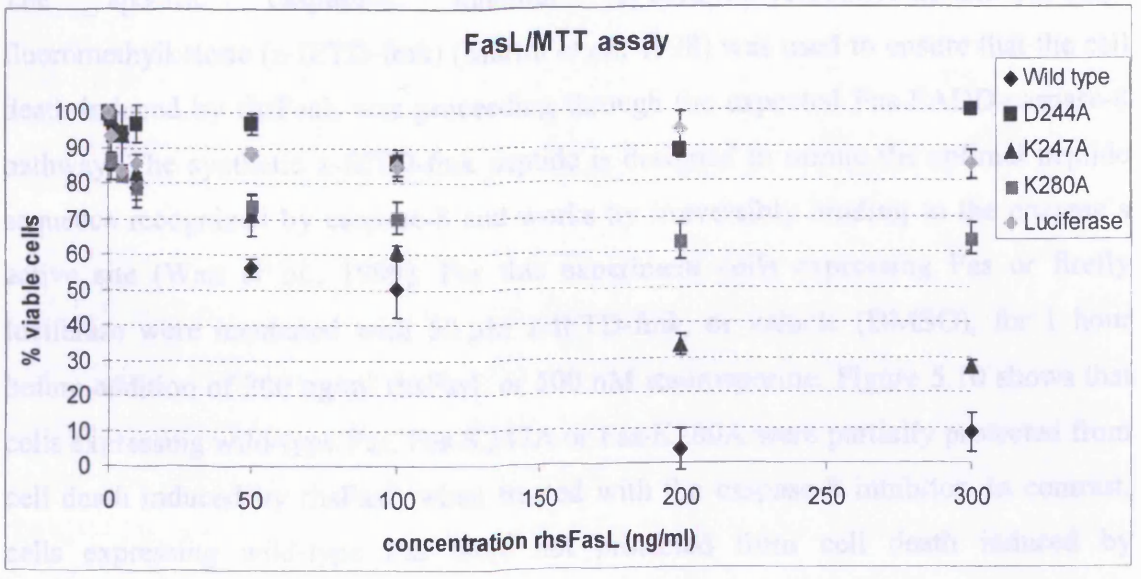

Figure 5.9: The response of cell lines expressing Fas, Fas mutants or luciferase to rhsFasL. This data shows the percentage of living (actively metabolising) cells – as measured by the MTT assay – after incubation of the five double-stable cell lines with increasing doses of rhsFasL. Cells expressing wild-type Fas or the K247A mutant die with similar, dose-dependent kinetics. Cells expressing Fas-D244A or luciferase are completely resistant to rhsFasL and cells expressing Fas-K280A die with reduced kinetics relative to the wild-type protein.

Each of the five transfected Huh7 cell lines was incubated with increasing concentrations of rhsFasL for a period of 24 hours after which cell survival was measured using the MTT assay. It can be seen from Figure 5.9 that the cell line expressing wild-type Fas underwent FasL-dependent cell death in a dose-response manner. When incubated with rhsFasL at a concentration of 200 ng/ml the cells are almost 100% dead. In contrast, the luciferase-expressing cell line was completely

resistant to rhsFasL at the concentrations tested. This data suggested that the reconstituted Fas receptor was able to function correctly, to bind FasL and induce cell death in the Huh7T-Fas cell line. In contrast to the situation for transfected wild-type Fas, the mutant Fas receptor, Fas-D244A, was unable to respond to rhsFasL. The cell-line expressing Fas-K247A showed a very similar response to the cells expressing wild-type Fas and the cell line expressing Fas-K280A showed some response to rhsFasL but this response was greatly attenuated relative to that of wild-type Fas.

5.9.1 Caspase-8 inhibition assay

The specific caspase-8 inhibitor *N*-benzyloxycarbonyl-Ile-Glu-Thr-Asp-fluoromethylketone (z-IETD-fmk) (Martin *et al.*, 1998) was used to ensure that the cell death induced by rhsFasL was proceeding through the expected Fas-FADD-caspase-8 pathway. The synthetic z-IETD-fmk peptide is designed to mimic the optimal peptide sequence recognized by caspase-8 and works by irreversibly binding to the enzyme's active site (Watt *et al.*, 1999). For this experiment cells expressing Fas or firefly luciferase were incubated with 50 μM z-IETD-fmk, or vehicle (DMSO), for 1 hour before addition of 200 ng/ml rhsFasL or 500 nM staurosporine. Figure 5.10 shows that cells expressing wild-type Fas, Fas-K247A or Fas-K280A were partially protected from cell death induced by rhsFasL when treated with the caspase-8 inhibitor. In contrast, cells expressing wild-type Fas were not protected from cell death induced by staurosporine. This data suggests that cell death induced by rhsFasL in these cells is dependent on the action of caspase-8.

5.9.2 TUNEL assay

To investigate whether that the caspase-8 dependent cell death induced by rhsFasL was apoptosis, the TUNEL assay was used to detect DNA fragmentation in the dying cells. DNA fragmentation is one of the hallmark events of apoptotic cell death (Saraste and Pulkki, 2000) occurring downstream of the caspase cascade. If it could be shown that the cell death induced by rhsFasL in the Fas-expressing cell lines involved DNA fragmentation then this data, along with the caspase-8 dependence shown above, would constitute compelling evidence that these cells are undergoing Fas-induced apoptosis.

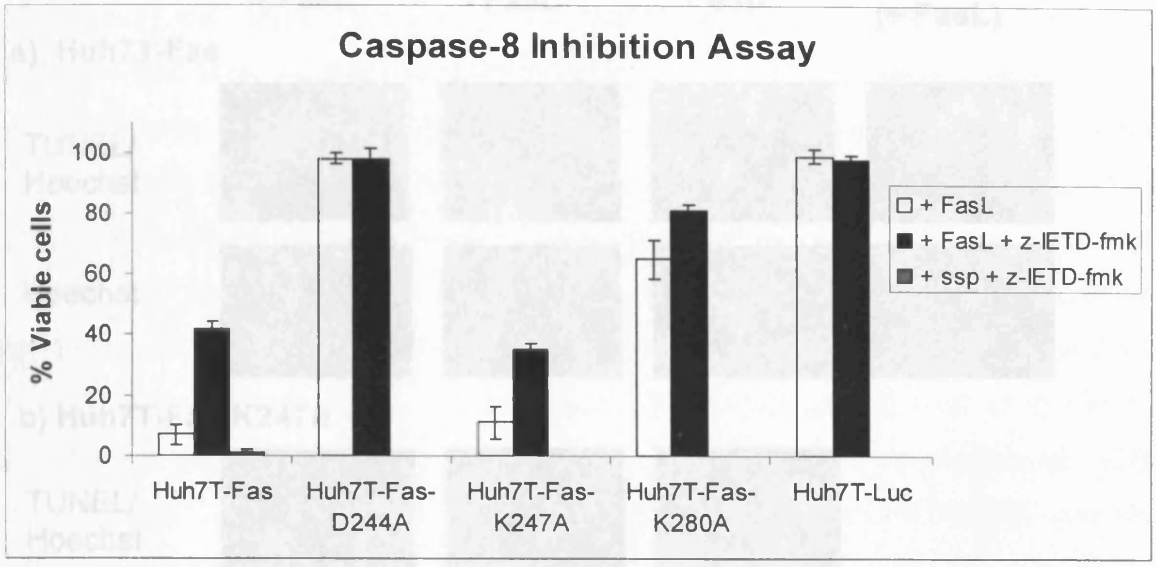

Figure 5.10: Inhibition of rhsFasL-induced cell death with the caspase-8 inhibitor z-IETD-fmk. Cells were incubated with or without z-IETD-fmk for 1 hour before being treated with 200 ng/ml rhsFasL. Cells expressing wild-type Fas, Fas-K247A or Fas-K280A could be partially protected by this inhibitor from cell death induced with FasL. Death of cells expressing wild-type Fas induced by staurosporine (ssp) could not be inhibited.

Each of the five transfected Huh7 cell lines was subjected to the TUNEL assay (as outlined in Section 2.5.9). Following this assay, cells were counterstained with bisbenzimide H 33342 – also known as Hoechst stain – before being examined by fluorescent microscopy. Hoechst stain has a very similar mechanism of action to DAPI, giving rise to blue fluorescence when bound to AT-rich DNA sequences (Otto and Tsou, 1985), but has also been shown to increase in fluorescent intensity when bound to fragmented DNA and hence is useful for identifying apoptotic nuclei (Hardin *et al.*, 1992).

Sample images from these experiments are shown in Figure 5.11. It can be seen by Hoechst staining that cells undergoing apoptosis (either from treatment with rhsFasL or with staurosporine) showed nuclear condensation and fragmentation. Such apoptotic cells were positively labelled by the TUNEL assay. As expected, the cell lines expressing wild-type Fas, Fas-K247A and Fas-K280A all contained TUNEL positive nuclei upon treatment with rhsFasL whereas the cell-line expressing Fas-D244A showed very few such positively labelled cells. On the other hand, all cell lines produced TUNEL positive cells upon treatment with staurosporine. These experiments, taken together with the caspase-8 inhibitor data strongly suggest that Huh7 cells re-engineered to express Fas undergo apoptosis following exposure to rhsFasL.

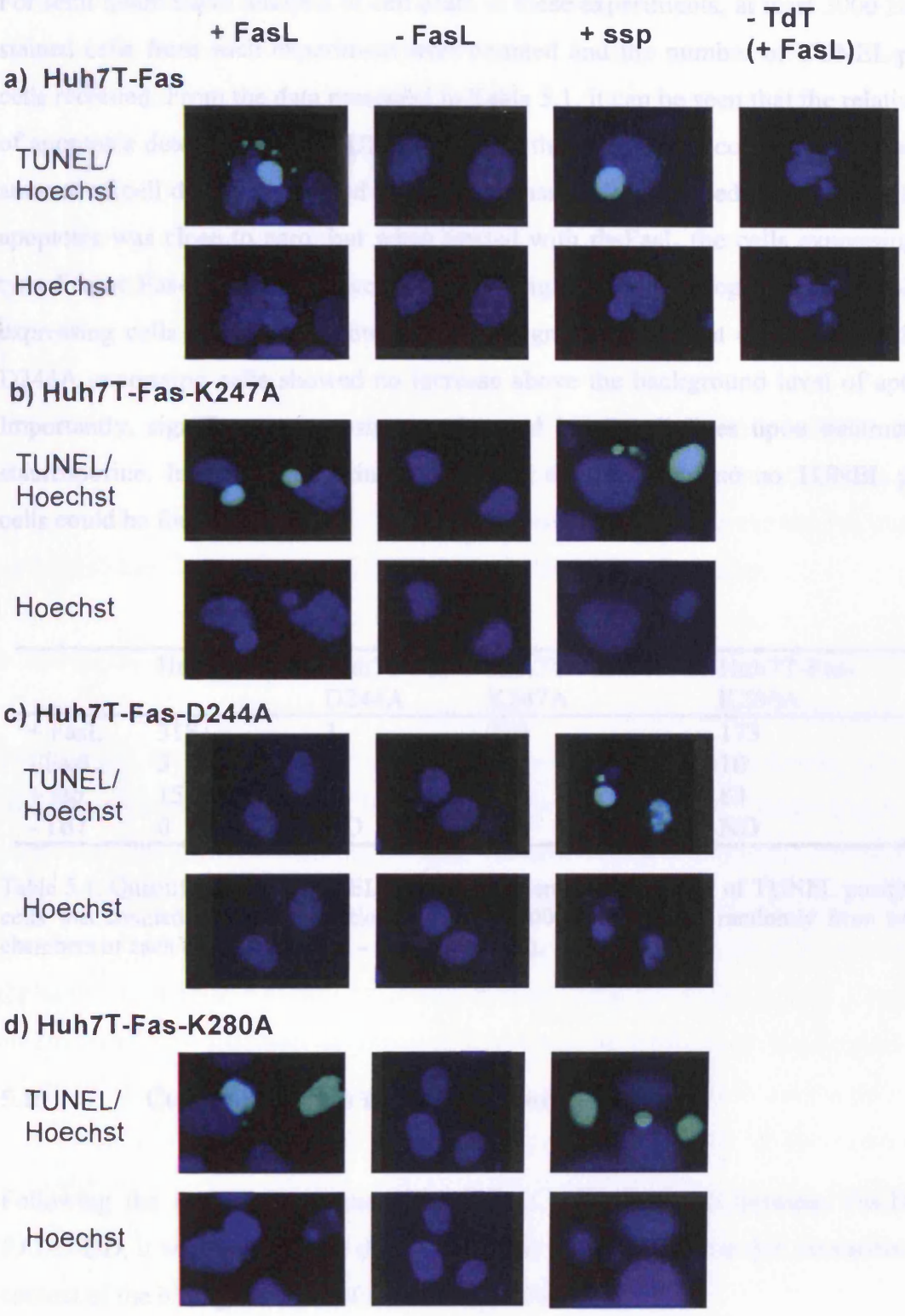

Figure 5.11: Sample fluorescence images of TUNEL and Hoechst staining of Fas expressing Huh7 cell lines. Monolayers of cells on chamber slides were treated with rhsFasL, staurosporine (ssp) or left untreated. A fluorescent TUNEL assay was then carried out to label fragmented DNA with FITC and cells were couterstained with Hoechst. The pairs of images seen here are of the same cells with the green, TUNEL-positive, fragmented nuclei superimposed with the blue Hoechst-staining in the top image and the Hoeshct staining by itself below.

For semi-quantitative analysis of cell death in these experiments, at least 3000 Hoechst-stained cells from each experiment were counted and the number of TUNEL-positive cells recorded. From the data presented in Table 5.1, it can be seen that the relative level of apoptosis detected by the TUNEL assay in these cell lines correlates well with the amount of cell death determined by the MTT assay. In untreated cultures, the level of apoptosis was close to zero, but when treated with rhsFasL the cells expressing wild-type Fas or Fas-K247A underwent similarly high levels of apoptosis, the Fas-K280A expressing cells underwent a lower but still significant amount of death and the Fas-D244A expressing cells showed no increase above the background level of apoptosis. Importantly, significant apoptosis was detected in all cell lines upon treatment with staurosporine. In control experiments, without the TdT enzyme no TUNEL positive cells could be found.

	Huh7T-Fas	Huh7T-Fas-D244A	Huh7T-Fas-K247A	Huh7T-Fas-K280A
+ FasL	318	3	339	173
- FasL	3	5	1	10
+ ssp	158	96	106	83
- TdT	0	ND	ND	ND

Table 5.1: Quantification of TUNEL assay experiments. The number of TUNEL positive cells was counted from a population of at least 3000 cells chosen randomly from two chambers of each experiment (ND – not determined).

5.10 Conclusions from functional assay development

Following the *in vitro* mutagenesis studies of the interaction between Fas-DD and FADD-DD, it was necessary to develop an assay that could probe this interaction in the context of the biological roles of these two proteins.

To achieve this, three putatively Fas negative, human cell lines, A549, Hep3B and Huh7 were initially chosen. All three cell lines were shown to be resistant to FasL-induced death. A combination of Western blotting analysis and immunocytochemistry indicated that these cell lines did not express the Fas receptor protein but did express caspase-8 and FADD. It was necessary to use ICC to test for FADD expression as the anti-FADD

antibody could not be successfully used to probe Western blots. The incompatibility of this antibody with Western blotting stems from the nature of the experiments being conducted. For example, some antibodies rely on the correctly folded shape of their target protein for recognition and, since Western blotting results in protein denaturation, such antibodies will no longer be able to bind to their target protein in these experiments. In the case of the anti-FADD antibody used in this study, Western blotting did not work, but subsequent ICC experiments were successful and the three cell lines were shown to express the FADD protein.

The Tet-on expression system was then used to generate four individual, stably transfected cell lines that express the wild-type or one of three death domain mutants of the Fas receptor. A single Huh7-Tet-on clone was chosen to express the Fas constructs as this cell line showed the greatest response to doxycyclin induction.

Although the expression of Fas in the four cell lines was initially different, the Tet-on system allowed equalisation of these expression levels by titration with doxycyclin. Interestingly, during the Western blotting analysis that was used to follow this titration process, it was notable that the Fas signal in the control A20 cell lysate was regularly observed at 43 kDa – 8 kDa higher than the recombinantly expressed Fas in the Tet-responsive cell lines (35 kDa). These two molecular weights are consistent with the glycosylated and unglycosylated forms of the receptor respectively. It is probable that, for an unknown reason the recombinantly expressed Fas is not being fully glycosylated by the transfected cell line. However it is unlikely that this absence of glycosylation affected Fas activity as there have been no reports of glycosylation being important for the function of this receptor, and subsequent experiments were entirely consistent with this receptor being competent to induce apoptosis. A second interesting feature of the western blots for ectopically expressed Fas was the consistent appearance of several smaller bands above the main 35kDa signal (see Figures 5.6 and 5.7). The reason for the appearance of such bands is unclear since they may correspond to non-specific binding of the 1^{o} antibody. However there is also a possibility that these additional bands are due to post-translational modification of the Fas protein in the Huh7 cells. The Fas protein may be phosphorylated, (partially) glycosylated or SUMOylated following its expression resulting in a series higher molecular weight species being observed on the western blots.

These experiments showed the utility of inducible expression systems in allowing the parallel expression of different proteins in four individual, stably transfected cell lines to be titrated to the same level. Having established that the expression of Fas and the three Fas mutants could be controlled and equalised, the remaining cell death experiments could be quantitatively analysed to assess the effects of Fas mutants on the ability of Fas to induce apoptosis.

To achieve this, it was first shown that the expression of the wild-type Fas receptor in Huh7 cells sensitised the cells to death induced by recombinant Fas ligand. These Fas-expressing cells, when treated with rhsFasL, could be partially rescued from cell death by the use of z-IETD-fmk, a specific caspase-8 inhibitor, and were shown to undergo DNA fragmentation by the use of a fluorescent TUNEL assay. The TUNEL-positive cells in this assay were seen to exhibit shrunken and fragmented nuclei, consistent with the morphological changes caused by apoptotic cell death. Moreover, the same cells, when treated with staurosporine, underwent the same DNA fragmentation and morphological changes, but this death could not be inhibited by z-IETD-fmk. It is almost certain, therefore, that the treatment of Fas-expressing Huh7 cells with Fas ligand resulted in caspase-8-dependent apoptosis.

Previous studies of the specific signal transduction pathway initiated by the interaction between Fas and FasL have shown that this form of caspase-8 dependent apoptosis is dependent on the interaction between the death domains of Fas and FADD (e.g. Yeh *et al.*, 1998). The cell-based assay developed here can therefore serve effectively as an assay for the interaction between these two domains. Three Fas-DD mutants, D244A, K247A and K280A, were tested for their effects on Fas-induced apoptosis. The results showed that the K247A mutation had little or no effect on the activity of Fas, but the D244A mutation completely abrogated Fas-induced apoptosis, while the K280A mutation resulted in a significant reduction in the amount of cell death.

A significant correlation was noted between the effects of the three mutations chosen for analysis in the cell-based assay and their effects on FADD-DD binding in the NMR and yeast-based experiments. In each case the K247A mutant exhibited similar effects as the wild-type Fas, the D244A mutation knocked out the activity of the wild-type protein and the K280A mutant showed an intermediate behaviour (either weakened

FADD-DD binding or significantly reduced apoptosis). This correlation serves to strengthen the conclusions from the NMR-based assay, the yeast two-hybrid analysis and the cell-based assay.

Chapter 6

Discussion

THE data I have presented in this thesis serve to illustrate several key points regarding the nature of the interaction between the death domains of the Fas receptor and its adaptor protein FADD. This interaction plays a key role in the initiation of apoptosis of certain cell types though the extrinsic pathway leading to the activation of caspase-8 and caspase-10. Using a combined, multidisciplinary approach, involving structural and cell biological methods, this interaction has been probed in the context of the two isolated death domains as part of a wider effort to understand the molecular basis for the signal transduction carried out following ligation of the Fas receptor. The remainder of this discussion will focus on achievements of this study and outlines the possibilities for the future of the project.

In Chapter 3 it was initially confirmed, using the yeast two-hybrid assay, that Fas-DD and FADD-DD productively interact in a cellular environment and that this interaction can be effectively abrogated by the D244A substitution in Fas-DD. It was then shown how these two death domains could be produced in a tractable form for studies with biomolecular nuclear magnetic resonance spectroscopy. The requirement for such NMR-based studies is the production of multi-milligrams of protein that is stable at millimolar concentrations. As shown by the attempts to produce Fas-DD in a form that was suitable for interaction studies with FADD-DD there are often problems associated

with the production of proteins for structural biology. Several approaches were taken to overcome the self-aggregation of wild-type human Fas-DD which occurred during attempts to concentrate this protein in buffers at physiological pH. These approaches included the use of different fusion protein partners (namely GST and Gb1), alteration of the amino-acid sequence boundaries of the death domain and site-directed mutagenesis of solvent-exposed residues. Fas-DD was produced in a suitable form by through both the use of the Gb1 fusion partner (to create Gb1-Fas-DD) and by using the Fas-DD-K247A mutant. The fact that it was necessary to apply such a wide range of strategies to solve this problem is an illustration of the general non-generic nature of proteins and protein fragments. It is still largely impossible to accurately predict the properties of a protein in solution from its primary sequence or, once a protein is produced, to predict the effects of any changes in the DNA construct used to encode that protein, or the consequences of changes in the buffer used to solublise that protein. There are numerous examples of how all three of the approaches used in the attempts to increase the expression yield and solubility of Fas-DD, along with other strategies not attempted in this work, have been applied successfully to the production of other proteins or protein domains (reviewed in (Georgiou and Valax, 1996; Waldo, 2003)). Such issues are highlighted by the difficulties being encountered by the highly resourced efforts in structural genomics (SG) projects around the world. The aim of SG initiatives is to solve the three dimensional structures of all (or a representative number) of the proteins synthesised from a variety of species. Initial estimates of the success of rates of these projects suggested that each one would solve the structures of 10-15% of their targets (Thornton, 2001; Service, 2002). In fact these seemingly conservative targets are now seen as overestimates and, at the time of writing this thesis, only 1587 out of 84938 selected gene targets have produced three dimensional structures that have been submitted to the RSCB protein data bank (PDB) database (data taken from Targetdb – http://targetdb.pdb.org/). This amounts to an overall success rate of less than 2%. It is clear that the typical generic, high-throughput "pipeline" nature of these initiatives is, at present, incompatible with the non-generic nature of individual polypeptide chains. For example, an analysis of one set of SG target proteins showed no correlation between the primary amino-acid sequence (or composition) and the tractability of that polypeptide as a viable structure determination candidate as defined by the quality of a 2D [^{15}N-^{1}H]-HSQC NMR spectrum (Yee *et al.*, 2002).

Having successfully produced the wild-type human FADD-DD and Fas-DD proteins in such a form that is suitable for structural studies, a series of titrations, monitored by [^{15}N-^{1}H]-HSQC NMR spectroscopy, was carried out in an attempt to characterise the interaction between these two domains in solution. Titration of either unlabelled Gb1-Fas-DD into ^{15}N-FADD-DD, or unlabelled FADD-DD into ^{15}N-Gb1-Fas-DD, resulted in the monotonic loss of the NMR signals from the ^{15}N-labelled death domain component. The resultant complex was evidently itself soluble as indicated by the presence of signals from mobile elements in the isotope-labelled component of the titration (either the terminal residues and side-chain carboxyamide groups from ^{15}N-FADD or the entire Gb1 domain of ^{15}N-Gb1-Fas-DD). The interaction was also shown to be specific to the death domains – as it could be essentially abrogated by the use of the Fas-DD-D244A mutant – and at least partially governed by electrostatic interactions as it could be disrupted by increasing the ionic strength of the buffer. However, the hydrodynamic size of the resultant complex, as well as its component stoichiometry, remains unknown and requires to be investigated by further biophysical analysis.

In Chapter 4 I presented a mutational analysis of the Fas death domain. In this study several previously reported Fas-DD mutants along with a range of novel mutants were analysed for their ability to interact with FADD-DD. This analysis was carried out using both yeast two-hybrid and NMR-based interaction assays. The yeast two-hybrid analysis established twelve Fas-DD mutants that appear to not interact with FADD-DD. These twelve mutants were further analysed by 2D [^{15}N-^{1}H]-HSQC NMR spectroscopy and the residue substitutions were all found not to disrupt the three dimensional fold of Fas-DD. Hence the substituted side-chains could be identified as being important for Fas-DD/FADD-DD interaction because of their effect in the yeast two-hybrid assay. Among this list of twelve mutants, four correspond to substitutions that have been previously reported to cause ALPS type 1a, a human lymphoproliferative disorder caused by defective Fas-induced apoptosis. The molecular basis of this disease is, in many cases, the disruption of the Fas/FADD interaction which is vital for apoptosis to occur through the Fas pathway (Martin *et al.*, 1999). In addition to these four, another six residues on the surface of Fas-DD were newly identified as being important for FADD-DD binding. This data represents an extension of our knowledge of the surface regions of Fas-DD that are important for FADD-DD interaction. Previous reports have shown that the surfaces of the α2 and α3 helices of Fas-DD constitute at least part of

the FADD-binding surface (Huang *et al.*, 1996; Lahm *et al.*, 2003), however the mutational analysis presented here has established that there are residues on the surfaces of α-helices 2, 3, 4, 5 and 6 that can modulate this interaction, at least *in vitro*. The extension of the Fas-DD interaction surface complements the data of Hill *et al.* who discovered, using a mutational analysis coupled with both *in vitro* pull-down and cell-based functional assays, an "expanded binding surface on the FADD death domain" that mediates the Fas-DD/FADD-DD interaction (Hill *et al.*, 2004).

To date, there are two published three dimensional structures of homotypic complexes of death fold family members – namely the *Drosophila* Pelle/Tube death domain complex (Xiao *et al.*, 1999) and the APAF-1/caspase-9 CARD complex (Qin *et al.*, 1999). Structures of the death domains of Fas and FADD were modelled onto the individual domains of these two complexes and the inventory of residues found at the interfaces in these simple models was compared to the list of residues that, when mutated, were found to disrupt the interaction between Fas-DD and FADD-DD. This analysis ultimately proved inconclusive and suggested that the 1:1 heterodimer structures of the Pelle-D/Tube-DD and APAF-1-CARD/caspase-9-CARD complexes are of not good starting points to use as templates for the creation of a model of the Fas-DD/FADD-DD interaction consistent with all the findings.

Evidence from the existing DD and CARD complex structures and the Fas-DD/FADD-DD interaction analysis points towards a non-conserved mode of homotypic interaction for the death fold domains. The Pelle-DD/Tube-DD interface consists of residues from α-helices 1, 3, and 4 of Pelle-DD and α-helices 1, 2 and 4 of Tube-DD along with the Tube-DD C-terminal extension that binds to the α4-α5 and α2-α3 loops of Pelle-DD. The CARD complex interface consists of mainly charged residues in α-helices 1 and 4 of caspase-9 CARD and α-helices 2 and 3 of APAF-1 CARD. It has been established by this work and that of Hill *et al.*, that Fas-DD and FADD-DD utilise residues from essentially each one of their respective helices (with the possible exception of the Fas-DD α1 helix). Moreover, there is extensive experimental evidence that the formation of these homotypic death fold complexes is dominated by electrostatic interactions (e.g. Zhou *et al.*, 1999; Bang *et al.*, 2000; Kaufmann *et al.*, 2002; Hill *et al.*, 2004). It is perhaps unsurprising then, that given the heterogeneity of the surface charge

distributions exhibited by these domains (see Figure 1.9), a common mode of interaction might not be established.

The data presented here, in Chapters 3 and 4, point to the formation of a multivalent complex between the death domains of Fas and FADD. The mutational analysis of Fas-DD revealed that several surface regions of the death domain are involved in its interaction with FADD-DD and, indeed, multiple surface regions of both Fas-DD and FADD-DD would be necessary for the formation of the large, mulitmeric complex suggested by the NMR-based titration studies of the two proteins.

In order to reinforce the *in vitro* mutational analysis of Fas-DD, Chapter 5 described the development of a functional, cell-based assay to analyse the effect of Fas mutations on the ability of the receptor to induce apoptosis. Wild-type Fas and three mutant forms (D244A, K247A and K280A) were introduced in the human Fas negative Huh-7 cell line utilising the fine control of expression level provided by the Tet-on expression system. FasL was shown to induce death in the cell line expressing wild-type Fas, Fas-K247A and, to a lesser extent, Fas-K280A but not in the cell line expressing Fas-D244A. Importantly, the cell death induced by FasL in these cultures was shown to be a result of caspase-8 dependent apoptosis by a combination of specific caspase-8 inhibition and *in situ* DNA fragmentation assays. The pattern of functional data established via the cell-based assay correlated well with *in vitro* analysis of the same three Fas-DD mutants. Such a correlation serves to highlight the utility of a multidisciplinary approach to the dissection of receptor-based signal transduction pathways.

Since the initiation of apoptosis through Fas depends on the activation of caspase-8, which in turn depends on the recruitment of FADD to the death receptor, the interaction between these two proteins is vital for the function of this apoptotic pathway. There is, at present, little understanding of the precise mechanism by which the effect of FasL ligation of the Fas receptor is transduced across the cell membrane. However, recent work identifying a specific series of events that follow Fas activation has increasingly suggested that the aggregation of Fas receptors in the membrane may be vital for the activation of sufficient quantities of caspase-8 to induce apoptosis (see Figure 6.1). First, high molecular weight oligomers of Fas have been reported to form as quickly as

5 seconds after FasL-binding. These oligomers are of unknown molecular weight as they have only been identified by Western-blotting techniques from whole-cell lysates (e.g. Algeciras-Schimnich *et al.*, 2002; Holler *et al.*, 2003) – curiously though, these Fas "micro-aggregates" are SDS-stable and, as such, may represent some form of covalently modified receptor. Without knowledge of the precise composition and oligomeric state of such micro-aggregates (or how, if at all, they are modified), it is hard to speculate upon their function in the signalling process. This issue is further confused by reports of the self-association of Fas receptors before ligand binding occurs and the subsequent identification of the pre-ligand assembly domain (PLAD) in the N-terminus of the extracellular domain of Fas (Siegel *et al.*, 2000). The Fas receptors may, therefore, undergo a form of structural rearrangement in the plasma membrane upon ligation with FasL that leads to or is coupled with micro-aggregate formation and receptor clustering, a hypothesis that is given weight by reports that disruption of the actin cytoskeleton can inhibit this process (Algeciras-Schimnich *et al.*, 2002).

Following these initial FasL-dependent events, FADD is rapidly recruited to the death domain of Fas reaching maximal levels of co-localisation after approximately 15 minutes (Kischkel *et al.*, 1995). A recent report by Siegel *et al.* indicates that FADD recruitment further drives the clustering of the Fas receptor in the cell membrane, allowing the detection of Fas aggregates using fluorescence confocal microscopy (Siegel *et al.*, 2004). Moreover, this process was found to be independent of caspase-8 recruitment but could be disrupted by overexpression of the ALPS mutation Fas-D244V and was independent of whether the apoptotic cell type was Type I or Type II (see Chapter 1).

In the next stage of apoptotic Fas signalling, caspase-8 is recruited to FADD to form the DISC thereby becoming activated to initiate the "caspase cascade". At this point Fas is further clustered (at least in Type I cells) (Barnhart *et al.*, 2003) to form receptor "caps" on the cell surface, in a caspase-dependent process (Siegel *et al.*, 2004). This receptor capping is also associated with ceramide production and acid sphingomyelinase activity and is, as such, thought to require lipid rafts (Cremesti *et al.*, 2001; Grassme *et al.*, 2001a). Finally these receptors are recycled via an uncharacterised endocytosis pathway (Algeciras-Schimnich *et al.*, 2002).

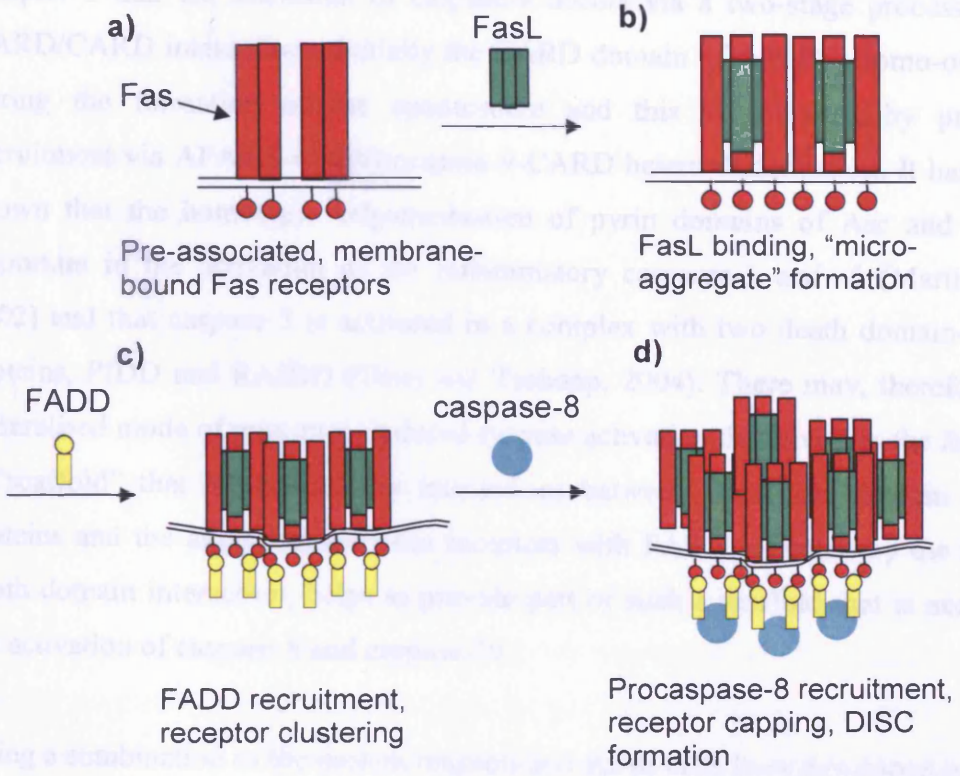

Figure 6.1: Stages of Fas receptor signalling and DISC formation. Fas receptors may be constitutively dimerised (based on the TNF-receptor structure – see Figure 1.9) or pre-associated in some other manner in the cell membrane via the PLAD region (a). Following FasL binding (b), the receptors form SDS-stable micro-aggregates that can be detected by Western blotting. A second stage of receptor clustering is dependent on FADD recruitment and actin filaments, and can be detected by fluorescent microscopy (c). In the final stage of DISC formation (d), procaspase-8 is recruited and activated. During this stage the receptors are further aggregated into polarised "caps" on one region of the cell surface. Receptor capping is dependent on both caspase-8 activation and the actin cytoskeleton and may involve the formation of lipid rafts. Following caspase activation DISCs are internalised by endocytosis.

Taking these data at face value it seems that there are at least three independent stages of Fas aggregation before caspase-8 activation occurs at the DISC. Coupled with the observation that, almost certainly, induced proximity of procaspase-8 is sufficient to induce caspase-8 activation (Donepudi *et al.*, 2003; Boatright *et al.*, 2003), it may be assumed that the scaffold produced by the aggregation of Fas receptors in the membrane allows the local concentration of activated caspase-8 molecules to significantly increase. If, as suggested by the data presented in this thesis, the interaction between Fas-DD and FADD-DD involves the co-aggregation of Fas receptors and full length FADD molecules, then this event may conceivably drive the clustering of Fas receptors post-FasL binding but before procaspase-8 recruitment. This hypothesis is given weight by the observations that the activation of other caspases is driven by the aggregation of various different death fold domain-containing proteins. For example it was shown in

Chapter 1 that the activation of caspase-9 occurs via a two-stage process driven by CARD/CARD interactions. Initially the CARD domain of APAF-1 homo-oligomerises during the formation of the apoptosome and this is followed by procaspase-9 recruitment via APAF-1-CARD/caspase-9-CARD hetero-dimerisation. It has also been shown that the homotypic oligomerisation of pyrin domains of Asc and NALP1 is important in the activation of the inflammatory caspases-1 and -5 (Martinon *et al.*, 2002) and that caspase-2 is activated in a complex with two death domain-containing proteins, PIDD and RAIDD (Tinel and Tschopp, 2004). There may, therefore, exist a generalised mode of proximity-induced caspase activation that involves the formation of a "scaffold" that is provided by interactions between death-fold domain containing proteins and the aggregation of Fas receptors with FADD, effected by the homotypic death domain interaction, helps to provide part of such a scaffold that is necessary for the activation of caspase-8 and caspase-10.

Using a combination of the protein reagents and stable cells lines developed in this work there is a wide range of possibilities for the future of this project. For example, attempts to understand the interaction between Fas-DD and FADD may be extended by working with full length FADD protein in place of the isolated death domain. Indeed, there have been reports that both the death domain and the death effector domain are required for efficient recruitment of FADD to the Fas receptor (Thomas *et al.*, 2004). Further to this, characterisation of the homotypic FADD/caspase-8 death effector domain interaction may lead to greater understanding of the precise molecular mechanism of caspase-8 activation, especially if this can be carried out in the context of the Fas/FADD interaction as a minimal *in vitro* reconstituted DISC.

In parallel to such efforts, utilisation of the stable Fas and Fas mutant expressing cell lines could enable comparative studies of the Fas receptor clustering and DISC formation using a combination of fluorescence microscopy and proteomic analysis. Although there have been reports of numerous other proteins involved in DISC formation such as FLIP, RIP, Daxx, FAP-1, FLASH, FAF-1, etc. (Peter *et al.*, 2003), none have been fully characterised in terms of their functional roles in Fas signalling or their precise molecular interactions. It is potentially feasible to "capture" the DISC proteome at varying points in the progression of its signalling by a combination of Fas activation and immunoprecipitation - as recently demonstrated for the TNF-R1

signalling complex (Kuai *et al.*, 2004). The availability of a cell-line expressing the wild-type Fas receptor along with others expressing a range of Fas mutants (including the D244A "knockout" mutant), would enable comparative studies to be carried out in parallel in order to decipher the precise functional role that each of these proteins may play with potential to reveal mechanistic details relevant to our understanding of health an in disease.

In summary, a combination of *in vitro* experiments using the yeast two-hybrid assay, NMR spectrsoscopy and point-mutation analysis indicated that an extended surface of the Fas death domain is required for its homotypic interaction with the FADD death domain, an interaction that provides the first step in the apoptotic signalling pathway of this death receptor. These results were reinforced by the development of a mammalian cell-based assay to test the effects of Fas-DD mutations on the efficiency of FasL-induced apoptosis. The biological assay yielded complementary data for several of the mutations tested *in vitro*. Therefore, this study has improved the understanding if the interaction between the death domains of the Fas receptor and the adaptor protein FADD and provided a basis for further structural and functional analyses.

References

Acehan, D., Jiang, X., Morgan, D. G., Heuser, J. E., Wang, X., and Akey, C. W. (2002). Three-dimensional structure of the apoptosome: implications for assembly, procaspase-9 binding, and activation. *Mol. Cell,* **9,** 423-432.

Algeciras-Schimnich, A., Pietras, E. M., Barnhart, B. C., Legembre, P., Vijayan, S., Holbeck, S. L., and Peter,M. E. (2003). Two CD95 tumor classes with different sensitivities to antitumor drugs. *Proc. Natl. Acad. Sci. U. S. A,* **100,** 11445-11450.

Algeciras-Schimnich, A., Shen, L., Barnhart, B. C., Murmann, A. E., Burkhardt, J. K., and Peter, M. E. (2002). Molecular ordering of the initial signaling events of CD95. *Mol. Cell Biol.,* **22,** 207-220.

Arends, M. J. and Wyllie, A. H. (1991). Apoptosis: mechanisms and roles in pathology. *Int. Rev. Exp. Pathol.,* **32,** 223-254.

Bang, S., Jeong, E. J., Kim, I. K., Jung, Y. K., and Kim, K. S. (2000). Fas- and tumor necrosis factor-mediated apoptosis uses the same binding surface of FADD to trigger signal transduction. A typical model for convergent signal transduction. *J. Biol. Chem.,* **275,** 36217-36222.

Banner, D. W., D'Arcy, A., Janes, W., Gentz, R., Schoenfeld, H. J., Broger, C., Loetscher, H., and Lesslauer, W. (1993). Crystal structure of the soluble human 55 kd TNF receptor-human TNF beta complex: implications for TNF receptor activation. *Cell,* **73,** 431-445.

Barnhart, B. C., Alappat, E. C., and Peter, M. E. (2003). The CD95 type I/type II model. *Semin. Immunol.,* **15,** 185-193.

Bateman, A., Coin, L., Durbin, R., Finn, R. D., Hollich, V., Griffiths-Jones, S., Khanna, A., Marshall, M., Moxon, S., Sonnhammer, E. L., Studholme, D. J., Yeats, C., and Eddy, S. R. (2004). The Pfam protein families database. *Nucleic Acids Res.,* **32 Database issue,** D138-D141.

Berglund, H., Olerenshaw, D., Sankar, A., Federwisch, M., McDonald, N. Q., and Driscoll, P. C. (2000). The three-dimensional solution structure and dynamic properties of the human FADD death domain. *J. Mol. Biol.,* **302,** 171-188.

Bettinardi, A., Brugnoni, D., Quiros-Roldan, E., Malagoli, A., La Grutta, S., Correra, A., and Notarangelo, L. D. (1997). Missense mutations in the Fas gene resulting in autoimmune lymphoproliferative syndrome: a molecular and immunological analysis. *Blood,* **89,** 902-909.

Beyaert, R., Van Loo, G., Heyninck, K., and Vandenabeele, P. (2002). Signaling to gene activation and cell death by tumor necrosis factor receptors and Fas. *Int. Rev. Cytol.*, **214,** 225-272.

Boatright, K. M., Renatus, M., Scott, F. L., Sperandio, S., Shin, H., Pedersen, I. M., Ricci, J. E., Edris, W. A., Sutherlin, D. P., Green, D. R., and Salvesen, G. S. (2003). A unified model for apical caspase activation. *Mol. Cell,* **11,** 529-541.

Brunger, A. T., Adams, P. D., Clore, G. M., DeLano, W. L., Gros, P., Grosse-Kunstleve, R. W., Jiang, J. S., Kuszewski, J., Nilges, M., Pannu, N. S., Read, R. J., Rice, L. M., Simonson, T., and Warren, G. L. (1998). Crystallography & NMR system: A new software suite for macromolecular structure determination. *Acta Crystallogr. D Biol. Crystallogr.*, **54 (Pt 5),** 905-921.

Brunner, T., Mogil, R. J., LaFace, D., Yoo, N. J., Mahboubi, A., Echeverri, F., Martin, S. J., Force, W. R., Lynch, D. H., Ware, C. F., and . (1995). Cell-autonomous Fas (CD95)/Fas-ligand interaction mediates activation-induced apoptosis in T-cell hybridomas. *Nature,* **373,** 441-444.

Budihardjo, I., Oliver, H., Lutter, M., Luo, X., and Wang, X. (1999). Biochemical pathways of caspase activation during apoptosis. *Annu. Rev. Cell Dev. Biol.,* **15,** 269-290.

Cagney, G., Uetz, P., and Fields, S. (2000). High-throughput screening for protein-protein interactions using two-hybrid assay. *Methods Enzymol.,* **328,** 3-14.

Cha, S. S., Sung, B. J., Kim, Y. A., Song, Y. L., Kim, H. J., Kim, S., Lee, M. S., and Oh, B. H. (2000). Crystal structure of TRAIL-DR5 complex identifies a critical role of the unique frame insertion in conferring recognition specificity. *J. Biol. Chem.,* **275,** 31171-31177.

Chai, J., Wu, Q., Shiozaki, E., Srinivasula, S. M., Alnemri, E. S., and Shi, Y. (2001). Crystal structure of a procaspase-7 zymogen: mechanisms of activation and substrate binding. *Cell,* **107,** 399-407.

Chinnaiyan, A. M. and Dixit, V. M. (1996). The cell-death machine. *Curr. Biol.,* **6,** 555-562.

Chinnaiyan, A. M., O'Rourke, K., Tewari, M., and Dixit, V. M. (1995). FADD, a novel death domain-containing protein, interacts with the death domain of Fas and initiates apoptosis. *Cell,* **81,** 505-512.

Chinnaiyan, A. M., Tepper, C. G., Seldin, M. F., O'Rourke, K., Kischkel, F. C., Hellbardt, S., Krammer, P. H., Peter, M. E., and Dixit, V. M. (1996). FADD/MORT1 is a common mediator of CD95 (Fas/APO-1) and tumor necrosis factor receptor-induced apoptosis. *J. Biol. Chem.,* **271,** 4961-4965.

Cottin, V., Doan, J. E., and Riches, D. W. (2002). Restricted localization of the TNF receptor CD120a to lipid rafts: a novel role for the death domain. *J. Immunol.,* **168,** 4095-4102.

Cremesti, A., Paris, F., Grassme, H., Holler, N., Tschopp, J., Fuks, Z., Gulbins, E., and Kolesnick, R. (2001). Ceramide enables fas to cap and kill. *J. Biol. Chem.*, **276,** 23954-23961.

Davis, G. D., Elisee, C., Newham, D. M., and Harrison, R. G. (1999). New fusion protein systems designed to give soluble expression in Escherichia coli. *Biotechnol. Bioeng.*, **65,** 382-388.

Delaglio, F., Grzesiek, S., Vuister, G. W., Zhu, G., Pfeifer, J., and Bax, A. (1995). NMRPipe: a multidimensional spectral processing system based on UNIX pipes. *J. Biomol. NMR,* **6,** 277-293.

DeLong, M. J. (1998). Apoptosis: a modulator of cellular homeostasis and disease states. *Ann. N. Y. Acad. Sci.,* **842,** 82-90.

Denault, J. B. and Salvesen, G. S. (2002). Caspases: keys in the ignition of cell death. *Chem. Rev.,* **102,** 4489-4500.

Deveraux, Q. L. and Reed, J. C. (1999). IAP family proteins--suppressors of apoptosis. *Genes Dev.,* **13,** 239-252.

Dhein, J., Walczak, H., Baumler, C., Debatin, K. M., and Krammer, P. H. (1995). Autocrine T-cell suicide mediated by APO-1/(Fas/CD95). *Nature,* **373,** 438-441.

Donepudi, M., Mac, S. A., Briand, C., and Grutter, M. G. (2003). Insights into the regulatory mechanism for caspase-8 activation. *Mol. Cell,* **11,** 543-549.

Eberstadt, M., Huang, B., Chen, Z., Meadows, R. P., Ng, S. C., Zheng, L., Lenardo, M. J., and Fesik, S. W. (1998). NMR structure and mutagenesis of the FADD (Mort1) death-effector domain. *Nature,* **392,** 941-945.

Eberstadt, M., Huang, B., Olejniczak, E. T., and Fesik, S. W. (1997). The lymphoproliferation mutation in Fas locally unfolds the Fas death domain. *Nat. Struct. Biol.,* **4,** 983-985.

Esnouf, R. M. (1997). An extensively modified version of MolScript that includes greatly enhanced coloring capabilities. *J. Mol. Graph. Model.,* **15,** 132-133.

Fesik, S. W. (2000). Insights into programmed cell death through structural biology. *Cell,* **103,** 273-282.

Fields, S. and Song, O. (1989). A novel genetic system to detect protein-protein interactions. *Nature,* **340,** 245-246.

Fisher, G. H., Rosenberg, F. J., Straus, S. E., Dale, J. K., Middleton, L. A., Lin, A. Y., Strober, W., Lenardo, M. J., and Puck, J. M. (1995). Dominant interfering Fas gene mutations impair apoptosis in a human autoimmune lymphoproliferative syndrome. *Cell,* **81,** 935-946.

Gavrieli, Y., Sherman, Y., and Ben Sasson, S. A. (1992). Identification of programmed cell death in situ via specific labeling of nuclear DNA fragmentation. *J. Cell Biol.,* **119,** 493-501.

Georgiou, G. and Valax, P. (1996). Expression of correctly folded proteins in Escherichia coli. *Curr. Opin. Biotechnol.*, **7,** 190-197.

Gill, S. C. and von Hippel, P. H. (1989). Calculation of protein extinction coefficients from amino acid sequence data. *Anal. Biochem.*, **182,** 319-326.

Grassme, H., Jekle, A., Riehle, A., Schwarz, H., Berger, J., Sandhoff, K., Kolesnick, R., and Gulbins, E. (2001a). CD95 signaling via ceramide-rich membrane rafts. *J. Biol. Chem.*, **276,** 20589-20596.

Grassme, H., Schwarz, H., and Gulbins, E. (2001b). Molecular mechanisms of ceramide-mediated cd95 clustering. *Biochem. Biophys. Res. Commun.*, **284,** 1016-1030.

Gravestein, L. A. and Borst, J. (1998). Tumor necrosis factor receptor family members in the immune system. *Semin. Immunol.*, **10,** 423-434.

Gronbaek, K., Straten, P. T., Ralfkiaer, E., Ahrenkiel, V., Andersen, M. K., Hansen, N. E., Zeuthen, J., Hou-Jensen, K., and Guldberg, P. (1998). Somatic Fas mutations in non-Hodgkin's lymphoma: association with extranodal disease and autoimmunity. *Blood,* **92,** 3018-3024.

Hacker, G. (2000). The morphology of apoptosis. *Cell Tissue Res.*, **301,** 5-17.

Hall, T.A. 1999. BioEdit: a user-friendly biological sequence alignment editor and analysis program for Windows 95/98/NT. *Nucl. Acids. Symp.* **Ser. 41**, 95-98.

Hansen, M. B., Nielsen, S. E., and Berg, K. (1989). Re-examination and further development of a precise and rapid dye method for measuring cell growth/cell kill. *J. Immunol. Methods,* **119,** 203-210.

Hardin, J. A., Sherr, D. H., DeMaria, M., and Lopez, P. A. (1992). A simple fluorescence method for surface antigen phenotyping of lymphocytes undergoing DNA fragmentation. *J. Immunol. Methods,* **154,** 99-107.

Helgstrand, M., Kraulis, P., Allard, P., and Hard, T. (2000). Ansig for Windows: an interactive computer program for semiautomatic assignment of protein NMR spectra. *J. Biomol. NMR,* **18,** 329-336.

Hengartner, M. O. (2000). The biochemistry of apoptosis. *Nature,* **407,** 770-776.

Hengartner, M. O. and Horvitz, H. R. (1994). C. elegans cell survival gene ced-9 encodes a functional homolog of the mammalian proto-oncogene bcl-2. *Cell,* **76,** 665-676.

Hill, J. M., Morisawa, G., Kim, T., Huang, T., Wei, Y., Wei, Y., and Werner, M. H. (2004). Identification of an expanded binding surface on the FADD death domain responsible for interaction with CD95/Fas. *J. Biol. Chem.*, **279,** 1474-1481.

Hill, J. M., Vaidyanathan, H., Ramos, J. W., Ginsberg, M. H., and Werner, M. H. (2002). Recognition of ERK MAP kinase by PEA-15 reveals a common docking site within the death domain and death effector domain. *EMBO J.*, **21,** 6494-6504.

Hiller, S., Kohl, A., Fiorito, F., Herrmann, T., Wider, G., Tschopp, J., Grutter, M. G., and Wuthrich, K. (2003). NMR structure of the apoptosis- and inflammation-related NALP1 pyrin domain. *Structure. (Camb.),* **11,** 1199-1205.

Holler, N., Tardivel, A., Kovacsovics-Bankowski, M., Hertig, S., Gaide, O., Martinon, F., Tinel, A., Deperthes, D., Calderara, S., Schulthess, T., Engel, J., Schneider, P., and Tschopp, J. (2003). Two adjacent trimeric Fas ligands are required for Fas signaling and formation of a death-inducing signaling complex. *Mol. Cell Biol.,* **23,** 1428-1440.

Huang, B., Eberstadt, M., Olejniczak, E. T., Meadows, R. P., and Fesik, S. W. (1996). NMR structure and mutagenesis of the Fas (APO-1/CD95) death domain. *Nature,* **384,** 638-641.

Hubbard, S. J., Campbell, S. F., and Thornton, J. M. (1991). Molecular recognition. Conformational analysis of limited proteolytic sites and serine proteinase protein inhibitors. *J. Mol. Biol.,* **220,** 507-530.

Hymowitz, S. G., Compaan, D. M., Yan, M., Wallweber, H. J., Dixit, V. M., Starovasnik, M. A., and de Vos, A. M. (2003). The crystal structures of EDA-A1 and EDA-A2: splice variants with distinct receptor specificity. *Structure. (Camb.),* **11,** 1513-1520.

Ivanov, V. N., Lopez, B. P., Maulit, G., Sato, T. A., Sassoon, D., and Ronai, Z. (2003). FAP-1 association with Fas (Apo-1) inhibits Fas expression on the cell surface. *Mol. Cell Biol.,* **23,** 3623-3635.

Jackson, C. E., Fischer, R. E., Hsu, A. P., Anderson, S. M., Choi, Y., Wang, J., Dale, J. K., Fleisher, T. A., Middelton, L. A., Sneller, M. C., Lenardo, M. J., Straus, S .E., and Puck, J. M. (1999). Autoimmune lymphoproliferative syndrome with defective Fas: genotype influences penetrance. *Am. J. Hum. Genet.,* **64,** 1002-1014.

Jacobson, M. D., Weil, M., and Raff, M. C. (1997). Programmed cell death in animal development. *Cell,* **88,** 347-354.

Jeong, E. J., Bang, S., Lee, T. H., Park, Y. I., Sim, W. S., and Kim, K .S. (1999). The solution structure of FADD death domain. Structural basis of death domain interactions of Fas and FADD. *J. Biol. Chem.,* **274,** 16337-16342.

Ju, S. T., Panka, D. J., Cui, H., Ettinger, R., el Khatib, M., Sherr, D. H., Stanger,B.Z., and Marshak-Rothstein, A. (1995). Fas(CD95)/FasL interactions required for programmed cell death after T- cell activation. *Nature,* **373,** 444-448.

Juo, P., Kuo, C. J., Yuan, J., and Blenis, J. (1998). Essential requirement for caspase-8/FLICE in the initiation of the Fas- induced apoptotic cascade. *Curr. Biol.,* **8,** 1001-1008.

Kabir, J., Lobo, M., and Zachary, I. (2002). Staurosporine induces endothelial cell apoptosis via focal adhesion kinase dephosphorylation and focal adhesion disassembly independent of focal adhesion kinase proteolysis. *Biochem. J.,* **367,** 145-155.

Karpusas, M., Hsu, Y. M., Wang, J. H., Thompson, J., Lederman, S., Chess, L., and Thomas, D. (1995). 2 A crystal structure of an extracellular fragment of human CD40 ligand. *Structure.,* **3,** 1031-1039.

Kaufmann, M., Bozic, D., Briand, C., Bodmer, J. L., Zerbe, O., Kohl, A., Tschopp, J., and Grutter, M. G. (2002). Identification of a basic surface area of the FADD death effector domain critical for apoptotic signaling. *FEBS Lett.*, **527,** 250-254.

Kaufmann, S. H. and Hengartner, M. O. (2001). Programmed cell death: alive and well in the new millennium. *Trends Cell Biol.*, **11,** 526-534.

Kay, L. E. (2001). Nuclear magnetic resonance methods for high molecular weight proteins: a study involving a complex of maltose binding protein and beta-cyclodextrin. *Methods Enzymol.*, **339,** 174-203.

Keegan, L., Gill, G., and Ptashne, M. (1986). Separation of DNA binding from the transcription-activating function of a eukaryotic regulatory protein. *Science,* **231,** 699-704.

Kerr, J. F., Wyllie, A. H., and Currie, A. R. (1972). Apoptosis: a basic biological phenomenon with wide-ranging implications in tissue kinetics. *Br. J. Cancer,* **26,** 239-257.

Kischkel, F. C., Hellbardt, S., Behrmann, I., Germer, M., Pawlita, M., Krammer, P. H., and Peter, M. E. (1995). Cytotoxicity-dependent APO-1 (Fas/CD95)-associated proteins form a death-inducing signaling complex (DISC) with the receptor. *EMBO J.*, **14,** 5579-5588.

Krammer, P. H. (2000). CD95's deadly mission in the immune system. *Nature,* **407,** 789-795.

Krueger, A., Fas, S. C., Baumann, S., and Krammer, P. H. (2003). The role of CD95 in the regulation of peripheral T-cell apoptosis. *Immunol. Rev.*, **193,** 58-69.

Kuai, J., Wooters, J., Hall, J. P., Rao, V. R., Nickbarg, E., Li, B., Chatterjee-Kishore, M., Qiu, Y., and Lin, L. L. (2004). NAK is recruited to the TNFR1 complex in a TNFalpha-dependent manner and mediates the production of RANTES: identification of endogenous TNFR-interacting proteins by a proteomic approach. *J. Biol. Chem.*, **279,** 53266-53271.

Lahm, A., Paradisi, A., Green, D. R., and Melino, G. (2003). Death fold domain interaction in apoptosis. *Cell Death. Differ.*, **10,** 10-12.

Lam, J., Nelson, C. A., Ross, F. P., Teitelbaum, S. L., and Fremont, D. H. (2001). Crystal structure of the TRANCE/RANKL cytokine reveals determinants of receptor-ligand specificity. *J. Clin. Invest,* **108,** 971-979.

Lee, S. H., Shin, M. S., Kim, H. S., Park, W. S., Kim, S. Y., Jang, J. J., Rhim, K. J., Jang, J., Lee, H. K., Park, J. Y., Oh, R. R., Han, S. Y., Lee, J. H., Lee, J. Y., and Yoo, N. J. (2000). Somatic mutations of Fas (Apo-1/CD95) gene in cutaneous squamous cell carcinoma arising from a burn scar. *J. Invest Dermatol.*, **114,** 122-126.

Lee, S. H., Shin, M. S., Park, W. S., Kim, S. Y., Kim, H. S., Han, J. Y., Park, G. S., Dong, S. M., Pi, J. H., Kim, C. S., Kim, S. H., Lee, J. Y., and Yoo, N .J. (1999). Alterations of Fas (Apo-1/CD95) gene in non-small cell lung cancer. *Oncogene,* **18,** 3754-3760.

Leist, M. and Jaattela, M. (2001). Four deaths and a funeral: from caspases to alternative mechanisms. *Nat. Rev. Mol. Cell Biol.*, **2,** 589-598.

Lenardo, M. J. (1991). Interleukin-2 programs mouse alpha beta T lymphocytes for apoptosis. *Nature,* **353,** 858-861.

Li, H. and Yuan, J. (1999). Deciphering the pathways of life and death. *Curr. Opin. Cell Biol.*, **11,** 261-266.

Liepinsh, E., Barbals, R., Dahl, E., Sharipo, A., Staub, E., and Otting, G. (2003). The death-domain fold of the ASC PYRIN domain, presenting a basis for PYRIN/PYRIN recognition. *J. Mol. Biol.*, **332,** 1155-1163.

Liepinsh, E., Ilag, L. L., Otting, G., and Ibanez, C. F. (1997). NMR structure of the death domain of the p75 neurotrophin receptor. *EMBO J.*, **16,** 4999-5005.

Lim, K., Ho, J. X., Keeling, K., Gilliland, G. L., Ji, X., Ruker, F., and Carter, D. C. (1994). Three-dimensional structure of Schistosoma japonicum glutathione S-transferase fused with a six-amino acid conserved neutralizing epitope of gp41 from HIV. *Protein Sci.*, **3,** 2233-2244.

Locksley, R. M., Killeen, N., and Lenardo, M. J. (2001). The TNF and TNF receptor superfamilies: integrating mammalian biology. *Cell,* **104,** 487-501.

MacCorkle, R. A., Freeman, K. W., and Spencer, D. M. (1998). Synthetic activation of caspases: artificial death switches. *Proc. Natl. Acad. Sci. U. S. A,* **95,** 3655-3660.

Martin, D. A., Siegel, R. M., Zheng, L., and Lenardo, M. J. (1998). Membrane oligomerization and cleavage activates the caspase-8 (FLICE/MACHalpha1) death signal. *J. Biol. Chem.*, **273,** 4345-4349.

Martin, D. A., Zheng, L., Siegel, R. M., Huang, B., Fisher, G. H., Wang, J., Jackson, C. E., Puck, J. M., Dale, J., Straus, S. E., Peter, M. E., Krammer, P. H., Fesik, S., and Lenardo, M. J. (1999). Defective CD95/APO-1/Fas signal complex formation in the human autoimmune lymphoproliferative syndrome, type Ia. *Proc. Natl. Acad. Sci. U. S. A,* **96,** 4552-4557.

Martin, S. J. and Green, D. R. (1995). Protease activation during apoptosis: death by a thousand cuts? *Cell,* **82,** 349-352.

Martinon, F., Burns, K., and Tschopp, J. (2002). The inflammasome: a molecular platform triggering activation of inflammatory caspases and processing of proIL-beta. *Mol. Cell,* **10,** 417-426.

Matsuzawa, A., Moriyama, T., Kaneko, T., Tanaka, M., Kimura, M., Ikeda, H., and Katagiri, T. (1990). A new allele of the lpr locus, lprcg, that complements the gld gene in induction of lymphadenopathy in the mouse. *J. Exp. Med.*, **171,** 519-531.

Medema, J. P., Scaffidi, C., Kischkel, F. C., Shevchenko, A., Mann, M., Krammer, P. H., and Peter, M. E. (1997). FLICE is activated by association with the CD95 death-inducing signaling complex (DISC). *EMBO J.*, **16,** 2794-2804.

Meier, P., Finch, A., and Evan, G. (2000). Apoptosis in development. *Nature,* **407,** 796-801.

Metzstein, M. M., Stanfield, G. M., and Horvitz, H. R. (1998). Genetics of programmed cell death in C. elegans: past, present and future. *Trends Genet.,* **14,** 410-416.

Muller, M., Strand, S., Hug, H., Heinemann, E. M., Walczak, H., Hofmann, W. J., Stremmel, W., Krammer, P. H., and Galle, P. R. (1997). Drug-induced apoptosis in hepatoma cells is mediated by the CD95 (APO-1/Fas) receptor/ligand system and involves activation of wild-type p53. *J. Clin. Invest,* **99,** 403-413.

Muzio, M., Chinnaiyan, A. M., Kischkel, F. C., O'Rourke, K., Shevchenko, A., Ni, J., Scaffidi, C., Bretz, J. D., Zhang, M., Gentz, R., Mann, M., Krammer, P. H., Peter, M. E., and Dixit, V. M. (1996). FLICE, a novel FADD-homologous ICE/CED-3-like protease, is recruited to the CD95 (Fas/APO-1) death--inducing signaling complex. *Cell,* **85,** 817-827.

Naismith, J. H., Devine, T. Q., Brandhuber, B. J., and Sprang, S. R. (1995). Crystallographic evidence for dimerization of unliganded tumor necrosis factor receptor. *J. Biol. Chem.,* **270,** 13303-13307.

Nambu, Y., Hughes, S. J., Rehemtulla, A., Hamstra, D., Orringer, M. B., and Beer, D. G. (1998). Lack of cell surface Fas/APO-1 expression in pulmonary adenocarcinomas. *J. Clin. Invest,* **101,** 1102-1110.

Newton, K., Harris, A. W., Bath, M. L., Smith, K. G., and Strasser, A. (1998). A dominant interfering mutant of FADD/MORT1 enhances deletion of autoreactive thymocytes and inhibits proliferation of mature T lymphocytes. *EMBO J.,* **17,** 706-718.

Nicholls, A., Sharp, K. A., and Honig, B. (1991). Protein folding and association: insights from the interfacial and thermodynamic properties of hydrocarbons. *Proteins,* **11,** 281-296.

Nicholson, D. W. (2000). From bench to clinic with apoptosis-based therapeutic agents. *Nature,* **407,** 810-816.

Nicholson, D. W. and Thornberry, N. A. (1997). Caspases: killer proteases. *Trends Biochem. Sci.,* **22,** 299-306.

Orengo, C. A. and Taylor, W. R. (1990). A rapid method of protein structure alignment. *J. Theor. Biol.,* **147,** 517-551.

Otto, F. and Tsou, K. C. (1985). A comparative study of DAPI, DIPI, and Hoechst 33258 and 33342 as chromosomal DNA stains. *Stain Technol.,* **60,** 7-11.

Park, W. S., Oh, R. R., Kim, Y. S., Park, J. Y., Lee, S. H., Shin, M. S., Kim, S. Y., Kim, P. J., Lee, H. K., Yoo, N. Y., and Lee, J. Y. (2001). Somatic mutations in the death domain of the Fas (Apo-1/CD95) gene in gastric cancer. *J. Pathol.,* **193,** 162-168.

Peter, M. E. and Krammer, P. H. (2003). The CD95(APO-1/Fas) DISC and beyond. *Cell Death. Differ.,* **10,** 26-35.

Peters, A. M., Kohfink, B., Martin, H., Griesinger, F., Wormann, B., Gahr, M., and Roesler, J. (1999). Defective apoptosis due to a point mutation in the death domain of CD95 associated with autoimmune lymphoproliferative syndrome, T-cell lymphoma, and Hodgkin's disease. *Exp. Hematol.*, **27,** 868-874.

Qin, H., Srinivasula, S. M., Wu, G., Fernandes-Alnemri, T., Alnemri, E. S., and Shi, Y. (1999). Structural basis of procaspase-9 recruitment by the apoptotic protease-activating factor 1. *Nature,* **399,** 549-557.

Richardson, H. and Kumar, S. (2002). Death to flies: Drosophila as a model system to study programmed cell death. *J. Immunol. Methods,* **265,** 21-38.

Rieux-Laucat, F., Blachere, S., Danielan, S., De Villartay, J. P., Oleastro, M., Solary, E., Bader-Meunier, B., Arkwright, P., Pondare, C., Bernaudin, F., Chapel, H., Nielsen, S., Berrah, M., Fischer, A., and Le Deist, F. (1999). Lymphoproliferative syndrome with autoimmunity: A possible genetic basis for dominant expression of the clinical manifestations. *Blood,* **94,** 2575-2582.

Rieux-Laucat, F., Fischer, A., and Deist, F. L. (2003a). Cell-death signaling and human disease. *Curr. Opin. Immunol.*, **15,** 325-331.

Rieux-Laucat, F., Le Deist, F., and Fischer, A. (2003b). Autoimmune lymphoproliferative syndromes: genetic defects of apoptosis pathways. *Cell Death. Differ.*, **10,** 124-133.

Rodseth, L. E., Brandhuber, B., Devine, T. Q., Eck, M. J., Hale, K., Naismith, J. H., and Sprang, S. R. (1994). Two crystal forms of the extracellular domain of type I tumor necrosis factor receptor. *J. Mol. Biol.*, **239,** 332-335.

Roths, J. B., Murphy, E. D., and Eicher, E. M. (1984). A new mutation, gld, that produces lymphoproliferation and autoimmunity in C3H/HeJ mice. *J. Exp. Med.*, **159,** 1-20.

Salvesen, G. S. and Dixit, V. M. (1999). Caspase activation: the induced-proximity model. *Proc. Natl. Acad. Sci. U. S. A,* **96,** 10964-10967.

Salvesen, G. S. and Renatus, M. (2002). Apoptosome: the seven-spoked death machine. *Dev. Cell,* **2,** 256-257.

Saraste, A. and Pulkki, K. (2000). Morphologic and biochemical hallmarks of apoptosis. *Cardiovasc. Res.*, **45,** 528-537.

Scaffidi, C., Fulda, S., Srinivasan, A., Friesen, C., Li, F., Tomaselli, K. J., Debatin, K. M., Krammer, P. H., and Peter, M. E. (1998). Two CD95 (APO-1/Fas) signaling pathways. *EMBO J.*, **17,** 1675-1687.

Scheel-Toellner, D., Wang, K., Singh, R., Majeed, S., Raza, K., Curnow, S. J., Salmon, M., and Lord, J. M. (2002). The death-inducing signalling complex is recruited to lipid rafts in Fas-induced apoptosis. *Biochem. Biophys. Res. Commun.*, **297,** 876-879.

Schneider, P. and Tschopp, J. (2000). Apoptosis induced by death receptors. *Pharm. Acta Helv.*, **74,** 281-286.

Service, R. F. (2002). Structural genomics. Tapping DNA for structures produces a trickle. *Science,* **298,** 948-950.

Siegel, R. M., Frederiksen, J. K., Zacharias, D. A., Chan, F. K., Johnson, M., Lynch, D., Tsien, R. Y., and Lenardo, M. J. (2000). Fas preassociation required for apoptosis signaling and dominant inhibition by pathogenic mutations. *Science,* **288,** 2354-2357.

Siegel, R. M., Muppidi, J. R., Sarker, M., Lobito, A., Jen, M., Martin, D., Straus, S. E., and Lenardo, M. J. (2004). SPOTS: signaling protein oligomeric transduction structures are early mediators of death receptor-induced apoptosis at the plasma membrane. *J. Cell Biol.,* **167,** 735-744.

Smith, D. B. and Johnson, K. S. (1988). Single-step purification of polypeptides expressed in Escherichia coli as fusions with glutathione S-transferase. *Gene,* **67,** 31-40.

Sneller, M. C., Wang, J., Dale, J. K., Strober, W., Middelton, L. A., Choi, Y., Fleisher, T. A., Lim, M. S., Jaffe, E. S., Puck, J. M., Lenardo, M. J., and Straus, S. E. (1997). Clincial, immunologic, and genetic features of an autoimmune lymphoproliferative syndrome associated with abnormal lymphocyte apoptosis. *Blood,* **89,** 1341-1348.

Sprick, M. R., Rieser, E., Stahl, H., Grosse-Wilde, A., Weigand, M. A., and Walczak, H. (2002). Caspase-10 is recruited to and activated at the native TRAIL and CD95 death-inducing signalling complexes in a FADD-dependent manner but can not functionally substitute caspase-8. *EMBO J.,* **21,** 4520-4530.

Starling, G. C., Bajorath, J., Emswiler, J., Ledbetter, J. A., Aruffo, A., and Kiener, P. A. (1997). Identification of amino acid residues important for ligand binding to Fas. *J. Exp. Med.,* **185,** 1487-1492.

Strasser, A., O'Connor, L., and Dixit, V. M. (2000). Apoptosis signaling. *Annu. Rev. Biochem.,* **69,** 217-245.

Straus, S. E., Jaffe, E. S., Puck, J. M., Dale, J. K., Elkon, K. B., Rosen-Wolff, A., Peters, A. M., Sneller, M. C., Hallahan, C. W., Wang, J., Fischer, R. E., Jackson, C. M., Lin, A. Y., Baumler, C., Siegert, E., Marx, A., Vaishnaw, A. K., Grodzicky, T., Fleisher, T. A., and Lenardo, M. J. (2001). The development of lymphomas in families with autoimmune lymphoproliferative syndrome with germline Fas mutations and defective lymphocyte apoptosis. *Blood,* **98,** 194-200.

Stuart, L. and Hughes, J. (2002). Apoptosis and autoimmunity. *Nephrol. Dial. Transplant.,* **17,** 697-700.

Suda, T. and Nagata, S. (1994). Purification and characterization of the Fas-ligand that induces apoptosis. *J. Exp. Med.,* **179,** 873-879.

Sukits, S. F., Lin, L. L., Hsu, S., Malakian, K., Powers, R., and Xu, G. Y. (2001). Solution structure of the tumor necrosis factor receptor-1 death domain. *J. Mol. Biol.,* **310,** 895-906.

Telliez, J. B., Xu, G. Y., Woronicz, J. D., Hsu, S., Wu, J. L., Lin, L., Sukits, S. F., Powers, R., and Lin, L. L. (2000). Mutational analysis and NMR studies of the death domain of the tumor necrosis factor receptor-1. *J. Mol. Biol.,* **300,** 1323-1333.

Thomas, L. R., Henson, A., Reed, J. C., Salsbury, F. R., and Thorburn, A. (2004). Direct binding of Fas-associated death domain (FADD) to the tumor necrosis factor-related apoptosis-inducing ligand receptor DR5 is regulated by the death effector domain of FADD. *J. Biol. Chem.*, **279,** 32780-32785.

Thorburn, A. (2004). Death receptor-induced cell killing. *Cell Signal.*, **16,** 139-144.

Thornton, J. (2001). Structural genomics takes off. *Trends Biochem. Sci.*, **26,** 88-89.

Tinel, A. and Tschopp, J. (2004). The PIDDosome, a protein complex implicated in activation of caspase-2 in response to genotoxic stress. *Science,* **304,** 843-846.

Trauth, B. C., Klas, C., Peters, A. M., Matzku, S., Moller, P., Falk, W., Debatin, K. M., and Krammer, P. H. (1989). Monoclonal antibody-mediated tumor regression by induction of apoptosis. *Science,* **245,** 301-305.

Vaishnaw, A. K., Orlinick, J. R., Chu, J. L., Krammer, P. H., Chao, M. V., and Elkon, K. B. (1999). The molecular basis for apoptotic defects in patients with CD95 (Fas/Apo-1) mutations. *J. Clin. Invest,* **103,** 355-363.

van den Berg A., Maggio, E., Diepstra, A., de Jong, D., van Krieken, J., and Poppema, S. (2002). Germline FAS gene mutation in a case of ALPS and NLP Hodgkin lymphoma. *Blood,* **99,** 1492-1494.

van Nuland, N. A., Kroon, G. J., Dijkstra, K., Wolters, G. K., Scheek, R. M., and Robillard, G. T. (1993). The NMR determination of the IIA(mtl) binding site on HPr of the Escherichia coli phosphoenol pyruvate-dependent phosphotransferase system. *FEBS Lett.*, **315,** 11-15.

Vaughn, D. E., Rodriguez, J., Lazebnik, Y., and Joshua-Tor, L. (1999). Crystal structure of Apaf-1 caspase recruitment domain: an alpha- helical Greek key fold for apoptotic signaling. *J. Mol. Biol.*, **293,** 439-447.

Vaux, D. L. and Korsmeyer, S. J. (1999). Cell death in development. *Cell,* **96,** 245-254.

Vogt, C. (1842) Untersuchungen uber die Entwicklungsbiologie der Geburtshelferkrote. *Alytes obstertricans*. Jent und Gassmann, Solothurn, Switzerland.

Waldo, G. S. (2003). Genetic screens and directed evolution for protein solubility. *Curr. Opin. Chem. Biol.*, **7,** 33-38.

Waldo, G. S., Standish, B. M., Berendzen, J., and Terwilliger, T. C. (1999). Rapid protein-folding assay using green fluorescent protein. *Nat. Biotechnol.*, **17,** 691-695.

Wallach, D., Varfolomeev, E. E., Malinin, N. L., Goltsev, Y. V., Kovalenko, A. V., and Boldin, M. P. (1999). Tumor necrosis factor receptor and Fas signaling mechanisms. *Annu. Rev. Immunol.*, **17,** 331-367.

Wang, J., Chun, H. J., Wong, W., Spencer, D. M., and Lenardo, M. J. (2001). Caspase-10 is an initiator caspase in death receptor signaling. *Proc. Natl. Acad. Sci. U. S. A,* **98,** 13884-13888.

Watanabe-Fukunaga, R., Brannan, C. I., Copeland, N. G., Jenkins, N. A., and Nagata, S. (1992). Lymphoproliferation disorder in mice explained by defects in Fas antigen that mediates apoptosis. *Nature,* **356,** 314-317.

Watt, W., Koeplinger, K. A., Mildner, A. M., Heinrikson, R. L., Tomasselli, A. G., and Watenpaugh, K. D. (1999). The atomic-resolution structure of human caspase-8, a key activator of apoptosis. *Structure. Fold. Des,* **7,** 1135-1143.

Weber, C. H. and Vincenz, C. (2001a). A docking model of key components of the DISC complex: death domain superfamily interactions redefined. *FEBS Lett.,* **492,** 171-176.

Weber, C. H. and Vincenz, C. (2001b). The death domain superfamily: a tale of two interfaces? *Trends Biochem. Sci.,* **26,** 475-481.

Wei, Y., Fox, T., Chambers, S. P., Sintchak, J., Coll, J. T., Golec, J. M., Swenson, L., Wilson, K. P., and Charifson, P .S. (2000). The structures of caspases-1, -3, -7 and -8 reveal the basis for substrate and inhibitor selectivity. *Chem. Biol.,* **7,** 423-432.

Xiao, T., Towb, P., Wasserman, S. A., and Sprang, S. R. (1999). Three-dimensional structure of a complex between the death domains of Pelle and Tube. *Cell,* **99,** 545-555.

Yee, A., Chang, X., Pineda-Lucena, A., Wu, B., Semesi, A., Le, B., Ramelot, T., Lee, G. M., Bhattacharyya, S., Gutierrez, P., Denisov, A., Lee, C. H., Cort, J. R., Kozlov, G., Liao, J., Finak, G., Chen, L., Wishart, D., Lee, W., McIntosh, L. P., Gehring, K., Kennedy, M. A., Edwards, A. M., and Arrowsmith, C. H. (2002). An NMR approach to structural proteomics. *Proc. Natl. Acad. Sci. U. S. A,* **99,** 1825-1830.

Yeh, W. C., Pompa, J. L., McCurrach, M. E., Shu, H. B., Elia, A. J., Shahinian, A., Ng, M., Wakeham, A., Khoo, W., Mitchell, K., El Deiry, W. S., Lowe, S. W., Goeddel, D. V., and Mak, T. W. (1998). FADD: essential for embryo development and signaling from some, but not all, inducers of apoptosis. *Science,* **279,** 1954-1958.

Yonehara, S., Ishii, A., and Yonehara, M. (1989). A cell-killing monoclonal antibody (anti-Fas) to a cell surface antigen co-downregulated with the receptor of tumor necrosis factor. *J. Exp. Med.,* **169,** 1747-1756.

Yuan, J., Shaham, S., Ledoux, S., Ellis, H. M., and Horvitz, H. R. (1993). The C. elegans cell death gene ced-3 encodes a protein similar to mammalian interleukin-1 beta-converting enzyme. *Cell,* **75,** 641-652.

Zhang, O., Kay, L. E., Olivier, J. P., and Forman-Kay, J. D. (1994). Backbone 1H and 15N resonance assignments of the N-terminal SH3 domain of drk in folded and unfolded states using enhanced-sensitivity pulsed field gradient NMR techniques. *J. Biomol. NMR,* **4,** 845-858.

Zhou, P., Chou, J., Olea, R.S., Yuan, J., and Wagner, G. (1999). Solution structure of Apaf-1 CARD and its interaction with caspase-9 CARD: a structural basis for specific adaptor/caspase interaction. *Proc. Natl. Acad. Sci. U. S. A,* **96,** 11265-11270.

Zhou, P., Lugovskoy, A. A., and Wagner, G. (2001). A solubility-enhancement tag (SET) for NMR studies of poorly behaving proteins. *J. Biomol. NMR,* **20,** 11-14.

Zuiderweg, E. R. (2002). Mapping protein-protein interactions in solution by NMR spectroscopy. *Biochemistry,* **41,** 1-7.

Zuzarte-Luis, V. and Hurle, J. M. (2002). Programmed cell death in the developing limb. *Int. J. Dev. Biol.,* **46,** 871-876.

Appendix

Appendix 1: The standard genetic code

First Position	Second Position								Third Position
	T		C		A		G		
T	TTT	Phe	TCT	Ser	TAT	Tyr	TGT	Cys	T
	TTC	Phe	TCC	Ser	TAC	Tyr	TGC	Cys	C
	TTA	Leu	TCA	Ser	TAA	Stop	TGA	Stop	A
	TTG	Leu	TCG	Ser	TAG	Stop	TGG	Trp	G
C	CTT	Leu	CCT	Pro	CAT	His	CGT	Arg	T
	CTC	Leu	CCC	Pro	CAC	His	CGC	Arg	C
	CTA	Leu	CCA	Pro	CAA	Gln	CGA	Arg	A
	CTG	Leu	CCG	Pro	CAG	Gln	CGG	Arg	G
A	ATT	Ile	ACT	Thr	AAT	Asn	AGT	Ser	T
	ATC	Ile	ACC	Thr	AAC	Asn	AGC	Ser	C
	ATG	Ile	ACA	Thr	AAA	Lys	AGA	Arg	A
	ATG	Met	ACG	Thr	AAG	Lys	AGG	Arg	G
G	GTT	Val	GCT	Ala	GAT	Asp	GGT	Gly	T
	GTC	Val	GCC	Ala	GAC	Asp	GGC	Gly	C
	GTA	Val	GCA	Ala	GAA	Glu	GGA	Gly	A
	GTG	Val	GCG	Ala	GAG	Glu	GGG	Gly	G

Appendix 2: Amino-acid one and three letter codes

A	**Ala**	Alanine	**M**	**Met**	Methionine
C	**Cys**	Cysteine	**N**	**Asn**	Asparagine
D	**Asp**	Aspartic acid (Aspartate)	**P**	**Pro**	Proline
E	**Glu**	Glutamic acid (Glutamate)	**Q**	**Gln**	Glutamine
F	**Phe**	Phenylalanine	**R**	**Arg**	Arganine
G	**Gly**	Glycine	**S**	**Ser**	Serine
H	**His**	Histidine	**T**	**Thr**	Threonine
I	**Ile**	Isoleucine	**V**	**Val**	Valine
K	**Lys**	Lysine	**W**	**Trp**	Tryptophan
L	**Leu**	Leucine	**Y**	**Tyr**	Tyrosine

Amino-acid nomenclature used in this thesis

D101: Aspartate residue number 101

D101A: Aspartate 101 mutated to alanine

Appendix 3: PCR cloning primers

Shown in the table below are the 5' to 3' base sequences of all oligonucleotide primers used in this project. Mutagenic bases are coloured red. When in pairs the forward (3') primer is listed first followed by the reverse (5') primer.

Primer Name	Purpose	Sequence
1	Yeast 2 hybrid –Fas-DD	AATTCCAGCTGACCACCATGGAAACAGTGGCAATAAATT
2	Yeast 2 hybrid –Fas-DD	GATCCCCGGGAATTGCCATGTTAGACCAAGCTTTGGATTTC
3	Yeast 2 hybrid –FADD-DD	ATTTCCAGCTGACCACCATGGGGGAAGAAGACCTGT
4	Yeast 2 hybrid –FADD-DD	GATCCCCGGGAATTGCCATGTTAGGCCCCACTCCTG
5	Yeast 2 hybrid – Re-PCR	CTATCTATTCGATGAAGATACCCCACCAAACCCAAAAAAA GAGATCGAATTCCAGCTGACCACCATG
6	Yeast 2 hybrid – Re-PCR	GTACCGTTAAGGGCCCCTAGGCAGCTGGACGTCTCTAGA TACTTAGCATCTATGACTTTTTGGGGCGTTC
7	His-Fas-DD PCR	CCGGCATATGGAAACAGTGGCAATAAAT
8	His-Fas-DD PCR	GCGCGGATCCTTATCTTGAGTCACTAGT
9	GST-Fas-DD PCR	CGGCGCGGATCCGAAACAGTGGCAATAAAT
10	GST-Fas-DD PCR	GCGGCCGGAATTCTTAGACCAAGCTTTGGA
11	GST-Fas-DD PCR	GGCGCGGATCCCTGAACCCGGAAACAGTGGCAATAAAT
12	GST-Fas-DD PCR	GGCGCGGATCCTCCCCGACCCTGAACCCGGAAACAGTG
13	GST-Fas-DD PCR	GGCGCGGATCCCACGAATCCCCGACCCTGAACCCGGAA
14	GST-Fas-DD PCR	GCGGCCGGAATTCTTATTCTGAGTCACTAGT
15	Fas-DD-D244A mutation	GTCAATGAAGCCAAAATAGCTGAGATCAAGAATG
16	Fas-DD-D244A mutation	CATTCTTGATCTCAGCTATTTTGGCTTCATTGAC
17	Fas-DD-K247A mutation	GCCAAAATAGATGAGATCGCGAATGACATTGTCCAA
18	Fas-DD-K247A mutation	GTCTTGGACATTGTCATTCGCGATCTCATCTATTTT
19	Gb1-Fas-DD PCR	GCCGGGATCCGAAACAGTGGCAATAAAT
20	Gb1-Fas-DD PCR	GGCCGGATCCTTATTCTGAGTCACTAGT
21	Fas-DD-S227A mutation	GGAGTCATGACACTAGCTCAAGTTAAAGGCTTTG
22	Fas-DD-S227A mutation	CAAAGCCTTTAACTTGAGCTAGTGTCATGACTCC
23	Fas-DD-R234A mutation	GTTAAAGGCTTTGTTGCAAAGAATGGTGTCAATG
24	Fas-DD-R234A mutation	CATTGACACCATTCTTTGCAACAAAGCCTTTAAC
25	Fas-DD-N239Q mutation	CGAAAGAATGGTGTCCAAGAAGCCAAAATAGATG
26	Fas-DD-N239Q mutation	CATCTATTTTGGCTTCTTGGACACCATTCTTTCG
27	Fas-DD-E240A mutation	GAAAGAATGGTGTCAATGCAGCCAAAATAGATGAG
28	Fas-DD-E240A mutation	CTCATCTATTTTGGCTGCATTGACACCATTCTTTC
29	Fas-DD-E240Q mutation	GAAAGAATGGTGTCAATCAAGCCAAAATAGATGAG
30	Fas-DD-E240Q mutation	CTCATCTATTTTGGCTTGATTGACACCATTCTTTC
31	Fas-DD-A241D mutation	GAATGGTGTCAATGAAGACAAAATAGATGAGATCAAG
32	Fas-DD-A241D mutation	GAATGGTGTCAATGAAGACAAAATAGATGAGATCAAG
33	Fas-DD-K242A mutation	GGTGTCAATGAAGCCGCAATAGATGAGATCAAG
34	Fas-DD-K242A mutation	CTTGATCTCATCTATTGCGGCTTCATTGACACC
35	Fas-DD-N248Dmutation	GATGAGATCAAGGATGACAATGTCCAAGAC
36	Fas-DD-N248D mutation	GTCTTGGACATTGTCATCCTTGATCTCATC
37	Fas-DD-V251Q mutation	GATCAAGAATGACAATCAGCAAGACACAGCAGAAC
38	Fas-DD-V251Q mutation	GTTCTGCTGTGTCTTGCAGATTGTCATTCTTGATC
39	Fas-DD-Q252Amutation	GAGATCAAGAATGAGCATGTCCAAGACACAGCAGAAC
40	Fas-DD-Q252A mutation	GTTCTGCTGTGTCTGCGACATTGTCATTCTTGATCTC
41	Fas-DD-E256Q mutation	CAATGTCCAAGACACAGCACAACAGAAAGTTCAAC

42	Fas-DD-E256Q mutation	GTTGAACTTTCTGTTGTGCTGTGTCTTGGACATTG
43	Fas-DD-R263A mutation	GAAAGTTCAACTGCTTGCTAATTGGCATCAACTTC
44	Fas-DD-R263A mutation	GAAGTTGATGCCAATTAGCAAGCAGTTGAACTTTC
45	Fas-DD-Q276E mutation	CTTCGTAATTGGCATGAACTTCATGGAAAGAAAG
46	Fas-DD-Q267E mutation	CTTTCTTTCCATGAAGTTCATGCCAATTACGAAG
47	Fas-DD-K272A mutation	CAACTTCATGGAAAGGCAGAAGCGTATGACACATTG
48	Fas-DD-K272A mutation	CAATGTGTCATACGCTTCTGCCTTTCCATGAAGTTG
49	Fas-DD-D276N mutation	GGAAAGAAAGAAGCGTATAACACATTGATTAAAGATC
50	Fas-DD-D276N mutation	GATCTTTAATCAATGTTTCATACGCTTCTTTCTTTCC
51	Fas-DD-K280A mutation	GCGTATGACACATTGATTGCAGATCTCAAAAAAGCC
52	Fas-DD-K280A mutation	GGCTTTTTTGAGATCTGCAATCAATGTGTCATACGC
53	Fas-DD-K284Q mutation	GATTAAAGATCTCAAACAAGCCAATCTTTGTACTC
54	Fas-DD-K284Q mutation	GAGTACAAAGATTGGCTTGTTTGAGATCTTTAATC
55	Fas-DD-N286K mutation	CTCAAAAAAGCCAAGCTTTGTACTCTTGCAGAG
56	Fas-DD-N286K mutation	CTCTGCAAGAGTACAAAGCTTGGCTTTTTTGAG
57	Fas-cDNA PCR	CCGCACGCGTGCCATGCTGGGCATCTGGACC
58	Fas-cDNA PCR	GTCAGCGGCCGCTCAGACCAAGCTTTGGATTTC

Appendix 4: Recombinant protein expression plasmids

Shown below are diagrammatical representations of the plasmid vectors used in this project. Each includes the following features: open reading frames (grey boxes), promoters (clear boxes) and unique restriction enzyme sites used for cloning.

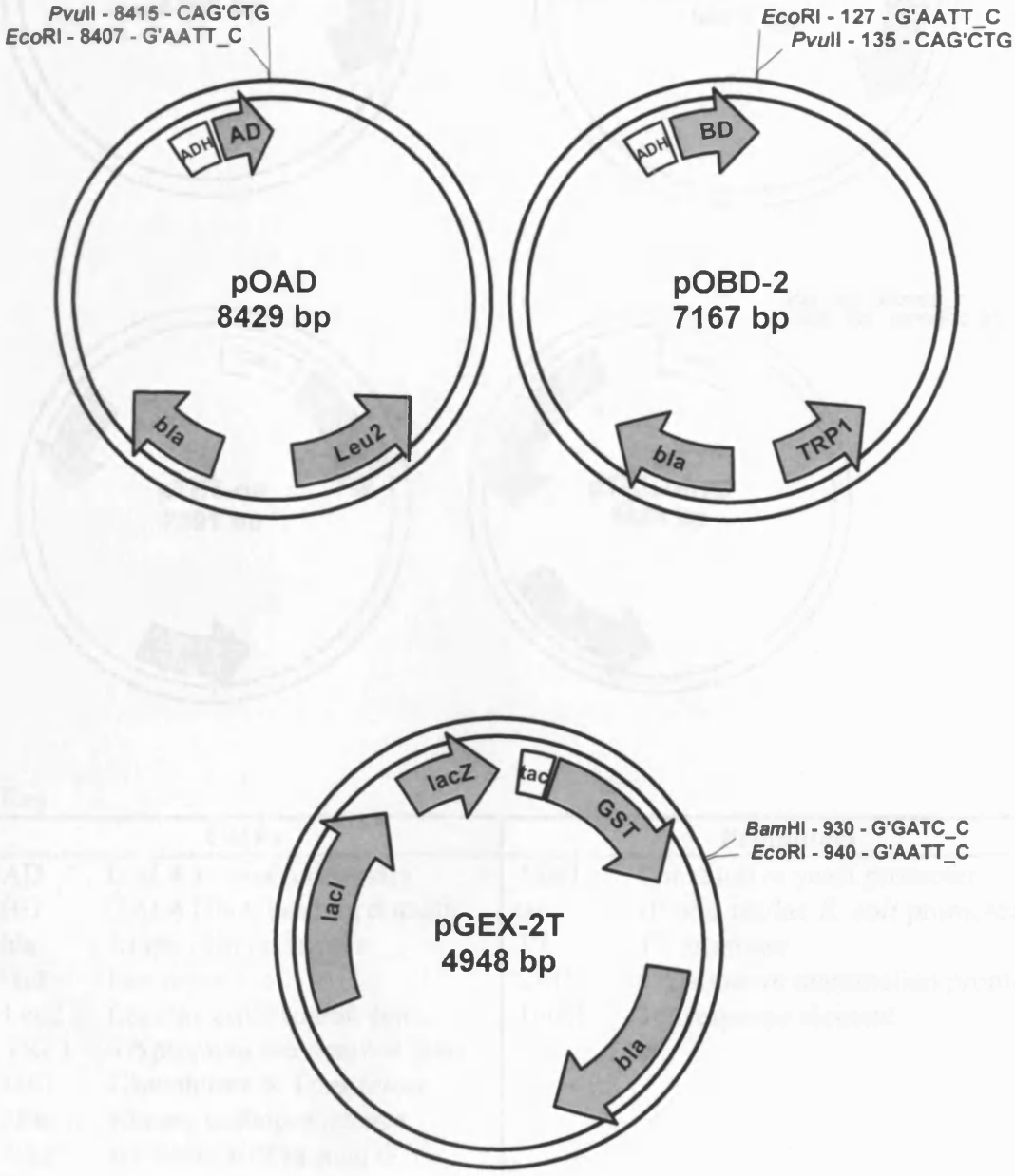

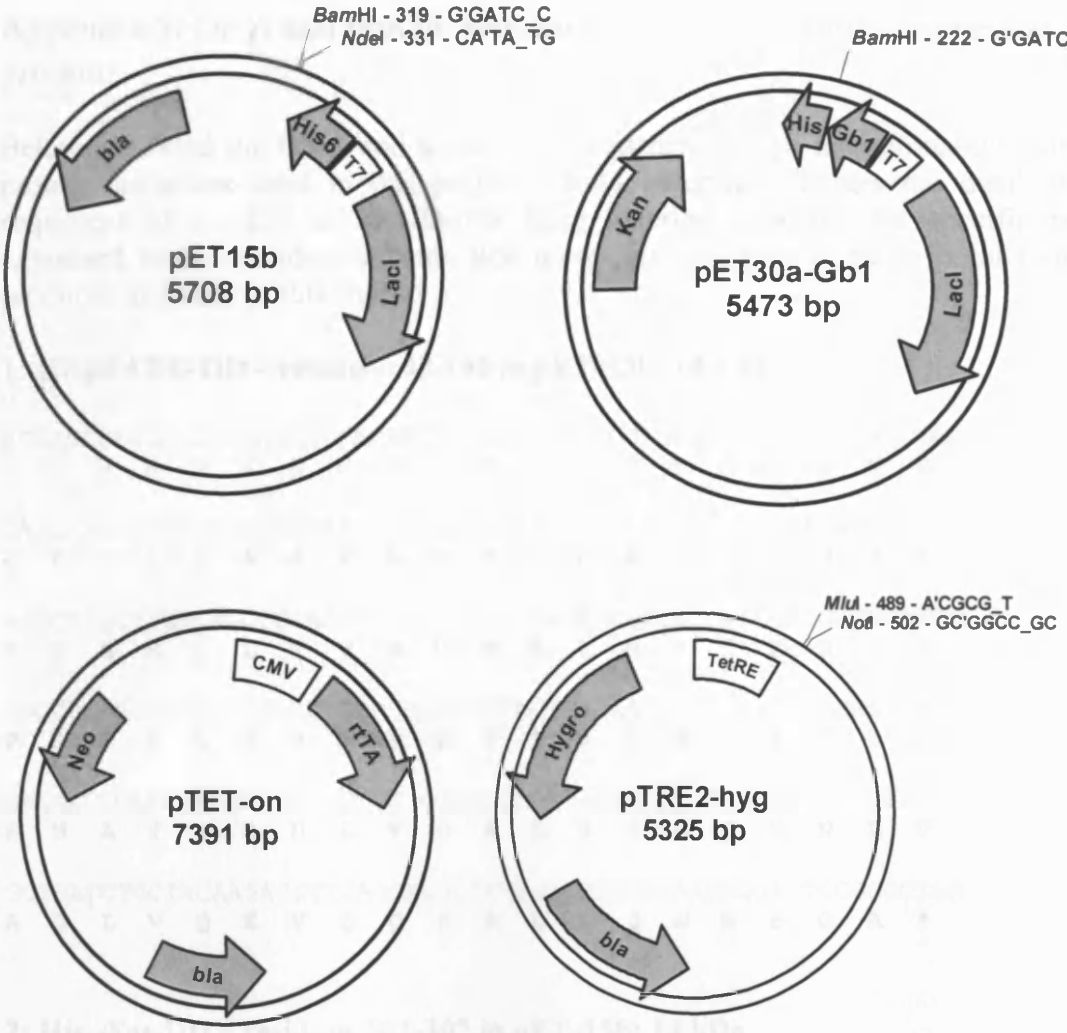

Key:

ORFs		Promoters	
AD	GAL4 activation domain	ADH	Constitutive yeast promoter
BD	GAL4 DNA binding domain	tac	Hybrid tac/lac *E. coli* promoter
bla	Ampicillin resistance	T7	T7 promoter
lacI	Lac repressor	CMV	Constitutive mammalian promoter
Leu2	Leucine auxotrophic gene	TetRE	Tet response element
TRP1	Tryptophan auxotrophic gene		
GST	Glutathione-S-Transferase		
His_6	His-tag coding sequence		
Gb1	B1 domain of protein G		
Kan	Kanamycin resistance gene		
Neo	Neomycin resistance gene		
Hygro	Hygromycin resistance gene		
rtTA	Tet-responsive transcription activator		

Appendix 5: DNA and protein sequences of recombinantly expressed proteins

Below are listed the DNA and amino-acid sequences for all recombinantly expressed protein constructs used in this project. Bold lettering indicates the death domain sequences of Fas-DD or FADD-DD. Blue lettering indicates the specific tags as expressed from individual vectors. Red letters indicate sites of those point mutations produced and used in this study.

1: His_6-FADD-DD – residues 93-192 in pET-15b: 14.5 kDa

```
ATGAGCCATCATCATCATCATCACAGCAGCGGCCTGGTGCCGCGCGGCAGCCATATGGGG
M  S  H  H  H  H  H  H  S  S  G  L  V  P  R  G  S  H  M  G

GAAGAAGACCTGTGCGCAGCATTTAACGTCATATGTGATAATGTGGGGAAAGATTGGAGA
E  E  D  L  C  A  A  F  N  V  I  C  D  N  V  G  K  D  W  R

AGGCTGGCTCGTCAGCTCAAAGTCTCAGACACCAAGATCGACAGCATCGAGGACAGATAC
R  L  A  R  Q  L  K  V  S  D  T  K  I  D  S  I  E  D  R  Y

CCCCGCAACCTGACAGAGCGTGTGCGGGAGTCACTGAGAATCTGGAAGAACACAGAGAAG
P  R  N  L  T  E  R  V  R  E  S  L  R  I  W  K  N  T  E  K

GAGAACGCAACAGTGGCCCACCTGGTGGGGGCTCTCAGGTCCTGCCAGATGAACCTGGTG
E  N  A  T  V  A  H  L  V  G  A  L  R  S  C  Q  M  N  L  V

GCTGACCTGGTACAAGAGGTTCAGCAGGCCCGTGACCTCCAGAACAGGAGTGGGGCCTGA
A  D  L  V  Q  E  V  Q  Q  A  R  D  L  Q  N  R  S  G  A  *
```

2: His_6-Fas-DD – residues 202-307 in pET-15b: 14 kDa

```
ATGAGCCATCATCATCATCATCACAGCAGCGGCCTGGTGCCGCGCGGCAGAAACA
M  S  H  H  H  H  H  H  S  S  G  L  V  P  R  G  S  E  T

GTGGCAATAAATTTATCTGATGTTGACTTGAGTAAATATATCACCACTATTGCTGGAGTC
V  A  I  N  L  S  D  V  D  L  S  K  Y  I  T  T  I  A  G  V

ATGACACTAAGTCAAGTTAAAGGCTTTGTTCGAAAGAATGGTGTCAATCAAGCCAAAATA
M  T  L  S  Q  V  K  G  F  V  R  K  N  G  V  N  Q  A  K  I

GATGAGATCAAGAATGACAATGTCCAAGACACAGCAGAACAGAAAGTTCAACTGCTTCGT
D  E  I  K  N  D  N  V  Q  D  T  A  E  Q  K  V  Q  L  L  R

AATTGGCATCAACTTCATGGAAAGAAAGAAGCGTATGACACATTGATTAAAGATCTCAAA
N  W  H  Q  L  H  G  K  K  E  A  Y  D  T  L  I  K  D  L  K

AAAGCCAATCTTTGTACTCTTGCAGAGAAAATTCAGACTATCATCCTCAAGGACATTACT
K  A  N  L  C  T  L  A  E  K  I  Q  T  I  I  L  K  D  I  T

AGTGACTCAGAATAA
S  D  S  E  *
```

3: GST-Fas-DD-1 – residues 202-307 in pGex-2T: 39 kDa (monomer mass)

ATGTCCCCTATACTAGGTTATTGGAAAATTAAGGGCCTTGTGCAACCCACTCGACTTCTT
M S P I L G Y W K I K G L V Q P T R L L

TTGGAATATCTTGAAGAAAAATATGAAGAGCATTTGTATGAGCGCGATGAAGGTGATAAA
L E Y L E E K Y E E H L Y E R D E G D K

TGGCGAAACAAAAAGTTTGAATTGGGTTTGGAGTTTCCCAATCTTCCTTATTATATTGAT
W R N K K F E L G L E F P N L P Y Y I D

GGTGATGTTAAATTAACACAGTCTATGGCCATCATACGTTATATAGCTGACAAGCACAAC
G D V K L T Q S M A I I R Y I A D K H N

ATGTTGGGTGGTTGTCCAAAAGAGCGTGCAGAGATTTCAATGCTTGAAGGAGCGGTTTTG
M L G G C P K E R A E I S M L E G A V L

GATATTAGATACGGTGTTTCGAGAATTGCATATAGTAAAGACTTTGAAACTCTCAAAGTT
D I R Y G V S R I A Y S K D F E T L K V

GATTTTCTTAGCAAGCTACCTGAAATGCTGAAAATGTTCGAAGATCGTTTATGTCATAAA
D F L S K L P E M L K M F E D R L C H K

ACATATTTAAATGGTGATCATGTAACCCATCCTGACTTCATGTTGTATGACGCTCTTGAT
T Y L N G D H V T H P D F M L Y D A L D

GTTGTTTTATACATGGACCCAATGTGCCTGGATGCGTTCCCAAAATTAGTTTGTTTTAAA
V V L Y M D P M C L D A F P K L V C F K

AAACGTATTGAAGCTATCCCACAAATTGATAAGTACTTGAAATCCAGCAAGTATATAGCA
K R I E A I P Q I D K Y L K S S K Y I A

TGGCCTTTGCAGGGCTGGCAAGCCACGTTTGGTGGTGGCGACCATCCTCCAAAATCGGAT
W P L Q G W Q A T F G G G D H P P K S D

CTGGTTCCGCGTGGATCCGAAACAGTGGCAATAAATTTATCTGATGTTGACTTGAGTAAA

L V P R G S **E T V A I N L S D V D L S K**

TATATCACCACTATTGCTGGAGTCATGACACTAAGTCAAGTTAAAGGCTTTGTTCGAAAG
Y I T T I A G V M T L S Q V K G F V R K

AATGGTGTCAATCAAGCCAAAATAGATGAGATCAAGAATGACAATGTCCAAGACACAGCA
N G V N E A K I D[1] E I K[2] N D N V Q D T A

GAACAGAAAGTTCAACTGCTTCGTAATTGGCATCAACTTCATGGAAAGAAAGAAGCGTAT
E Q K V Q L L R N W H Q L H G K K E A Y

GACACATTGATTAAAGATCTCAAAAAAGCCAATCTTTGTACTCTTGCAGAGAAAATTCAG
D T L I K D L K K A N L C T L A E K I Q

ACTATCATCCTCAAGGACATTACTAGTGACTCAGAATAA
T I I L K D I T S D S E *

[1]: **D244**
[2]: **K247**

4: Gb1-Fas-DD-His_6 – residues 202-307 in pET30a-Gb1: 20 kDa

ATGCAGTACAAACTGATCCTGAACGGTAAAACCCTGAAAGGTGAAACCACCACCGAAGCT
M Q Y K L I L N G K T L K G E T T T E A

GTTGACGCTGCTACCGCGGAAAAAGTTTTCAAACAGTACGCTAACGACAACGGTGTTGAC
V D A A T A E K V F K Q Y A N D N G V D

GGTGAATGGACCTACGACGACGCTACCAAAACCTTCACCGTTACCGAAGGATCCGAAACA
G E W T Y D D A T K T F T V T E G S **E T**

GTGGCAATAAATTTATCTGATGTTGACTTGAGTAAATATATCACCACTATTGCTGGAGTC
V A I N L S D V D L S K Y I T T I A G V

ATGACACTAAGTCAAGTTAAAGGCTTTGTTCGAAAGAATGGTGTCAATCAAGCCAAAATA
M T L S[1] Q V K G F V R[2] K N G V N[3] E[4] A[5] K[6] I

GATGAGATCAAGAATGACAATGTCCAAGACACAGCAGAACAGAAAGTTCAACTGCTTCGT
D[7] E I K[8] N[9] D N V[10] Q[11] D T A E[12] Q K V Q L L R[13]

AATTGGCATCAACTTCATGGAAAGAAAGAAGCGTATGACACATTGATTAAAGATCTCAAA
N W H Q[14] L H G K K[15] E A Y D[16] T L I K[17] D L K

AAAGCCAATCTTTGTACTCTTGCAGAGAAAATTCAGACTATCATCCTCAAGGACATTACT
K[18] A N[19] L C T L A E K I Q T I I L K D I T

AGTGACTCAGAAGGATCCCACCACCACCACCACCACTAA
S D S E G S H H H H H H *

[1]: **S227**
[2]: **R234**
[3]: **N239**
[4]: **E240**
[5]: **A241**
[6]: **K242**
[7]: **D244**
[8]: **K247**
[9]: **N238**
[10]: **V251**
[11]: **Q252**
[12]: **E256**
[13]: **R263**
[14]: **Q267**
[15]: **K272**
[16]: **D267**
[17]: **K280**
[18]: **K284**
[19]: **N286**

5: Fas – residues 1-319 in pTRE2-hyg: 35 kDa

ATGCTGGGCATCTGGACCCTCCTACCTCTGGTTCTTACGTCTGTTGCTAGATTATCGTCC
M L G I W T L L P L V L T S V A R L S S

AAAAGTGTTAATGCCCAAGTGACTGACATCAACTCCAAGGGATTGGAATTGAGGAAGACT
K S V N A Q V T D I N S K G L E L R K T

GTTACTACAGTTGAGACTCAGAACTTGGAAGGCCTGCATCATGATGGCCAATTCTGCCAT
V T T V E T Q N L E G L H H D G Q F C H

AAGCCCTGTCCTCCAGGTGAAAGGAAAGCTAGGGACTGCACAGTCAATGGGGATGAACCA
K P C P P G E R K A R D C T V N G D E P

GACTGCGTGCCCTGCCAAGAAGGGAAGGAGTACACAGACAAAGCCCATTTTTCTTCCAAA
D C V P C Q E G K E Y T D K A H F S S K

TGCAGAAGATGTAGATTGTGTGATGAAGGACATGGCTTAGAAGTGGAAATAAACTGCACC
C R R C R L C D E G H G L E V E I N C T

CGGACCCAGAATACCAAGTGCAGATGTAAACCAAACTTTTTTTGTAACTCTACTGTATGT
R T Q N T K C R C K P N F F C N S T V C

GAACACTGTGACCCTTGCACCAAATGTGAACATGGAATCATCAAGGAATGCACACTCACC
E H C D P C T K C E H G I I K E C T L T

AGCAACACCAAGTGCAAAGAGGAAGGATCCAGATCTAACTTGGGGTGGCTTTGTCTTCTT
S N T K C K E E G S R S N L G W L C L L

CTTTTGCCAATTCCACTAATTGTTTGGGTGAAGAGAAAGGAAGTACAGAAAACATGCAGA
L L P I P L I V W V K R K E V Q K T C R

AAGCACAGAAAGGAAAACCAAGGTTCTCATGAATCTCCAACCTTAAATCCTGAAACAGTG
K H R K E N Q G S H E S P T L N P E T V

GCAATAAATTTATCTGATGTTGACTTGAGTAAATATATCACCACTATTGCTGGAGTCATG
A I N L S D V D L S K Y I T T I A G V M

ACACTAAGTCAAGTTAAAGGCTTTGTTCGAAAGAATGGTGTCAATGAAGCCAAAATAGAT
T L S Q V K G F V R K N G V N E A K I D[1]

GAGATCAAGAATGACAATGTCCAAGACACAGCAGAACAGAAAGTTCAACTGCTTCGTAAT
E I K[2] N D N V Q D T A E Q K V Q L L R N

TGGCATCAACTTCATGGAAAGAAAGAAGCGTATGACACATTGATTAAAGATCTCAAAAAA
W H Q L H G K K E A Y D T L I K[3] D L K K

GCCAATCTTTGTACTCTTGCAGAGAAAATTCAGACTATCATCCTCAAGGACATTACTAGT
A N L C T L A E K I Q T I I L K D I T S

GACTCAGAAAATTCAAACTTCAGAAATGAAATCCAAAGCTTGGTCTAG
D S E N S N F R N E I Q S L V *

[1]: **D244**
[2]: **K247**
[3]: **K280**